
# *Using label-free proteomics to elucidate factors involved in the human response to orthohantavirus infection*

Thesis submitted in accordance with the requirements of the University of Liverpool for the degree of Doctor in Philosophy

by

Sarah Brun Bar-Yaacov (MSc)

January 2019

## *Acknowledgment*

This research was funded by the National Institute for Health Research Health Protection Research Unit (NIHR HPRU) in Emerging and Zoonotic Infections at the University of Liverpool in partnership with Public Health England and Liverpool School of Tropical Medicine.

I'd like to extend my thanks to my supervisors; Dr Nick Beeching, Dr Jackie Duggan, Prof Tom Solomon, Dr Tim Brooks, and a special thank you to Prof Julian Hiscox, whose lab I worked in for the majority of my PhD, for feedback and guidance throughout this project. I'm incredibly grateful that you all agreed and helped arranged for me to take time off in the middle of my PhD to work in Sierra Leone during the West-African Ebola outbreak, which was an invaluable experience.

Thank you to the Rare and Imported Pathogens Laboratory at Porton Down for providing all samples used for this thesis. Thank you to Sam Douthwaite and Catherine Nelson-Piercy, who allowed me to use their case report for the pregnant HFRS patient described in chapter 4 and for encouragement to report the case, and thank you very much to the patient for granting permission for her clinical details to be published.

I would like to say thank you to all the members of the Respiratory and Emerging Infections Group at the University of Liverpool, you have been a great bunch of people to work with for the past 4 years. Dr Olivier Touzelet and Dr Isabel Garcia-Dorival, you have both been an absolutely invaluable help with planning and conducting experiments, analysing data, and giving me feedback on my written work. Special mention is warranted for Dr. Stuart Armstrong, for conducting the mass spectrometry experiments for my project, and aiding

me with proteomic data analysis. At the University of Liverpool, I would also like to thank the Centre for Genomic Research for providing profile contrasting analysis of my datasets.

For the nine months I spent at Porton Down, I'd like to extend my thanks to Diagnostic Support for hosting me, especially Dr. Dan Baily for his knowledgeable guidance.

Thank you to my external advisory panel, Dr Jane Osborne and Prof Nigel Cunliffe, who listened interestedly to my complaints, and gave good advice and boosted my confidence for four years.

And finally, I would like to thank my supportive family:

> Mamma, pappa og Jonathan – for troen dere har i meg, særlig når jeg ikke har troen på meg selv. Tusen takk pappa for at du orket å lese gjennom hele avhandlingen min, og gi meg masse gode tips.
>
> Sam – without whom the days would be less bright and joyful.

# *Abstract*

## *Using label-free proteomics to elucidate factors involved in the human response to orthohantavirus infection*

Sarah Brun Bar-Yaacov

Orthohantaviruses are a genus of Bunyaviruses carried by a range of rodent hosts. They are found in endemic foci across the globe and are associated with the zoonotic diseases haemorrhagic fever with renal syndrome and hantavirus cardiopulmonary syndrome. Orthohantaviruses are enzootic to south-eastern, central and northern parts of continental Europe. The virus has historically been considered absent from the British Isles, but the endemic presence of Seoul orthohantavirus (SEOV) was demonstrated in wild and pet rats in the UK in 2012. For the last six years several human cases of orthohantavirus-infections have been diagnosed in the UK with associated acute renal failure. Currently, treatment for haemorrhagic fever with renal syndrome and hantavirus cardiopulmonary syndrome is purely symptomatic. The mechanisms underlying the pathogenesis of orthohantavirus infections are not fully understood though several lines of enquiry have demonstrated the multifaceted nature of the disease, with direct virally mediated mechanisms, indirect immune mediate mechanism and genetic host factors all likely contributors to the clinical picture.

Clinical proteomics is a field of study in which high-throughput analytical approaches are used to investigate proteins in clinical samples. A major advantage of the proteomic approach is that no *a priori* knowledge is required for proteome analysis, making it an excellent hypothesis generating experimental method. The high-throughput facets of proteomic methods also make the approach very useful for infections such as orthohantavirus, for which aspects of its pathology remains unclear, and the relative rarity of the associated diseases result in limited access to biological samples.

The aims of this study were to use label-free proteomics to discover biomarkers of orthohantavirus infection in clinical human sera and to study the cellular interactome of recombinant SEOV Cherwell glycoproteins in a human kidney cell line, with the objective of gaining further insights into mechanism involved in the processing of viral proteins through host cells.

A pipeline for investigating the human serum proteome during diseased and healthy conditions was established. Using label-free proteomics in association with immunological methods, afamin and galectin 3-binding protein were identified and evaluated as putative biomarkers of orthohantavirus infection. Both proteins showed promise as factors involved in the response to acute Seoul orthohantavirus infection. Their relevance as markers of disease were supported by their functional annotation, with afamin playing a possible role in the cellular response to oxidative stress, and galectin 3-binding protein being associated with pro-inflammatory and pro-coagulant activity. Further validation studies with larger sample cohorts are warranted. Initial investigations into the *in vitro* interactome of recombinant SEOV Cherwell glycoproteins identified 12 potential associations between host and viral proteins. While functional analysis of selected proteins revealed a potential for relevance in the viral life cycle, further follow-up of these findings will be required to establish whether the identified associations are firstly, true associations, and secondly, biologically relevant interactions.

# *List of tables*

## *List of figures*

# *List of abbreviations*

| | |
|---|---|
| **AKI** | Acute kidney injury |
| **ANDV** | Andes virus |
| **BCA** | Bicinchoninic acid assay |
| **BCCV** | Black Creek Canal virus |
| **CRP** | C-reactiv protein |
| **DNA** | Deoxyribonucleic acid |
| **DOBV** | Dobrava Belgrade virus |
| **EDTA** | Ethylenediamineteraacetic acid |
| **ELISA** | Enzyme-linked immunosorbent assay |
| **ER** | Endoplasmic reticulum |
| **FC** | Fold change |
| **G3BP** | Galectin 3-binding protein |
| **GCP** | Glycoprotein precursor |
| **GFP** | Green fluorescent protein |
| **GnCT** | Gn cytoplasmic tail |
| **GO** | Gene Ontology |
| **hCG** | Choriogonadotropin subunit beta variant 1 |
| **HEK** | Human embryonic kidney |
| **HFRS** | Haemorrhagic fever with renal syndrome |
| **HMVEC-L** | Lonza™ human lung microvascular endothelial cells |
| **HNTV** | Haantan virus |
| **HPS** | Hantavirus cardiopulmonary syndrome |
| **HRP** | Horseradish peroxidase |
| **HUVEC** | Human umbilical vein endothelial cell |
| **IFA** | Immunofluorescence assay |
| **IFN** | Interferon |
| Ig | Immunoglobulin |
| **IL** | Interleukin |
| **MS** | Mass spectrometry |
| **MS/MS** | Tandem mass spectrometry |
| **NCBI** | National Center for Biotechnology Information |
| **NE** | Nephropathia epidemica |
| **PBS** | Phosphate-buffered saline |
| **PCR** | Polymerase chain reaction |
| **PHE** | Public Health England |
| **PUUV** | Puumala virus |
| **RIPA** | Radioimmunoprecipitation assay |
| **RIPL** | Rare and Imported Pathogens Laboratory |
| **RNA** | Ribonucleic acid |
| **RT-PCR** | Real time polymerase chain reaction |
| **SDS-PAGE** | Sodium dodecyl sulphate polyacrylamide gel electrophoresis |
| **SEOV** | Seoul virus |
| **SNV** | Sin Nombre virus |

| | |
|---|---|
| **STRING** | Search tool for retrieval of interacting genes/proteins |
| **TBS-T** | Tris buffered saline - tween 20 |
| **TNF** | Tumour necrosis factor |
| **TULV** | Tula virus |

# *Chapter 1: Literature review*

## *1.1 Epidemiology of the Hantaviridae*

Orthohantaviruses are enzootic viruses maintained as apparently asymptomatic infections in rodent-, insectivore- and bat populations (Vaheri, Strandin, *et al.*, 2013). They belong to the Hantaviridae family of the order Bunyaviridae, and to date 41 orthohantavirus species have been officially recognized by the International Committee on Taxonomy of Viruses (ICTV, 2014).The phylogenetic division of orthohantaviruses coincide with the phylogenetic division of their carrier hosts; Murinae-borne, Arvicolinea-borne, Sigmodontinae/Neotominae-borne, and lastly Chiroptera- and Soricidae-borne (figure 1.1). The rodent-borne orthohantaviruses are the only ones currently known to cause human disease and will be the orthohantaviruses referred to in this thesis. Orthohantaviruses are found in endemic foci across the globe, though due to the close association of each viral species with a specific mammalian host, the presence of a specific orthohantavirus in a geographic location is dependent on the presence of its carrier. Seoul orthohantavirus (SEOV) is the only orthohantavirus with global distribution, a consequence of the ubiquitous dispersal of its host the brown rat (*Rattus norvegicus*) (Jonsson *et al.*, 2010; Vaheri, Henttonen, *et al.*, 2013).

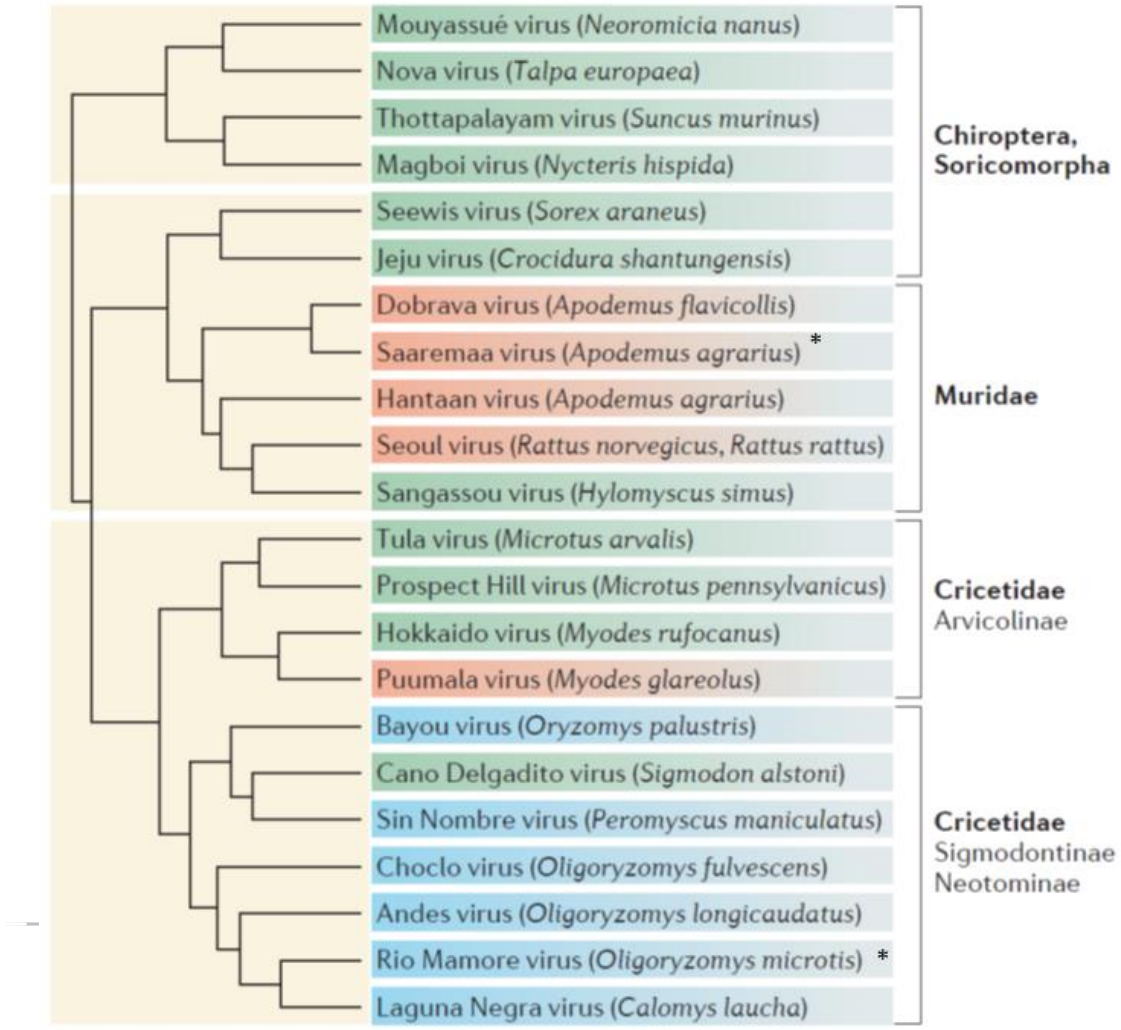


Figure 1.1. Orthohantavirus phylogeny reprinted by permission from Springer Nature: [Nature][Nature Reviews Microbiology](Vaheri, Strandin, *et al.*, 2013) [Copyright 2013] (license number: 4461321436935). Species in red are associated with hemorrhagic fever with renal syndrome, species in blue are associated with hantavirus cardiopulmonary syndrome, and species in green are not associated with human disease. *In a 2016 update on the Bunyavirales order, the ICTV removed Saarema virus and Rio Mamore virus as separate viral species of the Hantaviridae family. The ICTV have advised they should be considered strains of Dobrava-Belgrade virus and Laguna Negra virus respectively (Briese *et al.*, 2016).

Unlike other members of the Bunyavirdae family, no arthropod vector is involved in the viral transmission cycle of orthohantaviruses. In the rodent host viral replication is persistent. Virus is shed in saliva, urine and feces, and transmission occurs horizontally

within the population. Transmission to humans is mainly the result of inhalation of aerosolized rodent excreta in circumstances where humans come into direct contact with the animals or their dwellings (Vaheri, Strandin, *et al.*, 2013).

### *1.1.1 The Americas*

Several species of orthohantavirus, carried by a range of rodent hosts throughout the Americas, have been described in the literature (Jonsson *et al.*, 2010). So far 13 of these have been reported as causative agents of human disease (table 1). All pathogenic sigmodontinae-borne viruses are associated with the development of hantavirus cardiopulmonary syndrome (HPS). The first identification of a pathogenic orthohantavirus in the Americas occurred in 1993, during an outbreak of an unknown acute respiratory illness in the Four Corners Region of southwestern USA. The outbreak affected 48 people, and resulted in 27 fatalities (Prevention, 2017). The etiological agent was isolated from deer mice (*Peromyscus maniculatus*) in the area, and within a few weeks identified as a novel orthohantavirus species, given the name Sin Nombre virus (SNV). The respiratory disease has since become known as HPS. Compared to cases of haemorrhagic fever with renal syndrome (HFRS) in Europe and Asia, the prognosis of an infection with HPS-causing viruses seems to have a generally less favorable clinical course, with some outbreaks having reached mortality rates of approximately 60 %. Although the isolation of SNV was the first official recognition of the presence of a pathogenic orthohantavirus in the USA, sporadic cases displaying similar symptoms were anecdotally reported to have occurred by traditional healers living in the area (Jonsson *et al.*, 2010). Incidence of HPS in North America is low, and since the initial outbreak of 1993 through to December 2013, 637 were reported in the USA, with an overall case fatality rate of 36 % (Prevention, 2017)

**Table 1 Pathogenic orthohantaviruses**

| Distribution | Virus | Host | Host phylogeny | Disease |
|---|---|---|---|---|
| Global | | | | |
| | Seoul | Rattus spp. | Muridae | HFRS |
| Asia | | | | |
| | Haantan | *Apodemus agrarius* | Muridae | HFRS |
| | Amur | *Apodemus peninsulae* | Muridae | HFRS |
| | Thailand virus | *Bandicota indica* | Muridae | HFRS |
| Europe | | | | |
| | Puumala | *Myodes glareoles* | Cricetidae, arvicolinae | NE |
| | Dobrava – Belgrade | *Apodemius flavicollis*<br>*Apodemus ponticus*<br>*Apodemus agrarius* | Muridae | HFRS |
| | Tula* | *Microtus arvalis* | Cricetidae, arvicolinae | HFRS |
| America | | | | |
| | Sin nombre | *Peromyscus maniculatus* | Cricetidae, sigmodontinae | HPS |
| | Andes | *Oligoryzomys longicaudatus* | Cricetidae, sigmodontinae | HPS |
| | Choclo | *Oligoryzomys fulvescens* | Cricetidae, sigmodontinae | HPS |
| | Laguna Negra | *Calomys callidus*<br>*Calomys laucha* | Cricetidae, sigmodontinae | HPS |
| | Araraquara | *Necromys lasiurus* | Cricetidae, sigmodontinae | HPS |

| | | | |
|---|---|---|---|
| Bayou | *Oryzomys palustris* | Cricetidae, sigmodontinae | HPS |
| Black Creek Canal | *Sigmodon hispidus* | Cricetidae, sigmodontinae | HPS |
| Juquitiba | *Oligoryzomys nigripes* | Cricetidae, sigmodontinae | HPS |
| Monongahela | *Permomyscus leucopus*<br>*Peromyscus maniculatus* | Cricetidae, sigmodontinae | HPS |
| Bermejo | ***Oligoryzomys chocoensis*** | Cricetidae, sigmodontinae | HPS |
| Maciel | ***Bolomys obscurus*** | Cricetidae, sigmodontinae | HPS |
| Castelo dos Sohonos | ***Oligoryzomys moojeni*** | Cricetidae, sigmodontinae | HPS |
| Anajatuba | *Oligoryzomys fornesi* | Cricetidae, sigmodontinae | HPS |

*possible Tula-associated HFRS case from Switzerland diagnosed by serology, and molecular documented case in an immunocompromised patient from the Czech Republic (Schultze *et al.*, 2002; Zelena *et al.*, 2013)

1993 also saw the first reported cases of HPS from South America, with an outbreak in the Sao Paulo metropolitan area of Brazil. This outbreak was caused by Juquitiba virus, and is one of the most deadly outbreaks of a Hantaviridae species recorded, with a case fatality rate reaching 66 % (Jonsson *et al.*, 2010). Between 1993 and 2009 approximately 1000 HPS cases have been reported from Brazil. Viruses of five different lineages seem to be responsible for most of these: Juquitiba virus, Castelo dos Sonhos virus, Araraquara virus, Laguna Negra virus and Anajatuba virus. By 2013 more than 4000 cases of HPS caused by various hantaviral strains have been reported throughout South America (Kruger *et al.*, 2015). Andes virus (ANDV) is one of the most prominent disease-causing strains in South

America, especially important as a public health concern in Argentina and Chile. In Argentina three lineages of ANDV have been found to circulate in separate regions of endemnicity, whereas in neighboring Chile, a single ANDV strain has been described (Jonsson *et al.*, 2010). A unique feature of ANDV is the evidence of human-to-human transmission (Wells *et al.*, 1997; Padula *et al.*, 1998; Martinez-Valdebenito *et al.*, 2014). No cases of HPS have been reported from Mexico, despite cases occurring both north and south of its borders. There is, however, evidence that the area is endemic, as rodents have been found to harbor both hantavirus- specific antibodies and viral RNA, and seropositivity for Hantavirus infection has been detected in the general population of the Yucutan area (Jonsson *et al.*, 2010).

In July 2014, during an outbreak of an orthohantavirus in Panama, a case of HPS was diagnosed in a British woman returning to Britain after a residential stay in the area. Viral RNA was isolated from a serum sample from the woman, and sequence analysis by RT-PCR confirmed the causative virus to be Choclo virus, the only known orthohantavirus known to circulate in the region (Atkinson *et al.*, 2015).

Though orthohantavirus infection in the Americas is almost exclusively associated with HPS, there does exist reports of HFRS on this continent (Glass *et al.*, 1993). In 2008 a case of HFRS was reported from Maryland, Baltimore. The patient did not report to have travelled outside his residential area, leading to the conclusion of a domestically acquired infection. The etiological agent was identified as SEOV by serological and molecular methods (Woods *et al.*, 2009). In January 2017 a multi-state outbreak of SEOV linked to several rat-breeder sites in the USA was reported by the Center for Disease Control and Prevention. During the course of the outbreak 17 cases of human SEOV infection were laboratory confirmed across 11 states (Updates, no date).

### *1.1.2 Asia*

Hantaan virus (HNTV) was first isolated from the lung tissue of a striped field mouse (A*podemus agrarius*) in 1978 by Lee *et al*, and identified as the etiological agent of a disease known at the time as Korean hemorrhagic fever, outbreaks of which heavily affected UN troops during the Korean War in the 1950s (Lee *et al.*, 1978). Korean hemorrhagic fever is now known as a severe manifestation of HFRS, and HTNV is the major causative agent of the disease in Asia (Zhang *et al.*, 2010). HFRS has been reported in China since 1931, and there are descriptions of HFRS-like disease dating back approximately 1000 years, suggesting that the disease has long been considered a major public health problem. Annually more than 11 000 cases of HFRS are reported in China, caused by HTNV and SEOV. Cases have been reported nationwide, though the vast majority occurs in specific geographic regions. As human populations have become increasingly urban, a link has been made with the observed relative increase in the proportion of milder SEOV- caused HFRS cases compared to severe HTNV- associated cases and the accompanying migration of rats with human activity to urban centers (Zhang *et al.*, 2010). However, definitive data on the causative agent of HFRS in China is limited, as diagnosis relies on immunological testing where cross-reactions between the two strains are common (Zhang *et al.*, 2011). Korea is the second major endemic region for HFRS in Asia, and in South-Korea 300-400 HRFS cases were reported annually in the time period 2001 - 2008 (Kruger *et al.*, 2015). Since the early 1990's both China and Korea have made use of inactivated orthohantavirus vaccines as preventive control measures. In Korea Hantavax, a formalin inactivated HTNV vaccine derived from mouse brain tissue, has been used, while in China four inactivated vaccines targeting HNTV or HTNV and SEOV have been introduced (Sohn *et al.*, 2001; Zhang *et al.*, 2010). There seems to have been a trend towards a decrease in cases following the implementation of vaccination programs but public health education, rodent control and

improved living conditions are all measures that have certainly also contributed substantially to lowering the incidence of HFRS (Zhang *et al.*, 2010).

In the Asian parts of Russia, HRFS is caused by the same species of orthohantavirus as those found in China and Korea. The incidence of HFRS is higher in the European regions of the county, but the associated mortality rates are highest in the Far East (Lokugamage *et al.*, 2002; Garanina *et al.*, 2009). Thailand virus is a genetically unique rat-borne orthohantavirus carried by the bandicoot rat (*Bandicota indica*). Presence of Thailand virus-specific antibodies have been confirmed in rodents and patients presenting with unknown febrile illnesses in Sri Lanka, Thailand and India (Pattamadilok *et al.*, 2006; Nakamura *et al.*, 2008; Chandy *et al.*, 2009; Gamage *et al.*, 2011).

### *1.1.3 Africa*

2006 marked the first discovery of an orthohantavirus species on the African continent. Sangassou virus was isolated and cultured from an African wood mouse (*Hylomyscus simus*) in Guinea (Klempa *et al.*, 2006, 2012). The detection of a novel hanta-RNA genome was made possible by using a nested PCR-assay (figure 1.6) with highly degenerated primers designed from an alignment of all know nucleotide sequences of the conserved L segment of orthohantavirus genomes. Seroepidemiological investigations were conducted in the area to follow up on the discovery of this novel viral species and provided evidence of human infection by the detection of Sangassou virus-specific antibodies. A seroprevalance of 1.2 % was detected in a population-based survey conducted in Forest Guinea, while a seroprevalence of 4.4 % was detected in a cohort of patients with fever of unknown origin in Sangassou village (Klempa *et al.*, 2010).

### *1.1.4 Europe*

Orthohantaviruses have been found in both rodents and insectivores in Europe, and different species and strains co-circulate in the rodent populations in certain parts of the

continent (Vaheri, Henttonen, *et al.*, 2013). Rodent-borne viruses endemic to Europe are Puumala (PUUV), Dobrava-Belgrade (DOBV), SEOV and Tula (TULV). PUUV and TULV are carried by the bank vole (*Myodes glareolus*) and common vole (*Microtus spp.*) respectively, while DOBV is carried by Apodemus spp.

Cases of HFRS have been widely reported across continental Europe, though there are major regional differences in case numbers and the extent of human exposure. Most cases originate from specific endemic areas. In the period 2010 - 2014 the annual number of reported HFRS cases in the EU/EEA ranged between 2000 – 4000 (European Centre for Disease Control and Prevention, 2016). By including cases reported from Russia the annual incidence increases to more than 10 000 (Heyman *et al.*, 2011). The Nordic countries can be considered to be endemic hotspots, with Finland reporting as much as 70 % of all European HFRS cases, excluding Russia (Vaheri, Henttonen, *et al.*, 2013). In many regions of Europe, though few cases of HFRS are reported, serosurveillance has demonstrated a relatively high level of exposure to orthohantaviruses in the population.

The two viral species responsible for the vast majority of European HFRS cases are PUUV and DOBV. PUUV is the causative agent of a mild form of HFRS known as nephropathia epidemica (NE), a disease known to have occurred in Sweden since the 1930s (Lundkvist and Niklasson, 1992). This is the most common manifestation of orthohantaviral disease in Europe, and the clinical prognosis is generally good. DOBV infections, though less common, generally result in an infection with a far more severe clinical picture, with reported mortality rates as high as 12 % (Vaheri, Henttonen, *et al.*, 2013). DOBV is carried by three different Apodemus species; yellow-necked field mouse (*Apodemius flavicollis*), black sea field mouse (*Apodemus ponticus*) and the striped field mouse (*Apodemus agrarius*). Intriguingly different degrees of virulence are associated with DOBV infections originating from the different carriers. Generally, DOBV-af is associated with severe

disease, DOBV-ap with moderate-severe disease and DOBV-aa[1] with a mild clinical course (Klempa *et al.*, 2013). Though there is overlap between the geographic distributions of DOBV strains, DOBV-af infection is most prevalent in the Balkan states and southeastern parts of Europe, DOBV-aa occurs most frequently in central Europe and DOBV-ap is predominantly present in the European and Russian areas surrounding the Black Sea.

### *1.1.5 British Isles*

With no genetic confirmation of the viral genome in rodent populations, and only a handful of reported human clinical cases (table 2), orthohantaviruses have historically not been considered enzootic to the British Isles. However, growing evidence of viral exposure has been obtained through serosurveillance studies conducted over the past 30 years, by detection of hantavirus-specific antibodies in both humans and rodents (Pether and Lloyd, 1993; McKenna *et al.*, 1994; Webster and Macdonald, 1995; McCaughey *et al.*, 1996; Coleman, 2000; McCaughey and Hart, 2000). In 2013, a study conducted in the Yorkshire region reported a 7.6 % seroprevalence of orthohantavirus-specific IgG antibodies among a selected group of subjects expected to be at higher risk of acquiring an infection than the general population due to occupational exposure (Jameson *et al.*, 2014). The observed prevalence of this study was comparable to levels found in other known endemic regions of Europe (Vaheri, Henttonen *et al*. 2013).

[1] The taxonomic relationship between Saarema virus and DOBV has been much contested, with some groups considering them separate viral species and some considering Saarema virus a DOBV strain (i.e. DOBV-aa) (Plyusnin *et al.*, 2006). In 2016 Saarema virus was removed as a separate genus of the Hantaviridae by the ICTV, who have instructed it should be considered a DOBV strain.

**Table 2. Published cases of domestically acquired orthohantavirus infection in the UK prior to 2012**

| Year | Location | Source | # cases | Strain | Diagnositic modality | Reference |
|---|---|---|---|---|---|---|
| 1977 | Research laboratory, UK | Wistar rat (r. norvegicus) immunocytomas | 4* | HNTV/SEOV | IFA | (Lloyd and Jones, 1986) |
| 1983 | Scotland | Unknown | 1 | HNTV or related | IFA | (Walker *et al.*, 1985) |
| 1988 | Glasgow | Unknown | 1 | Unknown | IFA | (Kudesia *et al.*, 1988) |
| 1991 | Somerset | Unknown | 1 | Unknown | IFA | (Pether *et al.*, 1991) |
| 1991 | Somerset | Unknown | 1 | - | IFA | (Phillips *et al.*, 1991) |
| 1991 | Somerset | Unknown | 1 | Unknown | IFA | (Pether *et al.*, 1993) |
| 1992 | Somerset | Unknown | 25** | Unknown | IFA | (Pether and Lloyd, 1993) |

*Laboratory-acquired infection. **11-month study

In the current decade three novel orthohantaviral species have been isolated from rodents in the UK (Jameson, Logue, *et al.*, 2013; Jameson, Taori, *et al.*, 2013; Pounder *et al.*, 2013). In 2012 SEOV was detected in wild caught brown rats in the north-eastern region of England (Jameson, Logue *et al*. 2013). The investigation followed a case of severe acute kidney injury (AKI) in a patient from Yorkshire and the Humber, whom on serological testing presented with rising titers of orthohantavirus-reactive IgG antibodies. Phylogenetic studies

of the S and M genomic segments isolated from two rodents caught at the patient's place of residence showed that the virus clustered closely with a previously described SEOV strain, IR146, a strain associated with laboratory-acquired SEOV infections in the UK and Belgium (Lloyd and Jones, 1986). The isolation of the Humber strain confirmed, for the first time, the presence of an orthohantavirus in wild rodents in the UK. Not long after this initial discovery another case of AKI resulted in the detection of a related, yet genetically distinct SEOV among a colony of fancy pet agouti rats (*Rattus norvegicus*) (Jameson, Taori *et al*. 2013). The virus strain was named Cherwell. In addition to the original patient, two of three additional individuals that had been in contact with these rats were seropositive for hantavirus specific IgG antibodies, and one of them had been hospitalized some years earlier with an undiagnosed viral illness characterized by AKI and thrombocytopenia, both symptoms associated with HFRS. In a subsequent case of AKI in a pet rat owner in 2014, a partial viral sequence was recoverable form the patient's serum that exhibited 100 % homology to the Cherwell strain (Duggan *et al.*, 2017). Since these initial findings a further eight cases of HFRS with domestic origin have been diagnostically confirmed by the Rare and Imported Pathogens Laboratory (RIPL), Porton Down (table 3). In Sweden, SEOV was recently detected in a pedigree pet rat imported from England. Phylogenetic analysis revealed that the virus did not cluster with either of the newly described British strains, but with Belgium895, a strain previously isolated from wild rats in Belgium (Heyman *et al.*, 2009; Lundkvist *et al.*, 2013).

**Table 3. Cases of domestically acquired orthohantavirus infections diagnosed by RIPL 2012-2015**

| Year | Age | Sex | Renal failure | Animal exposure | Species (titre) | Reference |
|---|---|---|---|---|---|---|
| 2015 | 53 | M | | Rats | SEOV (1:1000) | RIPL |
| 2015 | 22 | M | | Reptiles and rodents | SEOV (1:100) | RIPL |
| 2015 | 20 | M | + | Rats | SEOV/HNTV (1:10000) | RIPL |
| 2015 | 28 | F | + | Rats | SEOV/HNTV (1:1000) | RIPL |
| 2014 | 10 | F | + | Rats | SEOV/HNTV (1:3200) | RIPL |
| 2014 | 41 | M | + | Rats | SEOV/HNTV (1:10000) | RIPL |
| 2013 | 11 | F | | Rats | HNTV (1:3200) | RIPL |
| 2013 | 20 | M | + | | SEOV/HNTV (1:10000) | RIPL |
| 2012 | 28 | M | + | Rats | SEOV (1:10000) | RIPL |
| 2012 | 59 | M | + | Rats | SEOV (1:10000) | RIPL |

In addition to the above mentioned SEOV strains, a virus clustering with the Arvicolinae-associated orthohantavirus species was recently isolated form a single field vole (*Micortus agrestis*) in Cheshire in north western England (Pounder *et al.*, 2013).The virus was named Tatenale, and subsequently a similar, but genetically distinct orthohantavirus, was found to be endemic in a field vole population in the Kielder Forest at the English - Scottish border (Thomason *et al.*, 2017). The pathogenic potential to humans of these viruses remain unknown, as no cases of human disease have been associated with them.

The Arvicolinae-associated orthoantaviruses include the NE-causing PUUV species and TULV. Interestingly, in the mid 80's, serosurveillance studies conducted in the UK reported a high prevalence of what was considered PUUV-specific antibodies, though without neutralization assays to verify, a determination of the specific viral species cannot be ascertained from these results (McCaughey and Hart 2000). In central and eastern Europe vole populations carry the Arvicolinae-associated TULV. The species is generally considered to be non-pathogenic, but there exists serological documentation of subclinical human infection, and there are reports of TULV–associated HFRS cases from Switzerland and the Czech Republic (table 1) (Schultze *et al.*, 2002; Heyman *et al.*, 2011; Zelena *et al.*, 2013).

## *1.2 Genomic structure and viral life cycle*

As is characteristic for Bunyaviruses, the Hantaviridae harbour a tri-segmented negative-sense, single-stranded RNA genome. The size of the total genome ranges from approx. 11, 8 kb to 12, 3 kb depending on the viral species. The three genomic segments are descriptively named small (S), medium (M) and large (L) based on their size, and each carries an open-reading frame that codes for the viral nucleoprotein (N), glycoprotein precursor (GCP) and RNA-dependent RNA-polymerase (RdRp) respectively. The open reading frames are flanked by non-transcribed regions at the 3' and 5' ends (Hepojoki, Strandin *et al*. 2012). The terminal nucleotides of the non-transcribed regions are complementary and highly conserved among orthohantaviruses; *3'AUCAUCAUCUG* (Meyer and Schmaljohn, 2000; Hussein *et al.*, 2011). Through hydrogen bonding between the 3' and 5' termini the viral RNA forms panhandle structures (Mir *et al.*, 2006). These structures are hypothesized to act as promoters, supported by observations that terminal deletions in the genomic segments correlate with decreased viral replication in persistently infected cell cultures (Meyer and Schmaljohn, 2000).

### *1.2.1 L segment*

With approximately 2150 amino acid residues, and with a molecular mass of about 250 kDa, the RdRp is the largest of the orthohantaviral proteins (Kukkonen *et al.*, 2005). The role of the RdRp is to copy negative-sense viral RNA into positive-sense mRNA and complementary RNA intermediates for protein synthesis and genome replication respectively. The RdRp is a highly conserved protein, not only among the Hantaviridae, but all viruses harboring RNA genomes, and sequence comparisons of the RNA polymerase of RNA viruses indicate that certain amino acids are essential for expression of a functional polymerase (figure 1.2)

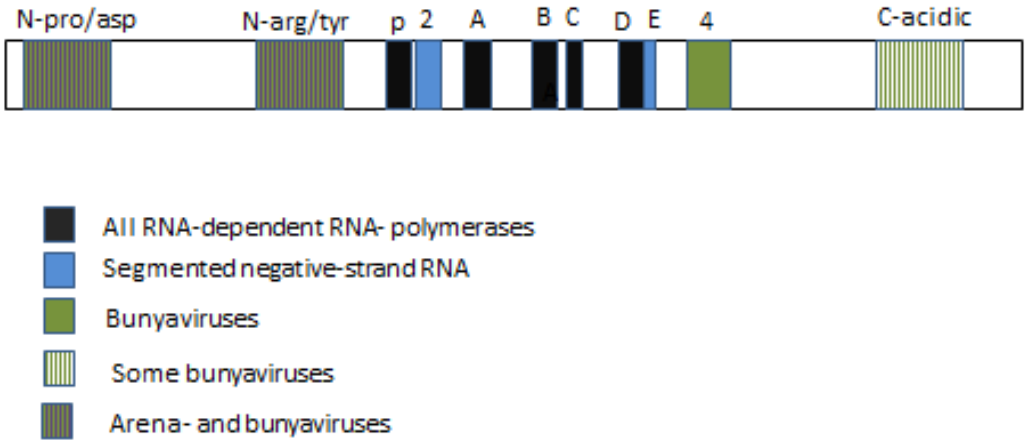


Figure 1.2 Schematic of conserved domains in ORF of Orthohantavirus L segment, adapted from (Kukkonen *et al.*, 2005). The color code shows which domains are also conserved among other RNA viruses. Domain A and C are centered on conserved aspartates, B a conserved glycine and D a conserved lysine. p (pre-motif A) contains a conserved lysine and two arginines. 2 indicate two conserved residues, a glutamate and lysine, located between p and A. 4 contains three conserved glycines and one tyrosine. The N-terminal conserved domains contain two conserved residues each, and the C-terminal conserved domain contains acidic residues. ORF; open reading frame.

### *1.2.2 M segment*

The GCP polypeptide, encoded by the M segment open reading frame, is not observed in infected cells, but is co-translationally cleaved by the cellular signal peptidase complex to the mature viral glycoproteins Gn and Gc (figure 1.3). These correlate to the amino terminus and carboxyl terminus of the GCP respectively, and the cleavage products have approximate sizes of 650 and 490 amino acid residues (Hepojoki, Strandin *et al*. 2012). The signal sequence WAASA has been experimentally demonstrated to be the cleavage site of the HTNV GCP (Lober *et al.*, 2001). This motif is highly conserved among orthohantaviruses, and it adheres to specific sequence rules required for localization to and cleavage of cellular proteins at the endoplasmic reticulum (ER) membrane (Lober *et al.*, 2001). This has marked it as a good candidate for a putative shared cleavage site of the Hantaviridae family. Gn and

Gc form hetero-oligomers, and their co-expression seems to be a necessity for exit from the ER, and translocation to the Golgi (Hepojoki, Strandin *et al*. 2012). The orthohantaviral glycoproteins have a high frequency of cysteine residues in their amino acid sequence (4-7 %), which gives them a propensity for forming disulfide bridges (Hussein *et al.*, 2011). Disulfide bridges are molecular structures important for protein folding and maintenance of their tertiary structure outside of the cytoplasm.

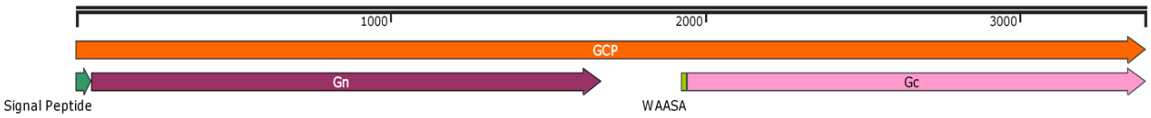


Figure 1.3. Schematic of the SEOV Cherwell GCP, created with SnapGene© Viewer using the Cherwell SEOV M segment sequence (3399bp). The SP (signal peptide) and WAASA sequences indicate cleavage sites within the GCP. Gn and Gc are the mature viral glycoproteins and correlate to the amino terminus and carboxyl terminus of the GCP respectively. GCP; glycoprotein precursor.

The Hantaviridae glycoproteins are modified by N-linked glycans, all of which are endoglycosidase H sensitive, identifying them as high-mannose type glycans (Shi and Elliott, 2004). This particular modification takes place at the cis-Golgi. N-glycans are commonly found attached to a nitrogen atom of an asparagine (Asn) residue which is present as part of the signal sequence Asn-X-Thr/Ser, where X is not a proline, threonine (Thr) or serine (Ser). By detecting this signal sequence it is possible to predict sites were N-linked glycans are likely to be present on a protein. Sequence analysis of the M segment open reading frame has revealed four conserved N-glycosylation sites for orthohantaviruses. On HTNV these are mapped to; Asn134, Asn347 and Asn399 on Gn, and Asn928 on Gc (Hepojoki *et al.*, 2012). Utilizing site-directed mutagenesis it has been demonstrated that all of the conserved sites carry functional N-glycans on HTNV and PUUV(Johansson *et al.*, 2004; Shi

and Elliott, 2004). In addition, a fifth N-glycosylation site specific for HTNV was identified on Gn at position Asn235 (Shi and Elliott, 2004). For PUUV, the presence of an O-glycan was identified on Gc at position Thr984 (Johansson *et al.*, 2004). Introduction of mutation at the conserved N-glycan sites has dramatic effects on glycoproteins function, affecting the intracellular trafficking of the proteins, their ability to properly fold and form heterodimers, and impairs their antigenic properties (Shi and Elliott, 2004).

The viral genome is contained within a particle that consists of a lipid envelope covered by spikes that protrude 10-12 nm from the surface. These spikes are made up of Gn:Gc hetero-oligomers (Cifuentes-Munoz *et al.*, 2014). Ultrastructural analysis of HNTV and TULV by cryo-electron tomography has made it possible to elucidate the surface structure of the virions (Huiskonen *et al.*, 2010; Battisti *et al.*, 2011). These analyses have revealed square shaped surface spike-complexes exhibiting four-fold symmetry. Molecular mass estimations of these complexes correspond to the presence of four copies each of the Gn and Gc subunits. Some differences in spike densities between HTNV and TULV have been noted, but whether this represents an actual difference in the organization of the spike complexes, or are artifacts caused by the experimental procedure remains undetermined (Cifuentes-Munoz *et al.*, 2014).

Members of the Bunyaviridae lack matrix proteins, proteins that for several other enveloped negative-sense RNA viruses are necessary for the interaction of envelope glycoproteins and ribonucleoproteins within the viral particle, facilitating assembly and budding of virions (Timmins *et al.*, 2004). It has been suggested that the Gn and Gc of orthohantaviruses act as surrogate matrix proteins, as they have ribonucleoprotein-binding abilities, and the Gn cytoplasmic tail (GnCT) harbours a YxxL sequence (figure 1.3), a sequence resembling the so called late domain sequences found in matrix proteins

(Hepojoki *et al.*, 2010; Wang *et al.*, 2010; Strandin *et al.*, 2013). In matrix proteins these sequences are responsible for recruiting host cell factors to the sites of viral budding.

### *1.2.3 S segment*

The N protein is an un-glycosylated protein of about 430 amino acid residues, and with an approximate molecular mass of 50kDA (Hepojoki *et al.*, 2012). Some viral species, specifically those carried by Cricetidae rodents, encode an additional non-structural protein in the S segment that overlaps the N protein open reading frame by +1 nucleotide (Jaaskelainen *et al.*, 2007). The function of this protein remains to be fully elucidated, though the non-structural proteins of PUUV and TULV have been demonstrated to act as weak antagonists of interferon (IFN) induction in fibroblasts (Jaaskelainen *et al.*, 2007). In addition, the non-structural protein of TULV has been shown to interact with ACBD3, a protein involved in the structural maintenance of the Golgi apparatus (Rönnberg *et al.*, 2012)

The N protein is the major structural component of the virus, and the most abundantly expressed protein in both virions and infected cells. Multiple functions have been ascribed to it, due to its interactions with both viral and host cell components (Kaukinen *et al.*, 2005). By binding to viral RNA at the panhandle structure the N protein encapsidates the genomic segments so that they exist as ribonucleoprotein complexes coupled to the RdRp within the virion (Mir *et al.*, 2006; Hepojoki *et al.*, 2012). The N protein is also able to bind cellular 5'mRNA caps and protect these from degradation, implicating it in the process of cap-snatching (Mir *et al.*, 2008, 2010). This tactic is used by several RNA viruses and entails the use of cellular 5' methylated-mRNA-caps as primers for the viral RdRp to initiate transcription (Decroly *et al.*, 2011). Additionally, the N protein has been shown to be capable of functioning as an initiation factor for viral translation by replacing and taking on the function of the eukaryotic cellular initiation complex eIF4F (Mir and Panganiban, 2008).

### *1.2.4 The viral life cycle*

An important function of orthohantaviral surface glycoproteins is to mediate the interaction between the virion and cell membrane through specific binding to cell surface receptors. Several putative receptors have been identified through *in vitro* studies though none have been definitely validated in *in vivo* infection. Several lines of evidence point to integrins as essential cellular receptors for viral entry. It has been demonstrated that orthohantaviruses enter human endothelial cells by binding to β3-integrins, and transfection of unpermissive cells with human recombinant β3-integrins render them susceptible to infection (Gavrilovskaya *et al.*, 1998, 1999; Mou *et al.*, 2006). A specific domain of the β3-integrin subunit was identified as a possible binding site for orthohantaviruses (Raymond *et al.*, 2005; Bondu *et al.*, 2017). Interestingly Prospect Hill Virus, which is a non-pathogenic orthohantavirus, does not utilize the β3-integrin receptor for cell entry, but requires the presence of β1-integrin (Gavrilovskaya *et al.*, 1998, 1999). The utilization by pathogenic and nonpathogenic viruses of different receptors, along with the role of β3-integrins in regulation of the vasculature, has led to speculations about the contribution integrins have as viral receptors in the pathogenesis of HFRS and HPS (Gavrilovskaya, Gorbunova *et al*. 2008, Wang, Zhang *et al*. 2012) CD55/DAF, a regulatory protein of the complement system, has also been demonstrated to facilitate viral infection by HTNV and PUUV, and SNV binds to this receptor with high affinity (Krautkramer and Zeier 2008, Buranda, Wu *et al.* 2010). A second protein involved in the complement system, gC1qR, was also shown to facilitate the entry of HTNV in human lung epithelial cells (Choi, Kwon *et al*. 2008). Likely, more than one receptor is involved *in vivo*, and other factors might also contribute. Depletion of cholesterol from lipid rafts in the plasma membrane lowers the susceptibility of cells to HTNV and ANDV infection (Krautkramer and Zeier 2008, Cifuentes-Munoz, Darlix *et al*. 2010).

The most common mode of cellular entry for orthohantaviruses seems to be by clathrin-mediated endocytosis, which has been demonstrated for HNTV, SEOV and Black Creek Canal virus (BCCV) (Jin *et al.*, 2002; Ramanathan *et al.*, 2007; Ramanathan and Jonsson, 2008). Intriguingly, ANDV does not rely on clathrin-mediated endocytosis to enter VeroE6 cells, but can use this mechanism to infect HMVEC-L cells (Ramanathan and Jonsson, 2008; Chiang *et al.*, 2016). In both VeroE6 cells and HMVEC-L cells, ANDV could also enter cells by an uncharacterised clathrin-independent endocytic mechanism. This suggests that ANDV, possibly uniquely among orhtohantaviruses, has the ability to utilize different mechanisms for cellular entry depending on the target cell. Once in the cell the virus traffics along the endocytic pathway, before escaping into the cytosol by low-pH-mediated fusion of the virion with the host-cell membrane (Jin *et al.*, 2002; Buranda *et al.*, 2013). Gc of ANDV has been identified as a class II fusion protein, placing it in the same structural category as Gc of other Bunyaviruses (Garry and Garry, 2004; Plassmeyer *et al.*, 2005; Tischler *et al.*, 2005; Cifuentes-Munoz *et al.*, 2011; Halldorsson *et al.*, 2016). A pH of 4.0 - 5.8 is necessary to trigger the fusogenic activity of Gc, a pH-range indicative of the virus probably reaching late endosomes (pH 4.9-6.0) before it is released into the cytosol (Ogino *et al.*, 2004; Cifuentes-Munoz *et al.*, 2011; Huotari and Helenius, 2011; Acuna *et al.*, 2015). Trafficking to late endosomes is further supported by observations that shortly following infection HNTV localises with the late endosomal/lysosome marker LAMP-1 and UV-inactivated SNV localises with and activates the GTPase Rab7, also associated with late endosomes (Jin *et al.*, 2002; Buranda *et al.*, 2013).

Intact cytoskeletal structures are essential for orthohantaviruses to complete their life-cycle (Ramanathan *et al.*, 2007; Ramanathan and Jonsson, 2008). Both old and new world orthohantaviruses require actin for efficient entry, as demonstrated by an inability of representatives of both species to replicate in permissive cells treated with an inhibitor or actin polymerisation one hour pre-infection. Seemingly however, only new world viruses

continue to require actin at later time points in the viral life cycle. ANDV seems especially reliant on an intact actin network, with loss of actin integrity almost completely inhibiting viral replication. BCCV, also a new world virus, experienced a 50 % reduction in viral yield under the same circumstances. The effect of disrupting actin at three hours and 12 hours post-infection with HNTV or SEOV was, on the other hand, negligible. The latter two viruses were conversely dependent on an intact microtubule network at these later time points, and while new world orthohantavirus replication was also negatively affected by microtubule dissociation, this was to a far lesser extent than for HNTV and SEOV.

The specific sites of orthohantaviral assembly and budding are currently under investigation. Several lines of evidence point to the Golgi complex as the main site of viral maturation. The glycoproteins accumulate and are retained in the Golgi complex when both Gn and Gc are expressed together or during viral infection, and budding of virions is observed there (Goldsmith *et al.*, 1995; Shi and Elliott, 2002; Kariwa *et al.*, 2003; Spiropoulou *et al.*, 2003; Deyde *et al.*, 2005). The timing of glycoprotein accumulation in the Golgi coincides with the time infectious viral particles are detectable in cell culture, and treatment of orthohantavirus infected cells with Brefeldin A, an antiviral compound that inhibits the transport of proteins from the ER to Golgi, inhibits viral replication (Kariwa *et al.*, 2003; Ramanathan *et al.*, 2007; Ramanathan and Jonsson, 2008). Orthohantaviral N proteins are transported to the ER-to-Golgi intermediate compartment (ERGIC) following infection, and the integrity of this complex seems to be essential for viral replication (Ramanathan *et al.*, 2007; Ramanathan and Jonsson, 2008). ANDV Gc, and to a lesser extent SNV Gc, can co-precipitate ERGIC-53, indicating a possible association of the glycoproteins with the ERGIC as well (Klaus *et al.*, 2013). Golgi maturation is considered a hallmark of Bunyaviruses and is the site of maturation for for Rift Valley Fever virus, Bunyamwera virus, Crimean-Congo Haemorrhagic Fever virus and Uukuniemi virus (Jäntti *et al.*, 1997; Haferkamp *et al.*, 2005; Novoa *et al.*, 2005; Carnec *et al.*, 2014). However, assembly of

orthohantaviral glycoproteins and viral budding has also been reported to occur at the plasma membrane, with ANDV, SNV, BCCV and HTNV glycoproteins having been observed to aggregate there at late stages post-infection or –transfection (Spiropoulou *et al.*, 2003; Ogino *et al.*, 2004; Xu *et al.*, 2007; Cifuentes-Munoz *et al.*, 2011). Viral budding at the plasma membrane has been observed for SNV and BCCV (Goldsmith *et al.*, 1995; Ravkov *et al.*, 1997). Even budding of virions at the rough ER has been reported for a species of HNTV (Xu *et al.*, 2007). These discrepancies in cellular trafficking and sites of maturation could be due to the use of different cell lines; HNTV glycoproteins do not assemble at the plasma membrane in P388D1 cells, but in VeroE6 and BHK cells, and SNV does not accumulate at the plasma membrane in NRK cells. The latter observation could, however, be a consequence of the timing of investigation rather than the cell line used. In the study, NRK cells were only monitored at 12 hours post transfection due to cytotoxic effects of the vaccinia expression system used (Spiropoulou *et al.*, 2003). As such it is possible to speculate that many studies have not observed glycoproteins at the plasma membrane because cells have not been monitored at late enough time-points for glycoprotein accumulation there. It is also possible that the sites of assembly are species-specific, or that orthohantaviruses can assemble at multiple sites in the cell.

## *1.3. Clinical course*

Clinically orthohantavirus infections generally manifest as HFRS in Eurasia and HPS in the Americas. Both syndromes primarily affect blood vessels and are characterized by altered barrier functions of the vascular endothelium, causing systemic vascular leakage. The major difference between the two syndromes is the primary afflicted organ. In HFRS this is the kidneys, whereas in HPS the lungs are targeted (Jonsson *et al.*, 2010). Though the primary target organs differ, HFRS and HPS are both generalized infections with multi-organ involvement. Cardiopulmonary and neurological complications have been noted in NE, and pulmonary oedema in severe HTNV infection is not uncommon (Mustonen et al. 2013; Du et al. 2014). Though rare, there are reports of renal involvement in cases of HPS from North America, and in South America it has been reported that as many as 50 % of ARAV patients present with raised serum creatinine, indicative of renal dysfunction (Hjelle *et al.*, 1996; Passaro *et al.*, 2001; Campos *et al.*, 2009).

The outcome of infection ranges from subclinical sero-conversion through mild, moderate and severe disease, to death. The infecting viral species is a major determinant of expected disease severity. For HFRS-causing viruses, HTNV and DOBV are associated with severe disease (10% - 15% mortality rate), SEOV with moderate (1% - 5% mortality rate) and PUUV with the mild form known as NE (< 1% mortality rate). This, however, is also subject to variability on a case by case basis, and an individual PUUV case might be severe while a HTNV case can present with a mild clinical course (Jonsson *et al.*, 2010).

The classical course of HFRS is divided into five distinct phases: (1) febrile, (2) hypotensive, (3) oliguric, (4) polyuric, and (5) convalescence. Variations among patients are however common, and this nicely structured division of clinical symptoms can be difficult to spot (Jonsson *et al.*, 2010). It has been noted that cases of SEOV infection display a less obviously staged disease course than HTNV, and this has been proposed to act as a

contributing factor to the relatively higher levels of initial misdiagnosis of SEOV cases (Zhang *et al.*, 2011).

The incubation period for HFRS is generally two – three weeks. The febrile phase that follows is sudden and characterized by development of quite indistinct flu-like symptoms, including fever, headache, backache and nausea. Typical laboratory findings during the hypotensive phase include thrombocytopenia, leukocytosis and increased C-reactive protein levels. The oliguric phase[2] accounts for approximately half of all HFRS related deaths, which is often due to disseminated intravascular coagulation causing multi organ failure or kidney failure. Restoration of renal function occurs during the polyuric phase, which leads on to convalescence and recovery (Jonsson *et al.*, 2010).

The usual incubation period for HPS lasts approximately two weeks. The course of disease progression, as well as laboratory findings, mirrors those of HFRS. A short febrile prodrome characterized by general symptoms of malaise transitions to an often severe, acute disease. Once respiratory symptoms manifest patients often rapidly deteriorate, and respiratory failure and cardiogenic shock ensues (Jonsson *et al.*, 2010).

In addition to variability in severity, the nature of clinical symptoms in both HRFS and HPS cases can differ between patients. Unspecific symptoms other than renal failure or pulmonary insufficiency can often dominate the clinical picture, complicating the diagnostic process (Vaheri *et al.*, 2008). Furthermore, typical laboratory findings in orthohantavirus infections are also symptomatic of other sepsis-causing infections. Leptospirosis is, due to its similar clinical presentation and epidemiology, often a differential diagnosis in cases of orthohantavirus infection (Gamage *et al.*, 2011; Goeijenbier *et al.*, 2014). Leptospirosis is a globally distributed spirochetal zoonosis, with highest associated morbidity rates occurring in tropical areas. It is increasingly being recognized as a cause of undifferentiated febrile

[2] Oliguria is defined as urine output of less than 400 ml / day

illness in these regions (Costa *et al.*, 2015). As is the case for orthohantaviral disease, leptospirosis spans a broad clinical spectrum ranging from a mild self-limiting influenza-like disease through to Weil's disease, which is the most severe manifestation of leptospirosis. Weil's disease is associated with AKI, liver failure and pulmonary haemorrhage (Forbes *et al.*, 2012). In the UK leptospirosis is a rare, but potentially fatal disease. Domestic exposure is predominantly environmental, through contact with bacterially contaminated soil or water during leisure or occupational activities. Asymptomatic rats and small rodents seem to be the main reservoirs of leptospira in the UK, and cases of disease acquired form domestic rats have occurred in this country (Forbes *et al.*, 2012).

## *1.4 Pathogenesis and biomarkers of disease severity*

The pathogenesis of orthohantavirus-induced disease is not fully understood; direct virally- mediated mechanisms, indirect immune-mediated mechanisms and host genetic factors, are all likely to be involved in the highly variable clinical course.

Orthohantaviruses exert no cytopathic effects *in vitro* or *in vivo*, rendering the cause of increased vascular permeability obscure. There is evidence that the virus itself can induce functional changes in infected cells. Alteration in endothelial cell barrier function was demonstrated in human kidney cells infected with HTNV or PUUV, as observed by a redistribution and reduction of ZO-1, a protein marker of cell tight junctions (Krautkramer *et al.*, 2011). Orthohantavirus infection has also been shown to sensitize and prolong the hyper-permeability response of human umbilical vein endothelial cells stimulated with VEGF and low doses of TNF-α, with no discernible effect on cell viability (Niikura *et al.*, 2004; Gavrilovskaya *et al.*, 2008). Furthermore, ANDV and HTNV displayed on endothelial cell surfaces seem to mediate the adherence of quiescent platelets to endothelial cells through binding of β3 integrin (Gavrilovskaya *et al.*, 2010). Microarray analysis of mRNA transcription in endothelial cells following orthohantavirus infection has revealed infection-specific alternations (Geimonen *et al.*, 2002; Khaiboullina *et al.*, 2004). Geimonen *et al* found that one day following infection with the nonpathogenic Prospect Hill several genes were specifically upregulated, whereas the pathogenic strains HTNV and New York-1 virus[3] did not cause notable change in the transcription of the same genes. At a later time point, four days post infection, the number of upregulated genes for all three strains were similar. Interestingly, the early response noted for Prospect Hill virus included several IFN-specific genes (Geimonen *et al.*, 2002). Orthohantavirus growth in cells is reduced by IFN pretreatment or early IFN addition, and it seems that the cytoplasmic tail of Gn of some

[3] New York virus has as of the ICTV report of 2016 on Bunyavirales, been removed as a separate orthohantaviral species. It has been advised it should be considered a strain of SNV.

orthohantaviruses regulates the early induction of IFN, thus permitting viral replication in endothelial cells (Alff *et al.*, 2006). The Gn cytoplasmic tail of PHV does not possess this ability, indicating that early inhibition of cellular IFN responses by Gn plays a role in determining the pathogenic potential of orthohantaviruses (Alff *et al.*, 2006; Matthys *et al.*, 2014). In support of this is the observation that interferon regulatory factor 3 translocation to the nucleus, which is necessary for transcription of type I IFNs, is greatly reduced in cells infected with pathogenic orthohantaviurses as compared to non-pathogenic species (Shim *et al.*, 2011). However, the ability of viruses to regulate early IFN responses does not fully explain why some orthohantaviruses causes human disease and some do not. TULV, also non-pathogenic, is in contrast to PHV capable of both replicating in human endothelial cells and regulating early IFN responses through its GnCT, like pathogenic orthohantaviruses do (Gavrilovskaya *et al.*, 2008; Matthys *et al.*, 2011).

A strong innate immune response is launched in response to orthohantavirus infection, evident as highly elevated serum levels of pro-inflammatory cytokines, such as TNF-α, interleukin (IL)-6, IL-2 and IL-8 in acute infection. As disease progresses towards convalescence the levels of these cytokines fall (Borges *et al.*, 2008; Sadeghi *et al.*, 2011; Korva *et al.*, 2013). Conversely, the anti-inflammatory cytokine TGF-β has the opposite kinetics, with marked increases in the late and convalescent stages of disease compared to acute, and a protective effect has been associated with the expression of this cytokine (Borges *et al.*, 2008; Sadeghi *et al.*, 2011; Korva *et al.*, 2013). In rats and deer mice elevated levels of TGF-β have been implicated in the maintenance of persistent infections (Easterbrook *et al.*, 2007; Schountz *et al.*, 2012). Interestingly, IL-10, another cytokine associated with anti-inflammatory activity, follows the kinetic profile of the above mentioned pro-inflammatory cytokines. It thus seems that any mitigating effect that might be expected in the presence of IL-10 is absent.

Due to their high levels in acute infection, along with their pro-inflammatory effector functions, the role of TNF-α and IL-6 as mediators of pathogenesis, and their utility as prognostic biomarkers, have been investigated. Sadeghi *et al* found higher levels of pro-inflammatory cytokines including IL-6 and TNF-α associated with higher maximum serum creatinine in PUUV infection (Sadeghi *et al.*, 2011). These results corroborated previous findings linking high levels of IL-6 with the severity of AKI measured by serum creatinine levels in NE (Outinen *et al.*, 2010). Takala *et al*, however, did not see the association of systemic inflammation with elevated serum creatinine in PUUV infection, though they did correlate it with other parameters reflecting disease severity (Takala *et al.*, 2000). In a fatal case of HFRS caused by DOBV, persistently elevated levels of TNF-α were highlighted to contrast with the kinetics of this cytokine in patients who recovered (Korva *et al.*, 2013). This study also noted that DOBV patients generally had higher levels of pro-inflammatory cytokines compared to PUUV patients, reflecting a stronger inflammatory response in the generally more severe clinical course of DOBV infections. Both IL-6 and TNF-α were found to be elevated among HPS patients, but only IL-6 seemed to be associated with disease severity, based on the finding that serum levels of IL-6 in two fatal cases were much higher than among survivors (Borges *et al.*, 2008). A genetic polymorphism involved in TNF-α production was later implicated as a genetic risk factor for development of fulminant HPS following ARAV infection. A hyper-secretor variant of the TNF-α allele (TNF-α2), in which a guanine at position -308 is substituted for alanine, was far more frequent among HPS cases (38 %) compared to a group of seroconverted individuals with no reported history of HPS (7 %). Furthermore, the TNF-α2 allele was less frequent among the healthy seroconverted group compared to a seronegative control group. In the latter group the frequency of TNF-a2 heterozygous individuals was similar to that observed among HPS patients (Borges *et al.*, 2010). The study did not detect any link between TNF-α2 and disease severity, in accordance with the authors' previous observations (Borges *et al.*, 2008). The TNF-α2 allele

is in high linkage disequilibrium with the HLA-B8 DRB1*3 haplotype, a HLA haplotype that has been associated with an increased risk of disease development and severe clinical course of NE in Finnish populations (Mustonen *et al.*, 1996; Mäkelä *et al.*, 2002). A trend was noted for TNF-α2 carriers to experience severe NE, however it was found not to be an independent risk factor, and the association was put down to the TNF-α2 polymorphism being a passive component of the extended HLA-B8 DRB1*3 haplotype (Mäkelä *et al.*, 2002).

Analyzing the humoral response during the clinical course has provided conflicting results. High levels of neutralizing antibodies in the acute stage were reported to be protective in SNV infection, as mild disease was associated with high titres and severe with low titres (Bharadwaj *et al.*, 2000). However, Terajima *et al* did not detect any difference in titres of neutralizing antibody between severe and moderate SNV patients (Terajima and Ennis, 2011). On the other extreme of the severity scale, Lindkvist *et al* observed markedly varying levels in antibody titre among NE patients, which did not provide any indication on the severity of the clinical course (Lindkvist *et al.*, 2008). In contrast, Petterson *et al* found low admission IgG titres to correlate with severe NE prognosis (Pettersson *et al.*, 2014). In both these studies the characterization of the humoral response was solely quantitative.

Thrombocytopenia and leukocytosis are both common clinical findings in the early stages of an acute orthohantavirus infection, and both parameters have been suggested to have value as predictive markers for severe kidney injury in NE and HFRS caused by PUUV and HTNV respectively (Rasche *et al.*, 2004; Kim *et al.*, 2007; Libraty *et al.*, 2012; Wang *et al.*, 2013). However, results reporting the causality of thrombocytopenia and leukocytosis with the severity of subsequent AKI are conflicting. Using univariate analysis Rasche *et al* associated an admission platelet count < 60x10^9/L in NE patients with development of subsequent severe AKI and requirement for hemodialysis. With a far lower cut-off value of

< 33x10^9/L, Wang *et al* found thrombocytopenia, especially nadir counts, predictive of AKI among HTNV infected patients. They also noted several other adverse outcomes, including death, to only occur among patients in the < 33x10^9/L group. Librarty *et al*, however, did not associate thrombocytopenia with severity of AKI in NE patients. In contrast, they reported a correlation with maximum leukocyte count, which on average occurred two days before max serum creatinine was reached (Libraty *et al.*, 2012). In HFRS caused by HTNV, Kim *et al* found leukocyte count at admission predictive of development of AKI in the oliguric phase. They noted that the maximum leukocyte count and minimum platelet count were more sensitive markers of oliguric AKI than admission values, but concluded they were not useful as predictive markers as they coincided too closely with the development of oliguria (Kim *et al.*, 2007). The way in which thrombocytopenia and leukocytosis manifest in HFRS means individual measurements are likely to be highly variable and will depend on for example when the patient presents at hospital. Furthermore, the complexity of pathogenesis following orthohantavirus infection means the use of any single biomarker is unlikely to be informative, though combinations of general and specific markers might be useful in both aiding diagnosis and predicting prognosis (Knust *et al.*, 2012). For HFRS, early clinical markers that might aid in identifying patients that are likely to experience kidney failure would be valuable. In addition, as AKI is a complication that can arises from a variety of clinical conditions and effective treatment is reliant on treating the underlying cause, being able to differentiate AKI caused by infection as compared to e.g. diabetes, would be useful for the prompt initiation of appropriate treatment.

## *1.5 Diagnostic methods*

Diagnosis of HFRS and HPS are based on clinical presentation and serological confirmation of infection. Obtaining background information from the patients about e.g. travel history, occupation and leisure activities can be important aids in the diagnostic process, in addition to providing valuable information for surveillance purposes.

The diagnostic methods in use for Hantavirus infection are various serological assays, namely commercial or in-house immunofluorescence assays (IFAs), immunoblots and enzyme immunoassays. These methods are all based on indirect confirmation of infection by the detection of hantavirus-specific IgM and/or IgG in patient sera. In the case of IgG detection, a ≥ four-fold increase in titre from serially obtained samples are required for confirmation of acute infection, as simply the presence of IgG in serum could indicate a previously resolved infection. IFA, based on acetone-fixed hantavirus infected cells, was the first modality in use for diagnosis of HFRS in Europe and Asia (Vaheri *et al.*, 2008). In the case of NE diagnosis by IFA a caveat to the method was the finding that due to the early antibody response and rapid seroconversion, many patients presented with already high, stable levels of IgG in the acute phase, and seroconversion or a ≥ four-fold increase in antibody titres from paired sera was not always possible to demonstrate (Niklasson and Kjelsson, 1988). In an effort to counter these complications, Finnish investigators developed an alternative method for discriminating between acute and previously acquired infections of PUUV. Fluorescence typing is based on a shift in functional affinity of IgG towards viral proteins during the course of infection, which can be visualized by IFA as characteristic fluorescence patterns corresponding to acute or old immunity. A granular staining pattern is associated with acute infection, while diffuse staining develops gradually with old immunity (figure 1.4). This method has allowed for IgG-based diagnosis from a single sample (Hedman *et al.*, 1991; Kallio-Kokko *et al.*, 2001).

Due to the safety aspects involved with handling whole live virus, the diagnostic antigens currently in use are most commonly derived from recombinant DNA methods (Jonsson *et al.*, 2010). Though antibodies targeting all three structural proteins develop in the course of *in vivo* infection the nature of the N-targeted response and characteristics of the N protein makes it highly suitable as a diagnostic tool (Jenison *et al.*, 1994; Yoshimatsu *et al.*, 1996; Kallio-Kokko *et al.*, 2001; Lindkvist *et al.*, 2008). Recombinant N protein produced in various expression systems have been widely applied as diagnostic antigens (table 4) (Wang *et al.*, 1993; Vapalahti *et al.*, 1996; Billecocq *et al.*, 2003; Meisel *et al.*, 2006). It is important to note that the type of expression system used impacts on the antigenicity of the protein being expressed. For instance, if glycosylation is required, an E. coli system should be avoided, as this system is not capable of glycosylation. For orthohantavirus N protein expression, lack of glycosylation is not an issue, as the protein is not glycosylated (Hepojoki *et al.*, 2012). However, some antigenic sites on the N protein are conformation dependent, and protein conformation can also be affected by the expression system. It was observed that linear, group-specific epitopes on the HNTV N protein were recognised equally using both a Baculovirus (insect) and E. coli (bacteria) expression system, however sero-specific antigens on the HNTV N protein were only detected using the Baculovirus system (Yoshimatsu *et al.*, 1996). This discrepancy was likely due to the protein being expressed as a monomer rather than a multimer when using E. coli (Yoshimatsu *et al.*, 1996; Yoshimatsu and Arikawa, 2014). Point-of care tests for PUUV and DOBV/HNTV are commercially available (Reagena, Toivala, Finland). These tests detect N protein-reactive IgM in acute serum, plasma or fingertip blood with sensitivities and specificities > 95 %. Test formats can be species specific or multiparametric, i.e. simultaneous screening for two or more hantavirus species (Hujakka *et al.*, 2001; Lederer *et al.*, 2013). The advantage of the latter approach is removing the risk of missing infections

caused by viruses from across the major phylogenic clusters, which is especially important to consider in areas of co-circulation. It is also useful when diagnosing imported cases where disease is due to a non-endemic species, or in cases of suspected infection in an area where hantavirus-infections are emerging and a local species remains unknown.

In 2012 the European Network for Diagnostics of Imported Viral Diseases organized an external quality assurance of European laboratories performing diagnosis of Hantavirus infection (Escadafal *et al.*, 2012). In all, 27 labs from 20 European countries participated. Laboratories were evaluated on assay sensitivity, i.e. correct detection of IgG and IgM antibodies, and specificity, i.e. identification of the infecting virus. The quality assurance concluded that with regards to sensitivity, there was little qualitative difference between the diagnostic modalities in use. However, it was noted that performance differed between laboratories using the same techniques, highlighting a need for standardization of assay protocols. In the case of specificity, half of the participating laboratories did not include specification of species type as part of their test results, as they only tested for the presence or absence of antibodies.

Identification of the infecting virus type is difficult to achieve by the conventional serological assays, as the immune response in the acute phase targets the highly cross-reactive amino-terminal region of the N protein (Jenison *et al.*, 1994; Yoshimatsu *et al.*, 1996; Lindkvist *et al.*, 2008). Endpoint titration, i.e. determination of the reciprocal of the highest serial dilution that retains measurable antibody activity, can be informative for differentiating orthohantaviruses from different phylogenic clusters, though with more closely related species such as SEOV, HTNV and DOBV results often remain indeterminate (table 5) (Lederer *et al.*, 2013).

**Table 4. Expression systems used to produce recombinant N protein for diagnostic application**

| Expression system | Antigen | Reactivity | Reference |
|---|---|---|---|
| E. coli | N protein; PUUV, HTNV, SEOV | Rat antisera (isotype not specified) | (Wang *et al.*, 1993) |
| Baculovirus | N protein; PUUV | Human antisera (IgM/IgG) | (Vapalahti *et al.*, 1996) |
| Saccharomyces cerevisiae | N protein; PUUV, DOBV | Human antisera (IgG/IgA) | (Meisel *et al.*, 2006) |
| BHK-21 | N protein; PUUV | Human antisera (IgM/IgG) | (Billecocq *et al.*, 2003) |

**Table 5. 4 sera obtained from a serosurveillance study conducted by Public Health England in the period October 2013 – June 2014* that were positive for hantavirus-specific antibodies by a multiparametric IFA (Euroimmune, Lubeck, Germany)**

| Serum no. | 1:100 | | | | | | 1:1000 | | | | | | 1:10,000 | | | | | |
|---|---|---|---|---|---|---|---|---|---|---|---|---|---|---|---|---|---|---|
| | HTNV | PUUV | SEOV | SAAV | DOBV | SNV | HTNV | PUUV | SEOV | SAAV | DOBV | SNV | HTNV | PUUV | SEOV | SAAV | DOBV | SNV |
| RP13000478 | + | - | + | + | ++ | + | - | - | - | - | + | - | - | - | - | - | - | - |
| RP13000571 | ++ | + | +++ | +++ | +++ | ++ | ++ | - | ++ | ++ | + | + | - | - | + | - | - | - |
| RP13000572** | +++ | ++ | +++ | +++ | +++ | +++ | +++ | + | +++ | ++ | + | + | ++ | - | ++ | + | + | - |
| RP13000580 | ++ | - | +++ | + | + | - | + | - | ++ | + | + | - | - | - | + | - | - | - |

* personal correspondence

**The infecting strain could be typed for three of four sera samples based on endpoint reactivity, while sample RP13000572 remained indeterminate at a 1:10,000 dilution.

The most sensitive method, and the gold standard for serotyping of orthohantaviruses, is the neutralisation assay, preferably on sera obtained at least one month post infection, as the neutralising antibody response of acute sera remains cross reactive (Lundkvist *et al.*, 1997). In addition to the necessity of using convalescent blood, the assay is laborious and slow, and must be conducted at biosafety level three facilities making it unsuitable for routine diagnostic use. An attractive alternative to the neutralization assay is the use of vesicular stomatitis virus (VSV) as a vector for the expression of the orthohantavirus glycoproteins. This so-called pseudovirus system consists of a replication-deficient VSV core, in which the VSV envelope glycoprotein has been replaced with a fluorescent reporter protein (VSVΔG). This system efficiently incorporates envelope proteins of foreign viruses (Ogino *et al.*, 2003). It has been used to express Gn and Gc of HTNV, SEOV, PUUV and ANDV, and though neutralizing titres generally are somewhat lower, it has produced comparable results in detection of neutralizing antibodies and ability for viral differentiation to the conventional neutralization assay with native virus (Ogino *et al.*, 2003; Ray *et al.*, 2010; Higa *et al.*, 2012). The method is faster and safer than the latter, with results obtained within a few days and circumventing the need for working in a containment laboratory. A proposed strategy for hantavirus diagnosis that is based on an initial screening utilizing the cross-reactive amino-terminal part of the N protein of pathogenic viral species spanning the three major rodent-associated phylogenic clusters, followed by serotyping with truncated N protein antigens retaining the sero-specific carboxyl-termini has been suggested as an alternative to the neutralization assay (Yoshimatsu and Arikawa, 2014).

The level of detectable viremia varies greatly in orthohantavirus infections. Generally, species associated with severe disease lead to higher viral loads and prolonged measurable viremia than do moderate- and mild disease causing species (Korva *et al.*, 2013). The viral

genome is detectable prior to the onset of clinical symptoms and the development of IgM antibodies, and an early high viral load seems to be associated with a severe prognosis (Evander *et al.*, 2007; Ferrés *et al.*, 2007; Korva *et al.*, 2013). In all orthohantavirus infections, viremia declines rapidly with disease progression, and the earlier a clinical sample is obtained the greater the chances are of successfully extracting genetic material (Korva *et al.*, 2013). RT-PCR has been successfully developed for both high and low virulence species, and is a valuable tool for early and rapid detection and identification of the infecting species, as well as providing information on viral load Importantly however, due to the often short and fluctuating levels of viremia seen with hantavirus infections, results of a PCR cannot be considered confirmative in a diagnostic setting and must be used in conjunction with other tests (Schilling *et al.*, 2007; Oldal *et al.*, 2014).

## *1.6 Clinical proteomics*

Proteomics is the study of proteins in a biological system, i.e. using state-of-the-art analytical tools to identify and quantify proteins, determine their structure and function or investigate protein interactions (Van Oudenhove and Devreese, 2013). A proteome can be defined as all expressed proteins, including post-translational modifications, produced by a cell or tissue. Unlike the genome, which remains essentially unchanged over time, the proteome is dynamic, and what is expressed varies depending on the specific condition the cell or tissue is experiencing at the time of investigation. The constituents of a proteome are also location specific, again in contrast to the genome, which is the same in any nucleated cell of an organism (Vizcaion, 2015). The field of clinical proteomics aims to answer questions of clinical significance using proteomic methods.

The plasma proteome comprises the total expressed protein content of blood plasma. This is a highly heterogenic collection of proteins including the classical blood resident proteins that exert their function in plasma, tissue resident proteins that leak into the circulation, and proteins originating from commensal or infecting organisms (Anderson and Anderson, 2002). Plasma is the fluid fraction of whole blood which remains when platelets and red and white blood cells are removed. Plasma is collected in the presence of an anti-coagulant, e.g. ethylenediamineteraacetic acid (EDTA), heparin or citrate to inhibit clotting. When plasma is allowed to clot the liquid fraction remaining is referred to as serum. The content of the serum proteome is comparable to the plasma proteome with the exception of most clotting factors (Issaq *et al.*, 2007). While the majority of the protein content of plasma and serum overlap, a comparison of EDTA plasma, heparin plasma and serum revealed that about 10 % of the total protein of each fraction was unique (Lan *et al.*, 2018). In addition to discrepancies between detectable protein content, the absolute levels of many proteins differ in serum and plasma, and in plasmas collected with different anti-coagulants, from the same individual (Tvedt *et al.*, 2015). It is therefore important that

quantitative comparisons between serum and plasma, or plasma collected using different anti-coagulants, are avoided. Since the turn of the century, through the field of proteomics, thousands of proteins have been detected and identified in blood (Nanjappa *et al.*, 2014). The dynamic range in concentration of the plasma and serum proteomes span more than 10 orders of magnitude between albumin, the most abundant protein, and the rarest proteins that are clinically measurable (Anderson and Anderson 2002). This far exceeds the range that is concurrently measurable by current proteomic methods (Patel *et al.*, 2011). In addition to its large dynamic range, extensive post-translational modifications and intra- and inter-individual variability of proteins contributes to the complexity of the proteomes, making both plasma and serum complicated samples to analyse (Nanjappa *et al.*, 2014). Nonetheless, blood is relatively easy to obtain, in contrast to many other clinical specimens, and it is therefore a very important and much analyzed sample in clinical settings. Combined with the nature of its constituent proteins, this makes blood an attractive, and potentially rich source of biomarkers for various disease states (Zhang *et al.*, 2007). Despite the difficulties faced with proteomic analysis, the ongoing efforts in optimizing workflows, and the identification of several potential plasma and serum biomarkers for a range of pathologies highlights the clinical importance of blood (Bauer *et al.*, 2006; Kumar *et al.*, 2012; Dagonnier *et al.*, 2017). Knowledge of relative and absolute concentrations of blood proteins in clinical samples can prove useful for monitoring and diagnosing disease, and an essential aspect of clinical proteomics is comparing the relative quantity of blood proteins in healthy and diseased conditions (Nanjappa *et al.*, 2014). Proteomics has been used to investigate outcome in HPS caused by SNV. A study identified the protein plasminogen activator inhibitor 1, elevated expression of which is associated with impaired fibrinolytic function and thrombosis, as a potential prognostic marker for fatal outcome (Bondu *et al.*, 2015). Interestingly, the plasminogen activator inhibitor 1 gene has also been linked to disease severity among patients with NE (Laine *et al.*, 2012).

In contrast to other conventional methods for identification and quantification of proteins such as western blot and ELISA, mass spectrometry is a high throughput method that allows for simultaneous quantification and identification of hundreds of proteins in a single experiment, with no need for *a priori* knowledge about specific proteins of interest (Nanjappa *et al.*, 2014). Mass spectrometers measure the molecular weight of a sample, or more specifically, the mass-to-charge (m/z) ratio of charged ions. The basic components of a mass spectrometer are; an ion source that ionizes sample molecules, an analyzer that uses electromagnetic fields to separates ions based on their mass, and a detector that records the presence of ions. The results are plotted as a mass spectrum with m/z on the x-axis and ion intensity on the y-axis, which, when searched against established databases predicts the identity of peptides and proteins in a sample (figure 1.4) (CE *et al.*, 2010).

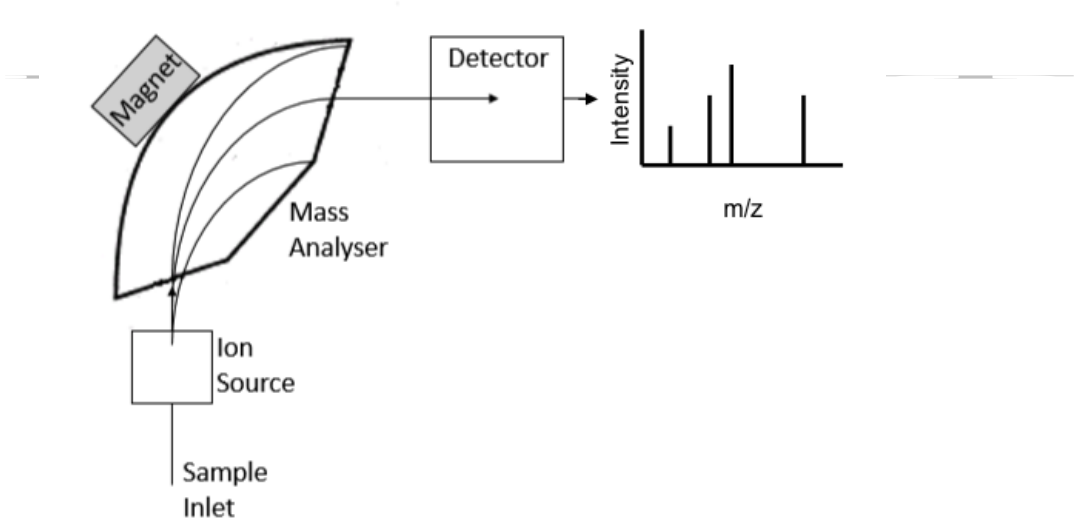


Figure 1.4. The basic components of a mass spectrometer. Figure modified from (theforensicslibrary n.d)

A commonly used strategy of mass spectrometry-based proteomics is the combination of 2D gel electrophoresis and mass spectrometry. With this method, proteins in a biological sample are separated by two gel-based techniques, firstly by charge using isoelectric focusing and secondly by molecular weight using SDS-PAGE. The gel is then stained and

proteins are quantified by determining the staining intensities of selected protein spots. Spots of interest are excised from the gel, digested into peptides, and the protein(s) is/are identified by mass spectrometery. As an alternative to gel-based approaches, gel-free methods can be used. In the latter proteins are directly digested in solution prior to a separation step. The peptides produced by digestion are subsequently separated by liquid chromatography and finally analysed by mass spectrometry ( van Oudenhove *et al* 2013).

Relative quantification of proteins can be achieved using either labelled or label-free strategies. A labelled approach entails labeling samples from different conditions with stable isotopes. This can be achieved either through metabolic labeling, where labels are incorporated into proteins by growing samples on media in which an element has been replaced with its corresponding stable isotope, or through chemical labeling, where, in an additional step following proteolysis, each sample is labeled with an unique isobaric tag. For the label-free approach protein abundance can be determined by spectral counting, a method in which the number of fragment-ion spectra acquired for peptides of a specific protein is counted and compared between samples. Alternatively it can be determined by measurement and comparison of ion intensities, which means comparing the chromatographic peak areas of corresponding peptides from different samples (figure 1.5) (Megger *et al.*, 2013). Both labelled and label-free approaches have been utilized to investigate serum proteome profiles of infectious diseases (Patel *et al.*, 2011; Kumar *et al.*, 2012).

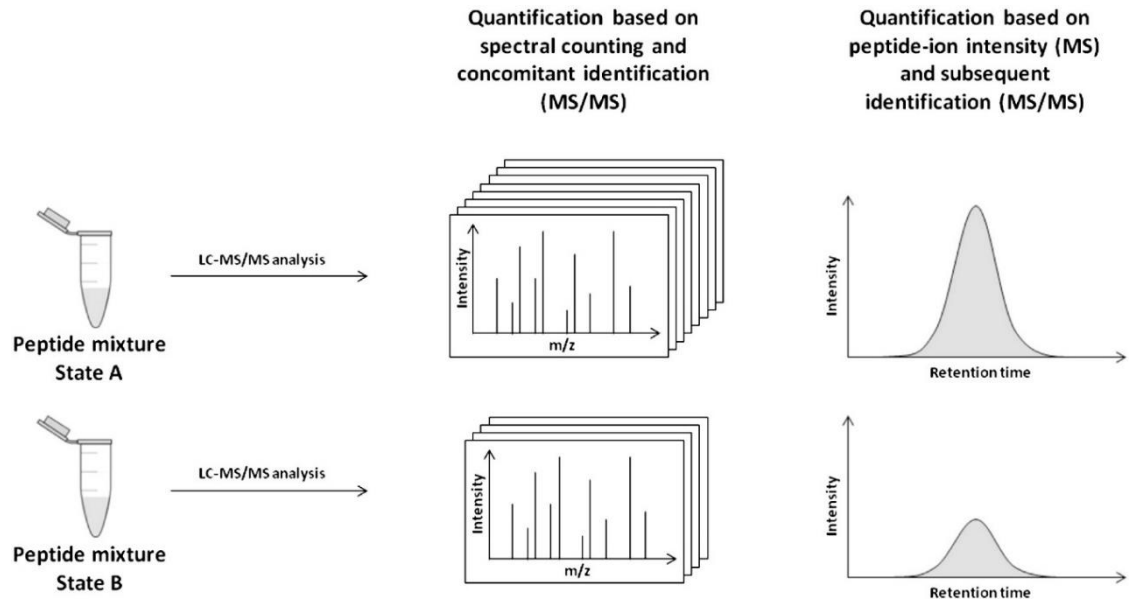


Figure 1.5. Relative quantification of proteins by label-free proteomics based on (left) spectral counting and (right) peptide-ion intensity, reprinted from Biochimica et Biophysica Acta (BBA) - Proteins and Proteomics, Megger et al, Label-free quantification in clinical proteomics, pp: 1581-1590, copyright (2013) with permission for reuse in a thesis/dissertation from Elsevier (license number: 4461341371341) (Megger *et al.*, 2013). With spectral counting the peptide and protein abundance is estimated by the number of acquired peptide spectrum matches, whereas quantification by peptide-ion intensity is achieved by measuring and comparing the chromatographic peak areas of corresponding peptides. In this schematic the protein abundance is highest in state A. MS; mass spectrometry, MS/MS; tandem mass spectrometry.

A major challenge for successful quantitative proteomics analysis is the requirement for reproducibility while performing a multi-step experimental workflow in which there is ample opportunity for introduction of error and bias. The different approaches all have their advantages and limitations. A major advantage of the 2D gel approach is the ability to visualize different isoforms of a protein, however the resolution of the method is relatively low (Lilley, 2015). When comparing label-free and labeled approaches, the depth of proteome coverage achieved by the former is greater. However, as samples are pooled in the latter, the reproducibility of labelled methods are more easily controlled (Li *et al.*, 2012; Megger *et al.*, 2013, 2014). Optimally, though not necessarily practically or financially feasible, using more than one approach would be beneficial, as comparative studies have

shown there to be significant complementarity between methods in regards to both proteins identified and the their relative quantities (Tian *et al.*, 2009; Collier *et al.*, 2011; Merl *et al.*, 2012)

## *Aims*

For this study label-free proteomics was utilized to investigate biomarkers of orthohantavirus infection and HFRS pathology in clinical human sera, and to study the cellular interactome of recombinant SEOV Cherwell glycoproteins in a human kidney cell line.

Biomarkers of infection and pathology were explored by;

1. Directly comparing the proteomes of a group of orthohantavirus-infected sera with non-infected sera to investigate differences in the abundance of specific proteins between the two groups that might be reflective of infection state.
2. Analysing a longitudal set of serum samples from a single individual including a seronegative baseline, samples obtained during active HFRS, and a convalescent sample, to identify proteins with abundance changes that correlate with disease, thus shedding light on mechanisms involved in the pathology of HFRS.

The interactome of SEOV Cherwell glycoproteins was analysed with the aim of discovering host proteins that associate with the viral proteins, thus establishing host factors that could be targeted to disrupt the function of the viral glycoproteins, and in extension inhibit the completion of the viral life-cycle.

.

# *Chapter 2: Materials and methods*

## *2.1 Samples*

### *2.1.1 Ethical approval*

Ethical approval for use of residual diagnostic sera of acute orthohantavirus and acute leptospirosis was obtained from the NRESComittee East-Midlands HRA (appendix A).

### *2.1.2 Human serum samples*

All human sera were provided by the Rare and Imported Pathogens Laboratory (RIPL), Public Health England (PHE), Porton Down. As a precautionary procedure all samples were heat-treated at 60 °C for 15 minutes prior to any experimental analysis, so as to inactivate any possible viral residue. Convalescent orthohantavirus samples and orthohantavirus-seronegative samples were surplus sera previously obtained by PHE during a 2013-2014 serosurveillance study done to ascertain the prevalence of orthohantavirus infections in presumed at-risk groups in the UK. Acute orthohantavirus infected samples and acute leptospirosis infected samples were residual archived sera originally received by RIPL for diagnostic purposes.

## *2.2. Immunodepletion of sera using spin columns*

Sera were depleted of the top 12 most highly abundant serum proteins (table 6) using a commercial immunodepletion kit (Pierce™ top 12 abundant protein depletion spin columns (Thermo Fisher Scientific)) according to the manufacturers' protocol. 10µl of sample was added to the depletion spin column and incubated with end-over-end mixing for one hour. The eluate contained the depleted sample in a final volume of 500µl. For each sample a matched undepleted control (crude) was prepared as a 1:50 dilution in a final volume of 500µl $dH_2O$. Processed samples were kept at -80°C until required for downstream analysis.

**Table 6. Proteins depleted by Pierce™ Top 12 Abundant Protein Depletion Spin Columns.**

| Protein |
|---|
| α 1-acid glycoprotein |
| α 1-antitrypsin |
| α 2 -macroglubulin |
| Abumin |
| Apolipoprotien a-I |
| Apolipoprotin A-II |
| Fibrinogen |
| Haptoglobin |
| IgA |
| IgG |
| IgM |
| Transferrin |

## *2.3 BCA procedure for determining protein concentration*

Determination of serum protein concentrations were done by the BCA method, using a commercial kit following the manufacturer's 96 well microplate protocol (Thermo Fisher Scientific). 25µl sample was transferred to each well and mixed with 200µl assay standard reagent (50:1 solution of reagents A: B) and incubated at 37°C for 30 minutes. Samples were measured in duplicate as undiluted (1:50 working concentration), 1:5 and 1:10. Absorbance was measured at 570nm on a microplate reader (TECAN). Bovine serum albumin (BSA) provided in the kit was serially diluted in $H_2O$ and used to make a standard curve ranging from 0 to 2000µg/µl to which the unknown samples could be compared. Protein concentrations were calculated accordingly;

*(([undiluted + undiluted] /2) + ([1:5 + 1:5]/2) + ([1:10+1:10]/2) /3) = X µg/ml.*

## *2.4 SDS-PAGE*

### *2.4.1 SDS electrophoresis*

Each sample was diluted to the appropriate protein concentration for antigen detection in $dH_2O$. Proteins were denatured by addition of 5x SDS buffer to the sample mixture and heat-treated at 95°C for 10 minutes. Samples were then loaded on to a Tris-acrylamide gel of an appropriate acrylamide percentage for the required molecular weight resolution (table 7). The gel was immersed in 1x running buffer (0.25M tris-base / 1.92M glycine / 0.5 % (w/v) SDS), and set to run at 150 V - 200 V, 400mA until optimal resolution of the protein ladder was (Colour protein standard, Broad-range, 11-245 kDa P7712, New England Biolabs) achieved (45 – 90 minutes).

**Table 7. Recipe for tris-acrylamide SDS resolving and stacking gels**

| **Resolving Gel (10 ml)** | | | | | **Stacking Gel (5 ml)** | |
|---|---|---|---|---|---|---|
| **% Gel** | 15% | 12% | 10% | 7.5% | **% Gel** | 5% |
| **30% Acrylamide** | 5 ml | 4 ml | 3.3 ml | 2.5 | **30 % Acrylamide** | 830 µl |
| **1.5M Tris-HCl pH8.8** | 2.5 ml | 2.5ml | 2.5ml | 2.5ml | **1M Tris-HCl pH6.8** | 630 µl |
| **$H_2O$** | 2.3 ml | 3.3 ml | 4 ml | 4.8 ml | **$H_2O$** | 3.4 ml |
| **10% (w/v) SDS** | 100 µl | 100µl | 100µl | 100µl | **10% (w/v) SDS** | 50 µl |
| **10% (w/v) APS** | 100 µl | 100µl | 100µl | 100µl | **10% (w/v) APS** | 50 µl |
| **TEMED** | 10 µl | 10µl | 10µl | 10µl | **TEMED** | 5 µl |
| **Resolution (Protein kDa)** | 10-40 | 20-100 | 30-100 | 25-200 | | |

### *2.4.2 Sypro Ruby whole protein gel stain*

Whole protein visualisation of SDS-PAGE gels were done with SYPRO Ruby protein gel stain (Molecular probes, Invitrogen, cat: S-12000). Following SDS-PAGE the gel was incubated in fix solution (50 % (v/v) methanol / 7 % (v/v) acetic acid) for 2 X 30 minutes at room temperature with shaking. The gel was then incubated in the dark with SYPRO Ruby gel stain overnight at room temperature. The following day the Sypro Ruby gel stain was discarded and the gel was incubated in the dark in wash solution (10 % (v/v) methanol / 7 % (v/v) acetic acid) for 30 minutes at room temperature with shaking. The gel was then rinsed in dd$H_20$ for 2 X 5 minutes. The gel was imaged at 488 nm on the ChemiDoc Touch Imaging System (BioRad), or on a GENEFLASH imager (Syngene bio-imaging).

## *2.5 Western blotting*

### *2.5.1 Semi-dry blot procedure*

PVDF membranes (Immobilon® –P, cat.no; IPVH00010) with 0.45 um pore size, were activated in 100 % methanol for 30 – 60 seconds before being equilibrated in Towbin buffer (25mM tris-base / 192 mM glycine / 20 % (v/v) methanol). Two filter papers and the SDS-PAGE gel itself were also soaked in Towbin buffer. One square of filter paper was placed on the surface of the semi-dry blotter, with the membrane and SDS-PAGE gel placed on top. Finally, the second filter paper was placed on top of the gel, and the sandwich was soaked with Towbin buffer. The transfer was run at: 10V, 400mA, 30 minutes or 30V, 45mA, 90 minutes up to 2 small gels, or 15V, 400mA, 60 minutes for three small gels or one large gel. After transfer the membrane was blocked in 5 % skimmed milk or 10 % skimmed milk for one hour at room temperature with shaking, or subjected to reversible whole protein staining as detailed in section 2.5.3 prior to blocking. Immobilized proteins were detected with the primary antibodies listed in table 9. Primary antibodies were diluted (see table 9 for antibody – specific dilutions) in TBS-T (0.25M Tris-base / 1.5M NaCl / 10 % (v/v) Tween 20). The membranes were incubated with approximately 5ml primary antibody solution overnight at 4°C with shaking. Following primary antibody incubation, the membrane was washed 3 X 5 minutes in TBS-T. Primary antibodies were detected with HRP-conjugated secondary antibodies (table 10) diluted 1:1000 in 5 % skimmed milk TBS-T or 2.5 % skimmed milk TBS-T. The membrane was incubated with the secondary antibody for one hour a room temperature with shaking. Before imaging the membrane was washed 3 X 5 minutes (when using mouse secondary antibody) or 4 X 5 minutes (when using rabbit secondary antibody) in TBS-T. Secondary antibodies were detected using enhanced chemiluminescence (ECL) and visualised on the ChemiDoc Touch Imaging System (BioRad). Relative densities of visualised bands were determined with FIJI (Schindelin *et al.*, 2012; Rueden *et al.*, 2017) or with ImageLab 5.2.1 (BioRad).

### *2.5.2 Dry-blot procedure*

For the dry-blot procedure the Iblot® System (Thermo Fisher Scientific) was used according to the manufacturers' protocol. The iBLOT Transfer Stack (Thermo Fisher Scientific) was assembled on the iBlot gel transfer device, with a Bolt™ 4 %-12% Bis-Tris Plus pre-cast gel (Life Technologies), and pre-soaked filter paper was placed between the bottom and top stacks. The transfer was run at 20V for seven minutes. The nitrocellulose membrane was blocked for one hour with Blotto® (5 % (w/v) non-fat powdered milk / 25mM Tris/ 150mM NaCl / pH 7.4 / 0.01 % Antifoam A / Kathon® anti-microbial agent, Thermo Fisher Scientific) at room temperature with shaking. The membrane was incubated overnight at 4 °C with primary antibody diluted (see table 9 for antibody-specific for dilutions) in TBS-T. Following overnight incubation the membrane was washed 3 X 5 minutes in TBS-T, before being incubate with HRP-conjugated secondary antibody diluted 1:1000 in Blotto®. Following incubation with the secondary antibody the membrane was washed 3 x 5 minutes in TBS-T. The secondary antibody was detected with ECL, and visualised on a G: box (Syngene). Relative densities of visualised bands were determined with FIJI / ImageJ2 (Schindelin *et al.*, 2012; Rueden *et al.*, 2017)or with ImageLab 5.2.1 (BioRad).

### *2.5.3 SYPRO Ruby blot stain*

To determine whole protein intensities, for use as normalisation reference and loading control, blots were reversibly stained with SYPRO Ruby blot stain. After semi-dry transfer the PVDF membrane was allowed to dry completely, before being activated in 100 % methanol for a few seconds. The membrane was then left to incubate in wash solution (10 % methanol (v/v) / 7 % acetic acid (v/v)) for 15 minutes at room temperature. The membrane was rinsed in $dH_20$ 4 X 5 minutes, before being incubated in Sypro Ruby Protein Blot Stain (Bio Rad, cat: 1703127) for 15 minutes at room temperature, in a dark container. The membrane was rinsed in $dH_20$ 3 X 1 minute to remove excess stain, before being

visualised with the ChemiDoc iTouch imaging System at 488 nm. Following visualisation, the semi-dry western blot protocol was continued as detailed in section 2.5.1.

### *2.5.4 Strip-blot procedure*

When probing a membrane for more than one protein, the membrane would be stripped after initial antibody detection using a Chemicon® Blot Restore Membrane Rejuvination Kit (Millipore, cat: 2520) according to the manufacturers' protocol. Following visualisation of the secondary antibody used for the first antibody detection, the membrane was submerged in 10ml blot restore solution A and incubated on a shaker for 10 minutes at room temperature. Solution A was then discarded, and the membrane was submerged in 10ml blot restore solution B and incubated on a shaker for 15 minutes at room temperature. Solution B was discarded, and the blot was blocked for 2 X 5 minutes in 5 % (w/v) skimmed milk TBS-T or 10 % (w/v) skimmed milk TBS-T, with shaking at room temperature. After blocking, the membrane was incubated with 5ml primary antibody at 4°C, overnight with shaking. The membrane was then washed 3 X 5 minutes with TBS-T and incubated one hour with 5ml secondary antibody at room temperature with shaking. The blot was washed 3 or 4 X 5 minutes with TBS-T, before the secondary antibody was detected with ECL, and protein bands were visualised with the ChemiDoc Touch Imager System (Bio-Rad).

## *2.6 ELISA*

Detection and quantitation of galectin-3-binding protein was done using the Human 90K/Mac-2BP Platinum sandwich ELISA (BM234 – Affymetrix eBiosciences) according to the manufactures protocol. Standards, ranging 200.0ng/ml – 12.5ng/ml, were provided ready for use in the kit. All buffers were brought to room temperature before beginning the assay. Samples were diluted 1:100 in the sample diluent (1x) provided in the kit. 100µl standard or sample was added to the wells in duplicate, blank wells contained 100µl sample diluent only. After loading, the plate was incubated at 37°C for 45 minutes without shaking[4]. Following incubation wells were washed four times with the wash buffer (1x) provided in the kit. 100µl HRP-conjugate was then added to each well, and the plate incubated a second time at 37°C for 45 minutes, without shaking. Wells were washed four times and 100µl TMB substrate solution added to all wells. The plate was incubated at room temperature for 15 minutes protected from light. The enzyme reaction was stopped after 15 minutes by adding 100µl Stop solution to each well. Absorbance was measured at 450nm on an Infinite® F50 (Tecan) microplate reader coupled with Magellan™ software, or a GloMax microplate reader (Promega).

[4] OD values obtained without shaking may be lower than indicated in the manufacturers protocol but are still valid.

## *2.7 Mass spectrometry*

The steps described in the following section (section 2.7) were kindly done by Dr. Stuart Armstrong, Department of Infection Biology, Institute of Infection and Global Health, University of Liverpool.

### *2.7.1 Tryptic digestion*

Depleted samples were precipitated by addition of an equal volume of ice-cold 30 % (w/v) trichloroacetic acid in acetone with incubation at 20°C for two hours. Samples were centrifuged at 12,000g for 10 minutes (4$^{o}$C) to pellet proteins. Pellets were washed three times with ice-cold acetone and allowed to air dry. Protein pellets were re-suspended in 50mM ammonium bicarbonate, 0.1 % (w/v) RapiGest SF (Waters). Samples were heated at 80°C for 10 min, reduced with 3mM DTT at 60°C for 10 minutes, cooled, then alkylated with 9mM iodoacetamide (Sigma Aldrich) for 30 minutes (room temperature) protected from light; all steps were performed with intermittent vortex-mixing. Proteomic-grade trypsin (Sigma Aldrich) was added at a protein: trypsin ratio of 50:1 and incubated at 37°C overnight. To remove RapiGest SF, the samples were precipitated using 1% (v/v) trifluoroacetic acid at 37°C for two hours and centrifuged at 12,000g for one hour (4°C).

### *2.7.2 NanoLC MS ESI MS/MS analysis*

Peptides were analysed by on-line nanoflow LC using the Thermo EASY-nLC 1000 LC system (Thermo Fisher Scientific) coupled with Q-Exactive mass spectrometer (Thermo Fisher Scientific). Samples were loaded on a 50cm Easy-Spray column with an internal diameter of 75µm, packed with 2µm $C_{18}$ particles, fused to a silica nano-electrospray emitter (Thermo Fisher Scientific). The column was operated at a constant temperature of 35°C. Chromatography was performed with a buffer system consisting of 0.1 % formic acid (buffer A) and 80 % acetonitrile in 0.1 % formic acid (buffer B). The peptides were separated by a linear gradient of 3.8 % – 50 % buffer B over 157 min at a flow rate of 300nl/min. The

Q-Exactive was operated in data-dependent mode with survey scans acquired at a resolution of 70,000. Up to the top 10 most abundant isotope patterns with charge states +2, +3 and/or +4 from the survey scan were selected with an isolation window of $2.0^{Th}$ and fragmented by higher energy collisional dissociation with normalized collision energies of 30. The maximum ion injection times for the survey scan and the MS/MS scans were 250 and 100ms, respectively, and the ion target value was set to 1E6 for survey scans and 1E4 for the MS/MS scans. Repetitive sequencing of peptides was minimized through dynamic exclusion of the sequenced peptides for 20s.

### *2.7.3 Protein Identification and Quantification*

Thermo RAW files were imported into Progenesis LC–MS (version 4.1, Nonlinear Dynamics). Peaks were picked by the software using default settings and filtered to include only peaks with a charge state between +2 and +7. Spectral data were converted into mgf files with Progenesis LC–MS and exported for peptide identification using the Mascot (version 2.3.02, Matrix Science) search engine. Tandem MS data were searched against translated ORFs from the human genome (Uniprot release 2015_02; 20,367 sequences; 11,398,732 residues) and the Hanta (Seoul) genome (NCBI Refseq 3 sequences; 3,713 residues). The search parameters were as follows: precursor mass tolerance was set to 10 ppm and fragment mass tolerance was set to 0.01Da. Two missed tryptic cleavages were permitted. Carbamidomethylation (cysteine) was set as a fixed modification and oxidation (methionine) set as variable modification. Mascot search results were further validated using the machine learning algorithm Percolator embedded within Mascot. The Mascot decoy database function was utilised and the false discovery rate was <1%, while individual percolator ion scores >13 indicated identity or extensive homology ($p < 0.05$). Mascot search results were imported into Progenesis LC–MS as XML files. Relative quantification using non- conflicting peptides was calculated by Progenesis.

## *2.8 Data analysis*

Abundance was $log_2$-transformed. Proteins were identified based on detection of at least two unique peptides, and differential abundances were considered significant if there was a minimum two-fold difference (1 $log_2$) in abundance between comparative groups, and a q-value < 0.05. For clustering of longitudal mass spectrometry data the software GProX v.1.1.16 (Rigbolt *et al.*, 2011) was used. Parameters for clustering were; minimum fold change ≥ 2, unique peptides ≥ 2 and q-value ≤ 0.05. Functional annotation of identified proteins was done using Gene Ontology (GO) terms. Protein interactions and protein networks were determined using STRING© v.10.5 (Szklarczyk *et al.*, 2017) and Reactome© (Croft *et al.*, no date; Fabregat *et al.*, 2016). Profile contrasting was kindly done by Yongxiang Fang at the Centre for Genomic Research at the University of Liverpool.

## *2.9 Statistical analysis*

Statistical analysis was done using SigmaPlot 13.0 or Excel for Mac 14.7.6. Significance was determined by t-test for parametric and Mann Whitney U test on Ranks for non-parametric parameters. Kruskal-Wallis ANOVA on ranks was used to calculate significance for ELISA (G3BP). Determination of the correlation of protein abundances between individual healthy control samples was determined by calculating the Spearman's Rank Correlation Coefficient. $P < 0.05$ was considered significant findings.

## *2.10 Plasmids*

Vectors containing the full-length M segment of Seoul orthohantavirus, strain Cherwell (GenBank accession; KM948593.1) were produced by GeneArt Gene Synthesis (Invitrogen). The M segment was cloned into an eGFP-N1 plasmid (referred to as eGFP-N1-GCP) and eGFP-C1 (referred to as eGFP-C1-GCP) plasmid with kanamycin resistance. The plasmids were codon optimized for *homo sapiens.*

## *2.11 Large scale preparation of plasmid DNA*

### *2.11.1 Transformation*

Agar plates were prepared containing 50ug/ml of antibiotics by pouring approximately 20 ml pre-prepared agar (32g (w/v) + ref) onto culture plates with kanamycin or ampicillin depending on the specific antibiotic resistance of the plasmid. The plates were left to set at room temperature, and then dried out at 37°C for approximately 30 minutes. Cell cultures for propagating plasmid DNA were set up by adding 2µl plasmid to 50µl competent cells (DH5α™ Competent Cells, Invitrogen, cat: 18265-017) and leaving them to incubate on ice for 30 minutes. The cells were then subjected to a 45 seconds heat-shock at 42°Cs, before being placed on ice for two minutes. 250µl room temperature SOC media (Sigma Aldrich, cat: S1797) was added to each tube and the cells were incubated at 37°C for one hour with shaking (140rpm). Following incubation, 40µl of the cell culture was spread on an agar plate. The plates were incubated overnight at 37°C. A positive control to determine the quality of the competent cells was set up alongside the plasmid DNA, in which 5µl pUC19 was added to 50µl competent cells. Following overnight incubation, the plates were checked for colonies. At this point the plates could be stored at 4°C until further use. From each plate a single colony was picked using a pipette tip and placed in a 50ml Falcon tubes containing 5ml LB Broth with 0.1% (v/v) antibiotics. The tubes were incubated at 37°C with shaking (250rpm) for six – eight hours. 250µl of the pre-culture was then transferred to a 1L

Erlenmeyer tube containing 250ml LB Broth with 0.1% (v/v) antibiotics. The flask was incubated overnight at 37°C with shaking (200 rpm).

### *2.11.2 Maxi-prep*

Following transformation plasmid DNA was extracted using a Qiagen plasmid maxi kit (QIAGEN®, cat: 12162) following the manufacturers' protocol. Overnight bacterial cultures (see section 2.11.1) were harvested by centrifugation at 6000g for 15 minutes at 4°C. The supernatant was discarded and the bacterial pellet re-suspended in 10ml Buffer P1. 10 ml Buffer P2 was then added and the suspension was left to incubate at room temperature for 5 minutes. Following incubation 10 ml chilled Buffer P3 was added and the solution was left to incubate on ice for a further 20 minutes. The solution was centrifuged at 10,000g for one hour at 4°C, and then re-centrifuged for an additional 30 minutes. A QIQGEN-tip was equilibrated by allowing 10ml Buffer QBT to flow through it, before the supernatant of the bacterial suspension was loaded onto the QIAGEN tip and allowed to enter the resin by gravity flow. The QIAGEN tip was then washed two times by adding 30ml Buffer QC and allowing it to move through the resin by gravity flow. Plasmid DNA was eluted by adding 15ml Buffer QF to the Qiagen tip and collecting the eluate in a clean 50ml falcon tube. The DNA was precipitated with 10.5ml isopropanol at room temperature, and centrifuged at 4000g for 75 minutes. The supernatant was discarded, and the DNA pellet washed with 5ml room temperature ethanol (70 % (v/v)), centrifuged again at 4000g for 30 minutes and discarding the subsequent remaining supernatant. The pelleted DNA was left to air-dry for 10 minutes, before being re-dissolved in 300µl cold $dH_20$ (4°C). DNA concentrations were determined on a NanoDrop™ 2000 (Thermo Fisher Scientific), and plasmids were stored at -20°C or -80°C for downstream use.

## *2.12 Restriction digestion*

Agarose gel electrophoresis with SYBR safe staining was used for DNA visualisation and restriction enzyme digestion analysis of plasmid DNA. 1 % (w/v) agarose gels were prepared by melting 1g agarose (AGTC Bioproducts) in 100ml 1x TBE (890mM Tris-borate / 890MM boric acid / 20mM EDTA / pH 8.3). 5µl SYBR safe (Invitrogen, cat.no. S33102) was added to 50ml cooled agarose, and the agarose was poured into a gel-casting tray with a comb and allowed to set. Restriction enzyme reactions for eGFP-C1-GCP and eGPF-N1-GCP were set up as follows:

| Component | Volume |
|---|---|
| $dH_2O$ | To 50 µl |
| 10X CutSmart®(NEB) | 5 µl |
| DNA (1µg/µl) | 1 µl |
| **Mix by pipetting – then add** | |
| Restriction enzyme | 1 µl |
| Final volume | 50 µl |

The restriction enzymes used were; NheI (NEB, cat: R0131S) and BamHI (NEB, cat: R136S) for eGFP-N1-GCP and XhoI (NEB, cat: R0146S) and BamHI for eGFP-C1-GCP. After 1 hour incubation at the enzyme's optimal temperature (37°C for all enzymes used) the reaction was stopped by a 20 minute heat-inactivation step at 65°C. The solution was loaded onto the agarose gel, and run for 100 minutes at 80V and 200mA, or until the loading buffer front reached the end of the gel.

## *2.11 Cell culture*

HEK293T cells (ECCAC) were maintained at 37°C with 5 % $CO_2$. The cells were grown in Dulbecco's modified eagle's medium (DMEM) with 10 % (v/v) foetal bovine serum (FBS) and 1% (v/v) penicillin-streptomycin. The cells were passaged when they reached approximately 90 % confluence, every three - four days.

## *2.12 Calcium phosphate transfection*

HEK293T (ECCAC) cells were seeded 24 hours before transfection in DMEM 10 % FBS without antibiotics. For downstream immunofluorescent staining, cells were seeded in a six well plate in which a cover slip, washed in 70 % ethanol and PBS had been placed (see section 2.15 for immunofluorescent staining procedure). Depending on the scale of the transfection and the size of culture dish/plate used, the amounts of reagents were scaled up or down accordingly (table 8). 24 hours after seeding, the confluency of the cells reached approximately 50 %. 2M CaCl2 and DNA were mixed with $ddH_20$. This was added in a dropwise fashion to a separate tube of 2x HBS. This mixture was left to incubate for 30 minutes at room temperature. The mixture was then added drop by drop onto the cells kept in transfection media. The cells were left to incubate overnight (16- 24 hours) at 37°C with 5 % $CO_2$. Fluorescence microscopy was used to visually determine whether transfections had been successful.

**Table 8. Set-up for calcium phosphate transfections.**

| Format | Relative area | Cells | Culture media | Transfection media | 2X HBS | 2M $CaCl_2$ | DNA |
|---|---|---|---|---|---|---|---|
| **24 well** | 0.25x | $6 \times 10^4$ each well | 500µl | 280µl | 18µl | 2.18µl | 0.36µg |
| **12 well** | 0.5x | $1 \times 10^5$ each well | 1ml | 570µl | 36µl | 4.36µl | 0.71µg |
| **6 well** | 1.2x | $2 \times 10^5$ each well | 2ml | 1.4ml | 86µl | 10.5µl | 1.71µg |
| **10cm** | 7x | $1.25 \times 10^6$ | 10ml | 8ml | 500µl | 61µl | 10µg |
| **T25** | 3x | $5.2 \times 10^5$ | 5ml | 3.4ml | 214µl | 25.8µl | 4.28µg |
| **T75** | 9x | $1.5 \times 10^6$ | 12ml | 10ml | 643µl | 184µl | 12.9µg |
| **T175** | 21x | $3 \times 10^6$ | 30ml | 24ml | 1500µl | 183µl | 30µg |
| **500cm²** | 60x | $8 \times 10^6$ | 100ml | 68ml | 4280µl | 523µl | 86µg |
| **10cm dish** | | $4 \times 10^6$ | 25ml | 25ml | 1280µl | 156.16µl | 25.6µg |

## *2.13 Protein extraction methods*

### *2.13.1 Protein extraction with RIPA buffer (for downstream western blotting)*

Cells were harvested 24 hours after calcium phosphate transfection. The transfection media was discarded from the plate. All wells were gently washed with 1ml PBS to remove traces of media. The PBS was discarded and RIPA buffer (10mM Tris-Cl pH 7.5 / 150mM NaCl / 5mM EDTA / 0.1 % SDS / 1 % Triton X-100 / 1 % Deoxycholate) with 1x Halt Protease Inhibitor (Thermo Fisher Scientific, cat: 78440) was added to each well. Approximately 100µl RIPA with 1x protease inhibitor was added to each well (i.e. sufficient RIPA buffer to cover the wells completely). The plate was left to incubate for 15 minutes on ice. The cells were dissociated from the surface of the well/dish using a cell scraper, and the cells and buffer were transferred to a 1.5ml Eppendorf tube. This tube was centrifuged at 14000g at 4°C for 10 minutes. Following centrifugation the supernatant was transferred to a new 1.5ml Eppendorf tube and stored at –20°C or –80°C until needed for downstream analysis. The pellet was discarded or frozen for downstream western blotting. All reagents and materials used in the procedure were kept on ice throughout.

### *2.13.2 Protein extraction with lysis buffer (for downstream immunoprecipitation and mass spectrometry)*

Cells were harvested 24 hours after calcium phosphate transfection. The cells were dissociated from the dish using a cell scraper. The cells and media were then transferred to a 50ml Falcon tube. The cells were spun down for 10 minutes at 1000g at 4°C. The supernatant was discarded, 10ml ice cold PBS was added on to the pellet, and the cells were spun for 10 minutes at 1000g at 4°C. This was repeated two more times. Following the third wash, the pellet was re-suspended in 200µl Lysis buffer (10mM Tris-CL, pH 7.5 / 150mM NaCl / 0.5mM EDTA / 0.5 % NP-40 / 1x Halt Protease Inhibitor (Thermo Fisher Scientific)). The cells were left to incubate in lysis buffer for 30 minutes on ice. Every 10

minutes during the incubation the solution was pipetted up and down to aid re-suspension of the pellet. After incubation the lysate was transferred from the falcon tube to a 1.5ml Eppendorf tube and spun down for 10 minutes at 14000g at 4°C. The supernatant was transferred to a new Eppendorf tube, and wash/dilution buffer (10mM Tris-Cl pH 7.5 / 150mM NaCl / 0.5mM EDTA) with 1x Halt™ Protease Inhibitor (Thermo Fisher Scientific) was added to make a total volume of 1ml. This was stored at – 80°C until used for the GFP-trap procedure (section 2.14). Before freezing, 50µl of the diluted sample was taken off and used for western blotting. This fraction was considered the 'input' sample.

## *2.14 GFP-Trap*

Following protein extraction with lysis buffer (section 2.13.2), GFP-tagged proteins and proteins bound to GFP-tagged proteins were co-precipitated using GFP-Trap® (Chromotek, cat: gtm-20). 500µl wash/dilution buffer (10mM Tris-Cl pH 7.5 / 150mM NaCl / 0.5mM EDTA) with 1x Halt™ Protease Inhibitor (Thermo Fisher Scientific) was added to Eppendorf tubes. 25µl of GFP-trap beads were then added to the tubes. The beads were washed three times by spinning them down for two minutes at 2500g at 4°C, discarding the supernatant and adding 500µl fresh wash/dilution buffer. Once the beads were washed the lysates obtained from the procedure of extracting proteins for immunoprecipitation (section 2.13.2) were added to the tubes containing the beads, and left to incubate overnight at 4°C with end-over-end mixing. After overnight incubation, the tubes were centrifuged at 2500g for 2 minutes at 4°C, and the supernatant was discarded. The beads were re-suspended in 500µl wash/dilution buffer, centrifuged at 2500g for two minutes at 4°C, and the resulting supernatant was discarded. This was repeated two more times. After the final washing step, 25µl 0.2M glycine pH 2.5 was added onto the beads. The content was left to incubate at room temperature for 10 minutes at 300rpm. They were then centrifuged at 2500g for two minutes at 4°C. Following centrifugation, the supernatant was transferred to a new Eppendorf tube and 2.5µl 1M Tris-base pH 10.4 was added. This step was repeated three more times, so that the final volume of the eluate was 100µl. For down-stream western blotting, 15µl of the eluate was taken off. The remaining eluate was stored at -80°C until it was used in downstream mass spectrometry.

## *2.15 Immunofluorescence staining*

Immunofluorescence staining was done to visualise transfected protein localisation in HEK293T cells. Cells were fixed to cover slips 24 hours following calcium phosphate transfection (section 2.12). The cells were washed three times with 1ml PBS to remove any traces of media. 1ml 4 % paraformaldehyde was then added to each well, and the plates left to incubate at room temperature for 15 minutes. After incubation the paraformaldehyde was removed, and the cells were washed three times with 1ml PBS. Fixed cells could be left long-term in PBS at 4°C or proceed directly to downstream permeabilizing and staining.

To permeabilize cells after fixation, 1ml PBS 0.1 % Triton was added to each well and the plate was left to incubate for 10 minutes at room temperature. The cells were then washed three times with 1ml PBS 0.5 % Tween. After the third wash the cells were incubated in PBS 10 % FBS for one hour at room temperature to block unspecific binding of the primary antibody. After blocking the cells were washed with PBS 0.5 % Tween before 100µl of the primary antibody, diluted PBS 0.5 % Tween with 2 % FBS, was added directly onto the cover slips. The plate was left to incubate in the dark for one hour at room temperature. After incubation the cells were washed three times with PBS 0.5 % Tween before adding 100µl of the secondary antibody, diluted 1:200 in PBS 0.5 % Tween with 2 % FBS, directly onto the cover slips. The plate was again left to incubate in the dark for one hour at room temperature. The cells were again washed three times with 1ml PBS 0.5 % Tween. The cover slips with fixed, stained cells were carefully removed from the wells using forceps, inverted and placed on glass slides spotted with 10µl - 20µl mounting media containing DAPI (Invitrogen) for visualisation of the cell nucleus. Mounted cover slips were sealed with nail varnish and kept at 4°C.

## *2.16 Immunofluorescence microscopy*

The cellular localisation of transfected proteins was visualised and determined using an Axio Imager.M2 microscope (Carl Zeiss Micoscopy GmbH, 2011) coupled with ZEN 2 (blue edition) software, and using a HXP 120 C light source. Images were captured at 20X and 63X magnifications. Channels for capture of blue - (DAPI, excitation at 405 nm, emission at 470nm), green – (GFP, excitation at 488 nm, emission at 510 nm), and red fluorophores (ALEXA 546, excitation at 488 nm / 532 nm, emission at 573 nm, or ALEXA 568, excitation at 568 nm, emission at 603 nm) were selected.

**Table 9. Primary antibodies**

| Target | Vendor | WB dilution | IF dilution | Cat. number |
|---|---|---|---|---|
| **Afamin** | R and D systems | 1:1000 | - | MAB8065 |
| **Albumin** | Sigma Aldrich | 1:10 000 | - | A6684 |
| **Calnexin** | Abcam | - | 1:1000 | Ab22595 |
| **C-reactive protein** | Sigma Aldrich | 1:200 | - | C1688 |
| **GAPDH** | Abcam | 1:2000 | - | Ab8245 |
| **GFP** | Sigma Aldrich | 1:2000 | - | 11814 460 001 |
| **Giantin** | Abcam | - | 1:500 | Ab80864 |
| **TOM70** | Santa Cruz | - | 1:50 | sc26495 |

**Table 10. Secondary antibodies**

| Antigen | Species | Fluorophore | Vendor | Cat. number |
|---|---|---|---|---|
| Rabbit | Donkey | Alexa 546 | Life technologies | A-10040 |
| Mouse | Goat | Alexa 568 | Life technologies | A-11004 |
| Mouse | Goat | - | Sigma Aldrich | A4416 |
| Rabbit | Goat | - | Sigma Aldrich | A6154 |

# *Chapter 3: Discovery and evaluation of afamin as a biomarker of orthohantavirus infection in human sera*

## *3.1 Introduction*

Understanding how orthohantaviruses and similar infections impact humans can be evaluated by the severity of clinical symptoms, but also through changes in the proteome of tissues. Blood is a commonly used tissue for diagnostic purposes, due to its ease of sampling in a clinical setting. Blood can be fractionated depending on how the sample is taken and stored. These fractions include; whole blood, plasma and serum. Plasma is the liquid fraction of blood remaining once blood cells have been removed through centrifugation, while serum, which is very similar in composition to plasma, lacks both blood cells and clotting factors. The constituents of the serum proteome, including serum resident proteins and tissue-derived proteins leaking into the circulation, along with proteins originating from both commensal and infecting organisms, make it an attractive source for the putative detection of biomarkers for various disease states (Anderson and Anderson, 2002; Zhang *et al.*, 2007). Serum biomarkers for various pathological conditions, including stroke, autoimmune disorders and infectious disease, have been investigated, using proteomic methods such as label-free and labelled MS and protein microarrays (Bauer *et al.*, 2006; Kumar *et al.*, 2012; Dagonnier *et al.*, 2017). Proteomics has also been used to investigate factors determining outcome in orthohantavirus infection. In a retrospective analysis of plasma from 14 hantavirus cardiopulmonary syndrome (HPS) patients with serologically proven Sin Nombre virus (SNV) infection, 2D gel electrophoresis coupled with mass spectrometry was used to identify plasminogen activator inhibitor type 1 as a potential prognostic marker of fatal outcome (Bondu *et al.*, 2015). For the study the patients were divided into three classes depending on severity of illness and outcome; class I were patients experiencing mild-moderate disease, (i.e. did not experience

cardiopulmonary failure and did not need mechanical ventilation), class II covered patients who required extracorporeal membrane oxygenation due to cardiac insufficiency and ultimately recovered from illness, while class III patients required extracorporeal membrane oxygenation but had fatal outcomes. Samples from 10 healthy individuals were used as controls. For class I patients, admission day samples were analysed, while for class II and III patients' serial samples for up to five days from admission were examined. Among the fatal cases in the study (n = four, approximately 28 %) the abundance of plasminogen activator inhibitor type 1 was highly elevated imminent to death, as compared to healthy controls (Bondu *et al.*, 2015). Interestingly, a genetic polymorphism in the plasminogen activator inhibitor type 1 gene has also been associated with more severe renal impairment, measured as maximum creatinine levels, in Finnish nephropathia epidemica (NE) patients (Laine *et al.*, 2012) .

Translating proteomic discoveries into clinically viable assays is a long and complex road. Several aspects relating to the study design, sample acquisition, handling and analysis must be carefully considered (Kearney *et al.*, 2018). The initial step of this pipeline is the use of high-throughput methods to analyse proteomes of clinical interest. These discovery phase analyses will usually yield datasets consisting of hundreds of protein hits. Systems biology approaches are therefore used to make an informed selection of candidate biomarkers for further evaluation (Micheel *et al.*, 2012; Kearney *et al.*, 2018). Once a selection is made, the behaviour of candidate biomarkers are verified for consistency in an independent sample cohort. If an independent sample set is not possible to obtain, verification must be done on a subset of the original discovery set. Importantly, if a subset of the original sample cohort is used, this subset should not have been included in the initial analyses (Micheel *et al.*, 2012). When the aim of proteomic research is the development of a clinical assay, the next step of the process is the validation phase, which involves defining the clinical test method, analytical validation of the test and finally biological validation on a blinded sample set. If

the assay is successfully validated at this point, it can be brought to the final stages of evaluation in a clinical trial setting (Micheel *et al.*, 2012). Only a few proteomic assays have so far been introduced (Kearney *et al.*, 2018) PreTRM is a selected reaction monitoring mass spectrometry-based assay, which was approved for use in the USA in 2015. The test has been validated for use in the 19$^{th}$ and 20$^{th}$ week of pregnancy, to predict the risk of spontaneous pre-term birth through evaluating the relative ratio of two proteins; insulin-like growth factor-binding protein 4 and sex hormone-binding globulin (Saade *et al.*, 2016; Kearney *et al.*, 2018). In the field of infectious disease, various biomarker panels have been evaluated for the diagnosis of Hepatitis C virus- induced fibrosis (Castera, 2012; Schiavon *et al.*, 2014). Patented panels available for this indication include FibroTest$^{TM}$ (Biopredictive, France) and ELF$^{TM}$ (iQur, Southampton, UK), two assays that measure a combination of serum proteins to evaluate the degree of fibrotic damage (Poynard *et al.*, 2004, 2007; Rosenberg *et al.*, 2004; Parkes *et al.*, 2010). In practice a combination of non-invasive methods, such as biomarker algorithms complemented by imaging techniques, have produced more accurate results than biomarkers alone for diagnosing fibrosis in Hepatitis C virus (Castera, 2012) Importantly, while the incorporation of non-invasive methods could reduce the need for liver biopsies among Hepatitis C virus patients, which is the current diagnostic gold standard, there are still several caveats to their use in clinical practice, such as their general low accuracy for discriminating early stages of fibrosis, and confounding due to co-morbidities (Castera, 2012; Schiavon *et al.*, 2014).

### *3.1.1 Hypothesis*

SEOV infection causes measurable alterations in the human serum proteome that are indicative of viral infection and renal pathology.

This hypothesis was explored by comparing the proteomes of five orthohantavirus-seropositive (one x acute and four x convalescent) and five orthohantavirus-seronegative serum samples using label free mass spectrometry, to investigate whether there were differences in the abundance of specific proteins between the two groups that might be reflective of infection state.

## *3.2 Results*

### *3.2.1 Establishing an experimental pipeline for detection of serum proteins by label free mass spectrometry in healthy human sera*

The dynamic protein abundance range in serum samples taken for proteomic analysis can span more than ten orders of magnitude between the most abundant protein, which is serum albumin (34-54 mg/ml), and the lowest abundant proteins that are detectable, e.g. cytokines such as interleukin (IL)-6 with an approximate abundance of < 0.000000005 mg/ml in healthy individuals (Anderson and Anderson, 2002; Nanjappa *et al.*, 2014). Additionally, a few highly abundant proteins dominate the bulk mass of blood and these effectively mask detection of lower abundance proteins by proteomic methods. In an effort to increase the depth of coverage of mass spectrometric analysis, sera were depleted of the top 12 most highly abundant proteins as detailed in chapter 2.2 (table 6) using immunodepletion spin coloumns (Thermo Fisher Scientific). Following depletion, the protein concentrations of depleted samples and their undepleted (crude) counterparts were determined by BCA. Two biological and two technical replicates of orthohantavirus seronegative sera were depleted to test the efficiency of the immunodepletion spin columns. After depletion the average decrease in protein concentration from crude to depleted was 91.1 %. As the orthohantavirus infected sera provided by RIPL (see chapter 2.1.2) had been heat-inactivated at 60°C for 15 minutes as a precautionary procedure to inactivate any possible residual virus in the sera, the effect of this treatment on protein quality and detection was investigated on an orthohantavirus seronegative control sample. This sample was split into two equal parts, of which one aliquot was heat-treated as described above and one was left untreated. The samples were then depleted and compared as depleted and crude specimens by BCA, and then whole protein stain of SDS-PAGE separated extracts. Western blot was used to visualise albumin, a high abundance

protein targeted for depletion by the immunodepletion spin columns (see chapter 2.2). Subjecting sera to heat-inactivation did not have any discernible effect on the parameters measured (figure 3.1). After triplicate measurements of depleted and crude sera by BCA, the average protein concentration of the heat-inactivated specimen was 2.38µg/µl before and 0.48µg/µl after depletion. For the specimen that had not been subjected to heat-inactivation the average protein concentrations of crude and depleted sera were 2.27µg/µl and 0.42µg/µl respectively. The percentage decrease in protein content for the heat-inactivated and non-heat-inactivated specimens in depleted compared to crude samples were 79.8 % and 81.5 % respectively.

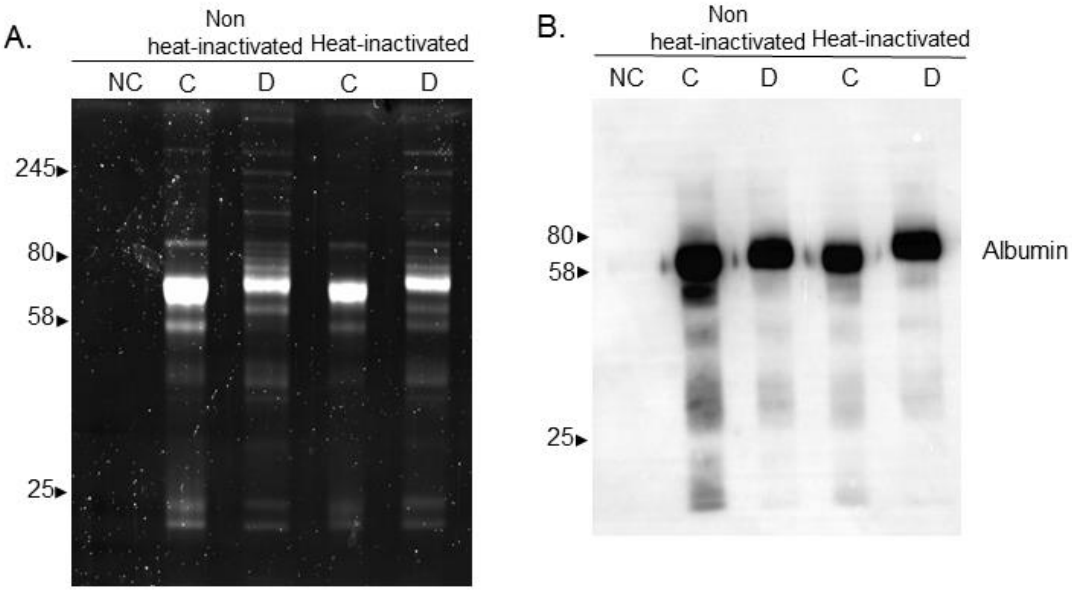


Figure 3.1. **A**, SYPRO ruby stain (whole protein stain) comparing non-heat-inactivated and heat-inactivated sera. **B**, western blot for albumin comparing non-heat inactivated and heat-inactivated sera. 12 ug protein was loaded in each lane. The experiment was repeated three times, and protein concentrations were calculated as the average concentration of three technical replicates. NC; negative control, C; crude, D; depleted.

To determine the baseline variability that could be expected when analysing sera by mass spectrometry and have an indication of the depth of proteome coverage to expect following immunodepletion, two healthy control sera samples were analysed by mass

spectrometry and compared (figure 3.2). In total, 202 proteins were identified across the two samples by mass spectrometry. Following removal of contaminants, i.e. keratins and non-human proteins introduced to the samples through use of upstream experimental reagents containing non-human protein constituents, along with removal of any protein only identified in one of the samples and all proteins identified by < 2 unique peptides, 124 proteins were common to the two samples tested. The label-free quantification (LFQ) intensities, which is a measure of the normalised, summed peptide intensities of identified proteins, were compared for the 124 proteins common to the two samples analysed (Cox *et al.*, 2014). The spearman correlation coefficient (rho= 0.97) between the samples was significant, $p < 0.000$

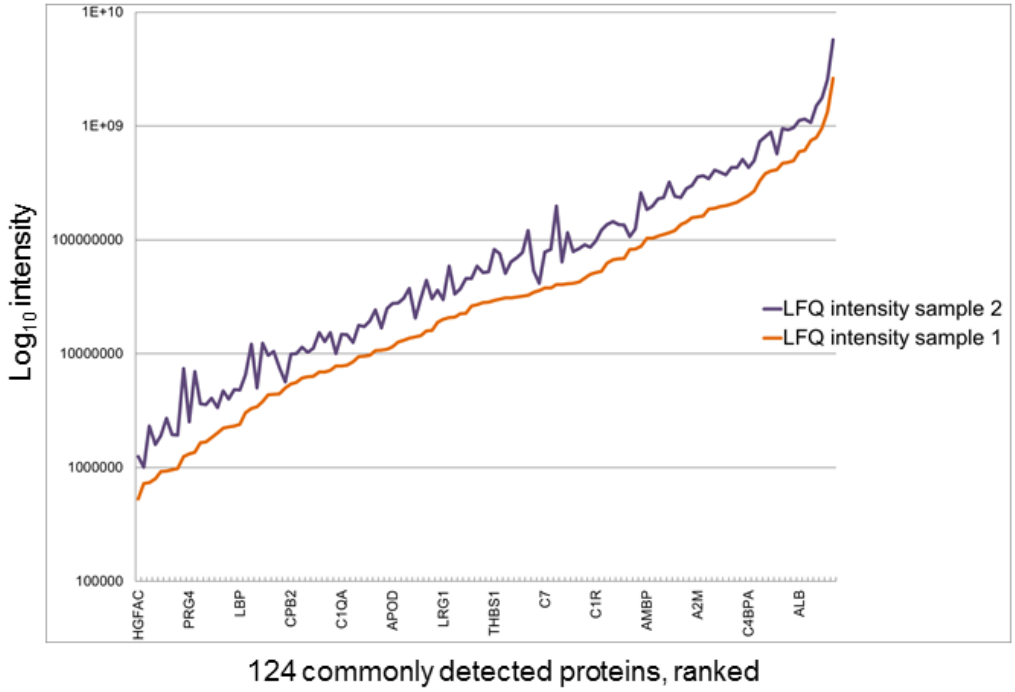


Figure 3.2. Label free quantification (LFQ) intensities for the 124 commonly detected proteins in two healthy (read orthohantavirus seronegative) control samples analyzed by mass spectrometry (sample 1 and sample 2). The Spearman correlation coefficient rho = 0.97 when comparing the LFQ intensities of the two samples. Rho was significant, $p < 0.0001$. Each tick on the x-axis represents one individual protein of the 124 proteins detected in both sample 1 and sample 2, ranked in ascending order of abundance for sample 1 (orange line). Selected proteins are highlighted: hepatocyte growth factor

activator (HGFAC), proteoglycan 4 (PRG4), lipopolysaccharide-binding protein (LBP), carboxypeptidase B2 (CPB2), complement C1q subcomponent subunit A (C1QA), apolipoprotein D (APOD), leucine-rich alpha-2-glycoprotein (LRG1), thrombospondin-1 (THBS1), complement component C7 (C7), complement C1r subcomponent (C1R), protein AMBP (AMBP), alpha-2-macroglobulin (A2M), C4b-binding protein alpha chain (C4BPA), serum albumin (ALB).

### *3.2.2 Preparing orthohantavirus infected samples for proteomic analysis*

With the objective of investigating if a measurable difference in the abundance of specific proteins in orthohantavirus-infected and non-infected sera could be detected, the proteomes of five orthohantavirus seropositive (four x convalescent, one x acute) and five orthohantavirus seronegative controls were compared. Each sample was depleted of the top 12 abundant serum proteins as described in chapter 2.2. The decrease in protein concentrations in individual samples from crude to depleted following immunodepletion ranged from 87.3 % - 96 %. The reduction was visualised by comparing crude and depleted specimens side by side on a SDS gel stained with a whole protein stain (figure 3.3A). To further validate that the process of immunodepletion had the desired effect, western blots were done in which depleted and crude samples were compared side by side for abundance of albumin (normal range: 34-54 g/L) and C-reactive protein (CRP) (normal range: <0.003 g/L). In depleted samples the detectable amount of albumin was reduced compared to crude, while the detectable amount of CRP was enriched in depleted samples as compared to crude (figure 3.3B), indicating that the depletion process enhanced the detection of lower abundance proteins relative to the detection of high abundance proteins.

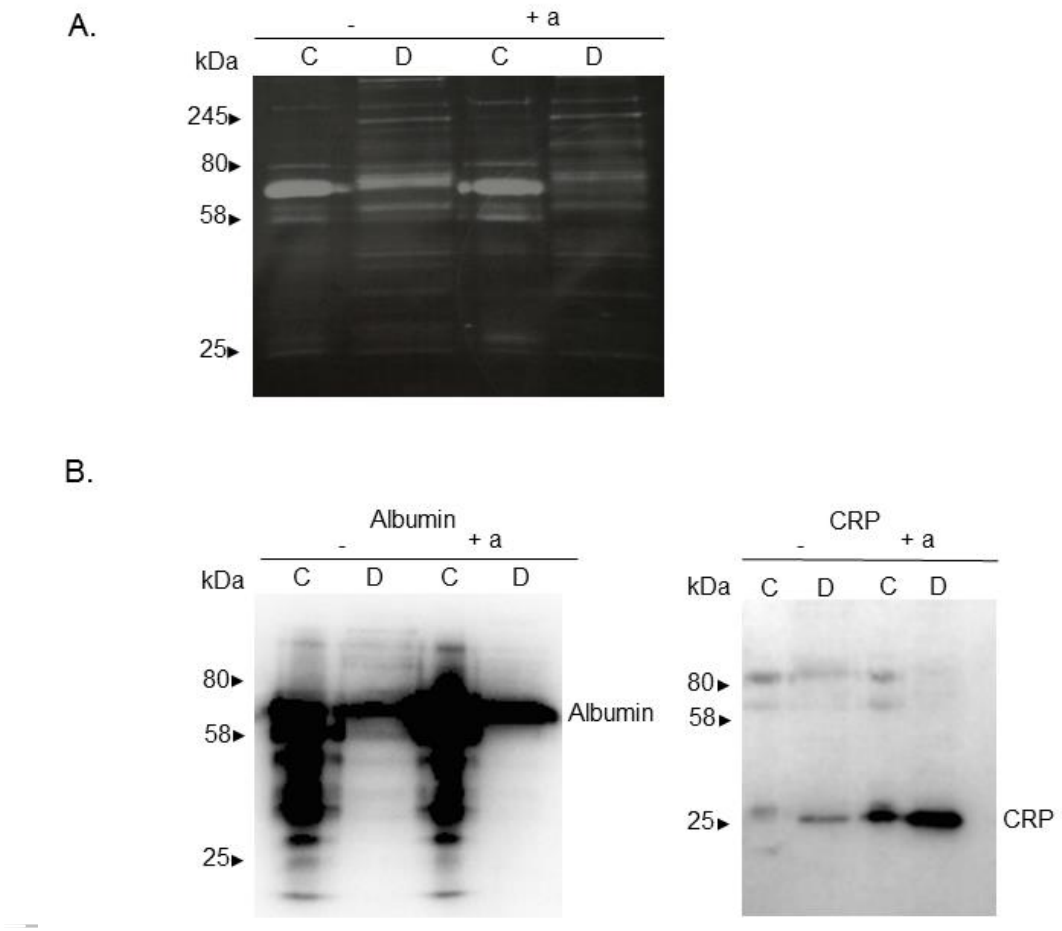


Figure 3.3 Changes in protein abundance before (lane marked C for crude) and after immunodepletion (lane marked D for depleted). The figure shows the crude and depleted specimens of two representative samples; one orthohantavirus seronegative (-) and one orthohantavirus seropositive during acute disease (+a). **A**, changes in protein pattern before and after depletion, visualized with Sypro ruby whole protein gel stain, and **B**, western blot showing reduced detection of albumin and enrichment of CRP in depleted samples compared to crude. 2.5µg protein was loaded per well. CRP; C-reactive protein.

### *3.2.3 Comparing orthohantavirus seronegative and seropositive samples by label-free mass spectrometry*

Following immunodepletion and determination of protein concentrations, the protein content of the samples were determined and quantified by mass spectrometry, as detailed in chapter 2.7. In total, 381 proteins identified by a minimum of two unique peptides were common to all 10 samples analysed (appendix B.1). Using threshold values of $q < 0.05$ and a

minimum fold change of 1 $log_2$, a total of 74 proteins were revealed to be differentially abundant between the two groups (figure 3.4). 20 proteins were increased in abundance in the seropositive group compared to controls and 54 proteins were decreased in abundance in the seropositive group compared to seronegative controls (table 11). Among the 20 proteins with increased abundance, STRING© network analysis (version 10.5) showed enrichment of several biological process gene ontology (GO) terms such as regulation of hydrolase activity, regulation of complement activation, cell adhesion and regulation of angiotensin levels in blood (figure 3.5, table 11). Among the proteins with decreased abundance a large number of immunoglobulin fragments were identified with biological process GO terms relating to complement activation and immune regulation. Most of the Ig-fragments were not recognised by the STRING© software, so GO term annotation was found by searching their UniProt entries. STRING© analysis of the remaining proteins in the decreased abundance group revealed functional associations relating to regulation of body fluid levels, lipid transport, localization and regulation of hydrolase activity (figure 3.5, table 11).

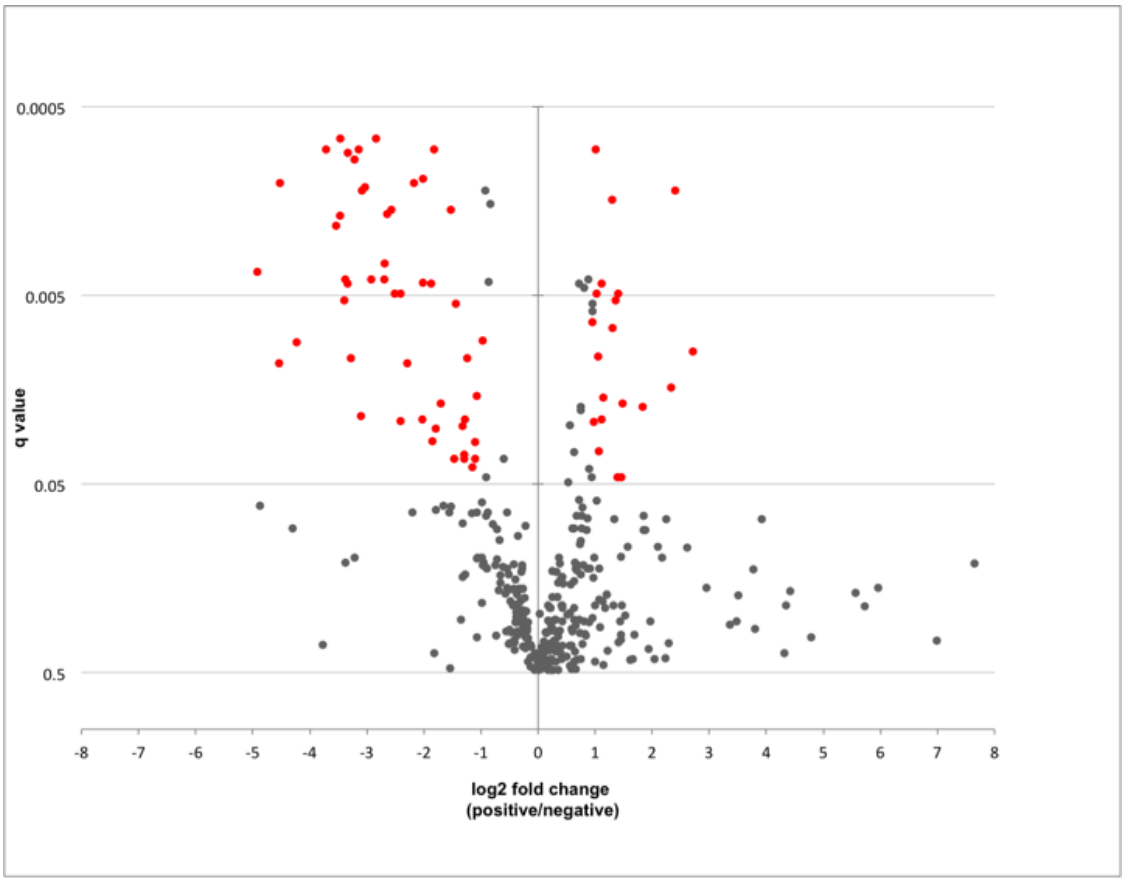


Figure 3.4. Differences in protein abundances between a group of five seropositive samples (four x convalescent and one x acute) and five seronegative controls. Serum proteins were identified and quantified by label-free mass spectrometry using Progenesis. Abundance was expressed as the mean $\log_2$ of positive/negative samples. Proteins were identified based on detection of at least two unique peptides, and significant findings had a minimum fold difference of 1 $\log_2$ in abundance between the positive and negative group and a q-value < 0.05. 74 proteins (highlighted red) were found to be significantly differentially abundant in seropositive samples compared to seronegative controls.

A.

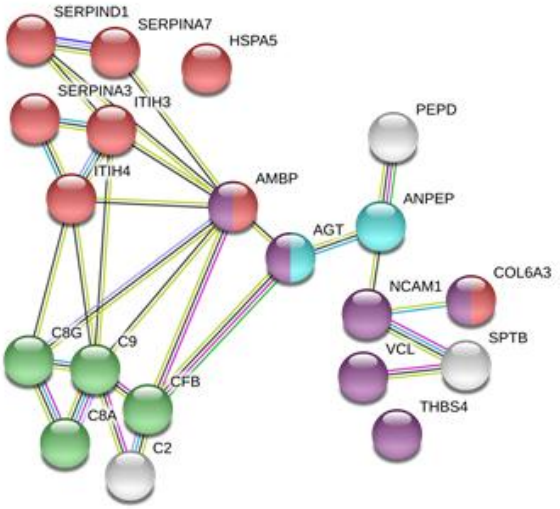


B.

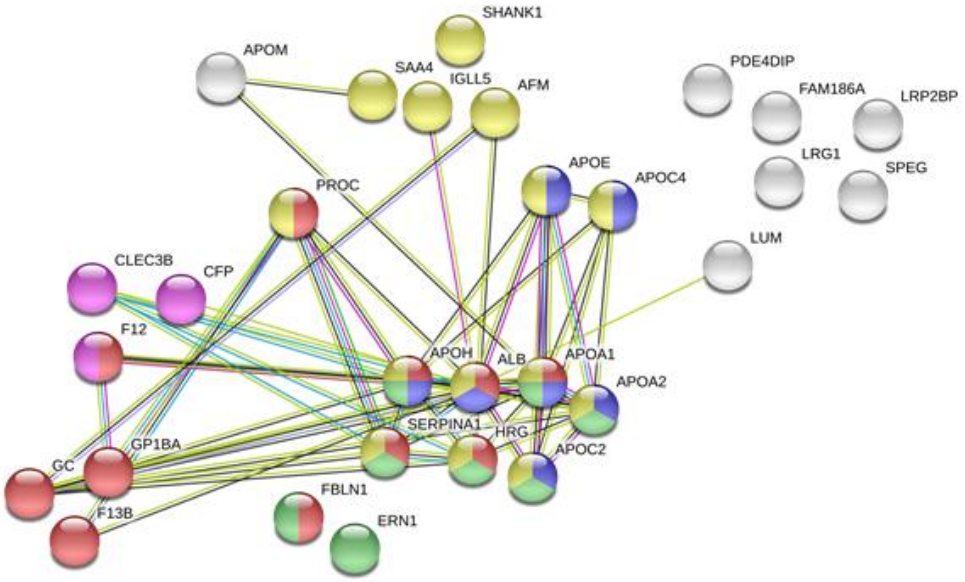


Figure 3.5. STRING© version 10.5 network analysis of 74 proteins with differential abundance in seropositive samples (n = five) compared to seronegative samples (n = five). **A**, 20 proteins with increased abundance in seropositive samples compared to seronegative samples. Green; regulation of complement activation, red; regulation of hydrolase activity, blue; regulation of angiotensin levels in blood, purple; cell adhesion. **B**, 29 proteins with decreased abundance in seropositive samples compared to seronegative samples. Several of the Ig-fragments (see table 11) were not recognised by STRING© and are therefore missing from the protein network. Red; regulation of body fluid levels, blue; lipid transport, green; regulation of hydrolase activity, yellow; localisation.

**Table 11. Proteins with significantly different abundance in the seropositive group compared to the seronegative group.**

| Increased in seropositive | | | | | |
|---|---|---|---|---|---|
| Description | Gene | FC log2 | q value | Accession | GO term |
| Thrombospondin-4 | THBS4 | 2.7 | 0.01 | P35443 | Cell adhesion |
| 78 kDa glucose-regulated protein | HSPA5 | 2.4 | 0.001 | P11021 | Regulation of hydrolase activity |
| Vinculin | VCL | 2.3 | 0.015 | P18206 | Cell adhesion |
| Spectrin beta chain, erythrocytic | SPTB | 1.8 | 0.019 | P11277 | Actin filament capping |
| Aminopeptidase N | ANPEP | 1.5 | 0.019 | P15144 | Regulation of angiotensin levels in blood |
| Xaa-Pro dipeptidase | PEPD | 1.5 | 0.046 | P12955 | Metabolic process |
| Inter-alpha-trypsin inhibitor heavy chain H3 | ITIH3 | 1.4 | 0.005 | Q06033 | Regulation of hydrolase activity |
| Neural cell adhesion molecule 1 | NCAM1 | 1.4 | 0.046 | P13591 | Cell adhesion |
| Complement component C8 gamma chain | C8G | 1.4 | 0.005 | P07360 | Regulation of complement activation |
| Heparin cofactor 2 | SERPIND1 | 1.3 | 0.007 | P05546 | Regulation of hydrolase activity |
| Alpha-1-antichymotrypsin | SERPINA3 | 1.3 | 0.002 | P01011 | Regulation of hydrolase activity |

| | | | | | |
|---|---|---|---|---|---|
| Complement component C8 alpha chain | C8A | 1.1 | 0.017 | P07357 | Regulation of complement activation |
| Complement factor B | CFB | 1.1 | 0.004 | P00751 | Regulation of complement activation |
| Complement component C9 | C9 | 1.1 | 0.022 | P02748 | Regulation of complement activation |
| Angiotensinogen | AGT | 1.1 | 0.034 | P01019 | Regulation of angiotensin levels in blood / cell adhesion |
| Inter-alpha-trypsin inhibitor heavy chain H4 | ITIH4 | 1.1 | 0.011 | Q14624 | Regulation of hydrolase activity |
| Complement C2 | C2 | 1.0 | 0.005 | P06681 | Complement activation |
| Collagen alpha-3(VI) chain | COL6A3 | 1.0 | 0.001 | P12111 | Regulation of hydrolase activity / cell adhesion |
| Protein AMBP | AMBP | 1.0 | 0.023 | P02760 | Regulation of hydrolase activity / Cell adhesion |
| Thyroxine-binding globulin | SERPINA7 | 1.0 | 0.007 | P05543 | Regulation of hydrolase activity |
| Decreased in seropositive | | | | | |
| **Description** | | **FC log2** | **q Value** | **Accession** | **Go term** |
| Ig lambda chain V-II | IGLV2-11 | -4.9 | 3.76E-03 | P01707 | Regulation of |

| | | | | | |
|---|---|---|---|---|---|
| region TRO | | | | | immune response |
| LRP2-binding protein | LRP2BP | -4.5 | 0.011 | Q9P2M1 | Protein binding |
| Ig kappa chain V-III region VH (Fragment) | -* | -4.5 | 0.001 | P04434 | -* |
| Ig kappa chain V-I region CAR | IGKV1-5 | -4.2 | 0.009 | P01596 | Regulation of immune response |
| Ig gamma-2 chain C region | IGHG2 | -4.0 | 0.0002 | P01859 | Complement activation |
| Ig gamma-3 chain C region | IGHG3 | -3.7 | 0.001 | P01860 | Complement activation |
| Platelet glycoprotein Ib alpha chain | GP1BA | -3.5 | 0.002 | P07359 | Regulation of body fluid levels |
| Ig gamma-4 chain C region | IGHG4 | -3.5 | 0.002 | P01861 | Complement activation |
| Afamin | AFM | -3.5 | 0.0007 | P43652 | Localization |
| Properdin | CFP | -3.4 | 0.005 | P27918 | Regulation of protein processing |
| Ig lambda chain V-III region LOI | IGLV3-21 | -3.4 | 0.0002 | P80748 | Regulation of immune response |
| Ig lambda chain V region 4A | IGLV7-43 | -3.4 | 0.004 | P04211 | Regulation of immune response |
| Coagulation factor XIII B chain | F13B | -3.3 | 0.004 | P05160 | Regulation of body fluid levels |
| Immunoglobulin lambda-like polypeptide 5 | IGLL5 | -3.3 | 0.001 | B9A064 | Localization |

| | | | | | |
|---|---|---|---|---|---|
| Ig heavy chain V-II region WAH | IGHV4-39 | -3.3 | 0.011 | P01824 | Regulation of immune response |
| Ig gamma-1 chain C region | IGHG1 | -3.2 | 0.001 | P01857 | Complement activation |
| Ig lambda-7 chain C region | IGLC7 | -3.1 | 0.001 | A0M8Q6 | Regulation of immune response |
| Ig heavy chain V-III region GA | IGHV3-30 | -3.1 | 0.022 | P01769 | Regulation of immune response |
| Ig heavy chain V-III region BUT | IGHV3-53 | -3.1 | 0.001 | P01767 | Regulation of immune response |
| Ig heavy chain V-III region WEA | IGHV3-48 | -3.0 | 0.001 | P01763 | Regulation of immune response |
| Apolipoprotein M | APOM | -3.0 | 0.0005 | O95445 | Lipoprotein metabolic process |
| Ig kappa chain V-III region IARC/BL41 | IGKV3-20 | -2.9 | 0.004 | P06311 | Regulation of immune response |
| Serum amyloid A-4 protein | SAA4 | -2.8 | 0.001 | P35542 | Localization |
| Ig lambda chain V-III region SH | IGLV3-19 | -2.7 | 0.004 | P01714 | Regulation of immune response |
| Ig alpha-2 chain C region | IGHA2 | -2.7 | 0.003 | P01877 | Complement activation |
| Ig alpha-1 chain C region | IGHA1 | -2.6 | 0.002 | P01876 | Complement activation |
| Ig kappa chain C region | IGKC | -2.6 | 0.002 | P01834 | Regulation of immune response |
| Lumican | LUM | -2.6 | 0.0002 | P51884 | Extracellular matrix |

| | | | | | |
|---|---|---|---|---|---|
| | | | | | organization |
| Ig heavy chain V-III region VH26 | IGHV3-23 | -2.5 | 0.005 | P01764 | Regulation of immune response |
| Ig heavy chain V-I region HG3 | IGHV1-46 | -2.4 | 0.005 | P01743 | Regulation of immune response |
| Apolipoprotein C-IV | APOC4 | -2.4 | 0.023 | P55056 | Lipid transport |
| Striated muscle preferentially expressed protein kinase | SPEG | -2.3 | 0.011 | Q15772 | Negative regulation of cell proliferation |
| SH3 and multiple ankyrin repeat domains protein 1 | SHANK1 | -2.2 | 0.001 | Q9Y566 | Localization |
| Serum albumin | ALB | -2.0 | 0.023 | P02768 | Regulatio of body fluid levels / Lipid transport |
| Ig kappa chain V-III region VG (Fragment) | IGKV3-11 | -2.0 | 0.004 | P04433 | Regulation of immune response |
| Apolipoprotein A-II | APOA2 | -2.0 | 0.001 | P02652 | Regulation of hydrolase activity / lipid transport |
| Ig kappa chain V-III region B6 | IGKV3-20 | -1.9 | 0.004 | P01619 | Regulation of immune response |
| Ig kappa chain V-I region HK102 (Fragment) | IGKV1-5 | -1.9 | 0.03 | P01602 | Regulation of immune response |
| Vitamin K-dependent protein C | PROC | -1.8 | 0.001 | P04070 | Regulation of body fluid leves / localization |

| | | | | | |
|---|---|---|---|---|---|
| Serine/threonine-protein kinase/endoribonuclease IRE1 | ERN1 | -1.8 | 0.025 | O75460 | Regulation of hydrolase activity |
| Ig kappa chain V-IV region Len | IGKV4-1 | -1.7 | 0.019 | P01625 | Regulation of immune response |
| Vitamin D-binding protein | GC | -1.5 | 0.002 | P02774 | Regulation of body fluid levels |
| Apolipoprotein C-II | APOC2 | -1.5 | 0.037 | P02655 | Regulation of hydrolase activity / Lipid transport |
| Myomegalin | PDE4DIP | -1.4 | 0.006 | Q5VU43 | Cellular protein-containing complex assembly |
| Apolipoprotein E | APOE | -1.3 | 0.025 | P02649 | Lipid transport |
| Apolipoprotein A-I | APOA1 | -1.3 | 0.035 | P02647 | Regulation of hydrolase activity / Lipid transport / Regulation of body fluid levels |
| Alpha-1-antitrypsin | SERPINA1 | -1.3 | 0.037 | P01009 | Regulation of hydrolase activity / Localization / Regulation of body fluid levels |
| Coagulation factor XII | F12 | -1.3 | 0.023 | P00748 | Regulation of body fluid levels / Regulation of protein |

| | | | | | |
|---|---|---|---|---|---|
| | | | | | processing |
| Beta-2-glycoprotein 1 | APOH | -1.2 | 0.011 | P02749 | Regulation of hydrolase activity / Lipid transport / Regulation of body fluid levels |
| Tetranectin | CLEC3B | -1.2 | 0.041 | P05452 | Regulation of protein processing |
| Leucine-rich alpha-2-glycoprotein | LRG1 | -1.1 | 0.03 | P02750 | Positive regulation of TF-β receptor signalling pathway |
| Fibulin-1 | FBLN1 | -1.1 | 0.037 | P23142 | Regulation of body fluid levels / Regulation of hydrolase activity |
| Protein FAM186A | FAM186A | -1.1 | 0.017 | A6NE01 | - |
| Histidine-rich glycoprotein | HRG | -1.0 | 0.009 | P04196 | Regulation of hydrolase activity / Localization / Regulation of body fluid levels |

*obsolete uniport entry, deleted from the database in 2016

Afamin was identified among the top 10 proteins with decreased abundance in seropositive samples, with a $q < 0.0007$ and a fold change of $\log_2 = -3.5$. Afamin was also highlighted when analysing the mass spectrometry-acquired dataset by a correlation analysis in which the seropositive and seronegative group was contrasted against each other (figure 3.6). It was therefore selected as a protein of interest for further investigation as a potential marker infection.

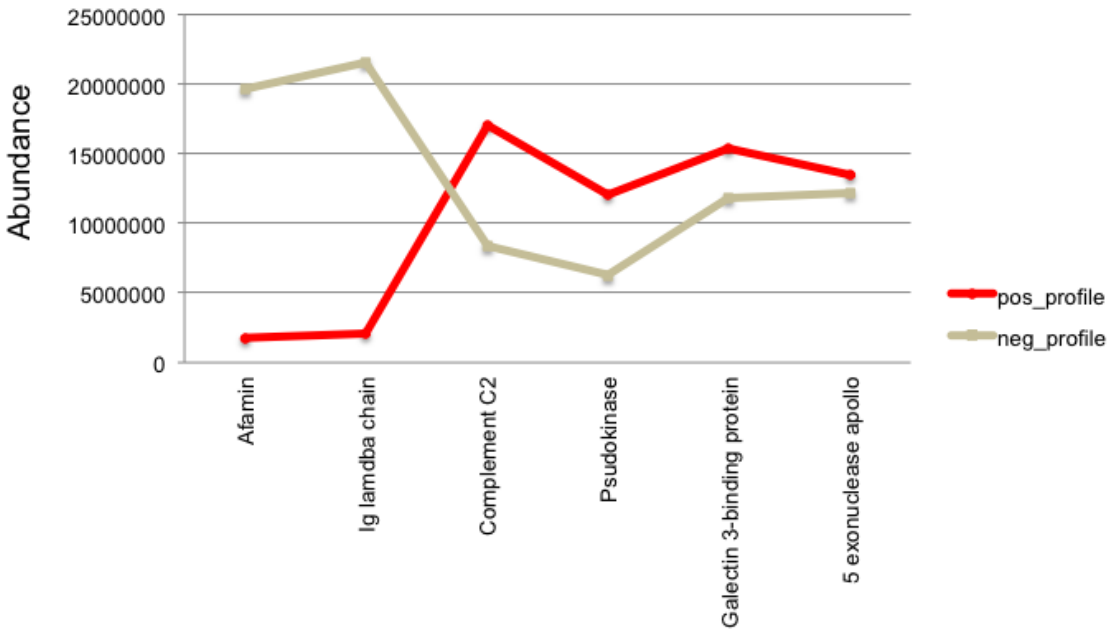


Figure 3.6. Profile contrasting of the seronegative (n = 5, white) and seropositive (n = 5, red) groups in a correlation analysis using raw mass spectrometry data.

To verify that afamin was decreased in the orthohantavirus seropositive samples compared to seronegative controls, a western blot was run probing specifically for the presence of afamin in the samples analysed by mass spectrometry (figure 3.7). The relative intensities (RI) of the bands were determined using the image processing software FIJI. A control sample of pooled seronegative sera was loaded on both gels to act as a reference to which the other samples of interest could be compared (figure 5, lane 1; GR). The average RI of afamin in seropositive samples was 0.56, and the average RI of seronegative was 0.48 (table 12). There was no statistically significant difference between the seropositive and seronegative groups, but notably the single acute disease sample of the seropositive group had the lowest measured relative intensity of all 10 samples investigated, with a RI = 0.10 (table 12, figure 3.7; seropositive lane 6).

**Table 12. Relative intensities of afamin in seropositive and seronegative samples.**

| Seropositive | | Seronegative | |
|---|---|---|---|
| Lane | Relative intensity | Lane | Relative intensity |
| 1 | 1 | 1 | 1 |
| 2 | 0.54 | 2 | 0.20 |
| 3 | 0.65 | 3 | 0.80 |
| 4 | 0.68 | 4 | 0.41 |
| 5 | 0.40 | 5 | 0.16 |
| 6 | 0.10 | 6 | 0.32 |
| **Average** | **0.56** | **Average** | **0.48** |

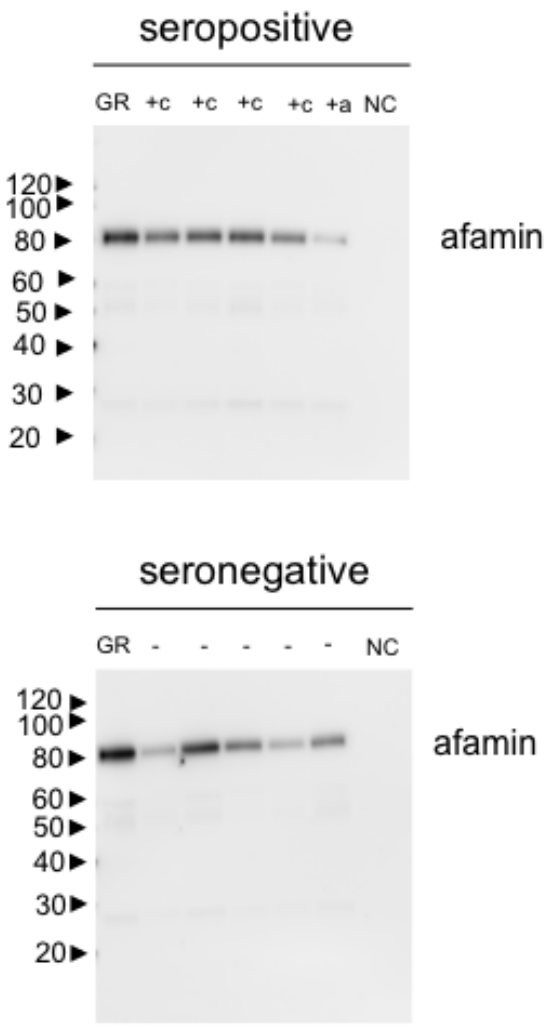


Figure 3.7. Verification of mass spectrometry and profile contrasting results for afamin by western blotting. 5µg protein was loaded per well. All samples were analyzed crude. GR; gel reference (a pool of 5 independent seronegative samples). For analysis of relative intensities across gels this band was arbitrarily set to a value of 1. NC; negative control (loading buffer only). - ; seronegative, +c ; seropositive convalescent, +a; seropositive acute.

### *3.2.4 Afamin abundance in patients with acute orthohantavirus infection compared to healthy controls*

A described above, western blotting indicated that the abundance of afamin was lowest in the single acute disease sample in the discovery cohort. Furthermore, the fold change for afamin remained above the set threshold level for significance when disregarding the seropositive convalescent samples and only comparing the seropositive acute sample to the seronegative controls, $\log_2 = -4.3$. It was therefore deemed appropriate to not follow up in convalescent samples, but only to consider acute disease samples compared to orthohantavirus-seronegative controls for the validation phase. To validate whether afamin was consistently decreased in acute orthohantavirus infection compared to healthy controls, an independent cohort of eight seronegative and eight acute disease samples were investigated for relative abundance of this protein by western blot (figure 3.8A). The median abundance of afamin in the seropositive group (median = 0.137) versus the seronegative groups (median = 0.181) was not found to be statistically significant in this cohort, $p < 0.463$ (figure 3.8B).

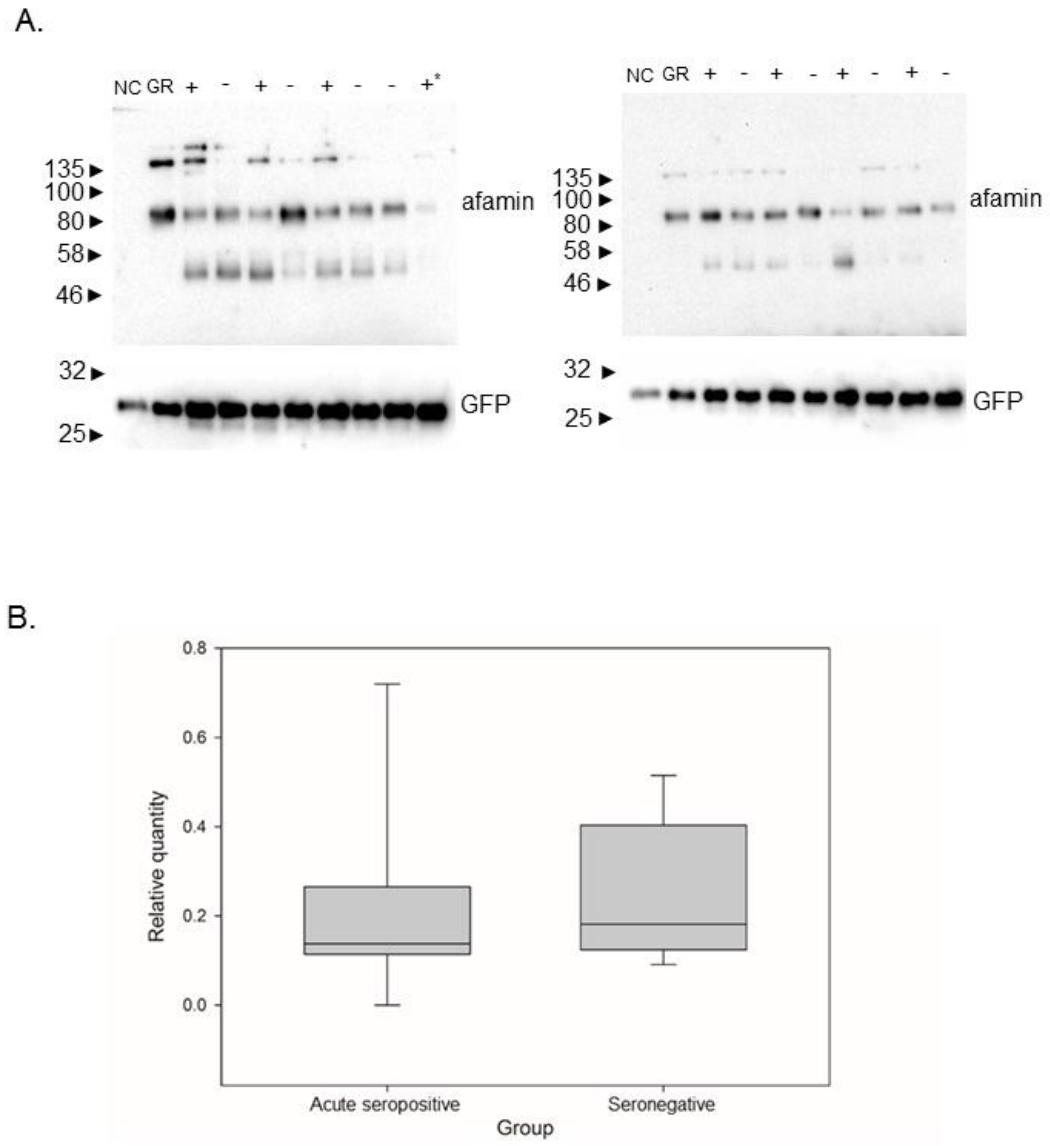


Figure 3.8. Validation of afamin abundance in an independent cohort of acute orthohantaviurs seropositive and orthohantavirus seronegative sera. **A**, Western blots. 5µg protein was loaded per well, with 5 ng rGFP spiked into each sample prior to protein denaturing. The rGFP acted as a loading control, and as a parameter to normalize afamin measurements against. NC; negative control ($H_20$ + loading buffer only), GR; gel reference (a seronegative sample loaded onto both gels to act as a reference value). The intensity if this band was arbitrarily set to value of one for relative intensity calculation. +*; the well was loaded with 2.5 µg protein. This sample was excluded from subsequent statistical analysis due to low protein load. **B**, comparison of the relative intensities of afamin measured by western blotting of the acute seropositive group (left) and the seronegative group (right). Relative intensities were measured using ImageLab (BioRad) and statistical analysis was done with SigmaPlot 13.0. The median quantity of the acute group = 0.137

(left box) and the seronegative group = 0.181 (right box). In the seropositive group there was one missing value). There was no significant difference in medians between acute and seronegative groups by Mann- Whitney Rank Sum test, $p < 0.463$. GFP; green fluorescent protein.

### *3.2.5 Afamin abundance measured on sequential days of hospitalisation in a patient with HFRS*

Protein abundance changes in relation to pathological conditions often occur within relatively short timeframes. Elevation of several plasma cytokines were observed within a week of admission in patients with dengue haemorrhagic fever (Jadhav *et al.*, 2017). Within 24 hours, abundance changes in Nt-proBNP, troponins and inflammatory mediators were demonstrated following myocardial infarction, and changes in serum vasopressin was observed within minutes of reperfusion of liver grafts (Keegan *et al.*, 2010; van Diepen *et al.*, 2016). As such, having the opportunity to look at temporal proteome changes within a single individual could more accurately capture biological changes in response to infection. If the abundance of afamin fluctuated during the course of HFRS, the results from the above investigated, single time point samples, might not accurately reflect proteome changes in response to disease, as the time points during illness at which these samples were collected was unknown. Afamin abundance was therefore additionally investigated in six sequential serum samples obtained from one individual who had been hospitalised with HFRS during pregnancy. The samples from the hospitalised pregnant patient consisted of one x orthohantavirus seronegative sample (prior to seroconversion), four x orthohantavirus seropositive samples obtained during acute illness and one x orhtohantavirus seropositive convalescent sample (see chapter 4). Changes in serum afamin abundance were evident in this individual when comparing levels of the healthy seronegative baseline, through acute disease, to convalescence (figure 3.9). Notably, afamin abundance was lowest in the earliest obtained acute disease sample (day three) and rose on sequential days of illness.

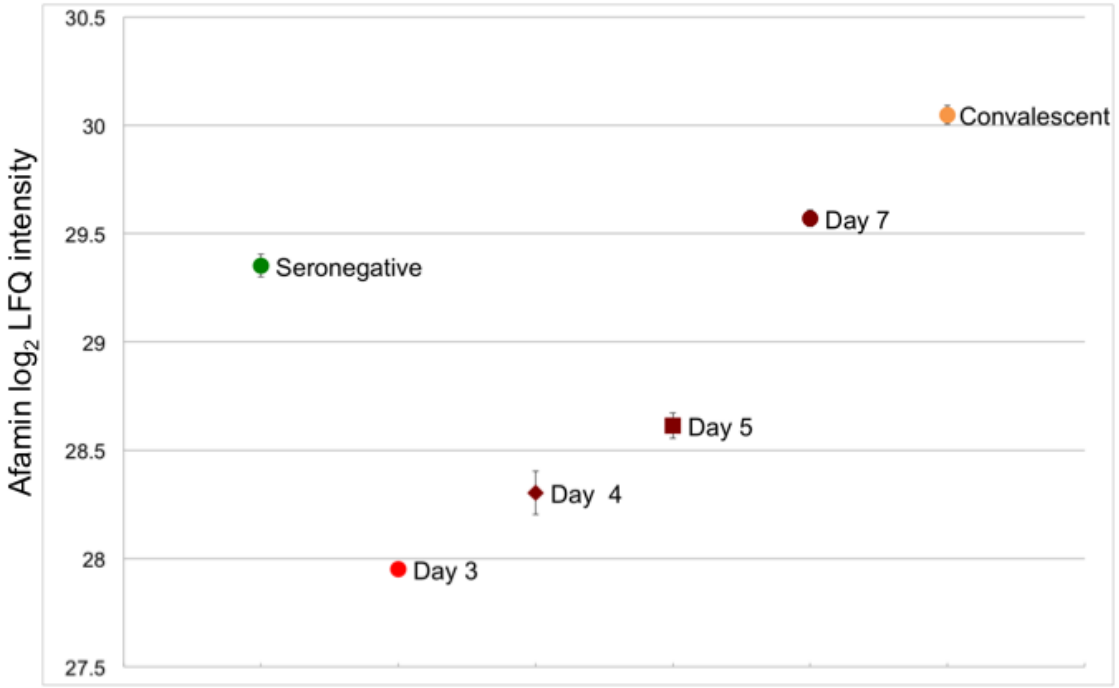


Figure 3.9. The average afamin abundance of sequential samples from a patient hospitalised with HFRS. Afamin abundance dropped to its lowest point during acute disease. Afamin levels rose on sequential days of illness. In the convalescent sample afamin abundance exceeded that of the patients' seronegative baseline. Day three – day seven equates days of clinical symptoms. Error bars are 2X standard error of the mean of triplicate measurements. LFQ; label free quantification

## *3.3 Discussion*

In this study the aim was to use label-free mass spectrometry as an exploratory method for discovery of novel biomarkers of orthohantavirus infection in human sera. For the initial discovery phase the seropositive sample cohort consisted of both acute and convalescent sera. This made true infection related links difficult to make, as a convalescent sample is likely to closely resemble that of an uninfected healthy control. Interestingly however, there were several proteins found to be differentially abundant in the seropositive compared to the seronegative group, despite most of the samples within the seropositive group originating from convalescent, presumably healthy, individuals. Whether the observed difference represents a true difference due to some chronic sequelae of a resolved infection or represents the variation in serum protein abundance for specific proteins that must be expected when looking at a random selection of healthy individuals with unknown medical histories, remains speculative, as follow up experiments of this study focused on differences between acutely ill patients and healthy controls. The question of whether orthohantavirus infections can cause long-term complications remains unresolved. In a five year follow up of Finnish NE patients there was evidence of higher glomerular filtration rate, increased proteinuria and hypertension among former patients compared to seronegative controls (Mäkelä *et al.*, 2000). However at a 10-year follow up of the same cohort, these differences between patients and controls were no longer significant (Miettinen *et al.*, 2006). In a large study in northern Sweden, in which 1600 people participated, no association was found between seropositivity for PUUV and increased incidence of hypertension or increased glomerular filtration rate, or of a higher risk of diabetes, heart attack or stroke (Bergstedt Oscarsson *et al.*, 2016). Similarly, no association was found between orthohantavirus seropositivity and chronic renal failure in a Czech multi-centre study (Pejcoch *et al.*, 2010).Interestingly, while the long-term outcome for renal and hypertensive complications following HFRS and NE seems favourable, in a

prospective study of HPS survivors, 50 % met the National Kidney Foundation's criteria for chronic kidney disease (Pergam *et al.*, 2009). There is also evidence that suggests patients who have recovered from HFRS and NE are at an increased risk of developing hormonal deficiencies (Stojanovic *et al.*, 2008; Makela *et al.*, 2010). It would be interesting to further investigate the apparent differences discovered in convalescent samples compared to seronegative in this study, to look at the potential for chronic complications associated with SEOV. This could initially be explored by comparing the incidence of pathological conditions in individuals with resolved SEOV infections to that of an orthohantavirus naïve cohort. Such a study would be greatly complicated by the fact that it would require access to a substantial number of long-term follow-up sera from individuals with proven exposure to SEOV, sampled at specified time-points following acute infection, along with samples from a demographically matched control group.

The decision to progress the study only comparing acute and seronegative samples was based on the observation that the acute seropositive specimen of the seropositive group presented with seemingly more outlying values than the convalescent ones for a specific protein of interest, i.e. afamin. Additionally, it was believed there would be a greater chance of identifying true differences by comparing more obviously phenotypically different conditions, especially considering the small sample size available for analysis.

Because the abundance of afamin was significantly decreased in the seropositive group by mass spectrometric measurement and highlighted as a protein of interest through a profile contrasting correlation analysis, it was selected for further investigation. Afamin is a highly glycosylated member of the albumin family, predominantly expressed in the liver and secreted into the bloodstream, but found in other extravascular fluids and tissues as well (Dieplinger and Dieplinger, 2015). The biological functions of afamin remain largely unknown. *In vitro* afamin binds vitamin E, and the concentrations of afamin and vitamin E

correlate in follicular and cerebrospinal fluid, though not in plasma. Notably, the two former fractions do not contain the proteins most closely associated with vitamin E transport in plasma, linking afamin to vitamin E transport in fluids were the lipoprotein system is lacking or insufficient (Jerkovic *et al.*, 2005). Absolute afamin levels seem to remain relatively stable across a range of parameters such as circadian rhythm, gender and age (Dieplinger *et al.*, 2013). It has been found to have altered abundance in various pathological conditions such as cancer, neurodegenerative disease and infection, however, its actual clinical relevance and utility remains questionable with results remaining unvalidated or controversial (Dieplinger and Dieplinger, 2015). Moderately decreased levels of afamin have been associated with ovarian cancer, inversely correlated with FIGO stage[5] and distant metastasis. Afamin did not, however add any significant value to the performance of cancer antigen 125, the most commonly used biomarker currently available for ovarian cancer, in differentiating ovarian cancer patients from healthy controls or benign gynaecological diseases (Dieplinger *et al.*, 2009). In a clinical study on therapy response in ovarian cancer, post-therapeutic afamin levels ≥ 48 mg/l was associated with increased survival (Melmer *et al.*, 2013). However, in another retrospective study no correlation between afamin and disease stage before intervention was seen, or with any measurements of therapy response and outcome (Aktas *et al.*, 2013). In a small study looking at prognostic biomarkers for the development of familial Alzheimer's disease, increased levels of afamin in cerebrospinal fluid were found in presymptomatic individuals carrying two high-risk gene mutations linked to the development of Alzheimer's compared to non-carriers of these mutations (Ringman *et al.*, 2012). Compared to healthy controls, significantly decreased plasma levels of afamin have been demonstrated in patients with

[5] A staging system for ovarian cancer established by the International Federation of Gynecological Oncologists. The system has 4 stages with stage 1 denoting a tumor limited to the ovaries or fallopian tube, and stage 4 denoting metastasis to another organ.

pneumonia and sepsis, but not in patients with chronic pathologies such as chronic obstructive pulmonary disease or chronic renal disease (Dieplinger *et al.*, 2013). A common denominator for cancer, neurodegenerative disease and acute infections is the induction of reactive oxygen species (Liu *et al.*, 2017; Yang and Lin, 2017). The role of vitamin E as a potent antioxidant and afamin's vitamin E-binding ability could implicate afamin in mechanisms associated with a response to oxidative stress during various pathological conditions. Afamin has also been implicated as a negative acute phase response protein, due to findings of an inverse relationship with CRP and IL-6 (Dieplinger *et al.*, 2013). While afamin was not decreased in abundance during orthohantavirus infection compared to controls in the validation phase of this study, the protein did follow some interesting kinetics in a sequential sera set from a patient with acute HFRS due to SEOV. In the sequential sera from this patient afamin was decreased in the earliest acute disease sample of the set compared to all the other samples from the patient but increased over the next few days of illness. The observation that afamin was higher in the convalescent sample than the seronegative, could be explained by the patient's pregnancy at the time of disease, as afamin increases almost two-fold during the course of an uncomplicated pregnancy (Hubalek *et al.*, 2014). Possibly, this could also account for the slightly higher abundance of afamin on acute day seven compared to the seronegative specimen. As it was observed in the sequential sera that afamin levels were altered during illness, it is difficult to say if the findings of no difference in the formerly analysed cohort was due to there being no biologically effect on afamin abundance in response to orthohantavirus infection, or that the acute disease samples used in this study were taken at time points of disease progression at which afamin had already returned to normal levels. Possibly, measuring the relative intensity of afamin using a semi-quantitative technique such as western blotting, might not be an accurate enough method in this case. To progress the findings of this study, investigating the absolute, rather than relative abundance of afamin using an afamin-

specific ELISA, could possibly provide more conclusive answers, as afamin levels could then be seen in relation to a normal range rather than an arbitrary normalisation value.

For HFRS it would be clinically useful with biomarkers that could aid in early identification of patients that are likely to experience acute kidney injury (AKI) and requirement for renal replacement therapy. Biomarkers of AKI have been investigated in both blood and urine in several settings (Alge and Arthur, 2015; Wasung *et al.*, 2015). Urine derived markers have showed most promise as accurate early diagnostic and prognostic markers. This is possibly because kidney function and damage can be better evaluated by detecting what the kidneys do or do not secrete during diseased compared to normal conditions. In combination, urinary tissue inhibitor of metalloproteinases-2 and insulin-like growth factor-binding protein 7 have demonstrated a very good ability to accurately predict the development of AKI within 12 hours of measurement (Kashani *et al.*, 2013; Bihorac *et al.*, 2014) As such, looking at urine samples from HFRS patients might provide more direct evidence of renal dysfunction than through analysing sera. In the case of HFRS, however, markers indicative of severe AKI might not necessarily be kidney specific. Exposure to inflammatory factors and immune cells induces endothelial activation, which in turn can can be a driver of renal disease (Imig and Ryan, 2013). Elevated levels of soluble thrombomodulin, a marker of endothelial injury, has been associated with development of AKI in septic and critically ill patients in the absence of urinary markers (Katayama *et al*. 2017; Bouchard *et al.* 2015). While AKI is a hallmark of HFRS, HFRS is predominantly a disease of the vascular endothelium (Krautkrämer *et al.*, 2013). If AKI is a consequence of infection-induced endothelial activation, early markers predictive of severe outcome, i.e. AKI, might be vascular rather than kidney specific.

In addition to biomarkers associated with the severity of AKI, it would also be beneficial with biomarkers capable of differentiating orthohantavirus infections from bacterial causes

of AKI, as leptospirosis is one of the most common differential diagnoses for HFRS (Gamage *et al.*, 2011; Goeijenbier *et al.*, 2014). Such biomarkers could possibly aid in the reduction of the use of provisional antibiotics. While it would be ideal with markers that could specifically point to a certain infection, in actuality this is quite unlikely, as similar symptoms generally mean similar pathologies and host responses on a clinical level. However, the intensity of the responses might differ, or certain shared factors may be more or less prominent depending on the infectious agent. As such, panels of biomarkers viewed in relation to each other and with well-defined thresholds could be informative for discriminating infections of different aetiologies. From the above datasets it would be interesting to look at several of the other proteins identified in addition to afamin. Angiotensinogen was found to be slightly elevated in infected samples. This protein is a competent of the renin-angiotensin system which regulates blood pressure, body fluid and electrolyte homeostasis, and it is a regulator of kidney function. Considering the pathology of HFRS this protein would be a very interesting candidate for further investigation, both in terms of acute disease and chronic complications. In addition, immune-function-associated proteins like properdin, a regulator of the alternative pathway of the complement system, and lumican, which mediates extravasation of neutrophils, would be very interesting to follow-up on(Hayashi *et al.*, 2010). Both these proteins were found to be decreased in seropositive samples compared to seronegative ones, indicating they might be involved in processes that are activated in the human response to orthohantavirus infection.

## *3.4 Conclusion*

In the above study label free mass spectrometry complimented by immunological validation techniques were used to investigate putative novel biomarkers of orthohantavirus infection in human sera. While the incorporation of convalescent sera at the discovery phase was not an optimal starting point for infection-related biomarkers, it did result in an interesting finding; the possibility of chronic changes in the serum proteome following a resolved orthohantavirus infection. While this would be fascinating to follow up, it could prove difficult because of the many possible confounders associated with long-term observations of populations, and the large numbers required for confident results.

The glycoprotein afamin was investigated as a putative biomarker for orthohantavirus infection. Whether or not the abundance of this protein was altered in response to infection remains inconclusive. In a cohort of eight acute disease samples compared against eight seronegative samples there was no measurable difference in afamin abundance. However, in a sequential set of sera from a single patient with HFRS, afamin abundance was decreased during acute disease compared to both a seronegative sample obtained pre-infection and a convalescent sample from the same patient. Certainly, having access to more longitudinal samples such as the one used in this study, would increase the ability of detecting relative abundance changes with biological relevance. In addition, considering a larger panel of proteins as biomarker candidates, and seeing them in relation to other infectious causes of AKI, especially leptospirosis, would provide stronger clinical relevance. Finally, it might be informative both in relation to rapid diagnosis of AKI and as an indication of the pathophysiology underlying AKI in HFRS, to consider changes in the urine proteome in response to orthohantavirus infection in addition to sera.

# *Chapter 4: Serum proteins associated with orthohantavirus infection in a pregnant patient*

## *4.1 Introduction*

One of the difficulties in studying the course of any infection in humans is gathering longitudinal samples. This is particularly with regards to obtaining a sample prior to infection that can act as a base line comparator. In this study the serum proteome from a pregnant patient was analysed at the time of orthohantavirus infection. Uniquely, a serum sample had been taken several months prior to both clinical symptoms and the positive diagnosis of orthohantavirus infection, and samples were also taken during acute infection and after the patient had recovered. This allowed for an unique analysis of temporal changes in protein abundance in her serum during and after disease, using the pre-infection seronegative specimen as a reference sample.

Proteomics has not previously been applied to the analysis of the serum proteome during pregnancies complicated by any species of orthohantavirus. While orthohantavirus infections have previously been analysed by proteomic means in the context of hantavirus cardiopulmonary syndrome (HPS), this is the first temporal analysis of proteome changes during a case of haemorrhagic fever with renal syndrome (HFRS) (Bondu *et al.*, 2015). Proteomic investigations of obstetric complications is an active area of research, with a focus on identifying biomarkers at an early screening stage that can predict later adverse pregnancy outcomes (Klein *et al.*, 2014; Kolialexi *et al.*, 2017). Proteomic investigations into infectious causes of obstetric complications mostly target amniotic fluids and placental tissue for analysis, as this is the site from which the most common infectious causes of adverse pregnancy outcomes stem from, such as Toxoplasma gondii infection and microbial invasion of the intra-amniotic cavity (Tambor *et al.*, 2013; Jiao *et al.*, 2017).

In this study the proteomes of the sera taken at different stages of infection were also compared to the serum proteomes from further patients taken either during acute orthohantavirus infection or when they were convalescent or from controls negative for orthohantavirus– specific antibodies. These control patients were not detectably pregnant, and in contrast to the sequential samples from the pregnant patient, only a single sample was available for each individual control patient. The data identified changes in the serum proteome that could be correlated with pregnancy and viral infection. The data also provided information on the underlying phenotypic changes caused by the infection including evidence of cellular stress, disruption of haemostasis and activation of the acute phase response.

### *4.1.1 Hypothesis*

Comparing the serum proteomes from a single individual prior to seroconversion, during active disease due to SEOV infection, and following recovery will reveal specific proteins with altered abundance levels as a result of clinical disease, shedding light on mechanisms involved in the pathology of HFRS.

### *4.1.2 Case report*

A 28-year-old woman was admitted to hospital in July 2015 with a two-day history of pyrexia and malaise, for which she had received empirical cefalexin for a presumed urinary tract infection. She was 25 weeks pregnant and had no significant past medical history. Her temperature was 39.6° C, heart rate 129 beats per minute and blood pressure 112/72. She remained pyrexial despite receiving empirical meropenem. She had thrombocytopenia (nadir 49 x $10^9$/L), raised transaminase levels (ALT 112 iu/L; normal <35) and raised serum creatinine, and was transferred to a tertiary obstetric unit on day four of illness with a diagnosis of possible HELLP syndrome (Hemolysis, Elevated Liver enzymes, and Low Platelet count) or acute fatty liver of pregnancy. At this point she was apyrexial and was

normotensive but had marked pitting oedema. She received dexamethasone 12 mg IM to induce fetal lung maturity in case urgent delivery was required. Investigations on day four of illness showed: haemoglobin 104 g/L (normal 118-148), platelets 78 x $10^9$/L (150-400), serum creatinine 234 µmol/L (50-130), serum ALT 122 iu/L (<35) and C reactive protein 157 mg/L (<5). Urine protein:creatinine ratio was raised at 76 mg/mmol (<45). Bacterial cultures of blood and urine were sterile. Abdominal ultrasound scans showed no renal or liver abnormalities and there was normal fetal growth appropriate for gestation, with no features of uteroplacental insufficiency. The patient mentioned that she kept and bred rats and suggested doing tests for leptospirosis and hantavirus. Paired serology was negative for leptospirosis but was strongly positive for Seoul (SEOV) and Hantaan virus (HNTV) IgG with titres of 1:1000 on day three of illness rising to 1:3200 on day five and a peak of 1:10000 on day 22, compared to negative results in the antenatal booking bloods taken 16 weeks previously. There was weaker cross reactivity at lower titres with Puumala virus (PUUV), Dobrava virus (DOBV), Sin Nombre virus (SNV) and Saarema virus (all 1:1000). The patient was managed conservatively, and her laboratory parameters improved over the following five days and had normalised by day 22. Her pregnancy proceeded uneventfully.

## *4.2 Results*

### *4.2.1 Preparing serum samples for proteomic analysis*

To enhance protein identification and quantification from these field samples (table 13), and to enrich detection of lower abundance proteins, the longitudinal samples from the pregnant female were depleted of the most common high abundance serum proteins as detailed in chapter 2.2. This resulted in an approximate 75% decrease in total protein concentration for each sample. This was visualized by SDS-PAGE where the crude and depleted samples were compared side by side (figure 4.1A). Depletion of high abundance proteins and concomitant enrichment of lower abundant proteins was confirmed by western blot, comparing human serum albumin (normal range; 34-54 g/L) and C-reactive protein (CRP) (normal range < 0.003 g/L) in crude and depleted samples (figure 4.1B). The comparative non-pregnant samples had been previously processed in the same manner (see chapter 3.2.2).

**Table 13. Sequential sera from a pregnant woman with HFRS**

| Sample identifier | Serostatus | Date of sampling | Total number of proteins identified by MS | Proteins identified by a single peptide |
|---|---|---|---|---|
| Negative | Seronegative | 06.03.2015 | 534 | 173 |
| Acute day 3 | Seropositive | 03.06.2015 | 561 | 196 |
| Acute day 4 | Seropositive | 04.06.2015 | 564 | 197 |
| Acute day 5 | Seropositive | 05.06.2015 | 553 | 187 |
| Acute day 7 | Seropositive | 07.06.2015 | 557 | 193 |
| Convalescent | Seropositive | 27.06.2015 | 549 | 186 |

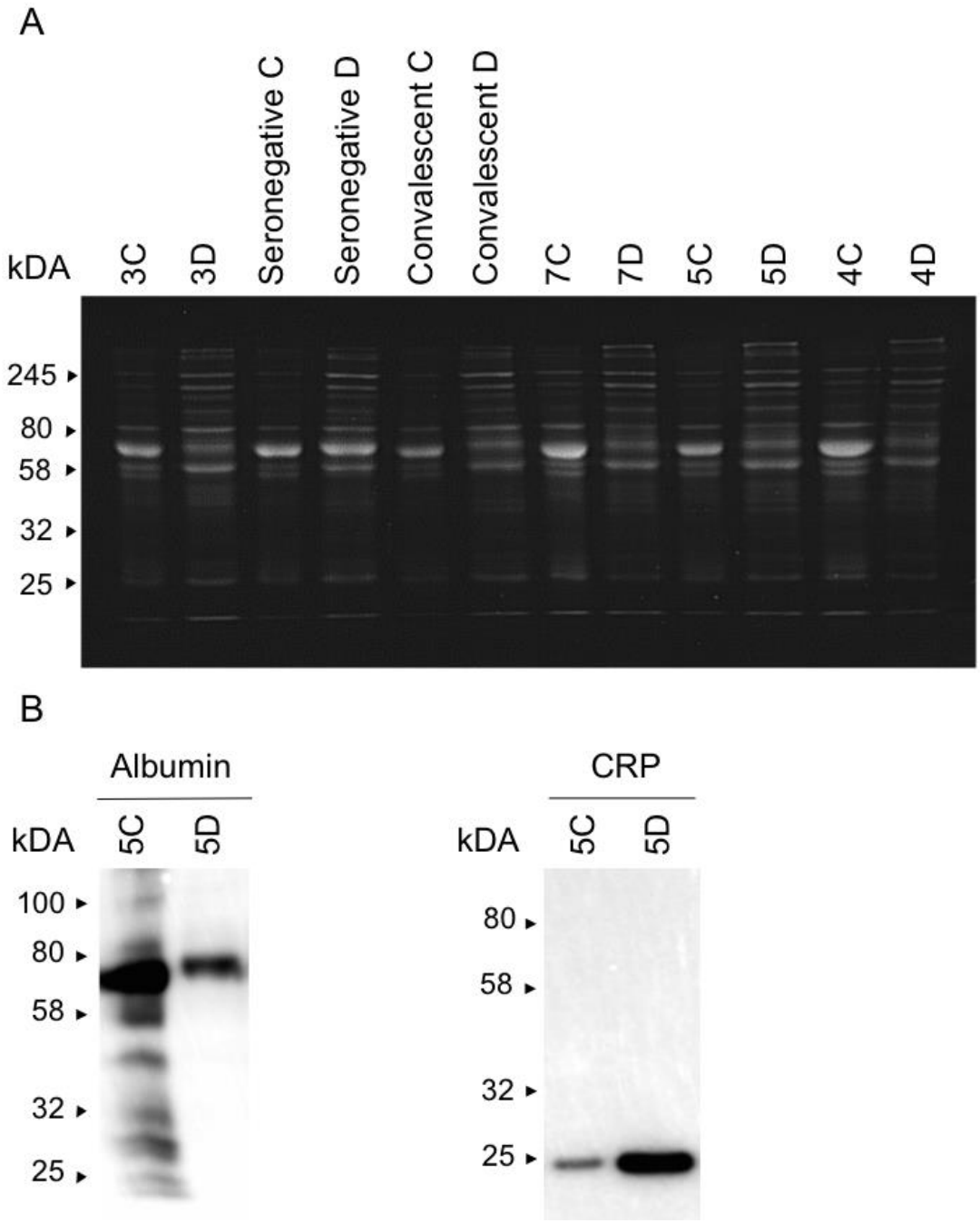


Figure 4.1. Total protein stain and western blot analysis of patient sera confirming depletion of high abundance proteins. **A**, SYPRO Ruby total protein stain of the sequential sera sample set, n = 6. Numbers 3-7 denotes day of clinical symptoms. For each sample an undepleted (lane marked C for crude) and a depleted (lane marked D for depleted) specimen was loaded next to each other on the gel to visualize the difference in protein

concentration before and after immunodepletion. Each lane was loaded with 2.5 µg protein. **B**, Western blot for albumin (75 kDa) left, and CRP (24kDa) right, of one representative sample (day five of clinical symptoms) from the sequential sera set. By western blotting the detection of a high abundance protein (albumin) and a low abundance protein CRP in a single sample before (C) and after (D) immunodepletion could be compared. Each lane was loaded with 2.5 µg protein. CRP; C-reactive protein.

### *4.2.2 Protein identification and quantitation by label free-mass spectrometry*

Proteins in the immunodepleted samples were identified and quantified by label-free mass spectrometry as detailed in chapter 2.7. Filtering the results for contaminants and proteins identified by a single unique peptide left a total of 357 proteins common to all the samples taken from the pregnant female and 381 proteins common to all the samples taken from the non-pregnant control group (appendix B.2 and appendix B.1, see chapter 3.2.3).

### *4.2.3 Analysis of protein abundance in the longitudinal sample set taken from a SEOV positive pregnant female*

In order to derive meaningful functional information from the longitudinal samples the proteome was clustered using GproX (Rigbolt *et al.*, 2011). Using this software, proteins with similar patterns of abundance change with time could be grouped together (figure 4.2, appendix B.3). Thus five clusters of distinct temporal regulation were identified. Clustered proteins were assigned membership values to their cluster ranging from 0-1. This value indicated the goodness of fit of the specific protein entry to a cluster, with higher membership values equating better fit. From the five clusters all proteins with high membership values (≥ 0.6) were extracted to investigate if there were any functional links associated with the patients' pregnancy and disease status that emerged from the regulatory patterns. Cluster 1 had a pattern of relatively low abundance at the seronegative time-point followed by sustained elevation in protein abundance from day one acute through to convalescence (figure 4.2). In this cluster 22 proteins had membership values ≥ 0.6, and of these 22 proteins 13 were specifically associated with pregnancy. Two blood

coagulation factors, fibrinogen alpha chain and coagulation factor VII, were also identified in cluster 1 (appendix B.3).

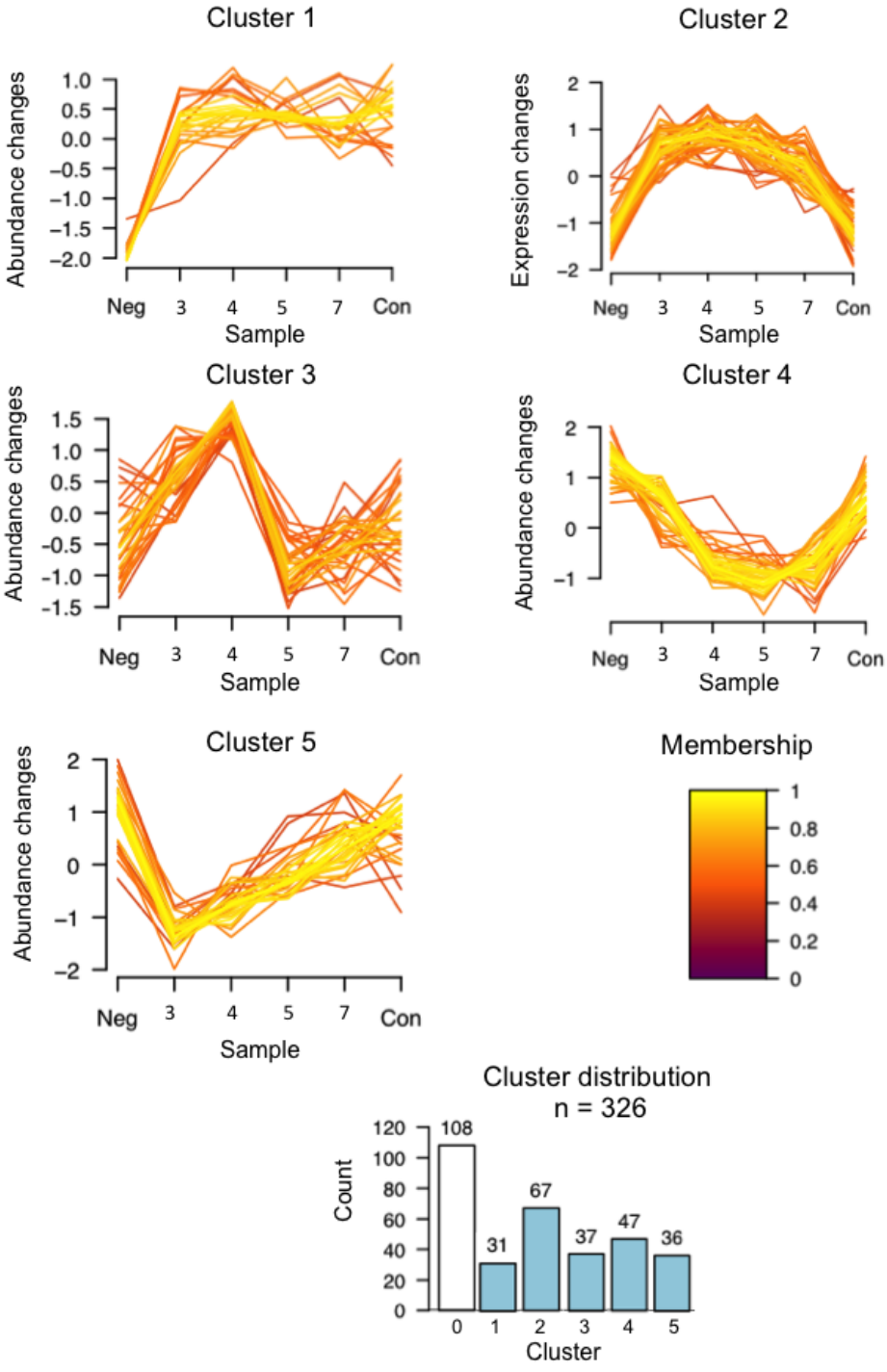


Figure 4.2. Clustering of proteins identified by the proteomics analysis into similar patterns of temporal changes in abundance. Unsupervised clustering by the Fuzzy C-means

algorithm was done using GProX software version 1.1.16. 357 proteins, filtered for human ID and ≥ 2 unique peptides, were included in this analysis. Of the 357 proteins, 31 were grouped in a cluster in which no proteins reached a membership value above 0.6. This cluster was therefore excluded from further analysis, leaving a total of 326 proteins. Proteins were included in a cluster if they reached a minimum fold change in abundance between highest and lowest state = 2 and a q-value < 0.05. Cluster 0 contained 108 proteins that did not reach these set filter thresholds, leaving a total of 218 proteins across clusters 1 - 5. The x-axis numeric 3-7 equates day of clinical symptoms. Neg; seronegative sample; Con; convalescent sample (22$^{nd}$ day of illness).

### *4.2.4 The pregnancy-associated protein hCG did not conform to the kinetics of cluster 1*

The pregnancy-associated protein choriogonadotropin subunit beta variant 1 (hCG) was detected in the patient's sera, as would be expected in pregnancy sera, as this protein is produced by the embryo and placenta early following conception. The longitudinal analysis showed that hCG did not, however, follow the temporal regulatory pattern of other pregnancy-associated proteins identified in cluster 1. Rather, it scored a 0.6 membership value to cluster 4 (figure 4.2, appendix B.3), a cluster dominated by antibody subunits and associated with a decrease in abundance during acute disease. The abundance of hCG was highest in the seronegative sample and declined during acute disease (figure 4.3). Compared to the acute samples the abundance of hCG was elevated in the convalescent specimen, though at this time point remained lower than the level measured at the seronegative baseline.

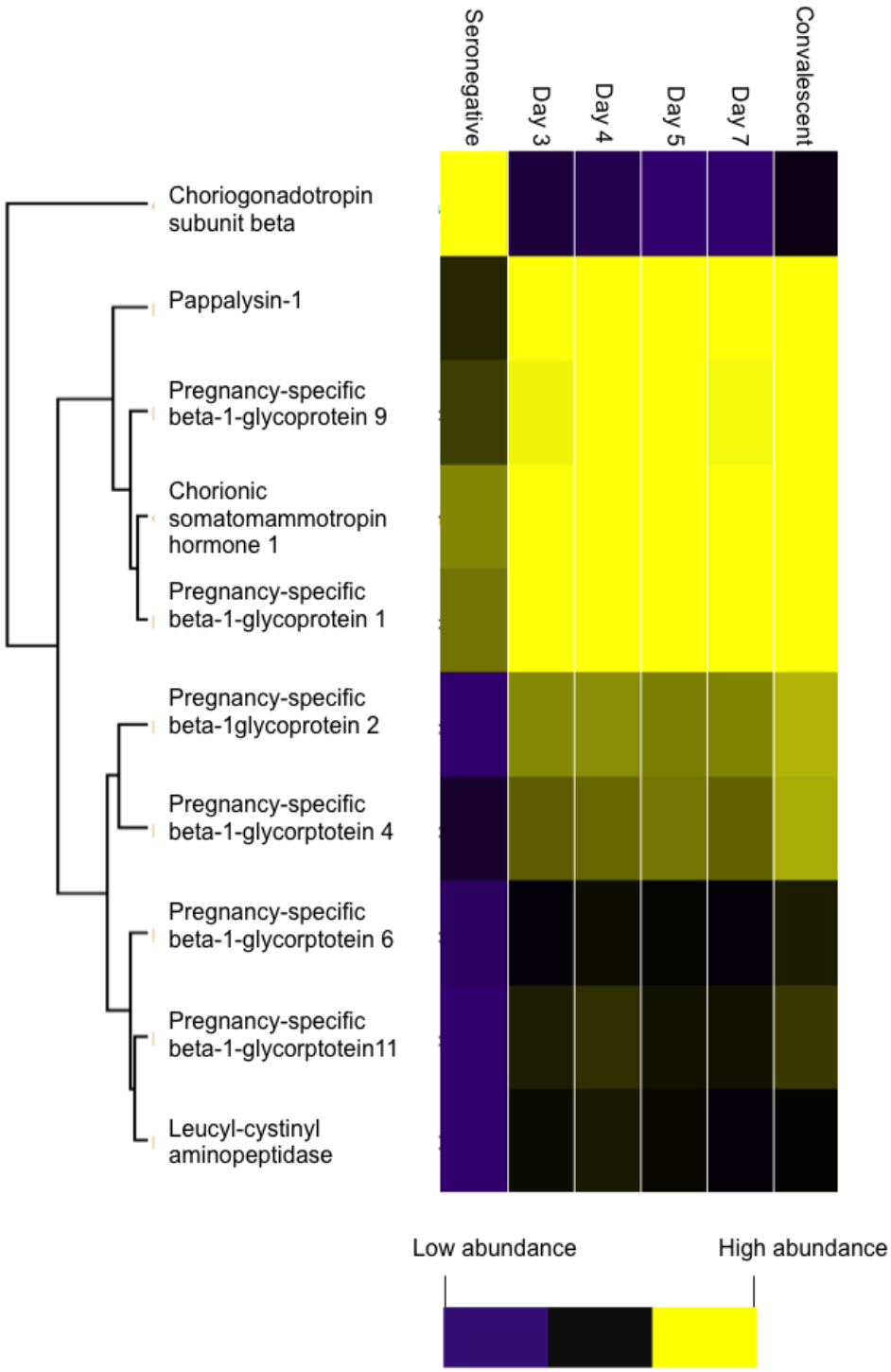


Figure 4.3. Heatmap of selected pregnancy-associated proteins from cluster 1 and choriogonadotropin subunit beta. The heatmap was made in Perseus ver. 1.5.1.6, using the k-means algorithm. hCG does not follow the temporal abundance pattern of the other pregnancy-associated proteins identified in cluster 1 but decreases during acute disease and subsequently increases somewhat in the convalescent sample.

### *4.2.5 Proteins in cluster 2 were elevated during illness and contained putative markers for orthohantavirus infection*

Proteins in cluster 2 were elevated in abundance during illness compared to the seronegative and convalescent specimens (figure 4.2). This cluster contained 41 high membership proteins (i.e. proteins scoring > 0.6). Of these several were immune response-associated proteins. Of the 41 proteins, eight proteins were classified as positive acute phase reactants (appendix B.3). The cluster also contained two innate immunity pattern recognition receptors, five receptors facilitating migration and adherence of immune cells to the vasculature, as well as proteins involved in angiogenic activity and proteasome subunits suggestive of increased proteolytic activity (appendix B.3). To identify proteins with abundance changes that might be specifically related to the patient's viral infection, high membership protein hits from cluster 2 were compared with an independent dataset of n = 10 single time-point serum samples. This comparison revealed 11 proteins present in both datasets with elevated abundance in acute samples compared to seronegative and seropositive convalescence samples (figure 4.4).

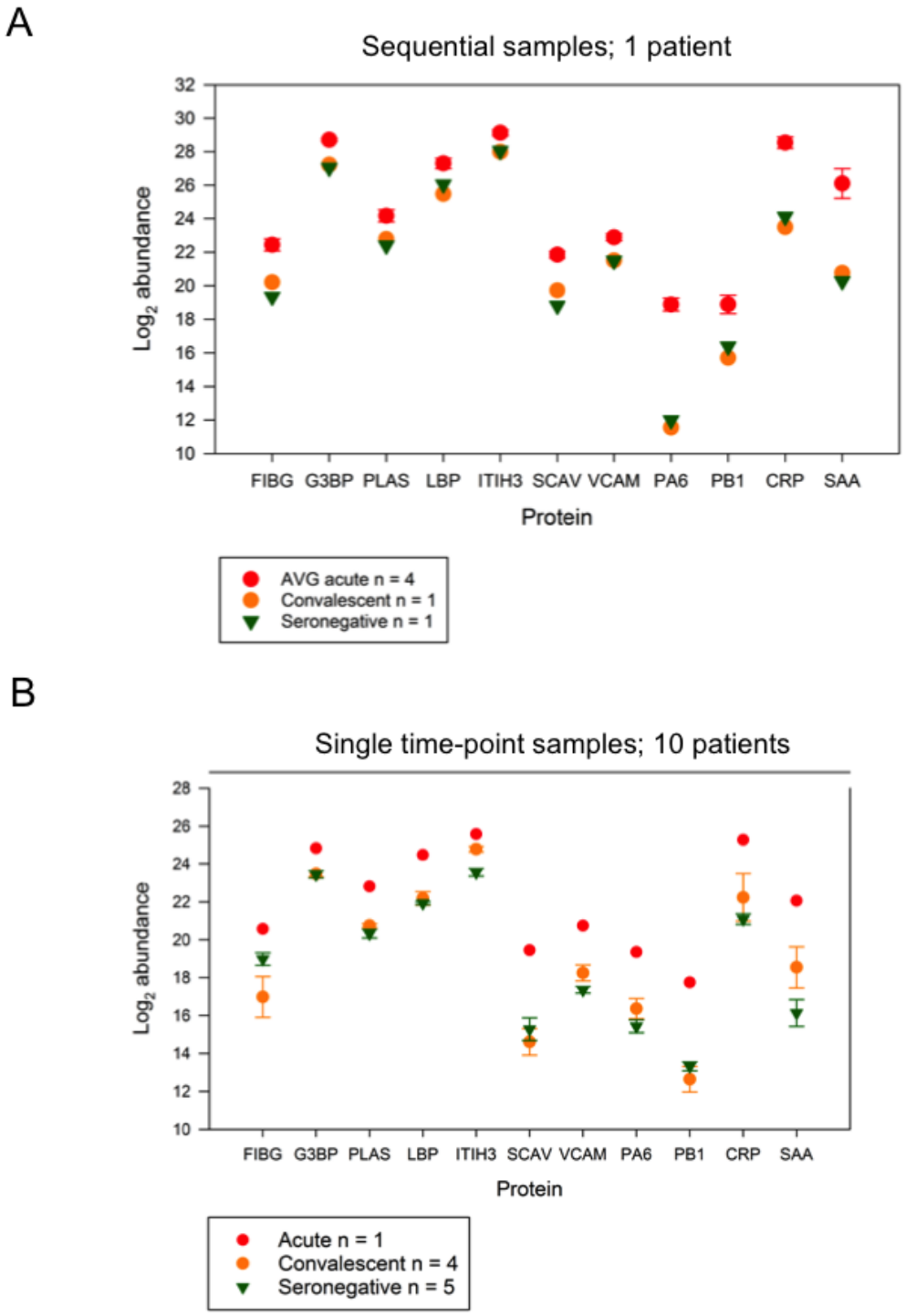


Figure 4.4. $Log_2$ transformed abundance levels of 11 selected proteins identified in cluster 2 (acute phase cluster) of the longitudinal dataset (n = six) with membership scores ≥ 0.6. These 11 proteins were additionally identified in an independent sample cohort of n = 10 individual samples, following the same trend of abundance change as the acute phase cluster. In both datasets protein abundance was increased in the acute disease samples

compared to seronegative and seropositive convalescent specimens. The independent sample set consisted of 10 single time point; one x acute hantavirus infection sample, four x seropositive convalescent for hanta-antibodies and five x hantavirus seronegative samples. Fibrinogen gamma chain (FIBG), galectin-3-binding protein (G3BP), plastin-2 (PLAS), lipopolysaccharide binding protein (LBP), inter alpha trypsin heavy chain H3 (ITIH3), scavenger receptor cysteine-rich (SCAV), vascular adhesion molecule 1 (VCAM), proteasome subunit alpha type-6 (PA6), proteasome subunit beta type-1 (PB1), c-reactive protein (CRP), serum amyloid a-1 (SAA). **A**, $\log_2$ abundance levels of the 11 selected proteins in the sequential samples from the pregnant patient. AVG acute = the average value of four acute disease samples obtained in sequential days of hospitalization. Convalescent = sample taken approx. three weeks after the patient recovered. Seronegative = sample taken approx. three months prior to the patient was hospitalized and seroconverted. Error bars indicate 1 x standard error. **B**, log2 abundance levels for the 11 selected proteins in the independent single time point sample cohort. The convalescent and seronegative values are the average values of four and five individual samples respectively, while the acute measurement is the value of a single sample. Error bars indicate 1 x standard error.

To investigate whether these results could be replicated in a larger sample cohort, an ELISA was done to quantify galectin-3-binding protein (G3BP) concentrations in an independent cohort of eight hantavirus seronegative, eight hantavirus seropositive convalescent and seven acute hantavirus-infected samples that had not previously been analysed by mass spectrometry (figure 4.5A). In the pregnant woman the abundance of G3BP was elevated in all four samples taken during her hospitalisation with HFRS as compared to the seronegative baseline and the convalescent sample from three weeks after hospitalisation (figure 4.4). G3BP was chosen for initial validation because increased levels of this protein has been associated with acute orthohantavirus infection previously (Hepojoki *et al.*, 2014). The median G3BP abundance concentration of the acute seropositive samples (53.9 ng/ml) was higher than both the seronegative and seropositive convalescent sample medians (42.9 ng/ml and 32.4 ng/ml respectively). Individual concentration measurements were variable in all groups, especially in the seropositive

acute group (interquartile range; 42.4ng/ml - 87.1 ng/ml). The difference between the groups was not found to be statistically significant by an ANOVA on ranks ($p = 0.06$). The highest concentration of G3BP was measured in an outlier of the seronegative group (99.4 ng/ml, interquartile range; 35.7ng/ml – 45.1ng/ml). To establish whether elevated G3BP was a generic response to infection or a specific response to orthohantavirus infection, levels of G3BP in acute orthohantavirus infected sera were compared to levels measured in acute leptospirosis infected sera. Leptospirosis was chosen because this bacterial disease is a common differential diagnosis for HFRS, due to its similar epidemiology and clinical presentation (Forbes *et al.*, 2012). The levels of G3BP were higher in leptospirosis-infected sera than in orthohantavirus infected sera, though not significantly so (median; 79.9 ng/ml and 31.7 ng/ml respectively, $p = 0.06$) (figure 4.5B). There was, however, a significant difference between acute leptospirosis and the healthy control samples ($p < 0.05$) while this was not the case when comparing acute orthohantavirus with healthy controls.

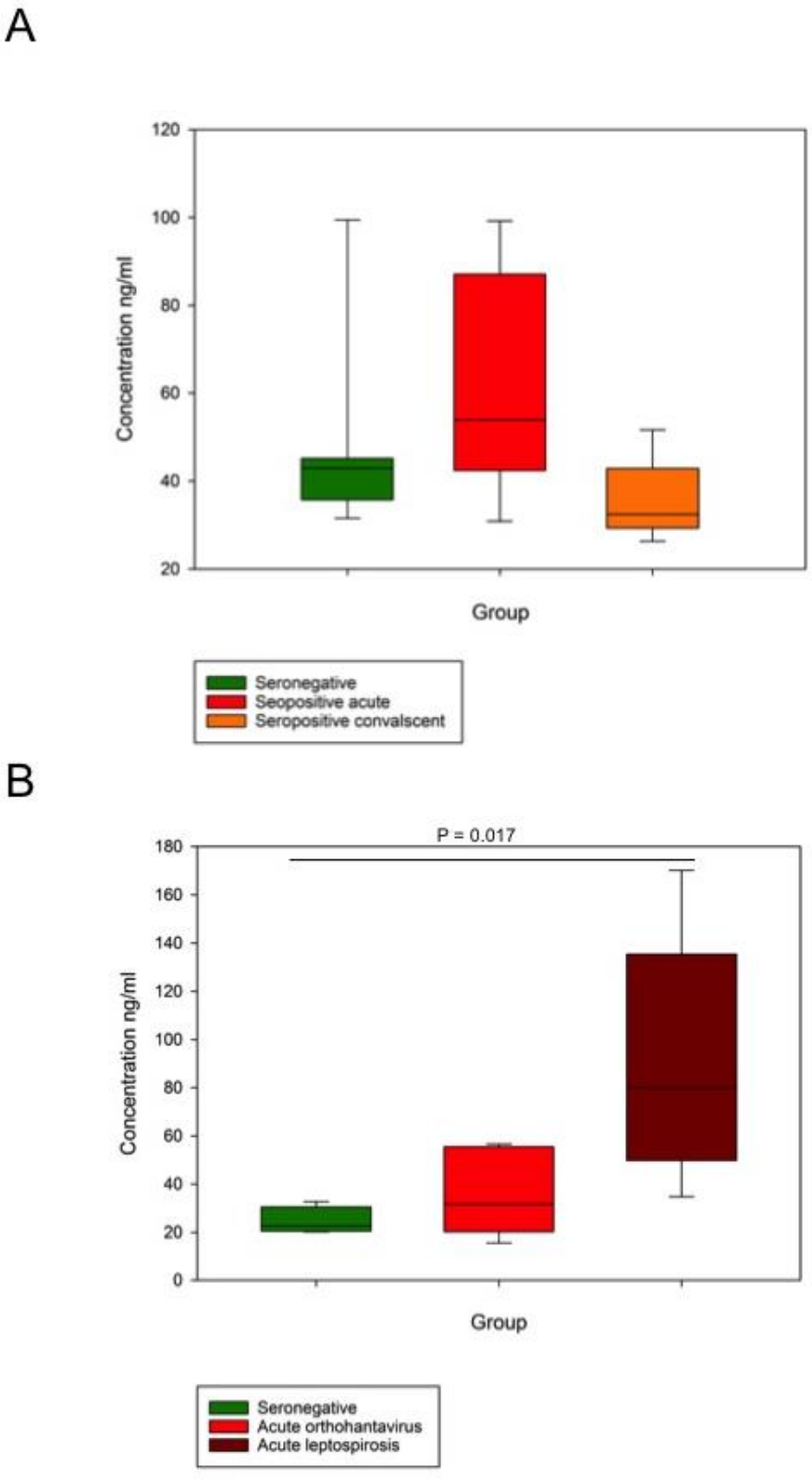


Figure 4.5 **A**, Galectin-3-binding protein (G3BP) concentrations in orthohantavirus - seronegative and orthohantavirus-seropositive human sera. G3BP concentrations were measured in eight seronegative (green), seven seropositive acute (red) and eight seropositive convalescent (orange) samples by a sandwich ELISA (Affymetric eBiosciences).

These 23 samples were independent of both mass spectrometry analysed datasets. Optical densities were measured at 450 nm. Standards and samples were measured in duplicate. Medians, 25 % - and 75 % - quartile ranges for the groups were, seronegative; 42.9 ng/ml, 35.7 ng/ml, 45.1 ng/ml, seropositive acute; 53,9 ng/ml, 42.4 ng/ml and 87.1 ng/ml, seropositive convalescent; 32.4 ng/ml, 29.3 ng/ml and 42.9 ng/ml. Kruskal-Wallis ANOVA on ranks p-value = 0.06. **B**, concentrations (of G3BP in orthohantavirus-seronegative (n = four, green), acute orthohantavirus (n = seven, red) and acute leptospirosis (n = seven, burgundy). Optical densities were measured at 450nm. Standards and samples were measured in duplicate. Medians and interquartile ranges for the groups were, seronegative; 22.6 ng/ml, 25%; 20.5 ng/ml, 75%; 30.5 ng/ml, acute orthohantavirus: 31.7 ng/ml, 25%; 20.3 ng/ml, 75%; 55.5 ng/ml, acute leptospirosis; 79.9 ng/ml, 25%; 49.8 ng/ml, 75%; 135.4 ng/ml. There was a significant difference in median values of seronegative and acute leptospirosis samples by Kruskal-Wallis one way ANOVA on Ranks with Dunn's multiple comparison, p = 0.017

### *4.2.6 Temporal regulatory patterns consistent with infection and consumption of **clotting factors***

Clusters 3 and 4 contained proteins associated with an activated immune or inflammatory response (figure 4.2, appendix B.3). Cluster 3 peaked at day two of hospitalisation and contained 19 proteins with membership values ≥ 0.6. 14 of these high membership proteins were functionally associated with a response to oxidative stress and neutrophil activity. Cluster 4 mainly contained Ig-subunits (25 of 37 high membership proteins), but also three common negative acute phase reactants, i.e. proteins that are generally reduced in blood during acute infection. Cluster 5 decreased in abundance at day one followed by a steady increase back to pre-infection levels at the convalescent time-point. Of 28 proteins with membership values ≥ 0.6, 18 were proteins associated with platelet activation and blood coagulation pathways. A few proteins involved in platelet activation were also present in cluster 2 (appendix B.3). Platelets become activated when encountering damaged endothelium or in response to pro-inflammatory mediators (Esmon,

2005). In contrast to inactive platelets that are repelled by the healthy endothelium, activated platelets become adhesive and attached to the endothelium and form aggregates. The platelets secrete the contents of their granules, which contain pre-formed pro-coagulative, pro-inflammatory mediators and factors promoting aggregation (Esmon, 2005; Van Hinsbergh, 2012). As identified for cluster 4, cluster 5 also contained some negative acute phase reactants.

## *4.3 Discussion*

In this study label-free mass spectrometry was used to investigate temporal abundance changes in the serum proteome of a pregnant patient before, during and following an incidence of HFRS. The proteome data could be grouped into five discrete clusters associated with time of infection and biological function. The identification in cluster 1 of pregnancy-associated proteins with a temporal abundance pattern consistent with an on-going pregnancy provided a qualitative and quantitative assurance that the method used was able to detect expected abundance changes in clinically relevant proteins. For instance, chorionic sommatomammotropin, is a hormone expressed exclusively during pregnancy (Walsh and Kossiakoff, 2006). Pappalysin-1 is expressed at high levels in the placenta and serum, with levels rising throughout pregnancy. It directly interacts with bone marrow proteoglycan, levels of which also increase in placenta and serum during pregnancy (Overgaard *et al.*, 1999). All three of these proteins had membership values of 0.9 to cluster 1. The detection of coagulation factors in the cluster is consistent with haemostatic changes that occur during the course of a normal pregnancy, as the concentration of fibrinogen and several coagulation factors increase, peaking around term (Brenner, 2004). Of interest, the pregnancy-associated protein hCG, though detected in the sera of the pregnant patient, did not follow the same regulatory pattern of other pregnancy-associated proteins identified in the dataset. hCG is a hormone important for maintaining a functional corpus luteum, an endocrine structure necessary for establishing and maintaining pregnancy. The abundance changes observed in the longitudinal dataset studied here could possibly be a reflection of the natural progression of hCG levels during an uncomplicated pregnancy, as the levels of this hormone rises drastically during early pregnancy, peaking around 10 weeks, after which it declines and reaches a stable level that is maintained until birth (Rull and Laan, 2005). However, the relatively lower hCG abundance during acute disease could also be caused by a direct or indirect suppressing effect that the viral infection had on abundance levels of this

hormone. As the seronegative specimen was taken around nine weeks of pregnancy, and the patient fell ill at 25 weeks, it is likely that the former scenario has been observed in this case (Nelson-Piercy 2014 , personal communication). It is important to add that the abundance changes observed for Cluster 1 may have been impacted by variable levels of depletion, especially with regards to the seronegative sample which was less efficiently depleted than the other samples of the set (figure 4.1A). This inconsistency may have resulted in a greater observed difference between the seronegative sample and the rest of the data set than is actually the case, due to a higher concentration of high abundance proteins sill present in the former. Though a rare occurrence, there are a few clinical reports of pregnancies complicated by PUUV, DOBV and Seoul virus (SEOV) infections from Europe, SNV infections from America, and Haantan virus (HNTV) infections from Asia (Howard *et al.*, 1999; Kim and Choi, 2006; Hofmann *et al.*, 2012; Macé *et al.*, 2013). SNV infection during pregnancy has resulted in both maternal and foetal mortality, while for HNTV there are no reports of maternal mortality, though a few cases resulting in the death of the infant. From Europe there are no reports of orthohantavirus infections during pregnancy that have ended with fatal outcomes for either mother or child. In all reported cases with positive outcomes for both mother and child, there is no evidence of vertical transmission of the virus or other adverse outcomes for the newborn infant.

From cluster 2 several proteins linked to an acute infection were identified. Acute phase reactants are proteins produced and secreted by the liver in response to inflammatory signals, such as cytokines (Murphy, 2012). Orthohantavirus infection is known to elicit a strong immune response, characterized by a so-called «cytokine-storm» with high levels of pro-inflammatory cytokines produced during acute disease and elevated CRP is a common clinical finding for HFRS (Borges *et al.*, 2008; Jonsson *et al.*, 2010; Sadeghi *et al.*, 2011; Korva *et al.*, 2013). As the temporal pattern of this cluster was such that increased protein

abundance was maintained at a relatively stable level throughout the patient's hospitalisation, these proteins were deemed appropriate candidates for comparison to non-sequential samples. This comparison revealed 11 proteins with corresponding patterns of abundance change in both datasets. Among these 11 proteins G3BP was identified, and in a cohort of n = 23 independent samples the same trend of elevated abundance during acute orthohantavirus infection was again observed for G3BP. Though a statistically significant difference could not be demonstrated between the groups in this latter cohort, the majority of the acute seropositive samples did have abundance levels of G3BP exceeding those observed for the two other groups. It is necessary to investigate changes in G3BP linked to orthohantavirus infection in larger cohorts of HFRS-diagnosed patients, as a major drawback of this study was the small sample size, which impacts on statistical power. G3BP is a secreted glycoprotein with pleiotropic functions associated with infection, inflammation, developmental regulation and cancer (Than *et al.*, 2015; Desmedt *et al.*, 2016). The binding partner of G3BP, galectin-3, has also been linked to both acute and chronic renal pathologies and infectious and inflammatory disorders of the female reproductive tract (Than *et al.*, 2015; Desmedt *et al.*, 2016). G3BP is linked to integrin function, which is notable considering that *in vitro* integrins act as essential cellular receptors for orthohantaviral entry to unpolarised host cells (Gavrilovskaya *et al*. 1999; Gavrilovskaya *et al.* 1998; Mou *et al*. 2006). Infection of human umbilical vein endothelial cell with the orthohantaviral species PUUV, Prospect Hill virus and Tula virus have been demonstrated to induce G3BP expression in these cells (Hepojoki *et al.*, 2014). *In vivo*, G3BP was increased in the serum of macaques experimentally infected with PUUV (Klingstrom *et al.*, 2002; Hepojoki *et al.*, 2014), and G3BP was also elevated in sera of patients with acute PUUV infection compared to convalescence and correlated to clinical symptoms of NE (Hepojoki *et al.*, 2014). G3BP has additionally been found to be elevated in the sera of patients with dengue fever, as well as in HIV positive individuals where its source has been postulated to

be latently infected T cells (Yang *et al.*, 2014; Liu *et al.*, 2016). In this study, by comparing acute orthohantavirus samples with acute leptospirosis samples it was demonstrated that G3BP, in addition to being elevated in orthohantavirus infection, was elevated in sera from individuals with an acute leptospirosis infection. The levels of G3BP were higher in acute leptospirosis sera than in acute orthohantavirus infected sera. Seeing as G3BP is elevated in several infections, it is likely involved in a generic response to infection. G3BP has been shown to be a stimulator of the proinflammatory cytokine interleukin (IL)-6 in cancer, and has been positively correlated with increased IL-6 production in cultured human peripheral blood mononuclear cells (Kalayci *et al.*, 2004; Silverman *et al.*, 2012). In a murine model, G3BP and its ligand galectin-3 contributed to venous thrombosis through a proinflammatory, IL-6 dependent, mechanism (Deroo *et al.*, 2015). IL-6 is elevated in both orthohantavirus and leptospirosis infections, as a factor of the "cytokine storm" (Borges *et al.*, 2008; Sadeghi *et al.*, 2011; Korva *et al.*, 2013; Haake and Levett, 2015). Elevated levels of IL-6 have been linked to disease severity in both NE and HPS (Borges *et al.*, 2008; Sadeghi *et al.*, 2011). The serum levels of G3BP differed quite substantially between the two infections investigated in this study, possibly a reflection of difference in disease severity between individual patients. Alternatively, it could be a reflection of a pathogenic mechanism, that though not specific for any of the infections, differs on a quantitative level. As the samples investigated were residual sera from diagnostic testing, and the length of storage of the samples before analysis was unknown, this could also have affected the quality and measurable levels of G3BP in individual samples. Putatively, better knowledge of the absolute and relative levels of this protein in acutely ill patients could contribute to differentiate infections of orthohantavirus from leptospirosis, or give insight into mechanisms of pathology and host response in illnesses characterized by haemorrhagic complications.

Cluster 3 contained several proteins related to oxidative stress and neutrophil function. The temporal pattern observed for this cluster was consistent with an acute infection, in which a rapid innate immune response is launched. The proteins identified for cluster 4 seemed to reduce in abundance throughout acute illness. Possibly this reflected a measurable consumption of orthohantavirus-specific antibodies, though this would indicate a very rapidly developed humoral response. Such a rapid humoral response is a possible scenario, as orthohantavirus-specific antibodies can be detectable very early on following infection, and in some cases high, stable levels of IgG are already detected when a patient presents acutely ill at hospital (Niklasson and Kjelsson, 1988).

Several blood clotting factors were identified in cluster 5, with a steep decrease in abundance at the first day of hospitalisation followed by a gradual increase in abundance on sequential days, reaching pre-infection levels at convalescence. Clinical orthohantavirus infections are characterized by altered barrier functions of the vascular endothelium, causing systemic vascular leakage in the absence of cytopathic effects (Jonsson *et al.*, 2010). Damage to the vasculature, inflammatory mediators and an endothelium responding to vasoactive agents are all triggers of the blood coagulation cascade (Esmon, 2005; Van Hinsbergh, 2012). While changes to the vasculature would be expected during an orthohantaviral infection, it is necessary in this case to consider that pregnancy causes a state of hypercoagulation, and as such could confound findings of vascular disturbance in the context of a haemorrhagic illness such as HFRS (Brenner, 2004). A putative mechanism for increased vascular leakage in orthohantavirus- infected HUVECs involves activation of the plasma kallikrein-kinin system and increased production of bradykinin, a peptide that promotes vasodilation and increased vascular permeability (Taylor *et al.*, 2013). Successful treatment of a near fatal PUUV infection with ictibant, a bradykinin receptor antagonist, supports the finding that increased bradykinin activity might play a role in orthohantavirus

pathogenesis (Antonen *et al.*, 2013). Plasma kallikrein was identified in cluster 5 with a membership value to the cluster of one, indicating its involvement during acute disease in the case of the pregnant patient analysed in this study. Possibly the dramatic fall in abundance measured at the first day of hospitalisation, could be due to an increased consumption of this protein as a result of an activated plasma kallikrein-kinin system. The end product of this system, bradykinin, was however not detected in this dataset.

## *4.4 Conclusion*

Using label-free mass spectrometry to measure temporal changes in the serum proteome of a pregnant patient with concomitant HFRS and using GProX to group proteins with similar patterns of temporal regulation, functional changes associated with an on-going pregnancy, an activated immune response, cellular stress and vascular disturbance could be identified. The fact that the investigated longitudinal sample set contained a pre-infection specimen was beneficial, as it allowed a direct comparison of the patient's diseased state with her own healthy baseline. This meant the difficulty of comparing the highly variable serum proteomes of random individuals could be circumvented. Conveniently, the pregnancy-associated proteins could also be viewed as an internal quality control for the proteomic approach. A number of specifically disease related proteins were identified as elevated during acute disease in a comparative analysis in which the longitudinal dataset was compared to a second proteomic dataset of non-sequential sera. The identification of the glycoprotein G3BP in this group of elevated proteins was notable, as it is a protein that has been demonstrated to be elevated and associated with disease severity in orthohantavirus infections by others. In this study, G3BP was additionally found to be elevated in an independent group of acute orthohantavirus infected sera compared to convalescent and seronegative controls. The protein was also elevated in sera from acute leptospirosis patients, with higher levels measured in acute leptospirosis compared to orthohantavirus infections. G3BP has both pro-inflammatory and pro-coagulant properties and has been associated with a range of pathological conditions in which inflammation, infection and vascular activation is involved. The results of this study further support its role as a factor that is involved in the host response to acute infections in which an activated vascular endothelium is a characteristic feature. Regarding the clotting factors identified in the longitudinal analysis, it is difficult to extrapolate these findings to other non-pregnant

orthohantavirus infected patients, due to the fact that pregnancy is a state that dramatically alters the equilibrium of haemostatic processes, which could confound the results.

# *Chapter 5: Interactome of Seoul Cherwell orthohantavirus glycoproteins in HEK293T cells*

## *5.1 Introduction*

The Hantaviridae genome consists of three genomic segments; small (S), medium (M) and large (L).The L segment encodes a RNA-dependent RNA-polymerase, the M segment the glycoprotein precursor (GCP) and the S segment the nucleoprotein (N) (Hepojoki *et al.*, 2012). The GCP is co-translationally cleaved at a conserved site to form the two mature viral glycoproteins; Gn and Gc (Lober *et al.*, 2001). On the viral envelope Gn and Gc form spike complexes made up of hetero-tetrameric associations of the two proteins (Huiskonen *et al.*, 2010; Battisti *et al.*, 2011). These complexes facilitate viral entry into host cells through interactions with cellular surface proteins. *In vitro*, integrins, CD55/DAF and gC1qR have all been implicated as viral receptors (Gavrilovskaya *et al.*, 1998, 1999; Mou *et al.*, 2006; Choi *et al.*, 2008; Krautkramer and Zeier, 2008). Interestingly, pathogenic and non-pathogenic orthohantaviruses rely on different host receptors for infection of human endothelial cells, with pathogenic strains binding to β3-integrins, while non-pathogenic species require the presence of β1-integrins (Gavrilovskaya *et al.*, 1998, 1999). Inside the cell, orthohantaviral glycoproteins interact with both viral and host proteins. Interactions between the glycoproteins, N protein and viral RNA is speculated to be the mechanism by which viral envelope proteins and ribonucleoproteins combine, facilitating assembly of virions in the absence of matrix proteins found in other viruses with negative strand RNA genomes (Hepojoki *et al.*, 2010; Wang *et al.*, 2010). The Gn cytoplasmic tail (GnCT) of new-world orthohantaviruses has been implicated as a virulence factor, with the ability to regulate the early anti-viral response. GnCT can interact with the cellular host protein TNF receptor associated factor 3 (TRAF3), an essential component of the signalling cascade leading to transcription of type-I interferon (IFN) in response to viral infections. Both viral

infection and expression of the GnCT alone inhibits the ability of TRAF3 to interact with TANK-binding kinase 1 (TBK1), an interaction which is necessary for downstream IFN production (figure 5.1) (Alff *et al.*, 2008). However, removal of the TRAF3 binding element of GnCT does not abrogate the proteins' ability to regulate IFN responses, indicating that TRAF3 binding alone is not sufficient to explain how this regulation occurs (Matthys *et al.*, 2014).

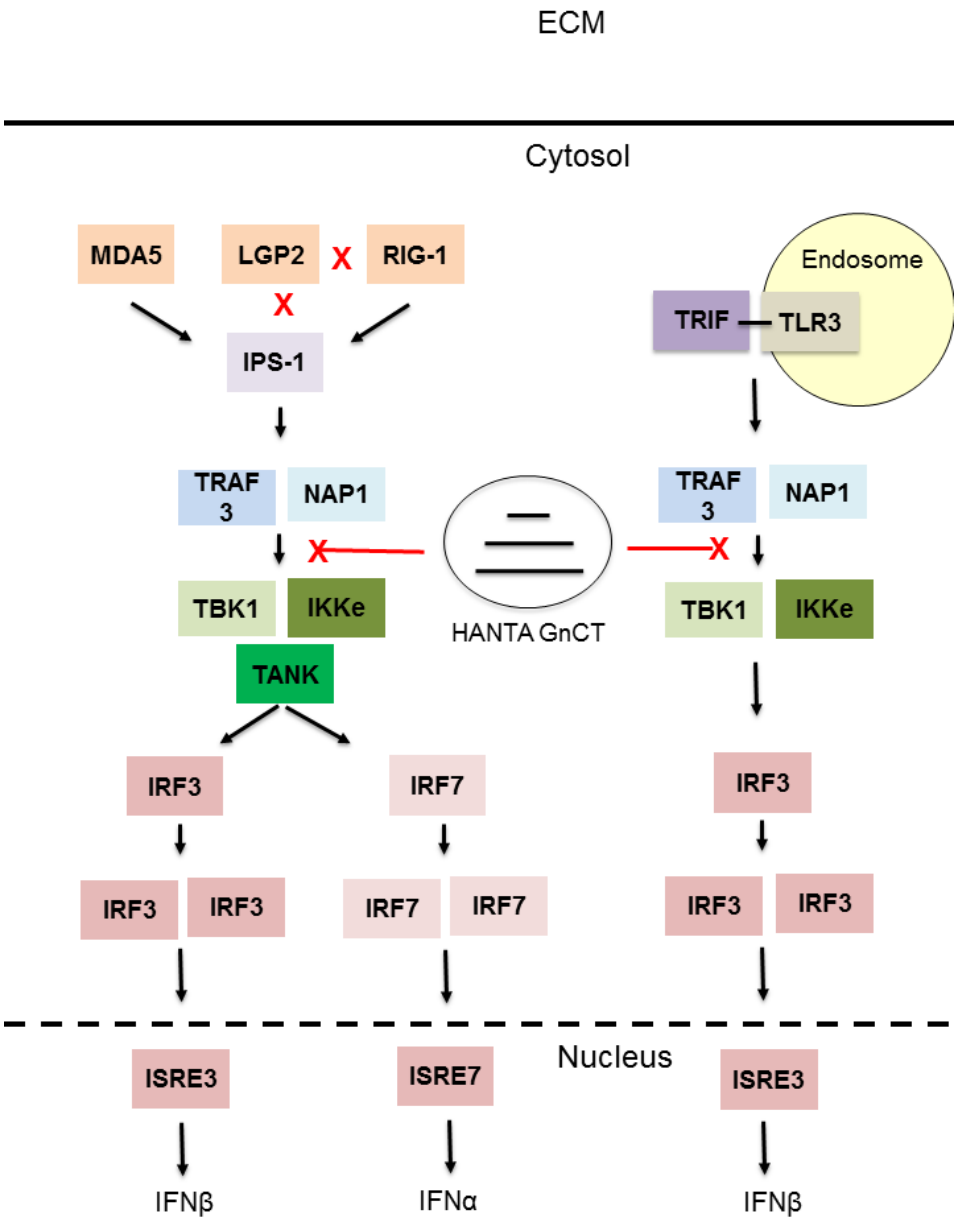


Figure 5.1. Type I IFN induction by viral infection through RLR and TLR3 signaling, adapted from www.invitrogen.com Copyright © 2011-2016 InvivoGen. The RLRs (MDA5, LGP2 and

RIG-I) and TLR3 initiates type I IFN production in response to viral infection. The GnCT of orthohantaviruses inhibits the interaction of TRAF3 and TBK1, thus abrogating downstream signaling events. MDA-5; melanoma differentiation associated gene, 5 LGP2; laboratory of genetics and physiology 2, RIG-I; retinoic acid inducible gene 1, IPS-1;interferon-β promoter stimulator 1, TRAF; TNF associated factor, NAP1; NF-κB–activating kinase-associated protein 1, TBK1; TANK-binding kinase 1, IKK; Inhibitor of nuclear factor kappa-B kinase, TANK; Traf family member-associated NF-κB activator, IRF; interferon regulatory factor, ISRE; interferon sensitive response element, IFN; interferon, TRIF; TIR domain-containing adaptor protein inducing interferon-β, TLR3; toll-like receptor 3, ECM; extracelluar matrix.

The sites of viral assembly and budding have not been definitely defined for orthohantaviruses. Like other Bunyaviruses they predominantly seem to assemble and mature at the Golgi complex (Shi and Elliott, 2002; Kariwa *et al.*, 2003; Spiropoulou *et al.*, 2003; Deyde *et al.*, 2005). However, aggregation of glycoproteins and viral budding has also been observed at the plasma membrane and endoplasmic reticulum (ER) for certain orthohantaviral species (Goldsmith *et al.*, 1995; Spiropoulou *et al.*, 2003; Ogino *et al.*, 2004; Xu *et al.*, 2007).

In their natural hosts, orthohantaviruses actively replicate and persist in the absence of disease (Easterbrook *et al.*, 2007; Schountz *et al.*, 2012; Vaheri, Strandin, *et al.*, 2013). As clinical disease in humans is believed to be, at least partially, a consequence of the host response, more insight into how the virus interacts with host factors might shed light on pathogenic mechanisms underlying clinical symptoms. In addition, understanding how the virus interacts with, and utilizes the cellular machinery to its advantage could provide novel drug target candidates. The current treatments for haemorrhagic fever with renal syndrome (HFRS) and hantavirus cardiopulmonary syndrome (HPS) are symptomatic. A clinical trial run in the mid 1980's demonstrated positive effects of ribavirin administration in Chinese HFRS patients, with reported lower case-fatality rate and decreased occurrence

of oliguria[6] among ribavirin-treated patients (Huggins *et al.*, 1991). These results have, however, not been convincingly replicated, and ribavirin has not shown efficacy in the treatment of HPS or nephropathia epidemica (NE) (Chapman *et al.*, 1999; Mertz *et al.*, 2004; Rusnak *et al.*, 2009; Malinin and Platonov, 2017). Administration of human immune sera has shown promise as a treatment of Andes virus (ANDV), and there are *in vitro* and *in vivo* indications that drugs that antagonise the increased vascular permeability induced by orthohantavirus infection might have value as clinical treatments (Gorbunova *et al.*, 2011; Antonen *et al.*, 2013; Vial *et al.*, 2015).

For this study label-free proteomics was used to study the interactome of recombinant SEOV Cherwell glycoproteins in HEK293T cells, a human embryonic kidney cell line. The objective of this investigation was to gain further insights into cellular mechanism involved in the processing of the viral glycoproteins through host cells, and the cellular proteins they associated with. Future work could be focused on disrupting these protein:protein interactions to e.g. reduce the viral load.

### *5.1.1 Hypothesis*

Orthohantaviral glycoproteins play a role in both the processing and assembly of the virus within cells and can act as a virulence factor with the ability to modify the cellular response to infection. By investigating the interactome of SEOV Cherwell glycoproteins, host proteins that interact with the viral proteins can be identified, providing insights into host factors that can be targeted in an effort to disrupt the function of the viral glycoproteins.

[6] Oliguria is defined as urine output of less than 400 ml / day

## *5.2 Results*

### *5.2.1 Production of plasmids carrying the full-length GCP of SEOV Cherwell*

Several studies have demonstrated that proper trafficking of the viral glycoproteins through cells require that they are co-expressed, either through a single plasmid encoding the full-length GCP or through co-transfection of separate plasmids encoding Gn and Gc respectively (Shi and Elliott, 2002; Spiropoulou *et al.*, 2003; Deyde *et al.*, 2005) As such, plasmids expressing the full length M segment open reading frame of Seoul virus (SEOV) Cherwell (GenBank accession; KM948593.1) were produced by GeneArt Synthesis (Invitrogen). Using the NCBI BLAST® tool, the sequence of the SEOV Cherwell GCP was 99% identical at the protein level and 95% identical at the nucleotide level to the SEOV glycoprotein reference sequence (SEOV 80-39, NCBI reference sequence; NP_942557.1). The inserted gene in the eGFP-C1 vector was 3419bp, making the entire plasmid (vector + insert) 8097bp, and in the eGFP-N1 vector the inserted gene was 3416bp, making the entire plasmid 8074bp. Following large scale production of plasmid DNA stocks, the size of the gene inserts were confirmed by restriction digestion.

### *5.2.2 Transfection of HEK293T cells with plasmids containing the SEOV Cherwell GCP.*

To express viral glycoproteins for downstream analysis, HEK293T cells were seeded in six well plates and transfected with either eGFP-C1 as a positive control, eGFP-N1-GCP, eGFP-C1-GCP or were mock transfected. To establish that the procedure had been successful, cells were visualised under fluorescent microscope 16-24 hours following transfection. Cells transfected with the eGFP-N1-GCP plasmid exhibited high expression levels of GFP-tagged proteins, while cells transfected with the eGFP-C1-GCP plasmid exhibited a much lower transfection efficiency (figure 5.2A). As the GCP is co-translationally cleaved into Gc and Gn, this indicated good expression of Gc but poor expression of Gn

following transfection with plasmids encoding the full-length M segment open reading frame. The GCP of SEOV Cherwell has a molecular weight of approximately 125kDa, while Gn and Gc have approximate weights of 65-75kDa and 55kDa respectively. To further validate appropriate protein expression, the cells were lysed and proteins were extracted and subsequently visualised by western blotting using a GFP-specific antibody (figure 5.2B). GFP-tagged Gc was detected at with an expected molecular weight of approximately 80kDa, while the GFP-tagged Gn protein, with an expected combined molecular weight of approximately 95kDa, was not detected. This corroborated what had been observed by fluorescent microscopy. Due to these results, subsequent experiments were conducted using only the eGFP-N1-GCP plasmid.

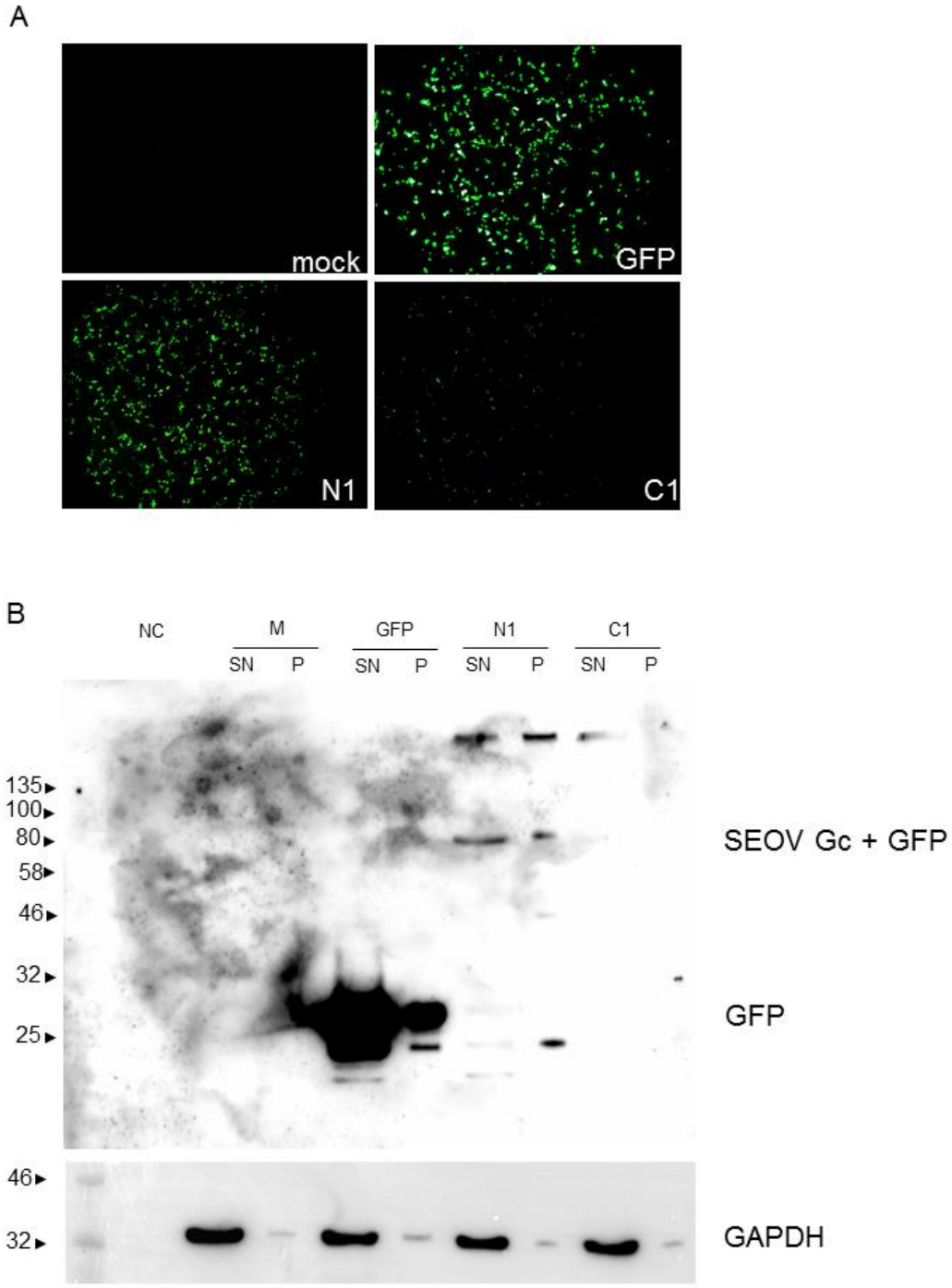


Figure 5.2 **A,** fluorescent microscopy visualizing GFP-tagged viral protein-expression 24 hours following calcium phosphate transfection of HEK293T cells. The expression of eGFP-N1-GCP was good (N1, bottom left), while the expression of eGFP-C1-GCP was poor (C1, bottom right). **B**, western blot for GFP-tagged Gn and Gc using a GPF-specific antibody. GAPDH was used as a loading control. The expected mw for GFP-Gc was 80kDA (55kDA + 27kDa). For GFP-Gn a band was expected, but not detected, at 95kDa (65kDa + 27kDa). The

high mw bands detected on the top of the blot could be heterodimers of Gn and Gc or possible multimers of one of the proteins. These unspecific high mw band could alternatively be IgG from the beads, as IgG has an approximate mw of 150kDa. Sn; supernatant, P; pellet, M; mock. GFP; GFP transfected, N1; eGFP-N1-GCP transfected, C1; eGFP-C1-GCP transfected, NC; negative control, GFP; green fluorescent protein, SEOV; seoul virus.

### *5.2.3 12 cellular proteins form associations with Gc*

To elucidate cellular interacting partners of Gc, HEK293T cells were seeded in 10cm dishes and transfected with either eGFP-C1, eGFP-N1-GCP, or were mock transfected. For each condition, transfections were performed in triplicate. Following successful transfection, as determined by fluorescent microscopy, the cells were lysed, and proteins were extracted and co-immunoprecipitated using GFP-trap (Chromotek) as detailed in chapter 2.14. Expression of the GFP-tagged Gc protein was validated by western blotting (figure 5.3), before the lysates were analysed by mass spectrometry (see chapter 2.7.2 and 2.7.3).

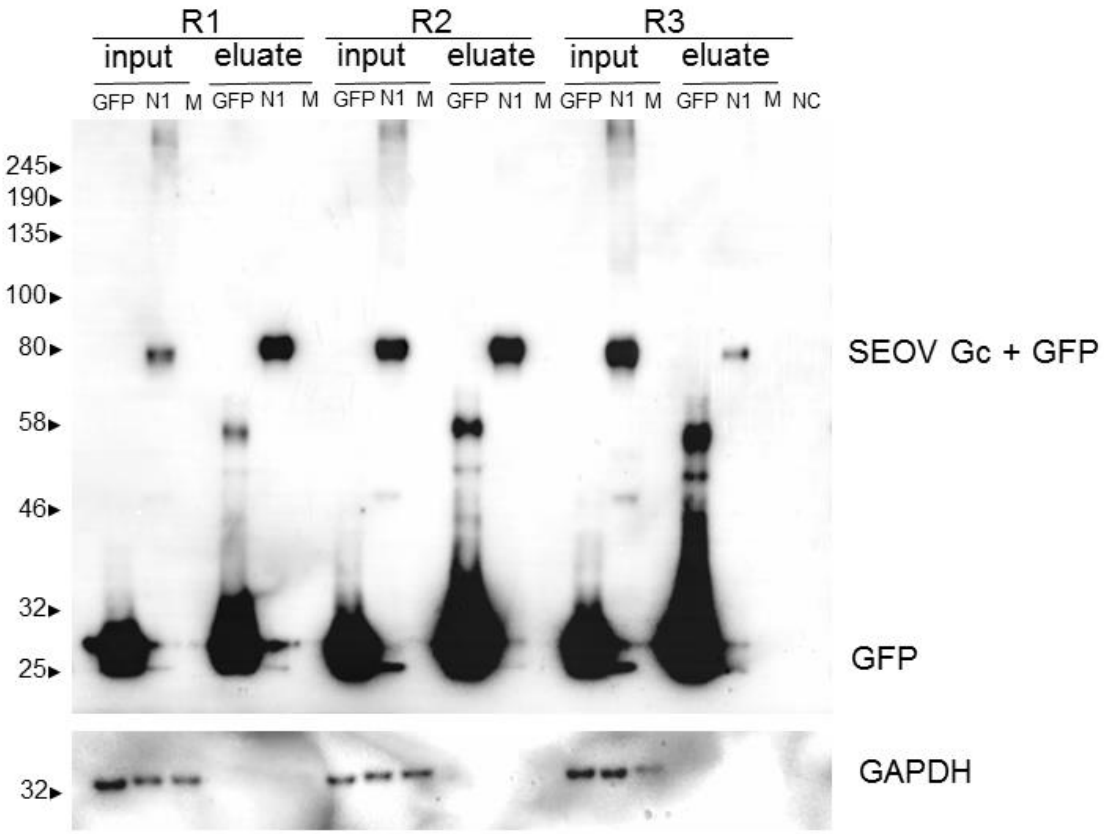


Figure 5.3. Western blot for Gc using a GFP-specific antibody. The expected band for Gc (with GFP-tag) was 80kDa. Transfections were done in triplicate, and protein extractions were performed with non-denaturing lysis buffer. GAPDH was used as a loading control. R1-R3; replicate one-three. GFP; GFP transfected. N1; eGFP-N1-GCP transfected. M; mock transfected. NP; negative control. GFP; green fluorescent protein, SEOV; seoul virus.

By mass spectrometric analysis 233 proteins were commonly identified across the three conditions. Filtering of the results to include only those proteins identified by ≥ 2 unique peptides left 211 proteins (appendix B.4). In a comparison of eGFP-N1-GCP and eGFP-C1 pulldowns, 12 proteins, excluding the viral glycoprotein itself, exceeded the threshold levels for fold change (FC) and p-value (FC > 2 and p-value < 0.05) required to be considered interacting partners of Gc (table 13, figure 5.4). Based on GO annotations the 12 identified proteins were functionally associated with mRNA processing, ER-translocation,

glycosylation, mitochondrial electron transport, ER-to-Golgi vesicular transport, and cell movement.

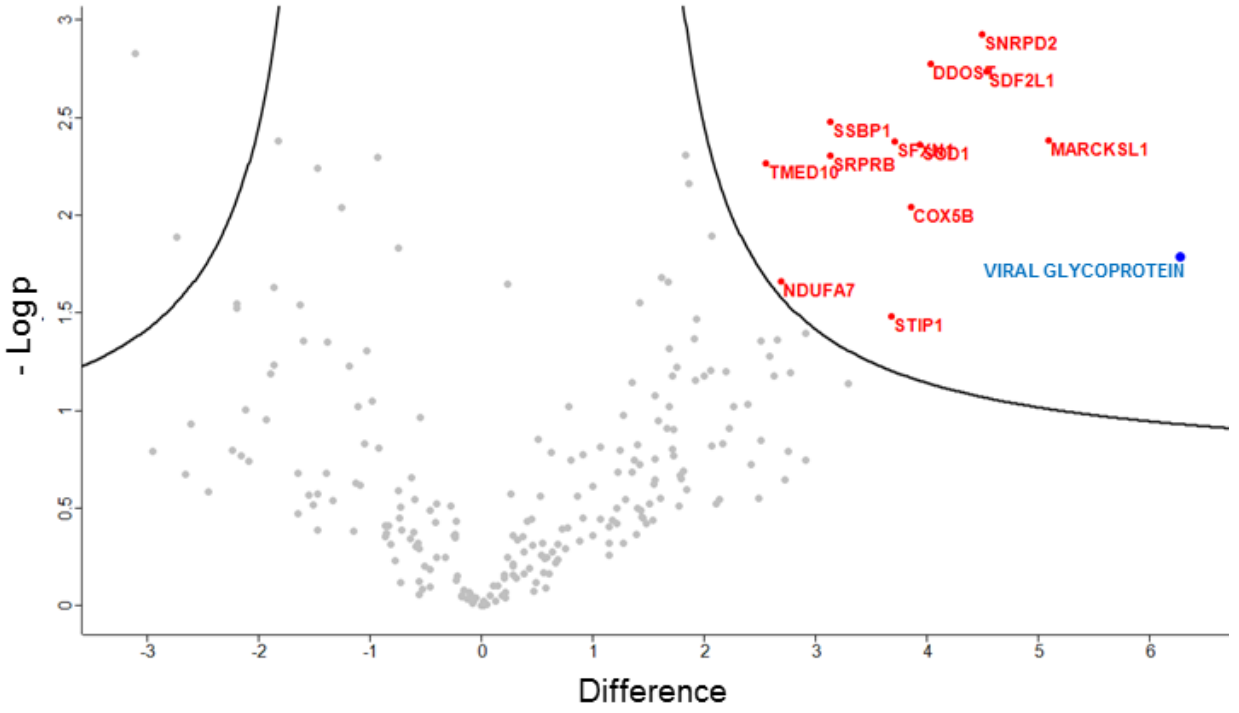


Figure 5.4. 12 cellular proteins co-immunoprecipitated Gc by GFP-trap. The point highlighted in blue is the viral glycoprotein. 12 proteins (in red and labelled) were identified as interactors of Gc. Thresholds for association were set at FC > 2 and p-value < 0.05. DDOST; Dolichyl-diphosphooligosaccharide--protein glycosyltransferase 48 kDa subunit , SNRPD2; Small nuclear ribonucleoprotein Sm D2, SDF2L1; Stromal cell-derived factor 2-like protein 1, SSBP1; Single-stranded DNA-binding protein, mitochondrial, MARCKS; MARCKS-related protein, COX5B; Cytochrome c oxidase subunit 5B, mitochondrial, SFXN1; Sideroflexin-1, SOD1; Superoxide dismutase [Cu-Zn], NDUFA7; NADH dehydrogenase [ubiquinone] 1 alpha subcomplex subunit 7, STIP1; Stress-induced-phosphoprotein 1, SRPRB; Signal recognition particle receptor subunit beta.

**Table 14. All proteins that co-immunoprecipitated with Gc**

| Protein names | Gene | GO term | Accession | FC | -log(P-value) |
|---|---|---|---|---|---|
| Small nuclear ribonucleoprotein Sm D2 | SNRPD2 | mRNA processing factor | P62316 | 4.5 | 2.93 |
| Dolichyl-diphosphooligosaccharide--protein glycosyltransferase 48 kDa subunit | DDOST | Glycosyltransferase | P39656 | 4.0 | 2.77 |
| Stromal cell-derived factor 2-like protein 1 | SDF2L1 | Mannosyl-transferase activity | Q9HCN8 | 4.5 | 2.74 |
| Single-stranded DNA-binding protein, mitochondrial | SSBP1 | DNA binding protein | Q04837 | 3.1 | 2.48 |
| MARCKS-related protein | MARCKS | Non-motor actin binding protein; Signaling molecule; Structural protein | P49006 | 5.1 | 2.39 |
| Sideroflexin-1 | SFXN1 | Cation transporter; Transfer/carrier protein | Q9H9B4 | 3.7 | 2.38 |
| Superoxide dismutase [Cu-Zn] | SOD1 | Oxidoreductase | P00441 | 3.9 | 2.37 |
| Transmembrane emp24 domain-containing protein 10 | TMED10 | Transfer/carrier protein; Vesicle coat protein | P49755 | 2.6 | 2.27 |

| | | | | | |
|---|---|---|---|---|---|
| Cytochrome c oxidase subunit 5B, mitochondrial | COX5B | Oxidase | P10606 | 3.9 | 2.05 |
| SEOV 80-39 | SEOVsMgp1 | Glycoprotein precursor | NP_942557.1 | 6.3 | 1.79 |
| NADH dehydrogenase [ubiquinone] 1 alpha subcomplex subunit 7 | NDUFA7 | Mitochondrial electron transport | O95182 | 2.7 | 1.66 |
| Stress-induced-phosphoprotein 1 | STIP1 | Chaperon | P31948 | 3.7 | 1.48 |
| Signal recognition particle receptor subunit beta | SRPRB | Receptor | Q9Y5M8 | 3.1 | 2.30 |

### *5.2.4 The cellular location of Gc corresponds with the ER*

To further validate the interaction of the identified host proteins with the viral glycoprotein, the intracellular location of Gc was investigated by immunofluorescent microscopy. By visual inspection the location of Gc was found to corresponded largely with that of the ER marker calnexin (figure 5.5), and to some extent with the Golgi marker giantin (figure 5.6). This correlated well with the functional annotation of several of the identified associated host proteins; Dolichyl-diphosphooligosaccharide--protein glycosyltransferase 48 kDa subunit (DDOST), Signal recognition particle receptor subunit beta (SRPRB) and Stromal cell-derived factor 2-like protein 1 (SDF2L1) are all ER-resident proteins, while Transmembrane emp24 domain-containing protein 10 (TMED10) is a protein involved in vesicular trafficking between the ER and Golgi complex, and Stress-induced-phosphoprotein 1 (STIP1) can also localize to the Golgi (Honore *et al.*, 1992;

Fukuda *et al.*, 2001; Potter and Nicchitta, 2002; Bonnon *et al.*, 2010; Roboti and High, 2012). However, by quantitative analysis using the Coloc2 plugin for FIJI to calculate the Pearson's correlation coefficient (PCC) of two probes (red / green and red / blue) there was good correlation of the GFP signal with the ER marker calnexin but only weak correlation between GFP and giantin (figure 5.8 and figure 5.9). Calnexin/GFP PCC = 0.76 and giantin/GFP PCC = 0.37. For both markers the PCC was close to 0 (i.e. no correlation, 1 = perfect correlation) with DAPI (table 15)(Schindelin *et al.*, 2012). By visual examination there seemed to be no significant overlap between expression of the viral glycoprotein and the mitochondrial marker TOM70 (figure 5.7), even though four (COX5B, NDFUA7, SDXN1 and SSBP1) of the 12 interactors identified by mass spectrometry were mitochondrial proteins. The PCC for TOM70/GFP was however 0.55, which indicated stronger correlation between GFP and TOM70 than between GFP and giantin (figure 5.10, table 15). However, as the PCCs for both TOM70 and giantin were in an intermediate range, it is difficult to make conclusions on the true correlation of GFP with these markers based on the above results.

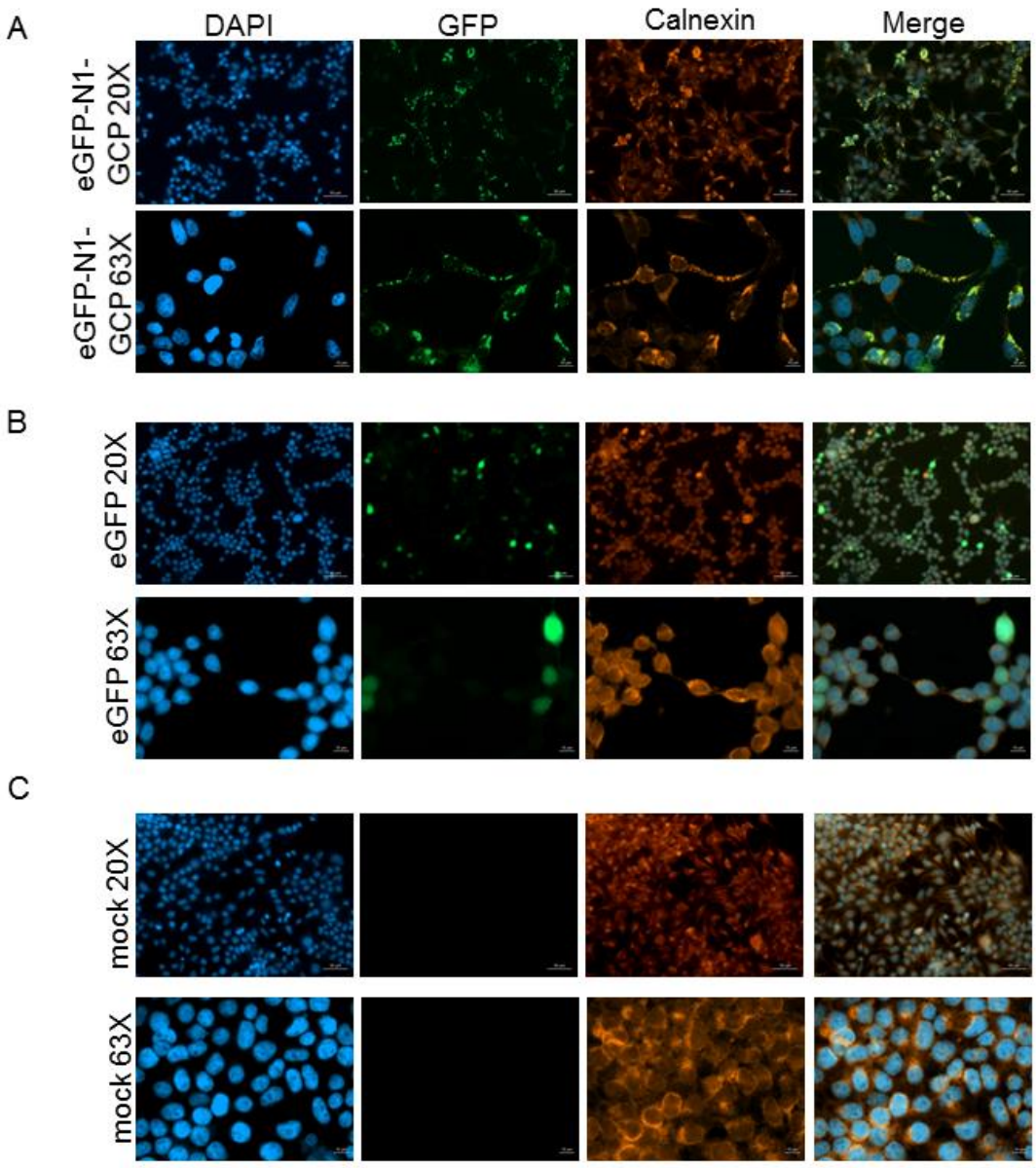


Figure 5.5. Immunofluorescent microscopy of transfected or mock transfected HEK293T cells. Cells were stained with DAPI for visualisation of the nucleus. Expression of the viral protein was determined by visualisation of GFP. Cells were co-stained with calnexin (ER marker). **A**, eGFp-N1-Cherwell-transfected cells at 20X at 63X magnification. **B**, eGFP-transfected cells at 20X and 63X magnification. **C**, mock-transfected cells at 20X and 63X magnification. GFP; green fluorescent protein.

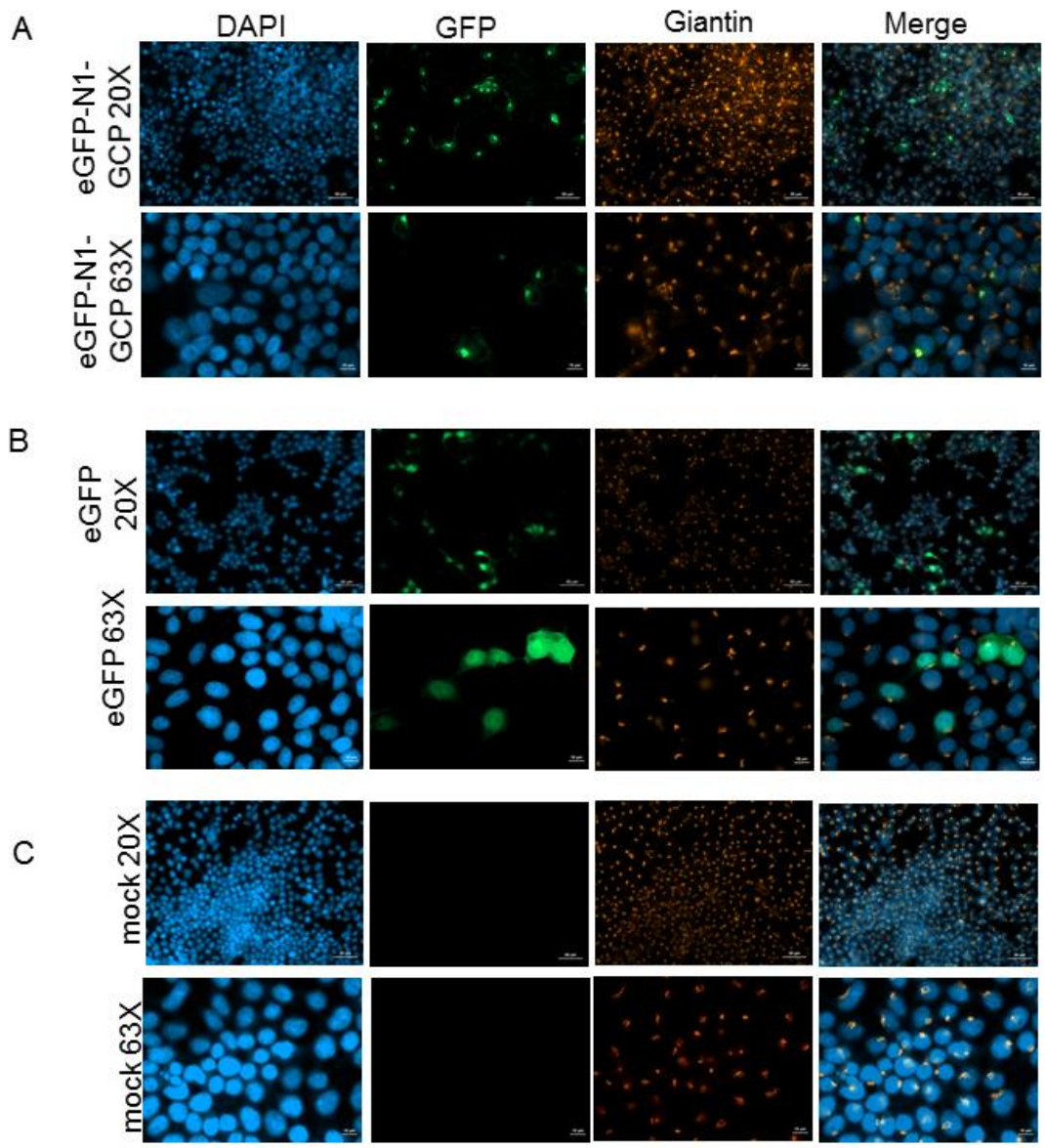


Figure 5.6. Immunofluorescent microscopy of transfected or mock transfected HEK293T cells. Cells were stained with DAPI for visualisation of the nucleus. Expression of the viral protein was determined by visualisation of GFP. Cells were co-stained with giantin (Golgi marker). **A**, eGFp-N1-Cherwell-transfected cells at 20X at 63X magnification. **B**, eGFP-transfected cells at 20X and 63X magnification. **C**, mock-transfected cells at 20X and 63X magnification. GFP; green fluorescent protein.

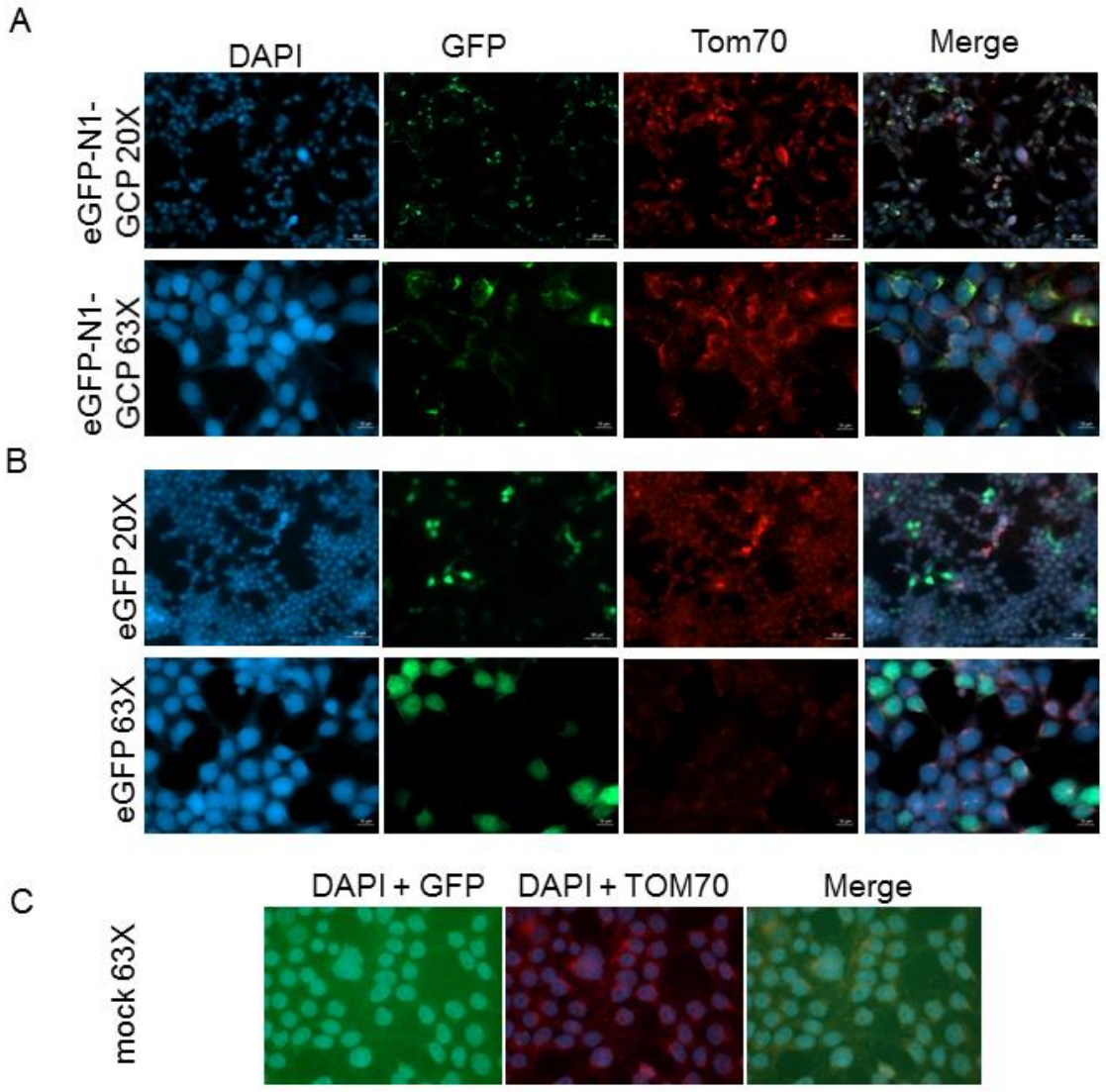


Figure 5.7. Immunofluorescent microscopy of transfected or mock transfected HEK293T cells. Cells were stained with DAPI for visualisation of the nucleus. Expression of the viral protein was determined by visualisation of GFP. Cells were co-stained with TOM70 (mitochondrial marker). **A**, eGFp-N1-Cherwell-transfected cells at 20X at 63X magnification. **B**, eGFP-transfected cells at 20X and 63X magnification. **C**, mock-transfected cells at 63X magnification. GFP; green fluorescent protein.

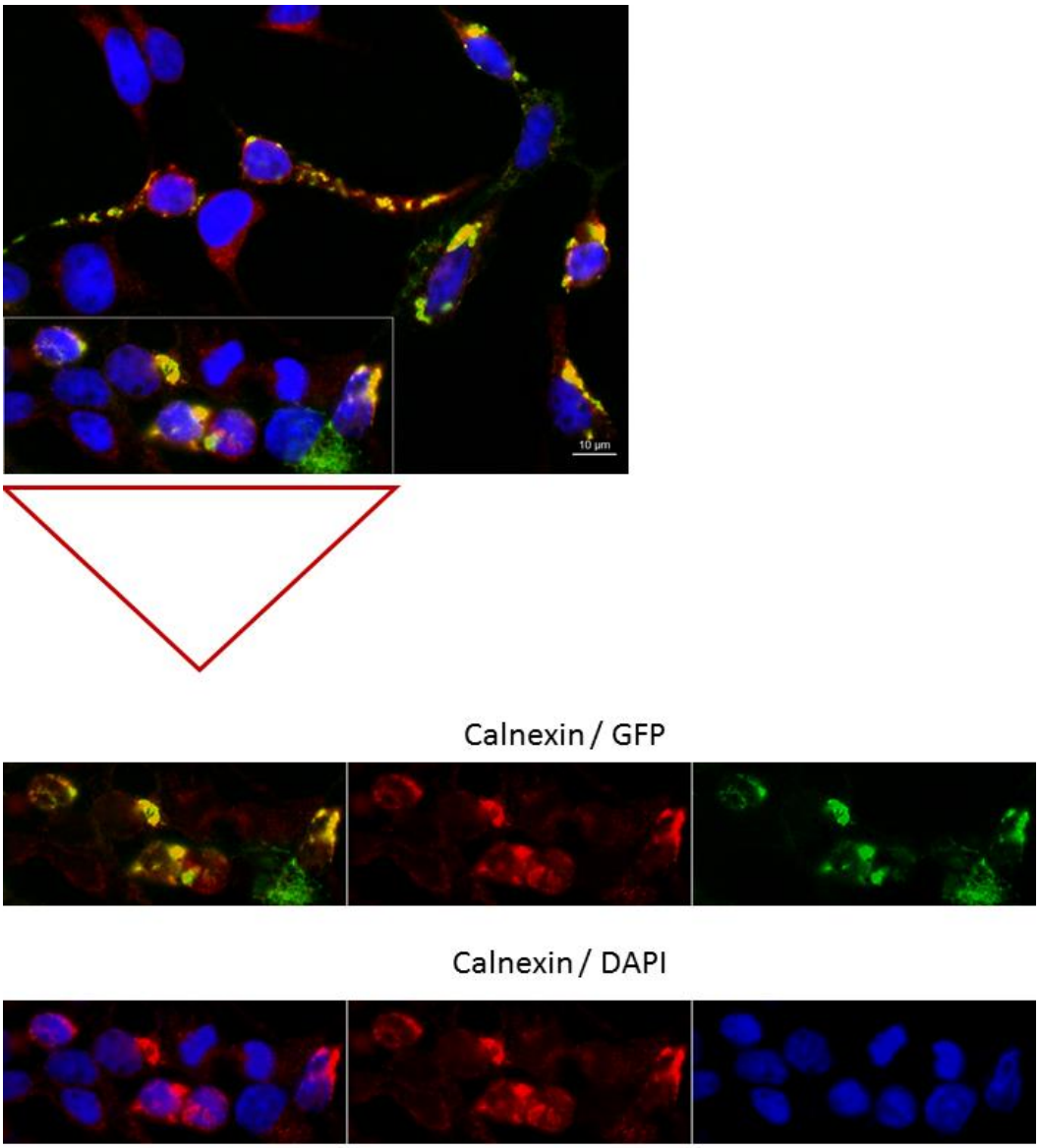


Figure 5.8. Immunofluorescence microscopy of eGFP-N1-Cherwell transfected HEK293T cells stained with Calnexin (ER marker) and DAPI (nuclear marker) at 63X magnification. Images were quantitatively analysed with the Coloc2 plugin for FIJI. The PCC for Calnexin/GFP = 0.76 and the above threshold PCC for Calnexin /DAPI = 0.23. GFP; green fluorescent protein.

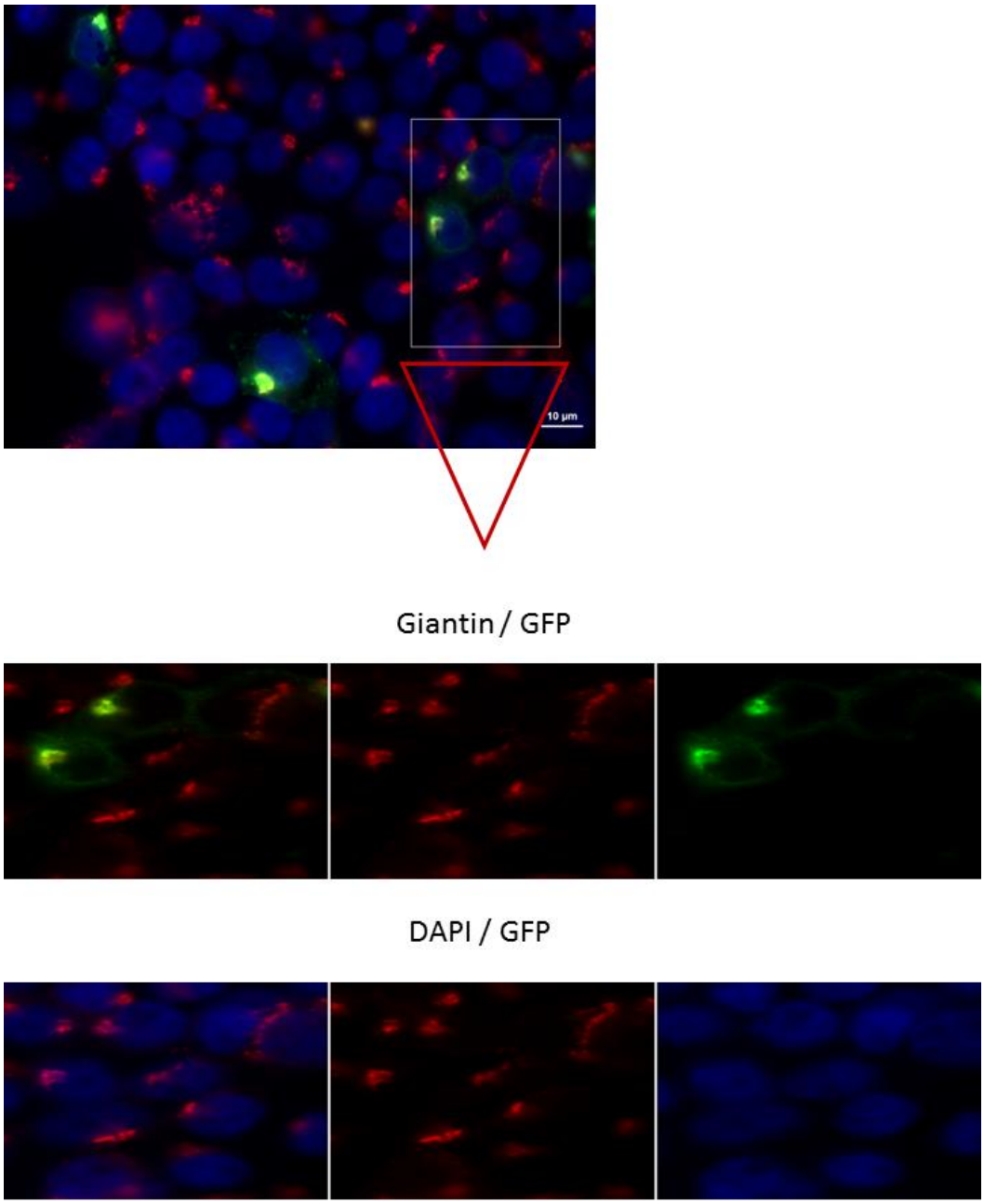


Figure 5.9. Immunofluorescence microscopy of eGFP-N1-Cherwell transfected HEK293T cells stained with giantin (Golgi marker) and DAPI (nuclear marker) at 63X magnification. Images were quantitatively analysed with the Coloc2 plugin for FIJI. The above threshold PCC for giantin/GFP = 0.37 and the above threshold PCC for giantin/DAPI = 0.01. GFP; green fluorescent protein.

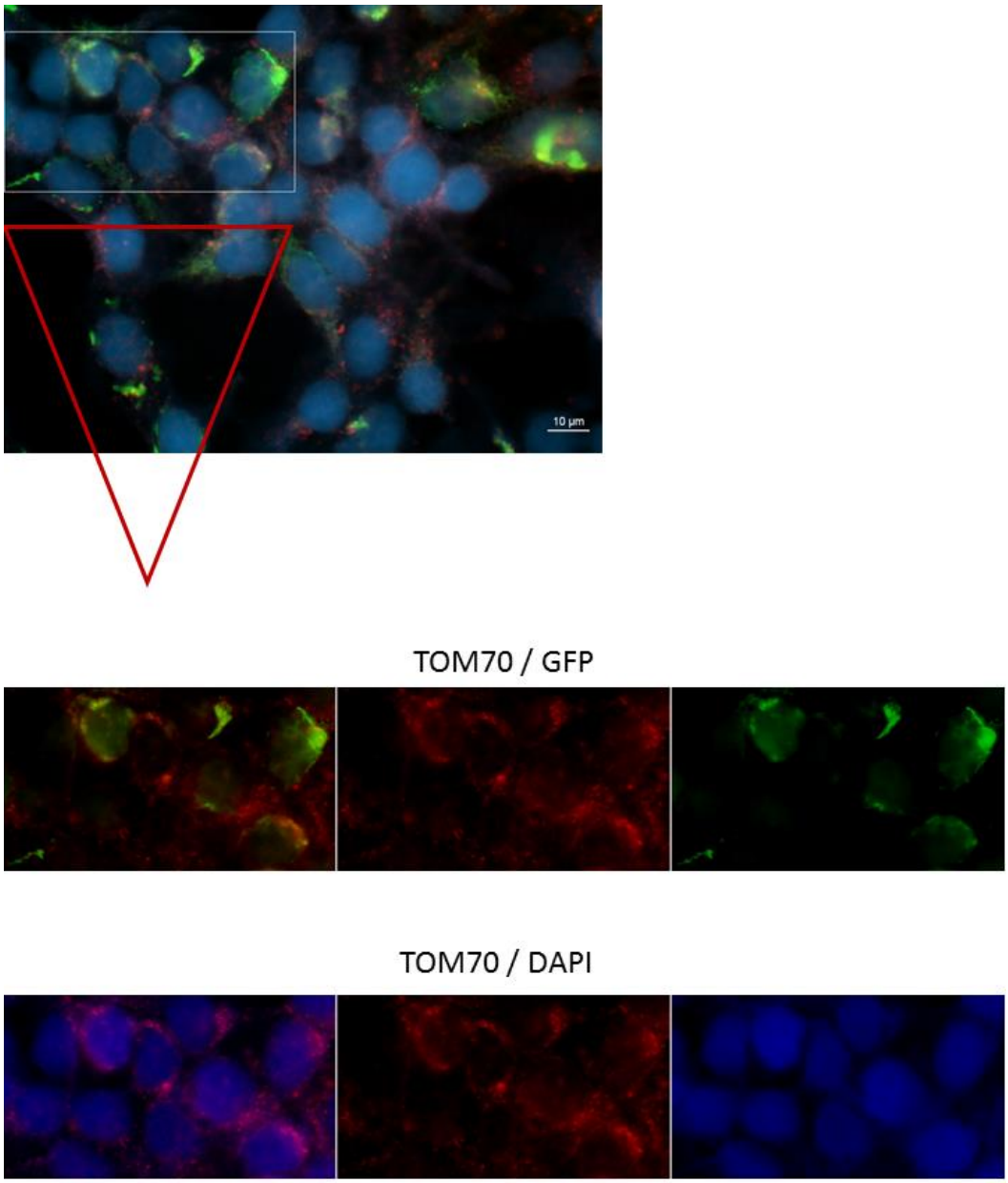


Figure 5.10. Immunofluorescence microscopy of eGFP-N1-Cherwell transfected HEK293T cells stained with TOM70 (mitochondrial marker) and DAPI (nuclear marker) at 63X magnification. Images were quantitatively analysed with the Coloc2 plugin for FIJI. The above threshold PCC for TOM70 /GFP = 0.55 and the above threshold PCC for giantin/DAPI = 0.18. GFP; green fluorescent protein.

**Table 15. Pearson's correlation co-efficient of GFP and DAPI with ER, Golgi and mitochondrial markers**

| Protein pairs | Pearson's correlation co-efficient |
|---|---|
| **Giantin / GFP** | 0.37 |
| **Giantin / DAPI** | 0.01 |
| **Calnexin / GFP** | 0.76 |
| **Calnexin/ DAPI** | 0.23 |
| **TOM70 / GFP** | 0.55 |
| **TOM70 / DAPI** | 0.18 |

### *5.2.5 Proteins of interest*

As the above results most strongly supported ER localisation of Gc, initial proteins of interest among the 12 identified interactors were postulated to be ER resident proteins based on GO annotation and network analysis using Reactome© 2017 and STRING© version 10.5.

#### 5.2.5.1 Endoplasmic reticulum

DDOST and SRPBP (table 14) are both involved in the process of signal receptor particle (SRP) – dependent co-translational translocation of polypetides from the cytosol to the ER lumen (figure 5.8). DDOST is a component of the ER resident translocon complex TRAP, which facilitates the transport of polypeptides to the ER lumen(Potter and Nicchitta, 2002). SRPBP acts upstream of TRAP, binding a complex consisting of the signal receptor particle in association with ribosomal proteins that are in the process of translating mRNA (Potter and Nicchitta, 2002). DDOST also has an essential role in N-linked glycosylation, as a subunit of the N-oligo-saccharyl transferase complex (OST), a complex that catalyses the transferee of high mannose oligosaccharides to the N-glycan associated signal sequence Asn-X-Ser/Thr

(Roboti and High, 2012). SDF2L1 (table 14) is also linked to the process of glycosylation. It is a component of the dolychyl-phosphate mannosyltransferase (figure 9B). Dolychol-phosphate mannosyltransferase subunit 1, a catalytic subunit of this complex embedded in the ER, was also identified in the dataset, though not in association with Gc (appendix B.4). In addition to glycosylation, SDF2L1 is also involved in the unfolded protein response (figure 5.9B).

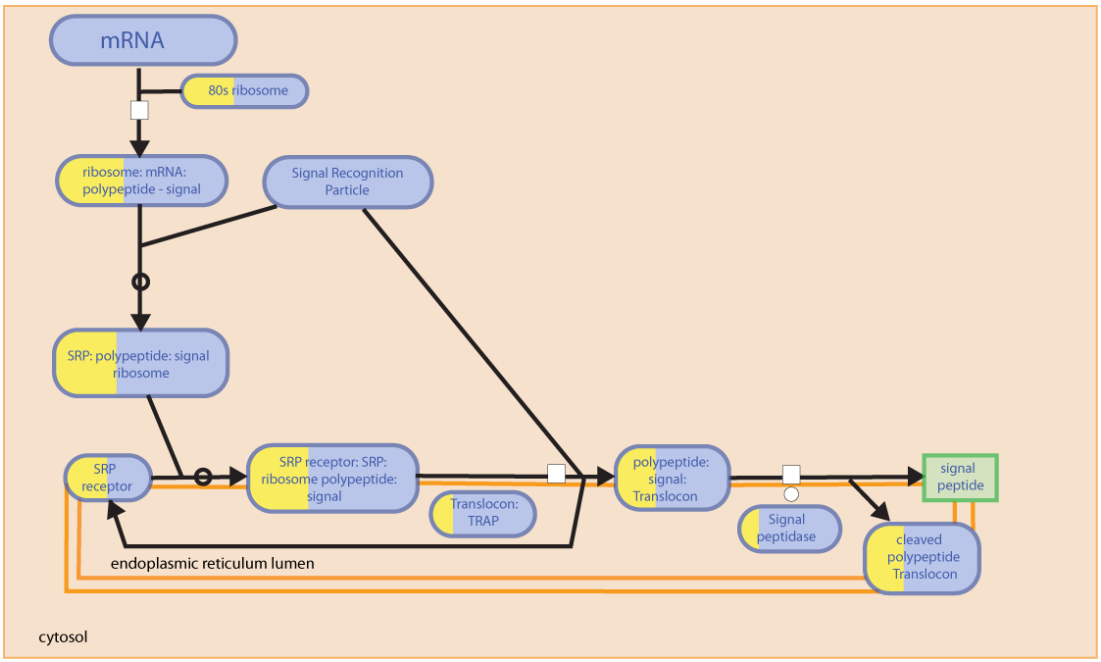


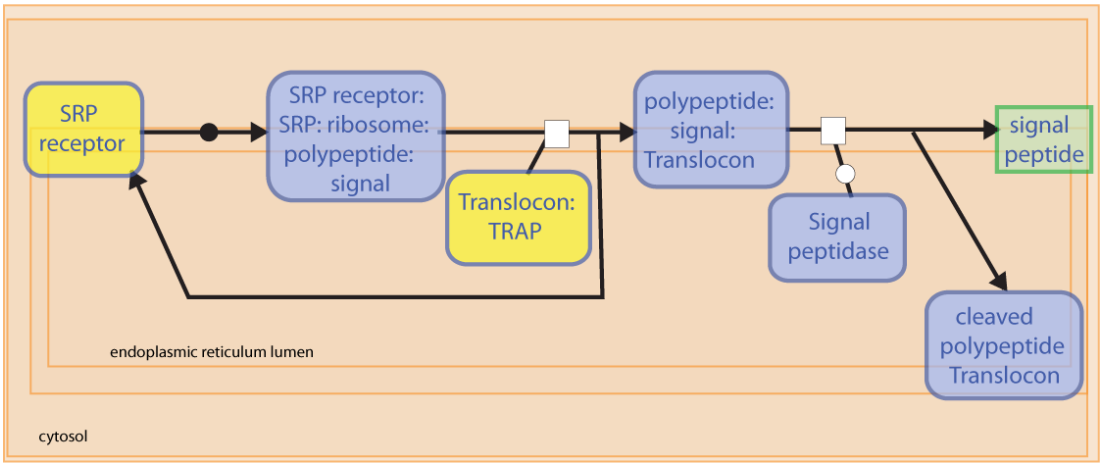


Figure 5.11. **Above**, overview of the pathway leading to co-translational translocation of proteins to the ER lumen. Boxes with yellow highlights represent complexes/components of the pathway for which identifiable proteins were present in the cell lysates analysed by

mass spectrometry. **Below**, detail of ER-specific part of the pathway. Orange boxes mark the protein-complexes of which SRPBP (SRP receptor) and DDOST (Translocon:TRAP) are components. (May, B, Gopinathrao,G (2008). Image for “SPR-dependent cotranslational protein target to membrane” pathway. Reactome© 2017. StableID: R-HSA1799339.).

## *5.3 Discussion*

In this study the interactome of SEOV Cherwell glycoproteins in HEK293T cells were investigated. 12 proteins were found to associate with the Gc subunit of the GCP, and GO annotation revealed that several of these proteins were functionally associated with cellular processes already known to be involved in orthohantaviral glycoprotein trafficking and maturation (Shi and Elliott, 2002; Spiropoulou *et al.*, 2003; Deyde *et al.*, 2005). Both DDOST and SDF2L are proteins involved in the process of glycosylation and might speculatively be cellular factors required for the proper glycosylation and assembly of orthohantaviral proteins in the ER prior to exit. In particular the link between DDOST and the N-glycan sequence motif Asn-X-Ser/Thr marks this protein as an interesting protein for follow-up. Orthohantaviral glycoproteins contain several of these conserved motifs (Shi and Elliott, 2004). N-glycosolation is essential for the proper functioning of orthohantaviral glycoproteins, with site specific mutations of these conserved N-glycan signal motifs resulting in proteins without the ability to form heterodimers or traffic through the cell, and that exhibit impaired antigenic properties (Shi and Elliott, 2004). Furthermore, DDOST and SDF2L1 have both previously been reported to associate with ANDV glycoproteins (Klaus et al). DDOST is a component of the TRAP translocon, a protein complex that facilitates transport of proteins to the ER lumen. Silencing of SEC61B, also a component of TRAP, reduced the detection of La Crosse Virus in HEK293T cells by approximately 25 % (Zhang *et al.*, 2017). La Crosse Virus is also a Bunyavirus, and like members of the Hantaviridae genus carries a genomic segment that codes for two glycoproteins in a single open reading frame (Pekosz *et al.*, 1995). SEC61B did not bind to SEOV Gc in our study (appendix B.4), but as DDOST and SRPBP are both involved in the same pathway as SEC61B, it is possible to speculate that inhibition of components of this pathway could have the same effect on the turn-over of orthohantaviruses as was observed for La Crosse Virus.

Localisation of the viral glycoproteins at the ER was observed to a much greater extent in this study than that reported by others (Shi and Elliott, 2002; Kariwa *et al.*, 2003; Spiropoulou *et al.*, 2003; Deyde *et al.*, 2005). It is possible that this observation was due to an unfolded protein response, which would cause retention of the proteins in the ER. This scenario was supported by the interaction of Gc with SDF2L1, which is involved in the unfolded protein response pathway. It is also feasible that Gc was retained in the ER due to a lack of interaction between Gc and Gn, because of inefficient expression of Gn or its rapid degradation. Interaction between Gc and Gn is necessary for their transport away from the ER (Shi and Elliott, 2002; Spiropoulou *et al.*, 2003; Deyde *et al.*, 2005). TULV infection of VeroE6 cells seemingly induces the unfolded protein response, and there is evidence that a certain amount of viral glycoproteins are retained in the ER following orthohantaviral infection; Gn tends to form high molecular weight aggregates, and the high mannose glycosylation of Gn and Gc and their association with calnexin and calreticulin points to a failure of passing the ER-control for properly folded proteins (Shi and Elliott, 2002; Spiropoulou *et al.*, 2003; Li *et al.*, 2005). It has been reported that expression of the viral N protein, or S segment RNA, rescues SNV Gn expression following transfection, raising the possibility that the accumulation of N protein induces a switch from Gn degradation to Gn accumulation (Ganaie and Mir, 2014). HNTV Gc has also been reported to traffic differently when expressed by transfection compared to infection, and co-transfection of the N protein and Gc results in a trafficking pattern that more closely resembles that observed following natural infection (Shimizu *et al.*, 2013). As such, it is possible that the absence of N protein in the above study resulted in impaired Golgi trafficking. It would be interesting to investigate if co-expression of the N protein with the glycoproteins would impact on the cellular localisation of the latter. The low levels of correlation between the Golgi marker giantin and GFP could also possibly be explained by the fairly low expression level of GFP, which as seen in figure 5.6 and 5.8, is only expressed in a low number of cells. Additionally,

in figure 5.3, it can be observed that the expression of the GFP-tagged viral protein was inconsistently expressed across replicates. Finally, it is possible that SEOV Cherwell glycoproteins aggregate to a greater extent at the ER membrane than is the case for other species of orthohantaviruses. Studies considering the trafficking and maturation of glycoproteins have not been performed using this particular strain of orthohantavirus before, and viral budding at the ER has previously been observed in VeroE6 cells for a specific species of HNTV (Xu 2017).

Four mitochondrial proteins were found to bind Gc. However, the results of immunofluorescence analysis were inconclusive for mitochondrial localisation of the viral protein, with an intermediate value obtained for quantitative analysis. This discrepancy could possibly be explained by the interaction of Gc with the protein SOD1. This protein is involved in the turn-over of toxic radicals produced by the mitochondria, and reportedly associates with COX5B, PRDX1 and NDUFA7 (figure 9C). Possibly the identification of these mitochondrial proteins does not reflect a direct interaction with Gc, but rather an association between them and another protein that interacts with Gc, i.e. SOD1. It's also possible that these interactions are the result of non-specific interactions with the viral protein or the associated GFP-tag. It is possible these mitochondrial proteins have been released into the cytosol and become available for unspecific binding as a result of the stress put on the cells during the experimental procedures.

To progress the above findings, the next step would be reverse pull-downs, i.e. determine if the viral proteins will reciprocally bind to the cellular proteins if the latter are used as the GFP-tagged bait proteins in immunoprecipitation. The initial focus would be on validating the interactions with the ER resident proteins, as these are the cellular structures the viral protein localised to. In addition it would be necessary to reimage the cells with better optimised parameters, so that further statistical tests could be reliable utilised,

providing stronger evidence for potential correlation and co-occurrence. As the PCC is less sensitive to differences in mean intensities between the probes and is less dependent on threshold values than the Manders split coefficients, the PCC was deemed the most appropriate coefficient to use for the images analysed above.

It is necessary to address the question of why the viral protein was poorly expressed from the plasmid in which the GFP-tag was linked to the Gn region of the GCP (eGFC-C1-GCP), while it was efficiently expressed from the plasmid in which the GFP-tag was linked to the Gc region (eGFP-N1-GCP). As Gn and Gc are both expressed from the same gene segment, and they need to form hetero-oligomeric interactions to traffic to cellular assembly sites and be expressed on the viral envelope, the intuitive assumption would be that they are expressed at similar levels in the cell. It is not possible from the above investigation to determine if the observed difference in Gc and Gn expression was a consequence of an inherently lower production of Gn, Gn being degraded to a larger degree than Gc, or if it was due to the GFP-tag interfering with protein expression when located at the N-terminus of the viral GCP. As sequencing was not done following large-scale production of viral DNA stocks, it is also possible that mutations occurred in the aa sequence of the viral protein at this step of the process, resulting in an aberrant viral protein. In a study looking at the cellular processing of Sin Nombre virus (SNV) glycoproteins, Gn was similarly detected at lower levels than Gc following transfection with a plasmid encoding the GCP (Spiropoulou *et al.*, 2003). It is possible that the reduced expression of Gn is a consequence of a selective degradation of this protein in the cell, and that this is a tactic for the virus to specifically control Gn turn-over for efficient viral replication. In HeLa cells the autophagosome machinery degrades SNV Gn, and SNV replication in HUVECs is dramatically reduced when either formation of autophagosomes or their degradative pathway is inhibited (Hussein et al 2012). Inhibition of the autophagosome machinery has, conversely, no effect on the expression of Gc. SNV Gn also

seems to aggregate in Lamp-1 containing cellular compartments when expressed from GCP or following viral infection (Spiropoulou *et al.*, 2003). LAMP-1 is a late-endosomal/lysosmal marker and this co-localisation has been postulated to represent lysosomal degradation of Gn. LAMP-1 co-localises with the autophage marker LC3 when autophage maturation is induced, and as such these results could be consistent with the former observations of autophagic clearance of Gn (Spiropoulou *et al.*, 2003; Jackson *et al.*, 2005). Autophagosomes are involved in several aspects of immunity, e.g. direct clearance of microbes, responding to inflammation, secretion of immune mediators, and antigen presentation (Deretic *et al.*, 2017). As such it is unsurprising that infecting pathogens have developed ways of circumventing their activity. For instance, several positive-sense RNA viruses seem to utilize the autophagosomal machinery for their benefit (Jackson *et al.*, 2005; Richards and Jackson, 2013; Shi *et al.*, 2016). *In vitro,* inhibiting the formation of autophagasome-like vesicles negatively affect the yield of poliovirus, rhinovirus and coxsacivirus B3.

It would be interesting to compare the findings of this study with the interactome of SEOV Cherwell glycoproteins in a second cell line. HUVECs would be ideal, as they are frequently used in studies of orthohantavirus infection, and as an endothelial cell line represent the major target cell for orthohantaviruses (Gavrilovskaya *et al.*, 2008). It would also be interesting to compare the interactome of SEOV, a cause of moderate HFRS in humans, with that of PUUV (NE), DOBV/HNTV (severe HFRS) and SNV/ANDV (HPS). Finally, comparing the interactome of SEOV in human and rat cell lines could possibly give insights into cellular factors that explain why human infection results in illness and viral clearance, while rats become persistently infected in the absence of clinical symptoms.

## *5.4 Conclusion*

In this hypothesis generating study, 12 cellular proteins were identified as interacting partners with recombinant SEOV Cherwell Gc in HEK293T cells. Using immunofluorescent microscopy, recombinant Gc was predominantly observed at the ER . This cellular localisation of Gc proved to be in line with the functional annotation of several of the identified binding proteins, of which three were ER resident. It still remains to further validate these protein interactions before more specific conclusions can be drawn. Speculatively, some of the associations described in this chapter could be indicative of cellular mechanisms involved in the maturation of the viral glycoproteins. In addition to advancing this work by validating the above results, this study has raised questions about the processing of the two viral glycoproteins that would be of interest to pursue further. The different turn-over of Gc and Gn has been reported by others, and it would be interesting to follow up the discrepancies in protein expression observed for the two different plasmids used in this study, in an effort to shed more light on mechanisms involved in the regulation of the viral life cycle.

# *Chapter 6: Conclusion*

The aims of this thesis were to use label-free proteomics to analyse orthohantavirus- positive human sera in an effort to discover biomarkers of HFRS infection caused by SEOV, and to investigate the cellular interactome of recombinant SEOV Cherwell glycoproteins, with the aim of gaining further insights into the mechanism involved in the processing of the viral proteins and the cellular protein interactions they formed.

Two strategies were used to examine the first of these aims:

1. Directly comparing the proteomes of a group of orthohantavirus-infected sera with non-infected sera and select biomarker candidates from among the proteins with significant differences in abundance between the two groups.

2. A proteomic case study in which abundance changes in the proteome of a single individual was followed during the course of a clinical HFRS infection and subsequently compared with a seronegative and convalescent sample obtained from the same individual, to identify proteins with abundance changes that correlated with disease.

By using a proteomic method to analyse changes in the serum proteome unique insights into protein alterations in response to orhtohantavirus infection have been made. The analysis of the longitudal sample set has allowed for novel insights into real-time changes during the course of active disease and recovery. These findings can be built on to gain a better understanding of the pathogenesis underlying HFRS. The glycoprotein afamin was investigated as a biomarker candidate based on initial findings of decreased abundance in seropositive samples compared to controls, though validation attempts of this finding produced conflicting results. No difference in afamin abundance was observed in a validation cohort of seven seropositive against eight seronegative samples. However, the relative abundance of afamin was observed to fluctuate in a temporal analysis of

longitudinal sera, with observed abundance changes temporally coinciding with disease progression. These discrepancies warrant further investigation into the response, or lack thereof, of afamin to acute orthohantavirus infection. Ideally this would be investigated in samples with well-defined times of sampling relative to infection, so as to take into account the transient nature of the abundance changes observed in the longitudinal sera. Galectin 3-binding protein was also investigated as a biomarker candidate, based on temporal analysis of sequential sera from a single individual. In addition to afamin, it would be very interesting to widen the investigation to include other proteins identified in this study, e.g. angiotensinogen which is intricately linked to hemostastis and kidney function, and properdin and lumican, which are proteins involved in the immune respons. It would also be interesting to further investigate the apparent differences discovered in convalescent samples compared to seronegative in this study, to investigate the potential for chronic complications associated with SEOV. Chronic complications are not an extensively studied area of orthohantavirus infections, and the results of studies looking at long term sequalae are controversial.

The increased abundance of G3BP in orthohantavirus infection was successfully validated in a larger, independent sample cohort. G3BP has been associated with PUUV infection and clinical symptoms of NE by others, and our results further support its relevance to orthohantaviral disease. We also found that leptospira-infected sera presented with elevated abundance of G3BP compared to controls, implicating G3PB in a generic response to infection The results of this study further support G3BPs role in the host response to acute infections in which an activated vascular endothelium is a characteristic feature. As mentioned above for afamin, it would be interesting to further investigate some of the other proteins identified in addition to G3BP. HNTV infection of endothelial cells has been shown by others to induce VCAM. This protein was, like G3BP, found to be elevated in the sera of the pregnant patient during acute disease and in the

single acute sample from the single-time-point cohort. VCAM mediates cell:cell adhesion, and as such it can be hypothesised that its alteration in response to orthohantavirus infection plays a direct role in the systemic vascular leakage characteristic of HFRS and HPS. For both afamin and G3BP, larger sample numbers would be required to confidently validate whether consistent abundance changes in relation to acute orthohantavirus infection occur, before speculations about their clinical utility could be further investigated.

The second part of the thesis focused on exploring the interactome of the SEOV Cherwell glycoprotein in a human kidney cell line. Using immunoprecipitation, mass spectrometry and cellular localisation studies, eight cellular proteins were identified as potential interacting partners of SEOV Gc in HEK293T cells. Functional annotation and network analysis revealed that several of these potential binding partners were involved in processes known to be required for the maturation of orthohantaviral proteins. A final validation step determining the specificity of the identified interactions, using reverse co-immunoprecipitation, remains to be done. If these findings are successfully validated, further studies could be pursued looking into the functional and biological relevance of these interactions and their associated pathways, by e.g. disrupting protein:protein interactions.

## *References*

Acuna, R., Bignon, E. A., Mancini, R., Lozach, P.-Y. and Tischler, N. D. (2015) 'Acidification triggers Andes hantavirus membrane fusion and rearrangement of Gc into a stable post-fusion homotrimer.', *The Journal of general virology*. England, 96(11), pp. 3192–3197. doi: 10.1099/jgv.0.000269.

Aktas, B., Kasimir-Bauer, S., Wimberger, P., Kimmig, R. and Heubner, M. (2013) 'Utility of mesothelin, L1CAM and afamin as biomarkers in primary ovarian cancer', *Anticancer Research*, 33(1), pp. 329–336. doi: http://dx.doi.org/10.1007/BF00783426.

Alff, P. J., Gavrilovskaya, I. N., Gorbunova, E., Endriss, K., Chong, Y., Geimonen, E., Sen, N., Reich, N. C. and Mackow, E. R. (2006) 'The pathogenic NY-1 hantavirus G1 cytoplasmic tail inhibits RIG-I- and TBK-1-directed interferon responses.', *Journal of virology*, 80(19), pp. 9676–9686. doi: 10.1128/JVI.00508-06.

Alff, P. J., Sen, N., Gorbunova, E., Gavrilovskaya, I. N. and Mackow, E. R. (2008) 'The NY-1 Hantavirus Gn Cytoplasmic Tail Coprecipitates TRAF3 and Inhibits Cellular Interferon Responses by Disrupting TBK1-TRAF3 Complex Formation', *Journal of Virology*, 82(18), pp. 9115–9122. doi: 10.1128/JVI.00290-08.

Alge, J. L. and Arthur, J. M. (2015) 'Biomarkers of AKI: A review of mechanistic relevance and potential therapeutic implications', *Clinical Journal of the American Society of Nephrology*, 10(1), pp. 147–155. doi: 10.2215/CJN.12191213.

Anderson, N. L. and Anderson, N. G. (2002) 'The human plasma proteome: history, character, and diagnostic prospects.', *Molecular & cellular proteomics : MCP*. American Society for Biochemistry and Molecular Biology, 1(11), pp. 845–867. doi: 10.1074/MCP.R200007-MCP200.

Antonen, J., Leppanen, I., Tenhunen, J., Arvola, P., Makela, S., Vaheri, A. and Mustonen, J. (2013) 'A severe case of Puumala hantavirus infection successfully treated with bradykinin receptor antagonist icatibant.', *Scandinavian journal of infectious diseases*, 45(6), pp. 494–496. doi: 10.3109/00365548.2012.755268.

Atkinson, B., Jameson, L. J., Bovill, B. A., Aarons, E. J., Clewlow, J., *et al.* (2015) 'A non-fatal case of hantavirus cardiopulmonary syndrome imported into the UK (ex Panama), July 2014', *Journal of Clinical Virology*. Elsevier Science, 67, pp. 52–55. doi: 10.1016/j.jcv.2015.04.007.

Battisti, A. J., Chu, Y.-K., Chipman, P. R., Kaufmann, B., Jonsson, C. B. and Rossmann, M. G. (2011) 'Structural studies of Hantaan virus.', *Journal of virology*, 85(2), pp. 835–841. doi: 10.1128/JVI.01847-10.

Bauer, J. W., Baechler, E. C., Petri, M., Batliwalla, F. M., Crawford, D., *et al.* (2006) 'Elevated serum levels of interferon-regulated chemokines are biomarkers for active human systemic lupus erythematosus.', *PLoS medicine*, 3(12), pp. e491–e491. doi: 10.1371/journal.pmed.0030491.

Bergstedt Oscarsson, K., Brorstad, A., Baudin, M., Lindberg, A., Forssén, A., Evander, M., Eriksson, M. and Ahlm, C. (2016) 'Human Puumala hantavirus infection in northern Sweden; increased seroprevalence and association to risk and health factors', *BMC Infectious Diseases*. BMC Infectious Diseases, 16(1), p. 566. doi: 10.1186/s12879-016-1879-2.

Bharadwaj, M., Nofchissey, R., Goade, D., Koster, F. and Hjelle, B. (2000) 'Humoral immune responses in the hantavirus cardiopulmonary syndrome.', *The Journal of infectious diseases*, 182(1), pp. 43–48. doi: 10.1086/315657.

Bihorac, A., Chawla, L. S., Shaw, A. D., Al-Khafaji, A., Davison, D. L., *et al.* (2014)

'Validation of cell-cycle arrest biomarkers for acute kidney injury using clinical adjudication.', *American journal of respiratory and critical care medicine*, 189(8), pp. 932–939. doi: 10.1164/rccm.201401-0077OC.

Billecocq, A., Coudrier, D., Boue, F., Combes, B., Zeller, H., Artois, M. and Bouloy, M. (2003) 'Expression of the nucleoprotein of the Puumala virus from the recombinant Semliki Forest virus replicon: characterization and use as a potential diagnostic tool.', *Clinical and diagnostic laboratory immunology*, 10(4), pp. 658–663.

Bondu, V., Schrader, R., Gawinowicz, M. A., McGuire, P., Lawrence, D. A., Hjelle, B. and Buranda, T. (2015) 'Elevated Cytokines, Thrombin and PAI-1 in Severe HCPS Patients Due to Sin Nombre Virus', *Viruses*. Edited by E. O. Freed. MDPI, 7(2), pp. 559–589. doi: 10.3390/v7020559.

Bondu, V., Wu, C., Cao, W., Simons, P. C., Gillette, J., Zhu, J., Erb, L., Zhang, X. F. and Buranda, T. (2017) 'Low-affinity binding in cis to P2Y2R mediates force-dependent integrin activation during hantavirus infection.', *Molecular biology of the cell*, 28(21), pp. 2887–2903. doi: 10.1091/mbc.E17-01-0082.

Bonnon, C., Wendeler, M. W., Paccaud, J.-P. and Hauri, H.-P. (2010) 'Selective export of human GPI-anchored proteins from the endoplasmic reticulum', *Journal of Cell Science*, 123(10), pp. 1705–1715. doi: 10.1242/jcs.062950.

Borges, A. A., Campos, G. M., Moreli, M. L., Moro Souza, R. L., Saggioro, F. P., Figueiredo, G. G., Livonesi, M. C. and Moraes Figueiredo, L. T. (2008) 'Role of mixed Th1 and Th2 serum cytokines on pathogenesis and prognosis of hantavirus pulmonary syndrome.', *Microbes and infection*, 10(10–11), pp. 1150–1157. doi: 10.1016/j.micinf.2008.06.006.

Borges, A. A., Donadi, E. A., Campos, G. M., Moreli, M. L., de Sousa, R. L. M., *et al.*

(2010) ‘Association of -308G/A polymorphism in the tumor necrosis factor-α gene promoter with susceptibility to development of hantavirus cardiopulmonary syndrome in the Ribeirão Preto region, Brazil’, *Archives of Virology*, 155(6), pp. 971–975. doi: 10.1007/s00705-010-0655-7.

Bouchard, J., Malhotra, R., Shah, S., Kao, Y.-T., Vaida, F., *et al.* (2015) ‘Levels of protein C and soluble thrombomodulin in critically ill patients with acute kidney injury: a multicenter prospective observational study.’, *PloS one*, 10(3), pp. e0120770–e0120770. doi: 10.1371/journal.pone.0120770.

Brenner, B. (2004) ‘Haemostatic changes in pregnancy’, *Thrombosis Research*, 114(5–6 SPEC. ISS.), pp. 409–414. doi: 10.1016/j.thromres.2004.08.004.

Briese, T., Alkhovsky, S., Beer, M., Calisher, C., Charrel, R. and Al., E. (2016) ‘Create a new order, Bunyavirales, to accommodate nine families (eight new, one renamed) comprising thirteen genera.’, (September), p. 46. doi: 10.13140/RG.2.2.27230.23368.

Buranda, T., Basuray, S., Swanson, S., Agola, J., Bondu, V. and Wandinger-Ness, A. (2013) ‘Rapid parallel flow cytometry assays of active GTPases using effector beads’, *Analytical Biochemistry*. Elsevier Inc., 442(2), pp. 149–157. doi: 10.1016/j.ab.2013.07.039.

Campos, G. M., Borges, A. A., Badra, S. J., Figueiredo, G. G., Souza, R. L. M. de, Moreli, M. L. and Figueiredo, L. T. M. (2009) ‘[Pulmonary and cardiovascular syndrome due to hantavirus: clinical aspects of an emerging disease in southeastern Brazil].’, *Revista da Sociedade Brasileira de Medicina Tropical*, 42(3), pp. 282–289.

Carnec, X., Ermonval, M., Kreher, F., Flamand, M. and Bouloy, M. (2014) ‘Role of the cytosolic tails of Rift Valley fever virus envelope glycoproteins in viral morphogenesis’, *Virology*. Elsevier, 448(2014), pp. 1–14. doi: 10.1016/j.virol.2013.09.023.

Castera, L. (2012) 'Noninvasive methods to assess liver disease in patients with hepatitis B or C', *Gastroenterology*. Elsevier Inc., 142(6), p. 1293–1302.e4. doi: 10.1053/j.gastro.2012.02.017.

CE, P., MR, W. and Mocanu, V. (2010) *Mass Spectrometry for Proteomics.*, *Neruoproteomics*. Available at: https://www.ncbi.nlm.nih.gov/books/NBK56011/.

Chandy, S., Okumura, M., Yoshimatsu, K., Ulrich, R. G., John, G. T., Abraham, P., Arikawa, J. and Sridharan, G. (2009) 'Hantavirus species in India: a retrospective study.', *Indian journal of medical microbiology*, 27(4), pp. 348–350. doi: 10.4103/0255-0857.55456.

Chapman, L. E., Mertz, G. J., Peters, C. J., Jolson, H. M., Khan, A. S., *et al.* (1999) 'Intravenous ribavirin for hantavirus pulmonary syndrome: safety and tolerance during 1 year of open-label experience. Ribavirin Study Group.', *Antiviral therapy*, 4(4), pp. 211–219.

Chiang, C. F., Flint, M., Lin, J. M. S. and Spiropoulou, C. F. (2016) 'Endocytic pathways used by andes virus to enter primary human lung endothelial cells', *PLoS ONE*, 11(10), pp. 1–19. doi: 10.1371/journal.pone.0164768.

Choi, Y., Kwon, Y.-C., Kim, S.-I., Park, J.-M., Lee, K.-H. and Ahn, B.-Y. (2008) 'A hantavirus causing hemorrhagic fever with renal syndrome requires gC1qR/p32 for efficient cell binding and infection.', *Virology*, 381(2), pp. 178–183. doi: 10.1016/j.virol.2008.08.035.

Cifuentes-Munoz, N., Barriga, G. P., Valenzuela, P. D. T. and Tischler, N. D. (2011) 'Aromatic and polar residues spanning the candidate fusion peptide of the Andes virus Gc protein are essential for membrane fusion and infection.', *The Journal of general virology*, 92(Pt 3), pp. 552–563. doi: 10.1099/vir.0.027235-0.

Cifuentes-Munoz, N., Salazar-Quiroz, N. and Tischler, N. D. (2014) 'Hantavirus Gn and Gc envelope glycoproteins: key structural units for virus cell entry and virus assembly.',

*Viruses*. Switzerland, 6(4), pp. 1801–1822. doi: 10.3390/v6041801.

Coleman, T. J. (2000) 'The Public Health Laboratory Service (PHLS) and its role in the control of zoonotic disease', *Acta Tropica*, 76(1), pp. 71–75. doi: 10.1016/S0001-706X(00)00093-0.

Collier, T. S., Randall, S. M., Sarkar, P., Rao, B. M., Dean, R. A. and Muddiman, D. C. (2011) 'Comparison of stable-isotope labeling with amino acids in cell culture and spectral counting for relative quantification of protein expression.', *Rapid communications in mass spectrometry : RCM*, 25(17), pp. 2524–2532. doi: 10.1002/rcm.5151.

Costa, F., Hagan, J. E., Calcagno, J., Kane, M., Torgerson, P., Martinez-Silveira, M. S., Stein, C., Abela-Ridder, B. and Ko, A. I. (2015) 'Global Morbidity and Mortality of Leptospirosis: A Systematic Review', *PLoS Neglected Tropical Diseases*. doi: 10.1371/journal.pntd.0003898.

Cox, J., Hein, M. Y., Luber, C. A., Paron, I., Nagaraj, N. and Mann, M. (2014) 'Accurate Proteome-wide Label-free Quantification by Delayed Normalization and Maximal Peptide Ratio Extraction, Termed MaxLFQ', *Molecular & Cellular Proteomics*, 13(9), pp. 2513–2526. doi: 10.1074/mcp.M113.031591.

Croft, D., Mundo, A. F., Haw, R., Milacic, M., Weiser, J., *et al.* (no date) 'The Reactome pathway knowledgebase'. doi: 10.1093/nar/gkt1102.

Dagonnier, M., Cooke, I. R., Faou, P., Sidon, T. K., Dewey, H. M., Donnan, G. A. and Howells, D. W. (2017) 'Discovery and Longitudinal Evaluation of Candidate Biomarkers for Ischaemic Stroke by Mass Spectrometry-Based Proteomics', *Biomarker Insights*, 12, p. 117727191774921. doi: 10.1177/1177271917749216.

Decroly, E., Ferron, F., Lescar, J. and Canard, B. (2011) 'Conventional and

unconventional mechanisms for capping viral mRNA.', *Nature reviews. Microbiology*, 10(1), pp. 51–65. doi: 10.1038/nrmicro2675.

Deretic, V., Saitoh, T. and Akira, S. (2017) 'Autophagy in infection, inflammation, and immunity', 13(10), pp. 722–737. doi: 10.1038/nri3532.Autophagy.

Deroo, E. P., Wrobleski, S. K., Shea, E. M., Al-khalil, R. K., Hawley, A. E., Henke, P. K., Jr, D. D. M., Wakefield, T. W. and Diaz, J. A. (2015) 'The role of galectin-3 and galectin-3 – binding protein in venous thrombosis', 125(11), pp. 1813–1822. doi: 10.1182/blood-2014-04-569939.Presented.

Desmedt, V., Desmedt, S., Delanghe, J. R., Speeckaert, R. and Speeckaert, M. M. (2016) 'Galectin-3 in Renal Pathology: More Than Just an Innocent Bystander?', *American Journal of Nephrology*, 43(5), pp. 305–317. doi: 10.1159/000446376.

Deyde, V. M., Rizvanov, A. A., Chase, J., Otteson, E. W. and St. Jeor, S. C. (2005) 'Interactions and trafficking of Andes and Sin Nombre Hantavirus glycoproteins G1 and G2', *Virology*, 331(2), pp. 307–315. doi: 10.1016/j.virol.2004.11.003.

van Diepen, S., Alemayehu, W. G., Zheng, Y., Theroux, P., Newby, L. K., Mahaffey, K. W., Granger, C. B. and Armstrong, P. W. (2016) 'Temporal changes in biomarkers and their relationships to reperfusion and to clinical outcomes among patients with ST segment elevation myocardial infarction', *Journal of Thrombosis and Thrombolysis*. Springer US, 42(3), pp. 376–385. doi: 10.1007/s11239-016-1390-z.

Dieplinger, B., Egger, M., Gabriel, C., Poelz, W., Morandell, E., *et al.* (2013) 'Analytical characterization and clinical evaluation of an enzyme-linked immunosorbent assay for measurement of afamin in human plasma()', *Clinica Chimica Acta; International Journal of Clinical Chemistry*. Elsevier, 425, pp. 236–241. doi: 10.1016/j.cca.2013.08.016.

Dieplinger, H., Ankerst, D. P., Burges, A., Lenhard, M., Lingenhel, A., Fineder, L., Buchner, H. and Stieber, P. (2009) 'Afamin and apolipoprotein A-IV: novel protein markers for ovarian cancer', *Cancer epidemiology, biomarkers & prevention : a publication of the American Association for Cancer Research, cosponsored by the American Society of Preventive Oncology*, 18(4), pp. 1127–1133. doi: 10.1158/1055-9965.EPI-08-0653.

Dieplinger, H. and Dieplinger, B. (2015) 'Afamin--A pleiotropic glycoprotein involved in various disease states.', *Clinica chimica acta; international journal of clinical chemistry*, 446, pp. 105–110. doi: 10.1016/j.cca.2015.04.010.

Du, H., Li, J., Jiang, W., Yu, H., Zhang, Y., Wang, J., Wang, P. and Bai, X. (2014) 'Clinical study of critical patients with hemorrhagic fever with renal syndrome complicated by acute respiratory distress syndrome', *PLoS ONE*, 9(2). doi: 10.1371/journal.pone.0089740.

Duggan, J. M., Close, R., McCann, L., Wright, D., Keys, M., *et al.* (2017) 'A seroprevalence study to determine the frequency of hantavirus infection in people exposed to wild and pet fancy rats in England.', *Epidemiology and infection*, 145(12), pp. 2458–2465. doi: 10.1017/S0950268817001480.

Easterbrook, J. D., Zink, M. C. and Klein, S. L. (2007) 'Regulatory T cells enhance persistence of the zoonotic pathogen Seoul virus in its reservoir host.', *Proceedings of the National Academy of Sciences of the United States of America*, 104(39), pp. 15502–15507. doi: 10.1073/pnas.0707453104.

Escadafal, C., Avšič-Županc, T., Vapalahti, O., Niklasson, B., Teichmann, A., Niedrig, M. and Donoso-Mantke, O. (2012) 'Second external quality assurance study for the serological diagnosis of hantaviruses in Europe', *PLoS Neglected Tropical Diseases*, 6(4). doi: 10.1371/journal.pntd.0001607.

Esmon, C. T. (2005) 'The interactions between inflammation and coagulation', *British Journal of Haematology*, 131(4), pp. 417–430. doi: 10.1111/j.1365-2141.2005.05753.x.

European Centre for Disease Control and Prevention (2016) 'Hantavirus infection.', *Advances in internal medicine*, (November).

Evander, M., Eriksson, I., Pettersson, L., Juto, P., Ahlm, C., Olsson, G. E., Bucht, G. and Allard, A. (2007) 'Puumala hantavirus viremia diagnosed by real-time reverse transcriptase PCR using samples from patients with hemorrhagic fever and renal syndrome.', *Journal of clinical microbiology*, 45(8), pp. 2491–2497. doi: 10.1128/JCM.01902-06.

Fabregat, A., Sidiropoulos, K., Garapati, P., Gillespie, M., Hausmann, K., *et al.* (2016) 'The reactome pathway knowledgebase', *Nucleic Acids Research*. doi: 10.1093/nar/gkv1351.

Ferrés, M., Vial, P., Marco, C., Yañez, L., Godoy, P., *et al.* (2007) 'Prospective Evaluation of Household Contacts of Persons with Hantavirus Cardiopulmonary Syndrome in Chile', *The Journal of Infectious Diseases*. United States, 195(11), pp. 1563–1571. doi: 10.1086/516786.

Forbes, A. E., Zochowski, W. J., Dubrey, S. W. and Sivaprakasam, V. (2012) 'Leptospirosis and weil's disease in the UK', *Qjm*, 105(12), pp. 1151–1162. doi: 10.1093/qjmed/hcs145.

Fukuda, S., Sumii, M., Masuda, Y., Takahashi, M., Koike, N., *et al.* (2001) 'Murine and human SDF2L1 is an endoplasmic reticulum stress-inducible gene and encodes a new member of the Pmt/rt protein family', *Biochemical and Biophysical Research Communications*, 280(1), pp. 407–414. doi: 10.1006/bbrc.2000.4111.

Gamage, C. D., Yasuda, S. P., Nishio, S., Kularatne, S. A., Weerakoon, K., *et al.* (2011) 'Serological evidence of Thailand virus-related hantavirus infection among suspected

leptospirosis patients in Kandy, Sri Lanka.', *Japanese journal of infectious diseases*, 64(1), pp. 72–75.

Ganaie, S. S. and Mir, M. A. (2014) 'The role of viral genomic RNA and nucleocapsid protein in the autophagic clearance of hantavirus glycoprotein Gn', *Virus Research*. Elsevier B.V., 187, pp. 72–76. doi: 10.1016/j.virusres.2013.12.034.

Garanina, S. B., Platonov, A. E., Zhuravlev, V. I., Murashkina, A. N., Yakimenko, V. V, Korneev, A. G. and Shipulin, G. A. (2009) 'Genetic diversity and geographic distribution of hantaviruses in Russia.', *Zoonoses and public health*, 56(6–7), pp. 297–309. doi: 10.1111/j.1863-2378.2008.01210.x.

Garry, C. E. and Garry, R. F. (2004) 'Proteomics computational analyses suggest that the carboxyl terminal glycoproteins of Bunyaviruses are class II viral fusion protein (beta-penetrenes).', *Theoretical biology & medical modelling*, 1, p. 10. doi: 10.1186/1742-4682-1-10.

Gavrilovskaya, I. N., Shepley, M., Shaw, R., Ginsberg, M. H. and Mackow, E. R. (1998) 'beta3 Integrins mediate the cellular entry of hantaviruses that cause respiratory failure.', *Proceedings of the National Academy of Sciences of the United States of America*, 95(12), pp. 7074–7079.

Gavrilovskaya, I. N., Brown, E. J., Ginsberg, M. H. and Mackow, E. R. (1999) 'Cellular entry of hantaviruses which cause hemorrhagic fever with renal syndrome is mediated by beta3 integrins.', *Journal of virology*, 73(5), pp. 3951–3959.

Gavrilovskaya, I. N., Gorbunova, E. E., Mackow, N. A. and Mackow, E. R. (2008) 'Hantaviruses Direct Endothelial Cell Permeability by Sensitizing Cells to the Vascular Permeability Factor VEGF, while Angiopoietin 1 and Sphingosine 1-Phosphate Inhibit

Hantavirus-Directed Permeability', *Journal of Virology*, 82(12), pp. 5797–5806. doi: 10.1128/JVI.02397-07.

Gavrilovskaya, I. N., Gorbunova, E. E. and Mackow, E. R. (2010) 'Pathogenic Hantaviruses Direct the Adherence of Quiescent Platelets to Infected Endothelial Cells', *Journal of Virology*, 84(9), pp. 4832–4839. doi: 10.1128/JVI.02405-09.

Geimonen, E., Neff, S., Raymond, T., Kocer, S. S., Gavrilovskaya, I. N. and Mackow, E. R. (2002) 'Pathogenic and nonpathogenic hantaviruses differentially regulate endothelial cell responses.', *Proceedings of the National Academy of Sciences of the United States of America*, 99(21), pp. 13837–13842. doi: 10.1073/pnas.192298899.

Glass, G. E., Watson, A. J., LeDuc, J. W., Kelen, G. D., Quinn, T. C. and Childs, J. E. (1993) 'Infection with a ratborne hantavirus in US residents is consistently associated with hypertensive renal disease.', *The Journal of infectious diseases*, 167(3), pp. 614–620.

Goeijenbier, M., Hartskeerl, R. A., Reimerink, J., Verner-Carlsson, J., Wagenaar, J. F., *et al.* (2014) 'The hanta hunting study: underdiagnosis of Puumala hantavirus infections in symptomatic non-travelling leptospirosis-suspected patients in the Netherlands, in 2010 and April to November 2011.', *Euro surveillance : bulletin Europeen sur les maladies transmissibles = European communicable disease bulletin*, 19(32).

Goldsmith, C. S., Elliott, L. H., Peters, C. J. and Zaki, S. R. (1995) 'Ultrastructural characteristics of Sin Nombre virus, causative agent of hantavirus pulmonary syndrome', *Archives of Virology*, 140(12), pp. 2107–2122. doi: 10.1007/BF01323234.

Gorbunova, E. E., Gavrilovskaya, I. N., Pepini, T. and Mackow, E. R. (2011) 'VEGFR2 and Src Kinase Inhibitors Suppress Andes Virus-Induced Endothelial Cell Permeability', *Journal of Virology*, 85(5), pp. 2296–2303. doi: 10.1128/JVI.02319-10.

Haake, D. A. and Levett, P. N. (2015) *Leptospirosis in Humans*. doi: 10.1007/978-3-662-45059-8.

Haferkamp, S., Fernando, L., Schwarz, T. F., Feldmann, H. and Flick, R. (2005) 'Intracellular localization of Crimean-Congo Hemorrhagic Fever (CCHF) virus glycoproteins', *Virol J*, 2, p. 42. doi: 10.1186/1743-422X-2-42.

Halldorsson, S., Behrens, A.-J., Harlos, K., Huiskonen, J. T., Elliott, R. M., Crispin, M., Brennan, B. and Bowden, T. A. (2016) 'Structure of a phleboviral envelope glycoprotein reveals a consolidated model of membrane fusion.', *Proceedings of the National Academy of Sciences of the United States of America*, 113(26), pp. 7154–7159. doi: 10.1073/pnas.1603827113.

Hayashi, Y., Call, M. K., Chikama, T., Liu, H., Carlson, E. C., *et al.* (2010) 'Lumican is required for neutrophil extravasation following corneal injury and wound healing.', *Journal of cell science*. England, 123(Pt 17), pp. 2987–2995. doi: 10.1242/jcs.068221.

Hedman, K., Vaheri, A. and Brummer-Korvenkontio, M. (1991) 'Rapid diagnosis of hantavirus disease with an IgG-avidity assay.', *Lancet (London, England)*, 338(8779), pp. 1353–1356.

Hepojoki, J., Strandin, T., Wang, H., Vapalahti, O., Vaheri, A. and Lankinen, H. (2010) 'Cytoplasmic tails of hantavirus glycoproteins interact with the nucleocapsid protein', *Journal of General Virology*, 91(9), pp. 2341–2350. doi: 10.1099/vir.0.021006-0.

Hepojoki, J., Strandin, T., Lankinen, H. and Vaheri, A. (2012) 'Hantavirus structure - Molecular interactions behind the scene', *Journal of General Virology*, 93(8), pp. 1631–1644. doi: 10.1099/vir.0.042218-0.

Hepojoki, J., Strandin, T., Hetzel, U., Sironen, T., Klingström, J., *et al.* (2014) 'Acute

hantavirus infection induces galectin-3-binding protein', *Journal of General Virology*, 95(2014), pp. 2356–2364. doi: 10.1099/vir.0.066837-0.

Heyman, P., Baert, K., Plyusnina, A., Cochez, C., Lundkvist, A., *et al.* (2009) 'Serological and genetic evidence for the presence of Seoul hantavirus in Rattus norvegicus in Flanders, Belgium.', *Scandinavian journal of infectious diseases*, 41(1), pp. 51–56. doi: 10.1080/00365540802459994.

Heyman, P., Ceianu, C. S., Christova, I., Tordo, N., Beersma, M., *et al.* (2011) 'A five-year perspective on the situation of haemorrhagic fever with renal syndrome and status of the hantavirus reservoirs in Europe, 2005-2010.', *Euro surveillance : bulletin Europeen sur les maladies transmissibles = European communicable disease bulletin*, 16(36).

Higa, M. M., Petersen, J., Hooper, J. and Doms, R. W. (2012) 'Efficient production of Hantaan and Puumala pseudovirions for viral tropism and neutralization studies.', *Virology*, 423(2), pp. 134–142. doi: 10.1016/j.virol.2011.08.012.

Van Hinsbergh, V. W. M. (2012) 'Endothelium - Role in regulation of coagulation and inflammation', *Seminars in Immunopathology*, 34(1), pp. 93–106. doi: 10.1007/s00281-011-0285-5.

Hjelle, B., Goade, D., Torrez-Martinez, N., Lang-Williams, M., Kim, J., Harris, R. L. and Rawlings, J. A. (1996) 'Hantavirus pulmonary syndrome, renal insufficiency, and myositis associated with infection by Bayou hantavirus.', *Clinical Infectious Diseases*, 23(November), pp. 495–500. Available at: file:///Users/sarahby/Downloads/23-3-495.pdf.

Hofmann, J., Fuhrer, A., Bolz, M., Waldschlager-Terpe, J., Meier, M., *et al.* (2012) 'Hantavirus infections by Puumala or Dobrava-Belgrade virus in pregnant women.', *Journal of clinical virology : the official publication of the Pan American Society for Clinical Virology*,

55(3), pp. 266–269. doi: 10.1016/j.jcv.2012.07.011.

Honore, B., Lefferssfl, H., Rasmussen, H. H., Vandekerckhove, J. and Celisg, J. E. (1992) 'Human Protein Containing the TPR Motif and Sharing Identity to the', *Journal of Biological Chemistry*, 267(12), pp. 8485–8491.

Howard, M. J., Doyle, T. J., Koster, F. T., Zaki, S. R., Khan, A. S., Petersen, E. A., Peters, C. J. and Bryan, R. T. (1999) 'Hantavirus pulmonary syndrome in pregnancy.', *Clinical infectious diseases : an official publication of the Infectious Diseases Society of America*, 29(6), pp. 1538–1544. doi: 10.1086/313513.

Hubalek, M., Buchner, H., Mörtl, M. G., Schlembach, D., Huppertz, B., *et al.* (2014) 'The vitamin E-binding protein afamin increases in maternal serum during pregnancy', *Clinica Chimica Acta*. Elsevier B.V., 434, pp. 41–47. doi: 10.1016/j.cca.2014.03.036.

Huggins, J. W., Hsiang, C. M., Cosgriff, T. M., Guang, M. Y., Smith, J. I., *et al.* (1991) 'Prospective, double-blind, concurrent, placebo-controlled clinical trial of intravenous ribavirin therapy of hemorrhagic fever with renal syndrome.', *The Journal of infectious diseases*, 164(6), pp. 1119–1127.

Huiskonen, J. T., Hepojoki, J., Laurinmaki, P., Vaheri, A., Lankinen, H., Butcher, S. J. and Grunewald, K. (2010) 'Electron cryotomography of Tula hantavirus suggests a unique assembly paradigm for enveloped viruses.', *Journal of virology*, 84(10), pp. 4889–4897. doi: 10.1128/JVI.00057-10.

Hujakka, H., Koistinen, V., Eerikainen, P., Kuronen, I., Laatikainen, A., Kauppinen, J., Vaheri, A., Vapalahti, O. and Narvanen, A. (2001) 'Comparison of a new immunochromatographic rapid test with a commercial EIA for the detection of Puumala virus specific IgM antibodies.', *Journal of clinical virology : the official publication of the Pan*

*American Society for Clinical Virology*, 23(1–2), pp. 79–85.

Huotari, J. and Helenius, A. (2011) 'Endosome maturation', *EMBO Journal*. Nature Publishing Group, 30(17), pp. 3481–3500. doi: 10.1038/emboj.2011.286.

Hussein, I. T. M., Haseeb, A., Haque, A. and Mir, M. A. (2011) 'Recent advances in hantavirus molecular biology and disease.', *Advances in applied microbiology*, 74, pp. 35–75. doi: 10.1016/B978-0-12-387022-3.00006-9.

ICTV (2014) 'ICTV Master Species List 2014 v3'.

Imig, J. D. and Ryan, M. J. (2013) 'Immune and inflammatory role in renal disease', *Comprehensive Physiology*, 3(2), pp. 957–976. doi: 10.1002/cphy.c120028.

Issaq, H. J., Xiao, Z. and Veenstra, T. D. (2007) 'Serum and plasma proteomics', *Chemical Reviews*, 107(8), pp. 3601–3620. doi: 10.1021/cr068287r.

Jaaskelainen, K. M., Kaukinen, P., Minskaya, E. S., Plyusnina, A., Vapalahti, O., Elliott, R. M., Weber, F., Vaheri, A. and Plyusnin, A. (2007) 'Tula and Puumala hantavirus NSs ORFs are functional and the products inhibit activation of the interferon-beta promoter.', *Journal of medical virology*, 79(10), pp. 1527–1536. doi: 10.1002/jmv.20948.

Jackson, W. T., Jr, T. H. G., Taylor, M. P., Mulinyawe, S., Rabinovitch, M., Kopito, R. R. and Kirkegaard, K. (2005) 'Subversion of Cellular Autophagosomal Machinery by RNA Viruses', 3(5). doi: 10.1371/journal.pbio.0030156.

Jadhav, M., Nayak, M., Kumar, S., Venkatesh, A., Patel, S. K., *et al.* (2017) 'Clinical Proteomics and Cytokine Profiling for Dengue Fever Disease Severity Biomarkers', *OMICS: A Journal of Integrative Biology*, 21(11), pp. 665–677. doi: 10.1089/omi.2017.0135.

Jameson, L. J., Taori, S. K., Atkinson, B., Levick, P., Featherstone, C. A., *et al.* (2013) 'Pet

rats as a source of hantavirus in England and Wales, 2013', *Eurosurveillance*, 18(9), pp. 8–10. Available at: file:///Users/sarahby/Documents/Artikler/Litteratur/Diagnose og identifisering/Hanta i Storbrittania/Jameson_eurosurveill_13 (9).pdf.

Jameson, L. J., Logue, C. H., Atkinson, B., Baker, N., Galbraith, S. E., Carroll, M. W., Brooks, T. and Hewson, R. (2013) 'The continued emergence of hantaviruses: isolation of a Seoul virus implicated in human disease, United Kingdom, October 2012.', *Euro surveillance : bulletin europ??en sur les maladies transmissibles = European communicable disease bulletin*, 18(1), pp. 4–7. Available at: file:///Users/sarahby/Documents/Artikler/Litteratur/Diagnose og identifisering/Hanta i Storbrittania/Jameson_eurosurveill_13.pdf.

Jameson, L. J., Newton, A., Coole, L., Newman, E. N. C., Carroll, M. W., Beeching, N. J., Hewson, R. and Christley, R. M. (2014) 'Prevalence of antibodies against hantaviruses in serum and saliva of adults living or working on farms in Yorkshire, United Kingdom.', *Viruses*, 6(2), pp. 524–534. doi: 10.3390/v6020524.

Jäntti, J., Hildén, P., Rönkä, H., Mäkiranta, V., Keränen, S. and Kuismanen, E. (1997) 'Immunocytochemical analysis of Uukuniemi virus budding compartments: role of the intermediate compartment and the Golgi stack in virus maturation.', *Journal of virology*, 71(2), pp. 1162–1172. Available at: http://www.pubmedcentral.nih.gov/articlerender.fcgi?artid=191169&tool=pmcentrez&rendertype=abstract.

Jenison, S., Yamada, T., Morris, C., Anderson, B., Torrez-Martinez, N., Keller, N. and Hjelle, B. (1994) 'Characterization of human antibody responses to four corners hantavirus infections among patients with hantavirus pulmonary syndrome.', *Journal of virology*, 68(5), pp. 3000–3006. Available at:

http://www.pubmedcentral.nih.gov/articlerender.fcgi?artid=236790&tool=pmcentrez&rendertype=abstract.

Jerkovic, L., Voegele, A. F., Chwatal, S., Kronenberg, F., Radcliffe, C. M., *et al.* (2005) 'Afamin is a novel human vitamin E-binding glycoprotein characterization and in vitro expression', *Journal of Proteome Research*, 4(3), pp. 889–899. doi: 10.1021/pr0500105.

Jiao, F., Zhang, D., Jiang, M., Mi, J., Liu, X., Zhang, H., Hu, Z., Xu, X. and Hu, X. (2017) 'Label-free proteomic analysis of placental proteins during Toxoplasma gondii infection.', *Journal of proteomics*, 150, pp. 31–39. doi: 10.1016/j.jprot.2016.08.013.

Jin, M., Park, J., Lee, S., Park, B., Shin, J., *et al.* (2002) 'Hantaan virus enters cells by clathrin-dependent receptor-mediated endocytosis.', *Virology*, 294(1), pp. 60–69. doi: 10.1006/viro.2001.1303.

Johansson, P., Olsson, M., Lindgren, L., Ahlm, C., Elgh, F., Holmstrom, A. and Bucht, G. (2004) 'Complete gene sequence of a human Puumala hantavirus isolate, Puumala Umea/hu: sequence comparison and characterisation of encoded gene products.', *Virus research*, 105(2), pp. 147–155. doi: 10.1016/j.virusres.2004.05.005.

Jonsson, C. B., Figueiredo, L. T. M. and Vapalahti, O. (2010) 'A global perspective on hantavirus ecology, epidemiology, and disease.', *Clinical microbiology reviews*, 23(2), pp. 412–441. doi: 10.1128/CMR.00062-09.

Kalayci, O., Birben, E., Tinari, N., Oguma, T., Iacobelli, S. and Lilly, C. M. (2004) 'Role of 90K protein in asthma and T H 2-type cytokine expression', *Annals of Allergy, Asthma and Immunology*. American College of Allergy, Astham, & Immunology, 93(5), pp. 485–492. doi: 10.1016/S1081-1206(10)61417-2.

Kallio-Kokko, H., Leveelahti, R., Brummer-Korvenkontio, M., Lundkvist, A., Vaheri, A.

and Vapalahti, O. (2001) ‘Human immune response to Puumala virus glycoproteins and nucleocapsid protein expressed in mammalian cells.’, *Journal of medical virology*, 65(3), pp. 605–613.

Kariwa, H., Tanabe, H., Mizutani, T., Kon, Y., Lokugamage, K., *et al.* (2003) ‘Synthesis of Seoul virus RNA and structural proteins in cultured cells’, *Archives of Virology*, 148(9), pp. 1671–1685. doi: 10.1007/s00705-003-0141-6.

Kashani, K., Al-Khafaji, A., Ardiles, T., Artigas, A., Bagshaw, S. M., *et al.* (2013) ‘Discovery and validation of cell cycle arrest biomarkers in human acute kidney injury’, *Critical Care*, 17(1), pp. R25–R25. doi: 10.1186/cc12503.

Katayama, S., Nunomiya, S., Koyama, K., Wada, M., Koinuma, T., Goto, Y., Tonai, K. and Shima, J. (2017) ‘Markers of acute kidney injury in patients with sepsis: the role of soluble thrombomodulin’, *Critical Care*. Critical Care, 21, pp. 1–9. doi: 10.1186/s13054-017-1815-x.

Kaukinen, P., Vaheri, A. and Plyusnin, A. (2005) ‘Hantavirus nucleocapsid protein: a multifunctional molecule with both housekeeping and ambassadorial duties.’, *Archives of virology*, 150(9), pp. 1693–1713. doi: 10.1007/s00705-005-0555-4.

Kearney, P., Boniface, J. J., Price, N. D. and Hood, L. (2018) ‘The building blocks of successful translation of proteomics to the clinic’, *Current Opinion in Biotechnology*. Elsevier Ltd, 51, pp. 123–129. doi: 10.1016/j.copbio.2017.12.011.

Keegan, M. T., Gali, B., Brown, D. R., Harrison, B. A., Plevak, D. J. and Findlay, J. Y. (2010) ‘Serum vasopressin concentrations during orthotopic liver transplantation’, *Transplantation Proceedings*. Elsevier Inc., 42(7), pp. 2594–2598. doi: 10.1016/j.transproceed.2010.04.051.

Khaiboullina, S. F., Rizvanov, A. A., Otteson, E., Miyazato, A., Maciejewski, J. and St Jeor, S. (2004) ‘Regulation of cellular gene expression in endothelial cells by sin nombre and

prospect hill viruses.', *Viral immunology*, 17(2), pp. 234–251. doi: 10.1089/0882824041310504.

Kim, B.-N. and Choi, B.-D. (2006) 'Hemorrhagic fever with renal syndrome complicated with pregnancy: A case report', *Korean Journal of Internal Medicine*, 21(2), pp. 150–153. Available at: http://www.scopus.com/inward/record.url?eid=2-s2.0-33748413918&partnerID=40&md5=2555876b47335a4af7e25752973cdac5.

Kim, Y. K., Lee, S. C., Kim, C., Heo, S. T., Choi, C. and Kim, J. M. (2007) 'Clinical and laboratory predictors of oliguric renal failure in haemorrhagic fever with renal syndrome caused by Hantaan virus.', *The Journal of infection*, 54(4), pp. 381–386. doi: 10.1016/j.jinf.2006.07.006.

Klaus, J. P., Eisenhauer, P., Russo, J., Mason, A. B., Do, D., *et al.* (2013) 'The intracellular cargo receptor ERGIC-53 is required for the production of infectious arenavirus, coronavirus, and filovirus particles.', *Cell host & microbe*, 14(5), pp. 522–534. doi: 10.1016/j.chom.2013.10.010.

Klein, J., Buffin-Meyer, B., Mullen, W., Carty, D. M., Delles, C., *et al.* (2014) 'Clinical proteomics in obstetrics and neonatology', *Expert Review of Proteomics*, 11(1), pp. 75–89. doi: 10.1586/14789450.2014.872564.

Klempa, B., Fichet-Calvet, E., Lecompte, E., Auste, B., Aniskin, V., *et al.* (2006) 'Hantavirus in African wood mouse, Guinea.', *Emerging infectious diseases*, 12(5), pp. 838–840. doi: 10.3201/eid1205.051487.

Klempa, B., Koivogui, L., Sylla, O., Koulemou, K., Auste, B., Kruger, D. H. and ter Meulen, J. (2010) 'Serological evidence of human hantavirus infections in Guinea, West Africa.', *The Journal of infectious diseases*, 201(7), pp. 1031–1034. doi: 10.1086/651169.

Klempa, B., Witkowski, P. T., Popugaeva, E., Auste, B., Koivogui, L., Fichet-Calvet, E., Strecker, T., Ter Meulen, J. and Kruger, D. H. (2012) 'Sangassou virus, the first hantavirus isolate from Africa, displays genetic and functional properties distinct from those of other murinae-associated hantaviruses.', *Journal of virology*, 86(7), pp. 3819–3827. doi: 10.1128/JVI.05879-11.

Klempa, B., Avsic-Zupanc, T., Clement, J., Dzagurova, T. K., Henttonen, H., *et al.* (2013) 'Complex evolution and epidemiology of Dobrava-Belgrade hantavirus: definition of genotypes and their characteristics', *Archives of Virology*, 158(3), pp. 521–529. doi: 10.1007/s00705-012-1514-5.

Klingstrom, J., Plyusnin, A., Vaheri, A. and Lundkvist, A. (2002) 'Wild-type Puumala hantavirus infection induces cytokines, C-reactive protein, creatinine, and nitric oxide in cynomolgus macaques', *J Virol*, 76(1), pp. 444–449. doi: 10.1128/JVI.76.1.444.

Knust, B., Macneil, A. and Rollin, P. E. (2012) 'Hantavirus pulmonary syndrome clinical findings: evaluating a surveillance case definition.', *Vector borne and zoonotic diseases (Larchmont, N.Y.)*, 12(5), pp. 393–399. doi: 10.1089/vbz.2011.0764.

Kolialexi, A., Mavreli, D. and Papantoniou, N. (2017) 'Proteomics for early prenatal screening of pregnancy complications: a 2017 perspective', *Expert Review of Proteomics*. Taylor & Francis, 14(2), pp. 113–115. doi: 10.1080/14789450.2017.1275574.

Korva, M., Saksida, a, Kejžar, N., Schmaljohn, C. and Avšič-Županc, T. (2013) 'Viral load and immune response dynamics in patients with haemorrhagic fever with renal syndrome.', *Clinical microbiology and infection : the official publication of the European Society of Clinical Microbiology and Infectious Diseases*, 19(8), pp. E358-66. doi: 10.1111/1469-0691.12218.

Krautkramer, E., Grouls, S., Stein, N., Reiser, J. and Zeier, M. (2011) 'Pathogenic Old World Hantaviruses Infect Renal Glomerular and Tubular Cells and Induce Disassembling of Cell-to-Cell Contacts', *Journal of Virology*, 85(19), pp. 9811–9823. doi: 10.1128/JVI.00568-11.

Krautkramer, E. and Zeier, M. (2008) 'Hantavirus causing hemorrhagic fever with renal syndrome enters from the apical surface and requires decay-accelerating factor (DAF/CD55).', *Journal of virology*, 82(9), pp. 4257–4264. doi: 10.1128/JVI.02210-07.

Krautkrämer, E., Zeier, M. and Plyusnin, A. (2013) 'Hantavirus infection: an emerging infectious disease causing acute renal failure.', *Kidney international*, 83(1), pp. 23–27. doi: 10.1038/ki.2012.360.

Kruger, D. H., Figueiredo, L. T. M., Song, J.-W. and Klempa, B. (2015) 'Hantaviruses--globally emerging pathogens.', *Journal of clinical virology : the official publication of the Pan American Society for Clinical Virology*, 64, pp. 128–136. doi: 10.1016/j.jcv.2014.08.033.

Kudesia, G., Christie, P., Walker, E., Pinkerton, I. and Lloyd, G. (1988) 'Dual infection with leptospira and hantavirus.', *Lancet (London, England)*. England, p. 1397.

Kukkonen, S. K. J., Vaheri, A. and Plyusnin, A. (2005) 'L protein, the RNA-dependent RNA polymerase of hantaviruses.', *Archives of virology*, 150(3), pp. 533–556. doi: 10.1007/s00705-004-0414-8.

Kumar, Y., Liang, C., Bo, Z., Rajapakse, J. C., Ooi, E. E. and Tannenbaum, S. R. (2012) 'Serum Proteome and Cytokine Analysis in a Longitudinal Cohort of Adults with Primary Dengue Infection Reveals Predictive Markers of DHF', *PLOS Neglected Tropical Diseases*. Public Library of Science, 6(11), pp. e1887–e1887. Available at: https://doi.org/10.1371/journal.pntd.0001887.

Laine, O., Joutsi-Korhonen, L., Makela, S., Mikkelsson, J., Pessi, T., *et al.* (2012) 'Polymorphisms of PAI-1 and platelet GP Ia may associate with impairment of renal function and thrombocytopenia in Puumala hantavirus infection.', *Thrombosis research*, 129(5), pp. 611–615. doi: 10.1016/j.thromres.2011.11.007.

Lan, J., Núñez Galindo, A., Doecke, J., Fowler, C., Martins, R. N., Rainey-Smith, S. R., Cominetti, O. and Dayon, L. (2018) 'Systematic Evaluation of the Use of Human Plasma and Serum for Mass-Spectrometry-Based Shotgun Proteomics', *Journal of Proteome Research*, p. acs.jproteome.7b00788. doi: 10.1021/acs.jproteome.7b00788.

Lederer, S., Lattwein, E., Hanke, M., Sonnenberg, K., Stoecker, W., *et al.* (2013) 'Indirect immunofluorescence assay for the simultaneous detection of antibodies against clinically important old and new world hantaviruses.', *PLoS neglected tropical diseases*, 7(4), pp. e2157–e2157. doi: 10.1371/journal.pntd.0002157.

Lee, H. W., Lee, P. W. and Johnson, K. M. (1978) 'Isolation of the etiologic agent of Korean Hemorrhagic fever.', *The Journal of infectious diseases*, 137(3), pp. 298–308.

Li, X. D., Lankinen, H., Putkuri, N., Vapalahti, O. and Vaheri, A. (2005) 'Tula hantavirus triggers pro-apoptotic signals of ER stress in Vero E6 cells', *Virology*, 333(1), pp. 180–189. doi: 10.1016/j.virol.2005.01.002.

Li, Z., Adams, R. M., Chourey, K., Hurst, G. B., Hettich, R. L. and Pan, C. (2012) 'Systematic comparison of label-free, metabolic labeling, and isobaric chemical labeling for quantitative proteomics on LTQ orbitrap velos', *Journal of Proteome Research*, 11(3), pp. 1582–1590. doi: 10.1021/pr200748h.

Libraty, D. H., Mäkelä, S., Vlk, J., Hurme, M., Vaheri, A., Ennis, F. A. and Mustonen, J. (2012) 'The degree of leukocytosis and urine GATA-3 mRNA levels are risk factors for severe

acute kidney injury in puumala virus nephropathia epidemica', *PLoS ONE*, 7(4), pp. 1–7. doi: 10.1371/journal.pone.0035402.

Lilley, K. (2015) 'Quantitative proteomics'. Hinxton.Cambridge: Cambridge Center for Proteomics, pp. 1–28. Available at: http://www.bio.cam.ac.uk/proteomics.

Lindkvist, M., Naslund, J., Ahlm, C. and Bucht, G. (2008) 'Cross-reactive and serospecific epitopes of nucleocapsid proteins of three hantaviruses: prospects for new diagnostic tools.', *Virus research*, 137(1), pp. 97–105. doi: 10.1016/j.virusres.2008.06.003.

Liu, K. T., Liu, Y. H., Chen, Y. H., Lin, C. Y., Huang, C. H., Yen, M. C. and Kuo, P. L. (2016) 'Serum galectin-9 and galectin-3-binding protein in acute dengue virus infection', *International Journal of Molecular Sciences*, 17(6). doi: 10.3390/ijms17060832.

Liu, Z., Zhou, T., Ziegler, A. C., Dimitrion, P. and Zuo, L. (2017) 'Oxidative Stress in Neurodegenerative Diseases: From Molecular Mechanisms to Clinical Applications', *Oxidative Medicine and Cellular Longevity*, 2017(Figure 1), pp. 1–11. doi: 10.1155/2017/2525967.

Lloyd, G. and Jones, N. (1986) 'Infection of laboratory workers with hantavirus acquired from immunocytomas propagated in laboratory rats.', *The Journal of infection*, 12(2), pp. 117–125. Available at: file:///Users/sarahby/Documents/Artikler/1-s2.0-S0163445386935334-main-2.pdf.

Lober, C., Anheier, B., Lindow, S., Klenk, H. D. and Feldmann, H. (2001) 'The Hantaan virus glycoprotein precursor is cleaved at the conserved pentapeptide WAASA.', *Virology*, 289(2), pp. 224–229. doi: 10.1006/viro.2001.1171.

Lokugamage, K., Kariwa, H., Hayasaka, D., Cui, B. Z., Iwasaki, T., *et al.* (2002) 'Genetic characterization of hantaviruses transmitted by the Korean field mouse (Apodemus

peninsulae), Far East Russia.', *Emerging infectious diseases*, 8(8), pp. 768–776. doi: 10.3201/eid0805.010494.

Lundkvist, A., Hukic, M., Horling, J., Gilljam, M., Nichol, S. and Niklasson, B. (1997) 'Puumala and Dobrava viruses cause hemorrhagic fever with renal syndrome in Bosnia-Herzegovina: evidence of highly cross-neutralizing antibody responses in early patient sera.', *Journal of medical virology*, 53(1), pp. 51–59.

Lundkvist, A., Verner-Carlsson, J., Plyusnina, A., Forslund, L., Feinstein, R. and Plyusnin, A. (2013) 'Pet rat harbouring Seoul hantavirus in Sweden, June 2013.', *Euro surveillance : bulletin Europeen sur les maladies transmissibles = European communicable disease bulletin*, 18(27).

Lundkvist, A. and Niklasson, B. (1992) 'Bank vole monoclonal antibodies against Puumala virus envelope glycoproteins: identification of epitopes involved in neutralization.', *Archives of virology*, 126(1–4), pp. 93–105.

Macé, G., Feyeux, C., Mollard, N., Chantegret, C., Audia, S., *et al.* (2013) 'Severe Seoul hantavirus infection in a pregnant woman, France, October 2012', *Eurosurveillance*, 18(17), pp. 14–17. Available at: file:///Users/sarahby/Documents/Artikler/Mace_euroseurveill_2012.pdf.

Makela, S., Jaatinen, P., Miettinen, M., Salmi, J., Ala-Houhala, I., *et al.* (2010) 'Hormonal deficiencies during and after Puumala hantavirus infection', *European Journal of Clinical Microbiology and Infectious Diseases*. Germany, 29(6), pp. 705–713. doi: 10.1007/s10096-010-0918-y.

Mäkelä, S., Ala-Houhala, I., Mustonen, J., Koivisto, A. M., Kouri, T., Turjanmaa, V., Vapalahti, O., Vaheri, A. and Pasternack, A. (2000) 'Renal function and blood pressure five

years after Puumala virus-induced nephropathy', *Kidney International*, 58(4), pp. 1711–1718. doi: 10.1046/j.1523-1755.2000.00332.x.

Mäkelä, S., Mustonen, J., Ala-Houhala, I., Hurme, M., Partanen, J., Vapalahti, O., Vaheri, A. and Pasternack, A. (2002) 'Human leukocyte antigen-B8-DR3 is a more important risk factor for severe Puumala hantavirus infection than the tumor necrosis factor-alpha(-308) G/A polymorphism.', *The Journal of infectious diseases*, 186(6), pp. 843–846. doi: 10.1086/342413.

Malinin, O. V and Platonov, A. E. (2017) 'Insufficient efficacy and safety of intravenous ribavirin in treatment of haemorrhagic fever with renal syndrome caused by Puumala virus.', *Infectious diseases (London, England)*, 49(7), pp. 514–520. doi: 10.1080/23744235.2017.1293841.

Martinez-Valdebenito, C., Calvo, M., Vial, C., Mansilla, R., Marco, C., *et al.* (2014) 'Person-to-person household and nosocomial transmission of andes hantavirus, Southern Chile, 2011.', *Emerging infectious diseases*, 20(10), pp. 1629–1636. doi: 10.3201/eid2010.140353.

Matthys, V., Gorbunova, E. E., Gavrilovskaya, I. N., Pepini, T. and Mackow, E. R. (2011) 'The C-Terminal 42 Residues of the Tula Virus Gn Protein Regulate Interferon Induction', *Journal of Virology*, 85(10), pp. 4752–4760. doi: 10.1128/JVI.01945-10.

Matthys, V. S., Cimica, V., Dalrymple, N. A., Glennon, N. B., Bianco, C. and Mackow, E. R. (2014) 'Hantavirus GnT Elements Mediate TRAF3 Binding and Inhibit RIG-I/TBK1-Directed Beta Interferon Transcription by Blocking IRF3 Phosphorylation', *Journal of Virology*, 88(4), pp. 2246–2259. doi: 10.1128/JVI.02647-13.

McCaughey, C., Montgomery, W. I., Twomey, N., Addley, M., O'Neill, H. J. and Coyle, P.

V (1996) ‘Evidence of hantavirus in wild rodents in Northern Ireland.’, *Epidemiology and infection*, 117(2), pp. 361–365.

McCaughey, C. and Hart, C. A. (2000) ‘Hantaviruses.’, *Journal of medical microbiology*, 49(7), pp. 587–599. doi: 10.1099/0022-1317-49-7-587.

McKenna, P., Clement, J., Matthys, P., Coyle, P. V and McCaughey, C. (1994) ‘Serological evidence of Hantavirus disease in Northern Ireland.’, *Journal of medical virology*, 43(1), pp. 33–38.

Megger, D. A., Bracht, T., Meyer, H. E. and Sitek, B. (2013) ‘Label-free quantification in clinical proteomics’, *Biochimica et Biophysica Acta - Proteins and Proteomics*, 1834(8), pp. 1581–1590. doi: 10.1016/j.bbapap.2013.04.001.

Megger, D. A., Pott, L. L., Ahrens, M., Padden, J., Bracht, T., Kuhlmann, K., Eisenacher, M., Meyer, H. E. and Sitek, B. (2014) ‘Comparison of label-free and label-based strategies for proteome analysis of hepatoma cell lines’, *Biochimica et Biophysica Acta - Proteins and Proteomics*. Elsevier B.V., 1844(5), pp. 967–976. doi: 10.1016/j.bbapap.2013.07.017.

Meisel, H., Wolbert, A., Razanskiene, A., Marg, A., Kazaks, A., Sasnauskas, K., Pauli, G., Ulrich, R. and Kruger, D. H. (2006) ‘Development of novel immunoglobulin G (IgG), IgA, and IgM enzyme immunoassays based on recombinant Puumala and Dobrava hantavirus nucleocapsid proteins.’, *Clinical and vaccine immunology : CVI*, 13(12), pp. 1349–1357. doi: 10.1128/CVI.00208-06.

Melmer, A., Fineder, L., Lamina, C., Kollerits, B., Dieplinger, B., *et al.* (2013) ‘Plasma concentrations of the vitamin E-binding protein afamin are associated with overall and progression-free survival and platinum sensitivity in serous ovarian cancer - A study by the OVCAD consortium’, *Gynecologic Oncology*. Elsevier Inc., 128(1), pp. 38–43. doi:

10.1016/j.ygyno.2012.09.032.

Merl, J., Ueffing, M., Hauck, S. M. and von Toerne, C. (2012) 'Direct comparison of MS-based label-free and SILAC quantitative proteome profiling strategies in primary retinal Muller cells.', *Proteomics*, 12(12), pp. 1902–1911. doi: 10.1002/pmic.201100549.

Mertz, G. J., Miedzinski, L., Goade, D., Pavia, A. T., Hjelle, B., *et al.* (2004) 'Placebo-controlled, double-blind trial of intravenous ribavirin for the treatment of hantavirus cardiopulmonary syndrome in North America.', *Clinical infectious diseases : an official publication of the Infectious Diseases Society of America*, 39(9), pp. 1307–1313. doi: 10.1086/425007.

Meyer, B. J. and Schmaljohn, C. S. (2000) 'Persistent hantavirus infections: Characteristics and mechanisms', *Trends in Microbiology*, 8(2), pp. 61–67. doi: 10.1016/S0966-842X(99)01658-3.

Micheel, C. M., Nass, S. J., Omenn, G. S. and Policy, H. S. (2012) *Evolution of Translational Omics Lessons Learned and the Path Forward*, *Evolution*. doi: 10.17226/13297.

Miettinen, M. H., Makela, S. M., Ala-Houhala, I. O., Huhtala, H. S. A., Koobi, T., Vaheri, A. I., Pasternack, A. I., Porsti, I. H. and Mustonen, J. T. (2006) 'Ten-year prognosis of Puumala hantavirus-induced acute interstitial nephritis.', *Kidney international*, 69(11), pp. 2043–2048. doi: 10.1038/sj.ki.5000334.

Mir, M. A., Brown, B., Hjelle, B., Duran, W. A. and Panganiban, A. T. (2006) 'Hantavirus N Protein Exhibits Genus-Specific Recognition of the Viral RNA Panhandle', *Journal of Virology*, 80(22), pp. 11283–11292. doi: 10.1128/JVI.00820-06.

Mir, M. A., Duran, W. A., Hjelle, B. L., Ye, C. and Panganiban, A. T. (2008) 'Storage of

cellular 5' mRNA caps in P bodies for viral cap-snatching.', *Proceedings of the National Academy of Sciences of the United States of America*, 105(49), pp. 19294–19299. doi: 10.1073/pnas.0807211105.

Mir, M. A., Sheema, S., Haseeb, A. and Haque, A. (2010) 'Hantavirus nucleocapsid protein has distinct m7G cap- and RNA-binding sites.', *The Journal of biological chemistry*, 285(15), pp. 11357–11368. doi: 10.1074/jbc.M110.102459.

Mir, M. A. and Panganiban, A. T. (2008) 'A protein that replaces the entire cellular eIF4F complex.', *The EMBO journal*, 27(23), pp. 3129–3139. doi: 10.1038/emboj.2008.228.

Mou, D. L., Wang, Y. P., Huang, C. X., Li, G. Y., Pan, L., Yang, W. S. and Bai, X. F. (2006) 'Cellular entry of Hantaan virus A9 strain: specific interactions with beta3 integrins and a novel 70kDa protein.', *Biochemical and biophysical research communications*, 339(2), pp. 611–617. doi: 10.1016/j.bbrc.2005.11.049.

Murphy, K. (2012) *Janeway's immunobiology*. Edited by 8th. Garkand Science.

Mustonen, J., Partanen, J., Kanerva, M., Pietilä, K., Vapalahti, O., Pasternack, A. and Vaheri, A. (1996) 'Genetic susceptibility to severe course of nephropathia epidemica caused by Puumala hantavirus', *Kidney International*, 49(1), pp. 217–221. doi: 10.1038/ki.1996.29.

Mustonen, J., Mäkelä, S., Outinen, T., Laine, O., Jylhävä, J., Arstila, P. T., Hurme, M. and Vaheri, A. (2013) 'The pathogenesis of nephropathia epidemica: New knowledge and unanswered questions', *Antiviral Research*. Elsevier B.V., 100(3), pp. 589–604. doi: 10.1016/j.antiviral.2013.10.001.

Nakamura, I., Yoshimatsu, K., Lee, B.-H., Okumura, M., Taruishi, M., Araki, K., Kariwa, H., Takashima, I. and Arikawa, J. (2008) 'Development of a serotyping ELISA system for Thailand virus infection.', *Archives of virology*. Austria, 153(8), pp. 1537–1542. doi:

10.1007/s00705-008-0128-4.

Nanjappa, V., Thomas, J. K., Marimuthu, A., Muthusamy, B., Radhakrishnan, A., *et al.* (2014) 'Plasma Proteome Database as a resource for proteomics research: 2014 update.', *Nucleic acids research*, 42(Database issue), pp. D959-65. doi: 10.1093/nar/gkt1251.

Nelson-Piercy, C. (2014) *Hantavirus with pt perspective SD*. Available at: file:///Users/sarahby/Documents/Artikler/Hantavirus with pt perspective SD.doc.

Niikura, M., Maeda, A., Ikegami, T., Saijo, M., Kurane, I. and Morikawa, S. (2004) 'Modification of endothelial cell functions by Hantaan virus infection: prolonged hyper-permeability induced by TNF-alpha of hantaan virus-infected endothelial cell monolayers', *Archives of Virology*, 149(7), pp. 1279–1292. doi: 10.1007/s00705-004-0306-y.

Niklasson, B. and Kjelsson, T. (1988) 'Detection of nephropathia epidemica (Puumala virus)-specific immunoglobulin M by enzyme-linked immunosorbent assay.', *Journal of clinical microbiology*, 26(8), pp. 1519–1523.

Novoa, R. R., Calderita, G., Cabezas, P., Elliott, R. M. and Risco, C. (2005) 'Key Golgi Factors for Structural and Functional Maturation of Bunyamwera Virus', *Journal of Virology*, 79(17), pp. 10852–10863. doi: 10.1128/JVI.79.17.10852-10863.2005.

Ogino, M., Ebihara, H., Lee, B.-H., Araki, K., Lundkvist, A., Kawaoka, Y., Yoshimatsu, K. and Arikawa, J. (2003) 'Use of vesicular stomatitis virus pseudotypes bearing hantaan or seoul virus envelope proteins in a rapid and safe neutralization test.', *Clinical and diagnostic laboratory immunology*, 10(1), pp. 154–160. doi: 10.1128/CDLI.10.1.154.

Ogino, M., Yoshimatsu, K., Ebihara, H., Lee, B., Okumura, M., Arikawa, J. and Araki, K. (2004) 'Cell Fusion Activities of Hantaan Virus Envelope Glycoproteins Cell Fusion Activities of Hantaan Virus Envelope Glycoproteins', *Journal of virology*, 78(19), pp. 10776–10782.

doi: 10.1128/JVI.78.19.10776.

Oldal, M., Nemeth, V., Madai, M., Kemenesi, G., Dallos, B., *et al.* (2014) 'Identification of hantavirus infection by Western blot assay and TaqMan PCR in patients hospitalized with acute kidney injury.', *Diagnostic microbiology and infectious disease*, 79(2), pp. 166–170. doi: 10.1016/j.diagmicrobio.2014.01.032.

Van Oudenhove, L. and Devreese, B. (2013) 'A review on recent developments in mass spectrometry instrumentation and quantitative tools advancing bacterial proteomics', *Applied Microbiology and Biotechnology*, 97(11), pp. 4749–4762. doi: 10.1007/s00253-013-4897-7.

Outinen, T. K., Mäkelä, S. M., Ala-Houhala, I. O., Huhtala, H. S., Hurme, M., Paakkala, A. S., Pörsti, I. H., Syrjänen, J. T. and Mustonen, J. T. (2010) 'The severity of Puumala hantavirus induced nephropathia epidemica can be better evaluated using plasma interleukin-6 than C-reactive protein determinations.', *BMC infectious diseases*, 10, p. 132. doi: 10.1186/1471-2334-10-132.

Overgaard, M. T., Oxvig, C., Christiansen, M., Lawrence, J. B., Conover, C. A., Gleich, G. J., Sottrup-Jensen, L. and Haaning, J. (1999) 'Messenger ribonucleic acid levels of pregnancy-associated plasma protein-A and the proform of eosinophil major basic protein: expression in human reproductive and nonreproductive tissues.', *Biology of reproduction*, 61(4), pp. 1083–1089.

Padula, P. J., Edelstein, A., Miguel, S. D. L., López, N. M., Rossi, C. M. and Rabinovich, R. D. (1998) 'Hantavirus Pulmonary Syndrome Outbreak in Argentina: Molecular Evidence for Person-to-Person Transmission of Andes Virus', *Virology*, 241(2), pp. 323–330. doi: 10.1006/viro.1997.8976.

Parkes, J., Roderick, P., Harris, S., Day, C., Mutimer, D., *et al.* (2010) 'Enhanced liver fibrosis test can predict clinical outcomes in patients with chronic liver disease', *Gut*, 59(9), p. 1245 LP-1251.

Passaro, D. J., Shieh, W. J., Hacker, J. K., Fritz, C. L., Hogan, S. R., Fischer, M., Hendry, R. M. and Vugia, D. J. (2001) 'Predominant kidney involvement in a fatal case of hantavirus pulmonary syndrome caused by Sin Nombre virus.', *Clinical infectious diseases : an official publication of the Infectious Diseases Society of America*, 33(2), pp. 263–264. doi: 10.1086/321832.

Patel, K., Lucas, J. E., Thompson, J. W., Dubois, L. G., Tillmann, H. L., *et al.* (2011) 'High predictive accuracy of an unbiased proteomic profile for sustained virologic response in chronic hepatitis C patients.', *Hepatology (Baltimore, Md.)*, 53(6), pp. 1809–1818. doi: 10.1002/hep.24284.

Pattamadilok, S., Lee, B.-H., Kumperasart, S., Yoshimatsu, K., Okumura, M., *et al.* (2006) 'Geographical distribution of hantaviruses in Thailand and potential human health significance of Thailand virus.', *The American journal of tropical medicine and hygiene*. United States, 75(5), pp. 994–1002.

Pejcoch, M., Pazdiora, P., Eiselt, J., Hajek, V., Vesela, E., Vlasak, J., Benesova, J., Kubatova, A. and Kriz, B. (2010) 'Seroprevalence of hantavirus antibodies among chronic hemodialysis patients in the Czech Republic.', *Epidemiologie, mikrobiologie, imunologie : casopis Spolecnosti pro epidemiologii a mikrobiologii Ceske lekarske spolecnosti J.E. Purkyne*, 59(1), pp. 48–51.

Pekosz, a, Griot, C., Nathanson, N. and Gonzalez-Scarano, F. (1995) 'Tropism of bunyaviruses: evidence for a G1 glycoprotein-mediated entry pathway common to the California serogroup.', *Virology*, 214, pp. 339–348. doi: 10.1006/viro.1995.0043.

Pergam, S. A., Schmidt, D. W., Nofchissey, R. A., Hunt, W. C., Harford, A. H. and Goade, D. E. (2009) 'Potential renal sequelae in survivors of hantavirus cardiopulmonary syndrome.', *The American journal of tropical medicine and hygiene*, 80(2), pp. 279–285.

Pether, J. V. S., Thurlow, J., Hospital, M. P., I, T. T. A., Hospital, D., Kingston, H. and Bai, Y. (1993) 'CASE REPORT Acute hantavirusinfection presenting as hypersensitivity', 1, pp. 75–77.

Pether, J. V, Jones, N. and Lloyd, G. (1991) 'Acute hantavirus infection.', *Lancet (London, England)*. England, p. 1025.

Pether, J. V and Lloyd, G. (1993) 'The clinical spectrum of human hantavirus infection in Somerset, UK.', *Epidemiology and infection*, 111(1), pp. 171–175.

Pettersson, L., Thunberg, T., Rocklov, J., Klingstrom, J., Evander, M. and Ahlm, C. (2014) 'Viral load and humoral immune response in association with disease severity in Puumala hantavirus-infected patients--implications for treatment.', *Clinical microbiology and infection : the official publication of the European Society of Clinical Microbiology and Infectious Diseases*, 20(3), pp. 235–241. doi: 10.1111/1469-0691.12259.

Phillips, M. J., Johnson, S. A., Thomson, R. K. and Pether, J. V (1991) 'Further UK case of acute hantavirus infection', *Lancet (London, England)*, 338(8781), pp. 1530–1531. doi: 10.1016/0140-6736(91)92355-6.

Plassmeyer, M. L., Soldan, S. S., Stachelek, K. M., Martín-García, J. and González-Scarano, F. (2005) 'California serogroup Gc (G1) glycoprotein is the principal determinant of pH-dependent cell fusion and entry', *Virology*, 338(1), pp. 121–132. doi: 10.1016/j.virol.2005.04.026.

Plyusnin, A., Vaheri, A. and Lundkvist, Å. (2006) 'Saaremaa hantavirus should not be

confused with its dangerous relative, Dobrava virus [10]', *Journal of Clinical Microbiology*, 44(4), pp. 1608–1609. doi: 10.1128/JCM.44.4.1608-1611.2006.

Potter, M. D. and Nicchitta, C. V. (2002) 'Endoplasmic reticulum-bound ribosomes reside in stable association with the translocon following termination of protein synthesis', *Journal of Biological Chemistry*, 277(26), pp. 23314–23320. doi: 10.1074/jbc.M202559200.

Pounder, K. C., Begon, M., Sironen, T., Henttonen, H., Watts, P. C., *et al.* (2013) 'Novel Hantavirus in field vole, United Kingdom', *Emerging Infectious Diseases*, 19(4), pp. 673–675. doi: 10.3201/eid1904.121057.

Poynard, T., Imbert-Bismut, F., Munteanu, M., Messous, D., Myers, R. P., *et al.* (2004) 'Overview of the diagnostic value of biochemical markers of liver fibrosis (FibroTest, HCV FibroSure) and necrosis (ActiTest) in patients with chronic hepatitis C', *Comparative Hepatology*, 3, pp. 1–12. doi: 10.1186/1476-5926-3-8.

Poynard, T., Morra, R., Halfon, P., Castera, L., Ratziu, V., *et al.* (2007) 'Meta-analyses of FibroTest diagnostic value in chronic liver disease', *BMC Gastroenterology*, 7, pp. 1–11. doi: 10.1186/1471-230X-7-40.

Prevention, C. F. D. C. and (2017) *Reported Cases of Hantavirus Disease*. Available at: https://www.cdc.gov/hantavirus/surveillance/.

Ramanathan, H. N., Chung, D.-H., Plane, S. J., Sztul, E., Chu, Y.-K., Guttieri, M. C., McDowell, M., Ali, G. and Jonsson, C. B. (2007) 'Dynein-dependent transport of the hantaan virus nucleocapsid protein to the endoplasmic reticulum-Golgi intermediate compartment.', *Journal of virology*, 81(16), pp. 8634–8647. doi: 10.1128/JVI.00418-07.

Ramanathan, H. N. and Jonsson, C. B. (2008) 'New and Old World hantaviruses differentially utilize host cytoskeletal components during their life cycles', *Virology*, 374(1),

pp. 138–150. doi: 10.1016/j.virol.2007.12.030.

Rasche, F. M., Uhel, B., Ulrich, R., Krüger, D. H., Karges, W., *et al.* (2004) 'Thrombocytopenia and acute failure in Puumala hantavirus infections', *Emerging Infectious Diseases*, 10(8), pp. 1420–1425. doi: 10.3201/eid1008.031069.

Ravkov, E. V, Nichol, S. T. and Compans, R. W. (1997) 'Polarized entry and release in epithelial cells of Black Creek Canal virus, a New World hantavirus.', *Journal of virology*, 71(2), pp. 1147–1154.

Ray, N., Whidby, J., Stewart, S., Hooper, J. W. and Bertolotti-Ciarlet, A. (2010) 'Study of Andes virus entry and neutralization using a pseudovirion system.', *Journal of virological methods*, 163(2), pp. 416–423. doi: 10.1016/j.jviromet.2009.11.004.

Raymond, T., Gorbunova, E., Gavrilovskaya, I. N. and Mackow, E. R. (2005) 'Pathogenic hantaviruses bind plexin-semaphorin-integrin domains present at the apex of inactive, bent alphavbeta3 integrin conformers.', *Proceedings of the National Academy of Sciences of the United States of America*, 102(4), pp. 1163–1168. doi: 10.1073/pnas.0406743102.

Richards, A. L. and Jackson, W. T. (2013) 'How positive-strand RNA viruses benefit from autophagosome maturation.', *Journal of virology*, 87(18), pp. 9966–9972. doi: 10.1128/JVI.00460-13.

Rigbolt, K. T. G., Vanselow, J. T. and Blagoev, B. (2011) 'GProX, a user-friendly platform for bioinformatics analysis and visualization of quantitative proteomics data.', *Molecular & cellular proteomics : MCP*, 10(8), p. O110.007450-O110.007450. doi: 10.1074/mcp.O110.007450.

Ringman, J. M., Schulman, H., Becker, C., Jones, T., Bai, U., *et al.* (2012) 'Proteomic changes in cerebrospinal fluid in presymptomatic nd affected persons carrying familial

alzheimer disease mutations', 69(1), pp. 96–104. doi: 10.1001/archneurol.2011.642.Proteomic.

Roboti, P. and High, S. (2012) 'The oligosaccharyltransferase subunits OST48, DAD1 and KCP2 function as ubiquitous and selective modulators of mammalian N-glycosylation', *Journal of Cell Science*, 125(14), pp. 3474–3484. doi: 10.1242/jcs.103952.

Rönnberg, T., Jääskeläinen, K., Blot, G., Parviainen, V., Vaheri, A., Renkonen, R., Bouloy, M. and Plyusnin, A. (2012) 'Searching for cellular partners of hantaviral nonstructural protein NSs: Y2H screening of mouse cDNA library and analysis of cellular interactome', *PLoS ONE*, 7(4). doi: 10.1371/journal.pone.0034307.

Rosenberg, W. M. C., Voelker, M., Thiel, R., Becka, M., Burt, A., *et al.* (2004) 'Serum markers detect the presence of liver fibrosis: A cohort study', *Gastroenterology*, 127(6), pp. 1704–1713. doi: 10.1053/j.gastro.2004.08.052.

Rueden, C. T., Schindelin, J., Hiner, M. C., DeZonia, B. E., Walter, A. E., Arena, E. T. and Eliceiri, K. W. (2017) 'ImageJ2: ImageJ for the next generation of scientific image data', *BMC Bioinformatics*, 18(1), p. 529. doi: 10.1186/s12859-017-1934-z.

Rull, K. and Laan, M. (2005) 'Expression of β-subunit of HCG genes during normal and failed pregnancy', *Human Reproduction*, 20(12), pp. 3360–3368. Available at: http://dx.doi.org/10.1093/humrep/dei261.

Rusnak, J. M., Byrne, W. R., Chung, K. N., Gibbs, P. H., Kim, T. T., *et al.* (2009) 'Experience with intravenous ribavirin in the treatment of hemorrhagic fever with renal syndrome in Korea.', *Antiviral research*, 81(1), pp. 68–76. doi: 10.1016/j.antiviral.2008.09.007.

Saade, G. R., Boggess, K. A., Sullivan, S. A., Markenson, G. R., Iams, J. D., *et al.* (2016)

'Development and validation of a spontaneous preterm delivery predictor in asymptomatic women', *American Journal of Obstetrics and Gynecology*, 214(5), p. 633e1-633e24. doi: 10.1016/j.ajog.2016.02.001.

Sadeghi, M., Eckerle, I., Daniel, V., Burkhardt, U., Opelz, G. and Schnitzler, P. (2011) 'Cytokine expression during early and late phase of acute Puumala hantavirus infection.', *BMC immunology*, 12, p. 65. doi: 10.1186/1471-2172-12-65.

Schiavon, L. de L., Narciso-Schiavon, J. L. and de Carvalho-Filho, R. J. (2014) 'Non-invasive diagnosis of liver fibrosis in chronic hepatitis C', *World Journal of Gastroenterology*, 20(11), pp. 2854–2866. doi: 10.3748/wjg.v20.i11.2854.

Schilling, S., Emmerich, P., Klempa, B., Auste, B., Schnaith, E., Schmitz, H., Krüger, D. H., Günther, S. and Meisel, H. (2007) 'Hantavirus disease outbreak in Germany: Limitations of routine serological diagnostics and clustering of virus sequences of human and rodent origin', *Journal of Clinical Microbiology*, 45(9), pp. 3008–3014. doi: 10.1128/JCM.02573-06.

Schindelin, J., Arganda-Carreras, I., Frise, E., Kaynig, V., Longair, M., *et al.* (2012) 'Fiji: an open-source platform for biological-image analysis', *Nature Methods*. Nature Publishing Group, a division of Macmillan Publishers Limited. All Rights Reserved., 9, p. 676.

Schountz, T., Acuna-Retamar, M., Feinstein, S., Prescott, J., Torres-Perez, F., *et al.* (2012) 'Kinetics of immune responses in deer mice experimentally infected with Sin Nombre virus.', *Journal of virology*, 86(18), pp. 10015–10027. doi: 10.1128/JVI.06875-11.

Schultze, D., Lundkvist, A., Blauenstein, U. and Heyman, P. (2002) 'Tula virus infection associated with fever and exanthema after a wild rodent bite.', *European journal of clinical microbiology & infectious diseases : official publication of the European Society of Clinical Microbiology*, 21(4), pp. 304–306. doi: 10.1007/s10096-002-0705-5.

Shi, X., Chen, Z., Tang, S., Wu, F., Xiong, S. and Dong, C. (2016) 'Coxsackievirus B3 infection induces autophagic flux, and autophagosomes are critical for efficient viral replication.', *Archives of virology*, 161(8), pp. 2197–2205. doi: 10.1007/s00705-016-2896-6.

Shi, X. and Elliott, R. M. (2002) 'Golgi Localization of Hantaan Virus Glycoproteins Requires Coexpression of G1 and G2.', *Virology*, 300(1), pp. 31–38. doi: 10.1006/viro.2002.1414.

Shi, X. and Elliott, R. M. (2004) 'Analysis of N-linked glycosylation of hantaan virus glycoproteins and the role of oligosaccharide side chains in protein folding and intracellular trafficking.', *Journal of virology*, 78(10), pp. 5414–5422.

Shim, S. H., Park, M. S., Moon, S., Park, K. S., Song, J. W., Song, K. J. and Baek, L. J. (2011) 'Comparison of innate immune responses to pathogenic and putative non-pathogenic hantaviruses in vitro', *Virus Research*. Elsevier B.V., 160(1–2), pp. 367–373. doi: 10.1016/j.virusres.2011.07.013.

Shimizu, K., Yoshimatsu, K., Koma, T., Yasuda, S. P. and Arikawa, J. (2013) 'Role of nucleocapsid protein of hantaviruses in intracellular traffic of viral glycoproteins', *Virus Research*. Elsevier B.V., 178(2), pp. 349–356. doi: 10.1016/j.virusres.2013.09.022.

Silverman, A. M., Nakata, R., Shimada, H., Sposto, R. and Declerck, Y. A. (2012) 'A Galectin-3 – Dependent Pathway Upregulates Interleukin-6 in the Microenvironment of Human Neuroblastoma', 72(26), pp. 2228–2239. doi: 10.1158/0008-5472.CAN-11-2165.

Sohn, Y. M., Rho, H. O., Park, M. S., Kim, J. S. and Summers, P. L. (2001) 'Primary humoral immune responses to formalin inactivated hemorrhagic fever with renal syndrome vaccine (Hantavax): consideration of active immunization in South Korea.', *Yonsei medical journal*, 42(3), pp. 278–284. doi: 10.3349/ymj.2001.42.3.278.

Spiropoulou, C. F., Goldsmith, C. S., Shoemaker, T. R., Peters, C. J. and Compans, R. W. (2003) 'Sin Nombre virus glycoprotein trafficking', *Virology*, 308(1), pp. 48–63. doi: 10.1016/S0042-6822(02)00092-2.

Stojanovic, M., Pekic, S., Cvijovic, G., Miljic, D., Doknic, M., *et al.* (2008) 'High risk of hypopituitarism in patients who recovered from hemorrhagic fever with renal syndrome.', *The Journal of clinical endocrinology and metabolism*, 93(7), pp. 2722–2728. doi: 10.1210/jc.2008-0311.

Strandin, T., Hepojoki, J. and Vaheri, A. (2013) 'Cytoplasmic tails of bunyavirus Gn glycoproteins-Could they act as matrix protein surrogates?', *Virology*. Elsevier, 437(2), pp. 73–80. doi: 10.1016/j.virol.2013.01.001.

Szklarczyk, D., Morris, J. H., Cook, H., Kuhn, M., Wyder, S., *et al.* (2017) 'The STRING database in 2017: quality-controlled protein-protein association networks, made broadly accessible.', *Nucleic acids research*. England, 45(D1), pp. D362–D368. doi: 10.1093/nar/gkw937.

Takala, A., Lahdevirta, J., Jansson, S. E., Vapalahti, O., Orpana, A., Karonen, S. L. and Repo, H. (2000) 'Systemic inflammation in hemorrhagic fever with renal syndrome correlates with hypotension and thrombocytopenia but not with renal injury.', *The Journal of infectious diseases*, 181(6), pp. 1964–1970. doi: 10.1086/315522.

Tambor, V., Kacerovsky, M., Lenco, J., Bhat, G. and Menon, R. (2013) 'Proteomics and bioinformatics analysis reveal underlying pathways of infection associated histologic chorioamnionitis in pPROM.', *Placenta*, 34(2), pp. 155–161. doi: 10.1016/j.placenta.2012.11.028.

Taylor, S. L., Wahl-Jensen, V., Copeland, A. M., Jahrling, P. B. and Schmaljohn, C. S.

(2013) ‘Endothelial Cell Permeability during Hantavirus Infection Involves Factor XII-Dependent Increased Activation of the Kallikrein-Kinin System’, *PLoS Pathogens*, 9(7). doi: 10.1371/journal.ppat.1003470.

Terajima, M. and Ennis, F. A. (2011) ‘T cells and pathogenesis of hantavirus cardiopulmonary syndrome and hemorrhagic fever with renal syndrome’, *Viruses*, 3(7), pp. 1059–1073. doi: 10.3390/v3071059.

Than, N. G., Romero, R., Balogh, A., Karpati, E., Mastrolia, S. A., *et al.* (2015) ‘Galectins: Double-edged Swords in the Cross-roads of Pregnancy Complications and Female Reproductive Tract Inflammation and Neoplasia INTRODUCTION TO THE GALECTIN FAMILY’, *Journal of Pathology and Translational Medicine*, 49, pp. 181–208. doi: 10.4132/jptm.2015.02.25.

Thomason, A. G., Begon, M., Bradley, J. E., Paterson, S. and Jackson, J. A. (2017) ‘Endemic Hantavirus in Field Voles, Northern England.’, *Emerging infectious diseases*, 23(6), pp. 1033–1035. doi: 10.3201/eid2306.161607.

Tian, Y., Tan, A. C., Sun, X., Olson, M., Xie, Z., *et al.* (2009) ‘Quantitative Proteomic Analysis of Ovarian Cancer Cells Identified Mitochondrial Proteins Associated with Paclitaxel Resistance’, *Proteomics. Clinical applications*, 3, pp. 1288–1295.

Timmins, J., Ruigrok, R. W. H. and Weissenhorn, W. (2004) ‘Structural studies on the Ebola virus matrix protein VP40 indicate that matrix proteins of enveloped RNA viruses are analogues but not homologues.’, *FEMS microbiology letters*, 233(2), pp. 179–186. doi: 10.1016/j.femsle.2004.03.002.

Tischler, N. D., Gonzales, A., Perez-Acle, T., Rosemblatt, M. and Valenzuela, P. D. T. (2005) ‘Hantavirus Gc glycoprotein: Evidence for a class ll fusion protein’, *Journal of General*

*Virology*, 86(11), pp. 2937–2947. doi: 10.1099/vir.0.81083-0.

Tvedt, T. H. A., Rye, K. P., Reikvam, H., Brenner, A. K. and Bruserud, Ø. (2015) 'The importance of sample collection when using single cytokine levels and systemic cytokine profiles as biomarkers — a comparative study of serum versus plasma samples', *Journal of Immunological Methods*. Elsevier B.V., 418, pp. 19–28. doi: 10.1016/j.jim.2015.01.006.

Updates, I. (no date) 'Multi-state Outbreak of Seoul Virus'.

Vaheri, A., Henttonen, H., Voutilainen, L., Mustonen, J., Sironen, T. and Vapalahti, O. (2013) 'Hantavirus infections in Europe and their impact on public health.', *Reviews in medical virology*, 23(1), pp. 35–49. doi: 10.1002/rmv.1722.

Vaheri, A., Strandin, T., Hepojoki, J., Sironen, T., Henttonen, H., Makela, S. and Mustonen, J. (2013) 'Uncovering the mysteries of hantavirus infections.', *Nature reviews. Microbiology*, 11(8), pp. 539–550.

Vaheri, A., Vapalahti, O. and Plyusnin, A. (2008) 'How to diagnose hantavirus infections and detect them in rodents and insectivores.', *Reviews in medical virology*, 18(4), pp. 277–288. doi: 10.1002/rmv.581.

Vapalahti, O., Lundkvist, A., Kallio-Kokko, H., Paukku, K., Julkunen, I., Lankinen, H. and Vaheri, A. (1996) 'Antigenic properties and diagnostic potential of puumala virus nucleocapsid protein expressed in insect cells.', *Journal of clinical microbiology*, 34(1), pp. 119–125.

Vial, P. A., Valdivieso, F., Calvo, M., Rioseco, M. L., Riquelme, R., *et al.* (2015) 'A non-randomized multicentre trial of human immune plasma for treatment of hantavirus cardiopulmonary syndrome caused by Andes virus.', *Antiviral therapy*, 20(4), pp. 377–386. doi: 10.3851/IMP2875.

Vizcaion, J. A. (2015) 'Proteomics:History and introduction to the course'. Hinxton.Cambridge: EMBL-EBI, pp. 1–11.

Walker, E., Boyd, A. J., Kudesia, G. and Pinkerton, I. W. (1985) 'A Scottish case of nephropathy due to Hantaan virus infection.', *The Journal of infection*. England, 11(1), pp. 57–58.

Walsh, S. T. R. and Kossiakoff, A. A. (2006) 'Crystal structure and site 1 binding energetics of human placental lactogen.', *Journal of molecular biology*. England, 358(3), pp. 773–784. doi: 10.1016/j.jmb.2006.02.038.

Wang, H., Alminaite, A., Vaheri, A. and Plyusnin, A. (2010) 'Interaction between hantaviral nucleocapsid protein and the cytoplasmic tail of surface glycoprotein Gn', *Virus Research*, 151(2), pp. 205–212. doi: 10.1016/j.virusres.2010.05.008.

Wang, M., Wang, J., Wang, T., Li, J., Hui, L. and Ha, X. (2013) 'Thrombocytopenia as a Predictor of Severe Acute Kidney Injury in Patients with Hantaan Virus Infections', *PLoS ONE*, 8(1), pp. 1–6. doi: 10.1371/journal.pone.0053236.

Wang, M., Rossi, C. and Schmaljohn, C. S. (1993) 'Expression of non-conserved regions of the S genome segments of three hantaviruses: evaluation of the expressed polypeptides for diagnosis of haemorrhagic fever with renal syndrome.', *The Journal of general virology*, 74 ( Pt 6), pp. 1115–1124. doi: 10.1099/0022-1317-74-6-1115.

Wasung, M. E., Chawla, L. S. and Madero, M. (2015) 'Biomarkers of renal function, which and when?', *Clinica Chimica Acta*. Elsevier B.V., 438(2015), pp. 350–357. doi: 10.1016/j.cca.2014.08.039.

Webster, J. P. and Macdonald, D. W. (1995) 'Parasites of wild brown rats (Rattus norvegicus) on UK farms.', *Parasitology*, 111 ( Pt 3, pp. 247–255.

Wells, R. M., Sosa Estani, S., Yadon, Z. E., Enria, D., Padula, P., Pini, N., Mills, J. N., Peters, C. J. and Segura, E. L. (1997) 'An unusual hantavirus outbreak in southern Argentina: person-to-person transmission? Hantavirus Pulmonary Syndrome Study Group for Patagonia.', *Emerging infectious diseases*, 3(2), pp. 171–174. doi: 10.3201/eid0302.970210.

Woods, C., Palekar, R., Kim, P., Blythe, D., de Senarclens, O., *et al.* (2009) 'Domestically acquired seoul virus causing hemorrhagic fever with renal syndrome-Maryland, 2008.', *Clinical infectious diseases : an official publication of the Infectious Diseases Society of America*, 49(10), pp. e109-12. doi: 10.1086/644742.

Xu, F., Yang, Z., Wang, L., Lee, Y. L., Yang, C. C., Xiao, S. Y., Xiao, H. and Wen, L. (2007) 'Morphological characterization of hantavirus HV114 by electron microscopy', *Intervirology*, 50(3), pp. 166–172. doi: 10.1159/000098959.

Yang, L. and Lin, P. C. (2017) 'Mechanisms that drive inflammatory tumor microenvironment, tumor heterogeneity, and metastatic progression', *Seminars in Cancer Biology*. Elsevier, (July), pp. 0–1. doi: 10.1016/j.semcancer.2017.08.001.

Yang, W., Zhou, J., Chen, L., Ao, M., Sun, S., Aiyetan, P., Simmons, A., Zhang, H. and Jackson, J. B. (2014) 'Glycoproteomic analysis identifies human glycoproteins secreted from HIV latently infected T cells and reveals their presence in HIV + plasma', *Clinical Proteomics*. Clinical Proteomics, 11(1), pp. 1–11. doi: 10.1186/1559-0275-11-9.

Yoshimatsu, K., Arikawa, J., Tamura, M., Yoshida, R., Lundkvist, A., Niklasson, B., Kariwa, H. and Azuma, I. (1996) 'Characterization of the nucleocapsid protein of Hantaan virus strain 76-118 using monoclonal antibodies.', *The Journal of general virology*, 77 ( Pt 4), pp. 695–704. doi: 10.1099/0022-1317-77-4-695.

Yoshimatsu, K. and Arikawa, J. (2014) 'Serological diagnosis with recombinant N antigen

for hantavirus infection.', *Virus research*, 187, pp. 77–83. doi: 10.1016/j.virusres.2013.12.040.

Zelena, H., Mrazek, J. and Kuhn, T. (2013) 'Tula hantavirus infection in immunocompromised host, Czech Republic.', *Emerging infectious diseases*, 19(11), pp. 1873–1875. doi: 10.3201/eid1911.130421.

Zhang, H., Liu, A. Y., Loriaux, P., Wollscheid, B., Zhou, Y., Watts, J. D. and Aebersold, R. (2007) 'Mass spectrometric detection of tissue proteins in plasma.', *Molecular & cellular proteomics : MCP*, 6(1), pp. 64–71. doi: 10.1074/mcp.M600160-MCP200.

Zhang, R., Miner, J. J., Gorman, M. J., Rausch, K., Ramage, H., *et al.* (2017) 'HHS Public Access', 535(7610), pp. 164–168. doi: 10.1038/nature18625.A.

Zhang, X., Chen, H.-Y., Zhu, L.-Y., Zeng, L.-L., Wang, F., *et al.* (2011) 'Comparison of Hantaan and Seoul viral infections among patients with hemorrhagic fever with renal syndrome (HFRS) in Heilongjiang, China.', *Scandinavian journal of infectious diseases*, 43(8), pp. 632–641. doi: 10.3109/00365548.2011.566279.

Zhang, Y.-Z., Zou, Y., Fu, Z. F. and Plyusnin, A. (2010) 'Hantavirus infections in humans and animals, China.', *Emerging infectious diseases*, 16(8), pp. 1195–1203. doi: 10.3201/eid1608.090470.

# *Appendix*

## *Appendix A. Ethical approval*

NHS
Health Research Authority

**East Midlands - Nottingham 1 Research Ethics Committee**

The Old Chapel
Royal Standard Place
Nottingham
NG1 6FS

23 February 2017

Ms Sarah Bar-Yaacov

University of Liverpool

Institute of Infection and Global Health

Department of Infection Biology

Liverpool

L3 5RF

Dear Ms Bar-Yaacov,

| | |
|---|---|
| **Study title:** | **Proteomic comparison of acute kidney injury due to Hantavirus infection and acute kidney injury due to leptospirosis** |
| **REC reference:** | **17/EM/0074** |
| **Protocol number:** | **NA** |
| **IRAS project ID:** | **201621** |

Thank you for your letter of 22 February 2017, responding to the Committee's request for further information on the above research and submitting revised documentation.

The further information has been considered on behalf of the Committee by the Chair.

We plan to publish your research summary wording for the above study on the HRA website, together with your contact details. Publication will be no earlier than three months from the date of this opinion letter. Should you wish to provide a substitute contact point, require further information, or wish to make a request to postpone publication, please contact hra.studyregistration@nhs.net outlining the reasons for your request.

*Confirmation of ethical opinion*

On behalf of the Committee, I am pleased to confirm a favourable ethical opinion for the above research on the basis described in the application form, protocol and supporting documentation as revised, subject to the conditions specified below.

*Conditions of the favourable opinion*

The REC favourable opinion is subject to the following conditions being met prior to the start of the study.

Management permission must be obtained from each host organisation prior to the start of the study at the site concerned.

*Management permission should be sought from all NHS organisations involved in the study in accordance with NHS research governance arrangements. Each NHS organisation must confirm through the signing of agreements and/or other documents that it has given permission for the research to proceed (except where explicitly specified otherwise).*

*Guidance on applying for NHS permission for research is available in the Integrated Research Application System, www.hra.nhs.uk or at http://www.rdforum.nhs.uk.*

*Where a NHS organisation's role in the study is limited to identifying and referring potential participants to research sites ("participant identification centre"), guidance should be sought from the R&D office on the information it requires to give permission for this activity.*

*For non-NHS sites, site management permission should be obtained in accordance with the procedures of the relevant host organisation.*

*Sponsors are not required to notify the Committee of management permissions from host organisations*

Registration of Clinical Trials

All clinical trials (defined as the first four categories on the IRAS filter page) must be registered on a publically accessible database within 6 weeks of recruitment of the first participant (for medical device studies, within the timeline determined by the current registration and publication trees).

There is no requirement to separately notify the REC but you should do so at the earliest opportunity e.g. when submitting an amendment. We will audit the registration details as part of the annual progress reporting process.

To ensure transparency in research, we strongly recommend that all research is registered but for non-clinical trials this is not currently mandatory.

If a sponsor wishes to request a deferral for study registration within the required timeframe, they should contact hra.studyregistration@nhs.net. The expectation is that all clinical trials will be registered, however, in exceptional circumstances non registration may be permissible with prior agreement from the HRA. Guidance on where to register is provided on the HRA website.

**It is the responsibility of the sponsor to ensure that all the conditions are complied with before the start of the study or its initiation at a particular site (as applicable).**

### *Ethical review of research sites*

NHS sites

The favourable opinion applies to all NHS sites taking part in the study, subject to management permission being obtained from the NHS/HSC R&D office prior to the start of the study (see "Conditions of the favourable opinion" below).

### *Approved documents*

The final list of documents reviewed and approved by the Committee is as follows:

| *Document* | *Version* | *Date* |
|---|---|---|
| Covering letter on headed paper [Cover letter] | 1 | 18 December 2016 |
| Evidence of Sponsor insurance or indemnity (non NHS Sponsors only) [Sponsor approval] | 1 | 18 December 2016 |
| IRAS Checklist XML [Checklist_22022017] | | 22 February 2017 |
| Letter from sponsor [Letter from sponsor] | 1 | 18 December 2016 |
| Other [Email Clarification Regarding Sponsor Signature] | | 02 February 2017 |
| REC Application Form [REC_Form_02022017] | | 02 February 2017 |
| Research protocol or project proposal [Project proposal] | 8 | 22 February 2017 |

| | | |
|---|---|---|
| Summary CV for Chief Investigator (CI) [CV for Ms Sarah Bar-Yaacov] | 2 | 01 February 2017 |
| Summary CV for supervisor (student research) [CV for Dr Beeching] | 1 | 01 February 2017 |
| Summary, synopsis or diagram (flowchart) of protocol in non technical language [Study design] | 3 | 04 October 2016 |

## *Statement of compliance*

The Committee is constituted in accordance with the Governance Arrangements for Research Ethics Committees and complies fully with the Standard Operating Procedures for Research Ethics Committees in the UK.

## *After ethical review*

Reporting requirements

The attached document *"After ethical review – guidance for researchers"* gives detailed guidance on reporting requirements for studies with a favourable opinion, including:

- Notifying substantial amendments
- Adding new sites and investigators
- Notification of serious breaches of the protocol
- Progress and safety reports
- Notifying the end of the study

The HRA website also provides guidance on these topics, which is updated in the light of changes in reporting requirements or procedures.

## *User Feedback*

The Health Research Authority is continually striving to provide a high quality service to all applicants and sponsors. You are invited to give your view of the service

you have received and the application procedure. If you wish to make your views known please use the feedback form available on the HRA website:

http://www.hra.nhs.uk/about-the-hra/governance/quality-assurance/

*HRA Training*

We are pleased to welcome researchers and R&D staff at our training days – see details at http://www.hra.nhs.uk/hra-training/

| **17/EM/0074** | **Please quote this number on all correspondence** |
|---|---|

With the Committee's best wishes for the success of this project.

Yours sincerely,

*Mr John Aldridge Chair*

Email:NRESCommittee.EastMidlands-Nottingham1@nhs.net

*Enclosures:* "After ethical review – guidance for researchers"

*Copy to:* *Julia West, Royal Liverpool And Broadgreen University Hospitals NHS Trust*

*Confidentiality Advise Team*

## *Appendix B. Tables*

### *Appendix B 1. 381 proteins common to 10 sera analysed by MS*

| Description | Accession | q Value | Unique peptides | Max fold change | Confidence score |
|---|---|---|---|---|---|
| 14-3-3 protein zeta/delta | P63104 | 0.18 | 3 | 1.23 | 192.31 |
| 28S ribosomal protein S9, mitochondrial | P82933 | 0.19 | 2 | 1.49 | 15.23 |
| 5' exonuclease Apollo | Q9H816 | 0.31 | 2 | 1.11 | 18.46 |
| 72 kDa type IV collagenase | P08253 | 0.26 | 2 | 1.55 | 32.8 |
| 78 kDa glucose-regulated protein | P11021 | 0.00 | 6 | 5.29 | 259.22 |
| A disintegrin and metalloproteinase with thrombospondin motifs 13 | Q76LX8 | 0.20 | 3 | 1.27 | 139.21 |
| Actin, cytoplasmic 1 | P60709 | 0.41 | 5 | 1.41 | 1208.44 |
| Actin-related protein 2 | P61160 | 0.05 | 2 | 1.89 | 35.37 |
| Adenosine deaminase 2 | Q9NZK5 | 0.31 | 2 | 1.78 | 22.59 |
| Adenylate kinase 8 | Q96MA6 | 0.36 | 3 | 1.34 | 14.71 |
| Adipocyte plasma membrane-associated protein | Q9HDC9 | 0.26 | 3 | 2.55 | 90.34 |
| Adiponectin | Q15848 | 0.35 | 3 | 1.42 | 303.8 |
| Afamin | P43652 | 0.00 | 28 | 11.06 | 1503.13 |
| Aggrecan core protein | P16112 | 0.29 | 2 | 2.12 | 68.08 |
| Alpha-1-acid glycoprotein 1 | P02763 | 0.27 | 5 | 1.34 | 600.54 |
| Alpha-1-acid glycoprotein 2 | P19652 | 0.43 | 6 | 1.02 | 735.17 |
| Alpha-1-antichmotrypsin | P01011 | 0.00 | 33 | 2.46 | 2633.26 |
| Alpha-1-antytrypsin | P01009 | 0.04 | 44 | 2.45 | 3077.02 |
| Alpha-1-glycoprotein | P04217 | 0.09 | 20 | 1.51 | 1933.95 |

| | | | | | |
|---|---|---|---|---|---|
| Alpha-2-antiplasmin | P08697 | 0.16 | 17 | 1.32 | 1219.36 |
| alpha-2-HS-glycoprotein | P02765 | 0.14 | 14 | 1.53 | 1953.36 |
| Alpha-2-macroglobulin | P01023 | 0.30 | 79 | 1.22 | 8223.76 |
| Alpha-actinin-1 | P12814 | 0.19 | 5 | 2.30 | 299.63 |
| Aminopeptidase N | P15144 | 0.02 | 5 | 2.79 | 231 |
| AMP deaminase 2 | Q01433 | 0.44 | 2 | 1.55 | 22.88 |
| Angiotensinogen | P01019 | 0.03 | 18 | 2.09 | 1917.19 |
| Antileukoproteinase | P03973 | 0.22 | 3 | 52.83 | 55.24 |
| Antithrombin-III | P01008 | 0.22 | 38 | 1.34 | 3335.62 |
| Apolipopriotein C-I | P02654 | 0.12 | 5 | 2.09 | 152.26 |
| Apolipoprotein A-I | P02647 | 0.03 | 30 | 2.45 | 1867.52 |
| Apolipoprotein A-II | P02652 | 0.00 | 6 | 4.05 | 385.77 |
| Apolipoprotein A-IV | P06727 | 0.34 | 29 | 1.33 | 2130.28 |
| Apolipoprotein B-100 | P04114 | 0.33 | 344 | 1.13 | 28040.43 |
| Apolipoprotein C-II | P02655 | 0.04 | 5 | 2.77 | 340.7 |
| Apolipoprotein C-III | P02656 | 0.13 | 5 | 1.34 | 446.83 |
| Apolipoprotein C-IV | P55056 | 0.02 | 7 | 5.29 | 189.46 |
| Apolipoprotein D | P05090 | 0.15 | 8 | 1.43 | 403.02 |
| Apolipoprotein E | P02649 | 0.02 | 23 | 2.50 | 1824.46 |
| Apolipoprotein F | Q13790 | 0.19 | 3 | 1.29 | 84.72 |
| Apolipoprotein L1 | O14791 | 0.35 | 15 | 1.13 | 943.81 |
| Apolipoprotein M | O95445 | 0.00 | 11 | 8.08 | 462.07 |
| Apolipoprotein(a) | P08519 | 0.20 | 54 | 1.19 | 3371.23 |

| | | | | | |
|---|---|---|---|---|---|
| Attractin | O75882 | 0.10 | 26 | 1.59 | 1585.89 |
| Autphagy-related protein 101 | Q9BSB4 | 0.04 | 2 | 1.52 | 14.33 |
| Band 3 anion transport protein | P02730 | 0.44 | 4 | 2.00 | 139.63 |
| Basement membrane-specific heparan sulfate proteoglycan core protein | P98160 | 0.22 | 17 | 1.13 | 531.79 |
| Beta-2-glyvoprotein 1 | P02749 | 0.01 | 15 | 2.37 | 1193.77 |
| Beta-Ala-his dipeptidase | Q96KN2 | 0.04 | 16 | 1.85 | 732.49 |
| Biotinidase | P43251 | 0.10 | 12 | 1.66 | 736.97 |
| BPI fold-containing family A member 1 | Q9NP55 | 0.19 | 5 | 47.43 | 485.21 |
| BPI fold-containing family B member 1 | Q8TDL5 | 0.43 | 8 | 3.17 | 305.11 |
| BPI fold-containing family B member 2 | Q8N4F0 | 0.34 | 2 | 127.38 | 31.58 |
| BTB/POZ domain-containing protein 16 | Q32M84 | 0.02 | 3 | 1.68 | 23.68 |
| C4b-binding protein alpha chain | P04003 | 0.31 | 33 | 1.10 | 2522.49 |
| C4b-binding protein beta chain | P20851 | 0.48 | 9 | 1.01 | 621.25 |
| Cadherin-1 | P12830 | 0.11 | 2 | 6.13 | 65.84 |
| Cadherin-5 | P33151 | 0.00 | 7 | 1.84 | 229.41 |
| Caherin 13 | P55290 | 0.34 | 2 | 1.23 | 79.03 |
| Capping protein, Arp2/3 and myosin-I linker protein 3 | Q8ND23 | 0.22 | 2 | 1.30 | 17.31 |
| Carbonic anhydrase 1 | P00915 | 0.43 | 7 | 1.68 | 427.6 |
| Carboxypeptidase B2 | Q96IY4 | 0.16 | 14 | 1.55 | 862.43 |
| Carboxypeptidase N catalytic chain | P15169 | 0.07 | 15 | 1.71 | 837.64 |
| Carboxypeptidase N subunit 2 | P22792 | 0.14 | 11 | 1.58 | 844.39 |
| Cartilage acidic protein 1 | Q9NQ79 | 0.43 | 9 | 1.01 | 516.52 |
| Cartilage oligomeric matrix protein | P49747 | 0.45 | 11 | 1.15 | 715.34 |

| | | | | | |
|---|---|---|---|---|---|
| Caspase recruitment domain-containing protein 11 | Q9BXL7 | 0.17 | 5 | 1.58 | 18.1 |
| Catalase | P04040 | 0.32 | 4 | 2.73 | 174.64 |
| Cathepsin D | P07339 | 0.30 | 4 | 1.22 | 77.27 |
| CD44 antigen | P16070 | 0.40 | 2 | 3.53 | 52.24 |
| CD5 antigen-lie | O43866 | 0.08 | 18 | 2.50 | 1189.55 |
| Cd9 antigen | P21926 | 0.32 | 3 | 1.28 | 54.43 |
| Cell surface glycoprotein MUC18 | P43121 | 0.01 | 6 | 1.93 | 106.98 |
| Centromere protein F | P49454 | 0.08 | 7 | 2.53 | 18.52 |
| Centromere-associated protein E | Q02224 | 0.29 | 4 | 1.17 | 25.08 |
| Ceruloplasmin | P00450 | 0.26 | 75 | 1.13 | 7612.42 |
| Cholesteryl ester transfer protein | P11597 | 0.13 | 12 | 1.68 | 602.72 |
| Cholinesterase | P06276 | 0.07 | 14 | 1.46 | 659.4 |
| Chromodomain-helicase-DNA-binding protein 1 | O14646 | 0.11 | 2 | 2.96 | 13.67 |
| Cllusterin | P10909 | 0.13 | 22 | 1.21 | 1351.29 |
| Coagulation facor XIII B chain | P05160 | 0.00 | 11 | 10.12 | 504.3 |
| Coagulation factor IX | P00740 | 0.22 | 11 | 1.33 | 500.18 |
| Coagulation factor V | P12259 | 0.08 | 39 | 1.83 | 1499.6 |
| Coagulation factor X | P00742 | 0.30 | 12 | 1.15 | 549.63 |
| Coagulation factor XI | P03951 | 0.09 | 25 | 1.81 | 1096.83 |
| Coagulation factor XIII A chain | P00488 | 0.45 | 13 | 2.20 | 584.48 |
| Cofilin-1 | P23528 | 0.30 | 3 | 1.41 | 18.64 |
| Cogulation factor XII | P00748 | 0.02 | 16 | 2.43 | 1038.17 |
| Collagen alpha-1(VI) chain | P12109 | 0.32 | 3 | 1.79 | 53.18 |

| | | | | | |
|---|---|---|---|---|---|
| Collagen alpha-3(VI) chain | P12111 | 0.00 | 9 | 2.01 | 198.78 |
| Collectin-11 | Q9BWP8 | 0.12 | 3 | 1.99 | 69.67 |
| Complement C1q subcomponent subunit B | P02746 | 0.00 | 10 | 1.82 | 676.8 |
| Complement C1q subcomponent subunit C | P02747 | 0.00 | 6 | 1.78 | 587.22 |
| Complement C1r subcomponent | P00736 | 0.12 | 31 | 1.29 | 1930.39 |
| Complement C1r subcomponent-like protein | Q9NZP8 | 0.01 | 6 | 1.93 | 417.88 |
| Complement C1s subcomponent | P09871 | 0.15 | 31 | 1.19 | 2006.45 |
| Complement C2 | P06681 | 0.00 | 25 | 2.04 | 1608.57 |
| Complement C3 | P01024 | 0.09 | 163 | 1.28 | 15903.41 |
| Complement C4-A | P0C0L4 | 0.36 | 3 | 1.47 | 10012.42 |
| Complement C4-B | P0C0L5 | 0.36 | 6 | 1.47 | 10435.6 |
| Complement C5 | P01031 | 0.00 | 96 | 1.65 | 6404.1 |
| Complement component C7 | P10643 | 0.23 | 37 | 1.34 | 2585.14 |
| Complement component C8 alpha chain | P07357 | 0.02 | 28 | 2.21 | 2076.58 |
| Complement component C8 beta chain | P07358 | 0.13 | 29 | 1.57 | 2608.94 |
| Complement component C8 gamma chain | P07360 | 0.01 | 12 | 2.56 | 1290.6 |
| Complement component C9 | P02748 | 0.02 | 29 | 2.17 | 2136.23 |
| Complement factor B | P00751 | 0.00 | 44 | 2.17 | 3472.63 |
| Complement factor C6 | P13671 | 0.13 | 38 | 1.30 | 2594.94 |
| Complement factor D | P00746 | 0.29 | 12 | 1.17 | 513.22 |
| Complement factor H | P08603 | 0.30 | 62 | 1.14 | 5447.59 |
| Complement factor H-related protein 2 | P36980 | 0.47 | 3 | 1.08 | 447.41 |
| Complement factor H-related protein 5 | Q9BXR6 | 0.47 | 11 | 1.02 | 446.65 |

| | | | | | |
|---|---|---|---|---|---|
| Complement factor I | P05156 | 0.02 | 25 | 1.67 | 1897.11 |
| Complemet C1q subcomponent subunit A | P02745 | 0.00 | 3 | 1.89 | 131.84 |
| Coronin-2A | Q92828 | 0.07 | 2 | 2.24 | 16.69 |
| Corticosteroid-binding globulin | P08185 | 0.06 | 15 | 2.04 | 1264.84 |
| C-reactive protein | P02741 | 0.18 | 7 | 7.70 | 281.09 |
| Cyetein-rich secretory protein 3 | P54108 | 0.27 | 3 | 1.31 | 80.5 |
| Cystatin-A | P01040 | 0.27 | 3 | 3.90 | 57.39 |
| Cytoplasmic tRNA 2-thiolation protein 1 | Q7Z7A3 | 0.10 | 2 | 1.68 | 14.7 |
| Cytosol aminpeptidase | P28838 | 0.28 | 11 | 1.58 | 255.34 |
| Deleted in malignant brain tumors 1 protein | Q9UGM3 | 0.13 | 9 | 201.24 | 660.15 |
| Dermicidin | P81605 | 0.39 | 2 | 1.27 | 125.44 |
| Desmoplakin | P15924 | 0.14 | 5 | 1.86 | 33.14 |
| Di-N-acetylchitobiase | Q01459 | 0.45 | 4 | 1.10 | 51.54 |
| Dipeptidyl peptidase 4 | P27487 | 0.16 | 5 | 1.31 | 100.79 |
| DNA excision repain protein ERCC-6-like 2 | Q5T890 | 0.27 | 3 | 1.14 | 17.08 |
| DNA repair-scaffolding protein | Q14159 | 0.47 | 2 | 1.10 | 17.44 |
| Docking protein 1 | Q99704 | 0.32 | 2 | 1.67 | 14.82 |
| Dopamine beta-hydroxylase | P09172 | 0.42 | 7 | 1.32 | 368.08 |
| Dynein heacy chain 11, axonemal | Q96DT5 | 0.47 | 4 | 1.06 | 42.8 |
| Dynein heacy chain 8, aonemal | Q96JB1 | 0.18 | 2 | 1.46 | 42.08 |
| Dynein heavy chain 10, axonemal | Q8IVF4 | 0.23 | 7 | 1.17 | 66.11 |
| Dynein heavy chain 12, axonemal | Q6ZR08 | 0.30 | 4 | 1.15 | 37.07 |
| Dynein heavy chain 5, axonemal | Q8TE73 | 0.13 | 3 | 1.93 | 38.08 |

| | | | | | |
|---|---|---|---|---|---|
| E3 ubiquitin-protein ligase UBR4 | Q5T4S7 | 0.07 | 5 | 1.84 | 17.91 |
| Ectonuleotide pyrophosphatase/phophodiseterase family member 2 | Q13822 | 0.40 | 2 | 1.32 | 48.32 |
| EGF-containing fibulin-like extracellular matric protein 1 | Q12805 | 0.30 | 11 | 1.16 | 457.17 |
| Endoplasmin | P14625 | 0.08 | 4 | 4.72 | 120.19 |
| Endothelial PAS domain-containing protein 1 | Q99814 | 0.26 | 3 | 1.24 | 14.2 |
| Erythrocyte band 7 integral membrane protein | P27105 | 0.22 | 2 | 2.77 | 151.61 |
| Extracellular matric protein 1 | Q16610 | 0.38 | 8 | 3.83 | 199.2 |
| Fermitin family homolog 3 | Q86UX7 | 0.12 | 3 | 2.73 | 94.11 |
| Fetuin-b | Q9UGM5 | 0.06 | 11 | 1.65 | 575.44 |
| Fibrinogen alpha chain | P02671 | 0.35 | 10 | 1.72 | 360.86 |
| Fibrinogen beta chain | P02675 | 0.43 | 7 | 1.60 | 282.19 |
| Fibrinogen gamma chain | P02679 | 0.24 | 7 | 1.02 | 336.32 |
| Fibronectin | P02751 | 0.09 | 81 | 1.64 | 7956.54 |
| Fibulin-1 | P23142 | 0.04 | 14 | 2.14 | 590.49 |
| Ficolin-2 | Q15485 | 0.14 | 9 | 1.62 | 464.55 |
| Ficolin-3 | O75636 | 0.40 | 13 | 1.06 | 976.9 |
| Filaggrin-2 | Q5D862 | 0.27 | 3 | 1.12 | 39.99 |
| Filamin-A | P21333 | 0.00 | 32 | 1.75 | 1109.95 |
| Filamin-C | Q14315 | 0.30 | 2 | 1.22 | 65.49 |
| Fructose-bisphosphate aldolase B | P05062 | 0.31 | 2 | 1.66 | 89.77 |
| Fumarylacetoacetase | P16930 | 0.23 | 2 | 2.26 | 27 |
| galectin-3-binding protein | Q08380 | 0.30 | 19 | 1.30 | 1223.46 |
| Gelsolin | P06396 | 0.23 | 38 | 1.55 | 2982.71 |

| | | | | | |
|---|---|---|---|---|---|
| Glucose-6-phosphate isomerase | P06744 | 0.21 | 2 | 2.10 | 54.06 |
| Glutathione peroxidase 3 | P22352 | 0.36 | 7 | 1.09 | 295.37 |
| Glyceraldehyde-3-phosphate dehydorgenase | P04406 | 0.38 | 4 | 2.33 | 154.51 |
| Golgin subfamily A member 6-like protein 22 | H0YM25 | 0.49 | 2 | 1.13 | 16.27 |
| Guanine nucleotide-binding protein G(I)/G(S)/G(T) subunit beta-1 | P62873 | 0.32 | 3 | 1.30 | 39.69 |
| Haptoglobin | P00738 | 0.15 | 17 | 2.41 | 2903.42 |
| Haptoglobin-related protein | P00739 | 0.13 | 11 | 1.96 | 2004.2 |
| Hemoglobin subunit alpha | P69905 | 0.49 | 6 | 1.20 | 225.18 |
| Hemoglobin subunit beta | P68871 | 0.25 | 10 | 1.28 | 660.51 |
| Hemopexin | P02790 | 0.24 | 36 | 1.15 | 2661.47 |
| Heparin cofactor 2 | P05546 | 0.01 | 30 | 2.48 | 1807.26 |
| Hepatocyte growth factor-like protein | P26927 | 0.06 | 8 | 1.98 | 435.26 |
| Heptaocyte growth factor activator | Q04756 | 0.33 | 11 | 1.16 | 431.78 |
| Hexokinase-1 | P19367 | 0.26 | 2 | 1.94 | 15.64 |
| Histidine-rich glycoprotein | P04196 | 0.01 | 24 | 1.96 | 2131.17 |
| Histone H4 | P62805 | 0.44 | 2 | 1.24 | 23.49 |
| Hornerin | Q86YZ3 | 0.45 | 4 | 1.03 | 207.13 |
| Hyaluronan-binding protein 2 | Q14520 | 0.23 | 14 | 1.16 | 832.59 |
| Hydrocephalus-inducing protein homolog | Q4G0P3 | 0.18 | 4 | 1.20 | 35.81 |
| ICOS ligand | O75144 | 0.14 | 2 | 1.74 | 34.58 |
| Ig heavy chain V-I region HG3 | P01743 | 0.00 | 2 | 5.31 | 191.83 |
| Ig heavy chain V-I region V35 | P23083 | 0.07 | 6 | 4.61 | 285.9 |
| Ig heavy chain V-II region WAH | P01824 | 0.01 | 2 | 9.72 | 50.83 |

| | | | | | |
|---|---|---|---|---|---|
| Ig heavy chain V-III region BUT | P01767 | 0.00 | 2 | 8.50 | 307.08 |
| Ig heavy chain V-III region GA | P01769 | 0.02 | 2 | 8.60 | 27.81 |
| Ig heavy chain V-III region GAL | P01781 | 0.13 | 2 | 10.40 | 85.26 |
| Ig heavy chain V-III region VH26 | P01764 | 0.00 | 2 | 5.70 | 196.98 |
| Ig heavy chain V-III region WEA | P01763 | 0.00 | 2 | 8.19 | 202.53 |
| Ig kappa chain V-I region CAR | P01596 | 0.01 | 2 | 18.79 | 126.59 |
| Ig kappa chain V-I region HK102 (Fragment) | P01602 | 0.03 | 2 | 3.61 | 258.36 |
| Ig kappa chain V-I region WEA | P01610 | 0.12 | 2 | 9.27 | 130.84 |
| Ig kappa chain V-III region B6 | P01619 | 0.00 | 2 | 3.67 | 146.11 |
| Ig kappa chain V-III region IARC/BL41 | P06311 | 0.00 | 2 | 7.55 | 135.39 |
| Ig kappa chain V-III region VG (Fragment) | P04433 | 0.00 | 3 | 4.05 | 186.08 |
| Ig kappa chain V-III region VH (Fragment) | P04434 | 0.00 | 2 | 22.92 | 90.11 |
| Ig kappa chain V-IV region Len | P01625 | 0.02 | 2 | 3.25 | 390.37 |
| Ig lambda chain V region 4A | P04211 | 0.00 | 2 | 10.37 | 83.58 |
| Ig lambda chain V-I region NEW | P01701 | 0.09 | 2 | 19.71 | 72.49 |
| Ig lambda chain V-II region TRO | P01707 | 0.00 | 2 | 30.17 | 29.19 |
| Ig lambda chain V-III region LOI OS=Homo sapiens PE=1 SV=1; TOPep_Count=5 | P80748 | 0.00 | 5 | 10.42 | 245.39 |
| Ig lambda chain V-III region SH | P01714 | 0.00 | 3 | 6.48 | 291.99 |
| Ig mu heavy chain disease protein | P04220 | 0.14 | 2 | 1.88 | 1716.85 |
| Immmunoglobulin heacy constant gamma 1 | P01857 | 0.00 | 6 | 9.28 | 1609.36 |
| immunoglobulin heacy constant alpha 1 | P01876 | 0.00 | 6 | 6.25 | 1574.71 |
| Immunoglobulin heacy constant alpha 2 | P01877 | 0.00 | 4 | 6.45 | 1109.68 |
| Immunoglobulin heavy constant delta | P01880 | 0.07 | 11 | 29.33 | 659.5 |

| | | | | | |
|---|---|---|---|---|---|
| Immunoglobulin heavy constant gamma 2 | P01859 | 0.00 | 5 | 16.15 | 1093.27 |
| Immunoglobulin heavy constant gamma 3 | P01860 | 0.00 | 6 | 13.10 | 1431.32 |
| Immunoglobulin heavy constant gamma 4 | P01861 | 0.00 | 6 | 11.09 | 1098.72 |
| Immunoglobulin heavy constant mu | P01871 | 0.12 | 6 | 2.10 | 1968.38 |
| Immunoglobulin J chain | P01591 | 0.07 | 5 | 2.11 | 426.69 |
| Immunoglobulin kappa constant | P01834 | 0.00 | 5 | 5.93 | 1074.97 |
| Immunoglobulin lambda constant 7 | A0M8Q6 | 0.00 | 2 | 8.84 | 407.76 |
| Immunoglobulin lambda-like polypeptide 1 | P15814 | 0.16 | 2 | 2.50 | 38.72 |
| Immunoglobulin lambda-like polypeptide 5 | B9A064 | 0.00 | 3 | 10.09 | 810.1 |
| Insulin-like growth factor-binding protein 3 | P17936 | 0.27 | 3 | 1.75 | 119.31 |
| Insulin-like growth factor-binding protein complex acid labile subunit | P35858 | 0.49 | 24 | 1.17 | 1539.11 |
| Integrin alpha-Iib | P08514 | 0.20 | 12 | 1.27 | 663.79 |
| Integrin beta-3 | P05106 | 0.08 | 9 | 1.74 | 340.63 |
| Inter-alpha-trypsin inhibitor heacy chain H1 | P19827 | 0.14 | 38 | 1.60 | 4154.63 |
| Inter-alpha-trypsin inhibitor heacy chain H4 | Q14624 | 0.01 | 51 | 2.07 | 4552.24 |
| Inter-alpha-trypsin inhibitor heavy chain H3 | Q06033 | 0.00 | 31 | 2.64 | 1932.16 |
| inter-alpha-trypsin inhibitor heavy chian H2 | P19823 | 0.07 | 45 | 1.60 | 4262.77 |
| Interleukin-1 receptor accessory protein | Q9NPH3 | 0.35 | 2 | 4.88 | 52.92 |
| IQ motif and SEC7 domain-containing protein 1 | Q6DN90 | 0.42 | 2 | 1.10 | 19.15 |
| Kallistatin | P29622 | 0.14 | 21 | 1.83 | 1790.32 |
| Keratin, type I cytoseletal 17 | Q04695 | 0.19 | 4 | 2.30 | 502.41 |
| Keratin, type I cytoskeletal 10 | P13645 | 0.29 | 27 | 1.16 | 3011 |
| Keratin, type I cytoskeletal 14 | P02533 | 0.37 | 4 | 1.17 | 1147.45 |

| | | | | | |
|---|---|---|---|---|---|
| Keratin, type I cytoskeletal 16 | P08779 | 0.48 | 9 | 1.04 | 987.68 |
| Keratin, type I cytoskeletal 28 | Q7Z3Y7 | 0.45 | 2 | 1.00 | 198 |
| Keratin, type I cytoskeletal 9 | K1C9_HUMAN | 0.27 | 37 | 1.32 | 2498.39 |
| Keratin, type II cuticular Hb5 | P78386 | 0.07 | 2 | 3.17 | 20.36 |
| Keratin, type II cytoskeletal 1 | P04264 | 0.18 | 36 | 1.41 | 2827.24 |
| Keratin, type II cytoskeletal 2 epidermal | P35908 | 0.22 | 21 | 1.36 | 1974.27 |
| Keratin, type II cytoskeletal 5 | P13647 | 0.30 | 13 | 1.18 | 930 |
| Keratinocyte proline-rich protein | Q5T749 | 0.30 | 3 | 1.22 | 59.32 |
| Kinesin-like protein KIF28P | B7ZC32 | 0.05 | 3 | 1.45 | 15.1 |
| Kininogen-1 | P01042 | 0.14 | 33 | 1.21 | 2458.4 |
| Lactotransferrin | P02788 | 0.29 | 38 | 13.90 | 2067.07 |
| Latent-transforming growth factor beta-binding protein 1 | Q14766 | 0.44 | 4 | 1.13 | 109.19 |
| Leucine-rich alpha-2-glycoprotein | P02750 | 0.03 | 12 | 2.14 | 798.78 |
| Leukocyte immunoglobulin-like receptor subfamily A member 3 | Q8N6C8 | 0.34 | 2 | 2.66 | 49.55 |
| LINE-1 retrotransposable element ORF2 protein | O00370 | 0.43 | 2 | 4.13 | 16.73 |
| Lipocalin-1 | P31025 | 0.20 | 2 | 11.40 | 75.5 |
| Lipopolysaccharide-binding protein | P18428 | 0.21 | 13 | 2.20 | 655.61 |
| L-lactate dehydorgenase B chain | P07195 | 0.14 | 6 | 1.89 | 269.52 |
| L-lactate dehydrogenase A chain | P00338 | 0.40 | 2 | 1.02 | 138.91 |
| Low affinity immunoglobulin gamma Fc region receptro III-A | P08637 | 0.22 | 2 | 2.51 | 23.83 |
| LRP2-binding protein | Q9P2M1 | 0.01 | 2 | 23.21 | 31.9 |
| L-selectin | P14151 | 0.36 | 3 | 13.69 | 120.64 |
| Lumican | P51884 | 0.00 | 12 | 5.92 | 828.14 |

| | | | | | |
|---|---|---|---|---|---|
| Lymphatic vessel endothelial hyaluronic acid receptor 1 | Q9Y5Y7 | 0.18 | 4 | 1.26 | 57.93 |
| Lysosomal-trafficing regulator | Q99698 | 0.21 | 5 | 1.99 | 25.5 |
| Lysosome-associated membrane glycoprotein 2 | P13473 | 0.35 | 2 | 1.43 | 123.63 |
| Lysozyme C | P61626 | 0.22 | 9 | 1.99 | 262.25 |
| Macrophage mannose receptor 1 | P22897 | 0.33 | 2 | 2.10 | 37.32 |
| Manganese-transpoting ATPase 13A1 | Q9HD20 | 0.23 | 2 | 1.24 | 27.49 |
| Mannan-binding lectin serine protease 2 | O00187 | 0.15 | 8 | 1.25 | 330.97 |
| Mannan-binding lectin serine protesase 1 | P48740 | 0.37 | 15 | 1.08 | 697.2 |
| Mannose-binding protein C | P11226 | 0.39 | 6 | 1.56 | 417.29 |
| Mannosyl-oligosaccharide 1,2-alpha-mannosidase IA | P33908 | 0.07 | 4 | 3.59 | 133 |
| Matrix metalloproteinase-9 | P14780 | 0.40 | 7 | 1.03 | 265.35 |
| Metalloproteinase inhibitor 1 | P01033 | 0.43 | 6 | 1.09 | 253.91 |
| Mixed lineaeg kinase domain-like protein | Q8NB16 | 0.05 | 3 | 1.92 | 13.97 |
| Mocnocyte differnetiation antigen CD14 | P08571 | 0.21 | 5 | 1.40 | 259 |
| Mucin-16 | Q8WXI7 | 0.37 | 2 | 1.10 | 28.78 |
| Mucin-5B | Q9HC84 | 0.26 | 8 | 1.65 | 193.14 |
| Multimerin-1 | Q13201 | 0.27 | 5 | 2.71 | 190.66 |
| Myomegalin | Q5VU43 | 0.01 | 6 | 2.71 | 34.4 |
| N-acetylmuramoyl-L-alanine amidase | Q96PD5 | 0.26 | 22 | 1.20 | 2319.05 |
| NACT, LRR and PYD domains-containing protein 12 | P59046 | 0.39 | 2 | 1.24 | 16.4 |
| Neural cell adhesion molecule 1 | P13591 | 0.05 | 2 | 2.62 | 76.65 |
| Neural cell adhesion molecule L1-like protein | O00533 | 0.37 | 4 | 1.29 | 68.22 |
| Nidogen-1 | P14543 | 0.26 | 8 | 1.23 | 234.91 |

| | | | | | |
|---|---|---|---|---|---|
| Noelin | Q99784 | 0.49 | 3 | 1.27 | 50.37 |
| Nucleolar protein 6 | Q9H6R4 | 0.42 | 2 | 1.05 | 24.74 |
| Nucleolas pre-ribosoma-associated protein 1 | O60287 | 0.02 | 2 | 1.47 | 16.75 |
| Obscurin | Q5VST9 | 0.16 | 3 | 1.95 | 43.62 |
| Panthetheinase | O95497 | 0.33 | 2 | 2.74 | 67.45 |
| Peptidyl-prolyl cis-trans isomerase A | P62937 | 0.29 | 3 | 1.18 | 52.9 |
| Periostin | Q15063 | 0.25 | 8 | 2.87 | 292.19 |
| Perociredocin-2 | P32119 | 0.34 | 3 | 1.23 | 103.73 |
| Phosphatidylcholine-sterol acyltrasferase | P04180 | 0.13 | 6 | 1.64 | 408.46 |
| Phosphatidylinositol 3,4,5-triphosphate-dependent Rac exchanger 1 protein | Q8TCU6 | 0.07 | 2 | 2.95 | 23.52 |
| Phosphatidylinositol-glycan-specific phspholipase D | P80108 | 0.29 | 22 | 1.49 | 1208.22 |
| Phospholipid transfer protein | P55058 | 0.24 | 6 | 1.47 | 367.31 |
| Pigment epithelium-derived factor | P36955 | 0.35 | 21 | 1.12 | 1400.25 |
| Plasma kallikrein | P03952 | 0.17 | 33 | 1.48 | 1976.74 |
| Plasma protease C1 inhibitor | P05155 | 0.43 | 27 | 1.02 | 1917.06 |
| Plasma serine proteas inhibitor | P05154 | 0.14 | 13 | 1.46 | 679.42 |
| Plasminogen | P00747 | 0.36 | 61 | 1.10 | 4672.49 |
| Plastin-2 | P13796 | 0.14 | 22 | 2.11 | 927.63 |
| Platelet basic protein | P02775 | 0.25 | 4 | 1.30 | 205.55 |
| Platelet factor 4 | P02776 | 0.07 | 3 | 3.46 | 80.53 |
| Platelet glycoprotein Ib alpga chain | P07359 | 0.00 | 5 | 11.60 | 137.38 |
| Platelet glycoprotein V | P40197 | 0.29 | 5 | 1.19 | 297.1 |
| Polymeric immunoglobulin receptor | P01833 | 0.32 | 9 | 3.22 | 348.05 |

| | | | | | |
|---|---|---|---|---|---|
| Polyubiquitin-B | P0CG47 | 0.36 | 3 | 1.50 | 110.39 |
| POTE ankyrin domain family member E | Q6S8J3 | 0.31 | 2 | 1.39 | 643.77 |
| Pregnancy zone protein | P20742 | 0.11 | 33 | 4.29 | 2790.76 |
| Prenylcystein oxidase 1 | Q9UHG3 | 0.34 | 8 | 1.07 | 400.97 |
| Procollagen C-denopeptidase enhancer 1 | Q15113 | 0.31 | 5 | 1.19 | 162.91 |
| Profilin-1 | P07737 | 0.35 | 2 | 1.19 | 53.65 |
| Prolactin inducible protein | P12273 | 0.27 | 3 | 11.20 | 90.3 |
| Properdin | P27918 | 0.01 | 4 | 10.53 | 197.63 |
| Proteasome subunit alpha type-3 | P25788 | 0.22 | 2 | 20.40 | 33.32 |
| Proteasome subunit beta type-1 | P20618 | 0.42 | 2 | 4.71 | 46.4 |
| Proteasome subunit beta type-8 | P28062 | 0.18 | 2 | 21.39 | 129.46 |
| Protein AMBP | P02760 | 0.02 | 23 | 1.97 | 1541.99 |
| Protein FAM184A | Q8NB25 | 0.48 | 2 | 1.58 | 23.4 |
| Protein FAM186A | A6NE01 | 0.02 | 2 | 2.10 | 19.78 |
| Protein kinase C zeta type | Q05513 | 0.07 | 4 | 2.88 | 54.9 |
| Protein S100-A7 | P31151 | 0.43 | 6 | 1.17 | 320.13 |
| Protein S100-A8 | P05109 | 0.38 | 3 | 1.32 | 45.01 |
| Protein S100-A9 | P06702 | 0.35 | 3 | 1.19 | 81.07 |
| Protein Shroom3 | Q8TF72 | 0.24 | 2 | 1.31 | 22.26 |
| protein Z-dependent protease inhibitor | Q9UK55 | 0.17 | 15 | 1.36 | 678.57 |
| Proteoglycan 4 | Q92954 | 0.30 | 14 | 1.47 | 687.24 |
| Protesome subunut alpha type-6 | P60900 | 0.12 | 6 | 4.51 | 139.14 |
| Prothrombin | P00734 | 0.38 | 44 | 1.14 | 3752.56 |

| | | | | | |
|---|---|---|---|---|---|
| Putative macrophage stimulating 1-like protein | Q2TV78 | 0.30 | 2 | 1.51 | 169.94 |
| Ras-related protein Rap-1b | P61224 | 0.17 | 2 | 1.28 | 82.75 |
| Receptor-type tyrosine-protein phosphatase eta | Q12913 | 0.30 | 2 | 1.15 | 22.2 |
| Retinol-binding protein 4 | P02753 | 0.31 | 13 | 1.17 | 1275.49 |
| RNA-binding protein 25 | P49756 | 0.47 | 2 | 2.92 | 14.9 |
| Scavenger receptor cystein-rich type 1 protein M130 | Q86VB7 | 0.43 | 4 | 3.07 | 147.88 |
| Secreted phosphoprotein 24 | Q13103 | 0.09 | 3 | 3.61 | 177.91 |
| Seglycin | P10124 | 0.12 | 4 | 1.97 | 144.12 |
| Selenoprotein P | P49908 | 0.18 | 6 | 1.35 | 296.59 |
| Serine/threonine-protein kinase LMTK1 | Q6ZMQ8 | 0.21 | 2 | 1.24 | 18.3 |
| Serine/threonine-protein kinase/endoribonuclease IRE1 | O75460 | 0.03 | 2 | 3.45 | 24.29 |
| Serotransferrin | P02787 | 0.37 | 56 | 1.07 | 5259.27 |
| Serpin B3 | P29508 | 0.40 | 3 | 19.84 | 92.49 |
| Serum albumin | P02768 | 0.02 | 56 | 4.08 | 5033.19 |
| serum amyloid a-1 protein | P0DJI8 | 0.08 | 4 | 15.11 | 171.87 |
| Serum amyloid A-4 protein | P35542 | 0.00 | 7 | 7.16 | 339.12 |
| Serum amyloid P-component | P02743 | 0.25 | 9 | 1.20 | 533.41 |
| Serum paraoxonase/arylesterase 1 | P27169 | 0.19 | 19 | 1.31 | 1488.82 |
| Serum paraoxonase/lactonase 3 | Q15166 | 0.18 | 5 | 1.61 | 234.46 |
| Sex hormone-binding globulin | P04278 | 0.34 | 15 | 1.35 | 740.99 |
| SH3 and multiple ankyrin repeat domains protein 1 | Q9Y566 | 0.00 | 4 | 4.50 | 25.95 |
| Solute carrier family 13 member 4 | Q9UKG4 | 0.37 | 2 | 1.16 | 13.5 |
| SPARC | P09486 | 0.36 | 6 | 1.20 | 190.24 |

| | | | | | |
|---|---|---|---|---|---|
| Spectrin beta chain, erythrocytic | P11277 | 0.02 | 3 | 3.57 | 18.66 |
| StAR-related lipeid transfeer protein 9 | Q9P2P6 | 0.09 | 2 | 1.55 | 44.03 |
| Stress-70 protein, mitochondrial | P38646 | 0.37 | 2 | 1.07 | 29.42 |
| Striated muscle preferentially expressed proein kinase | Q15772 | 0.01 | 2 | 4.89 | 15.07 |
| Sulfhydryl oxidase 1 | O00391 | 0.16 | 11 | 1.34 | 519.3 |
| Syntaxin-8 | Q9UNK0 | 0.09 | 2 | 1.70 | 14.56 |
| Talin-1 | Q9Y490 | 0.18 | 16 | 1.22 | 533.48 |
| Talin-2 | Q9Y4G6 | 0.15 | 2 | 1.22 | 24.14 |
| Tenascin | P24821 | 0.27 | 11 | 1.86 | 314.03 |
| Tenascin-X | P22105 | 0.40 | 18 | 1.05 | 665.44 |
| Tetranectin | P05452 | 0.04 | 8 | 2.22 | 496.42 |
| Thrombospondin-1 | P07996 | 0.15 | 50 | 1.57 | 3811.8 |
| Thrombospondin-4 | P35443 | 0.01 | 13 | 6.56 | 740.94 |
| Thyrocine-binding globulin | P05543 | 0.01 | 20 | 1.94 | 1001.51 |
| Titin | Q8WZ42 | 0.08 | 30 | 1.16 | 74.21 |
| Tonsoku-like protein | Q96HA7 | 0.07 | 2 | 1.71 | 16.93 |
| TPR and ankyrin repeat-containing protein 1 | O15050 | 0.20 | 3 | 1.18 | 18.55 |
| Transforming growth factor-beta-induced protein ig-h3 | Q15582 | 0.15 | 22 | 1.68 | 874.65 |
| Transketolase | P29401 | 0.14 | 5 | 13.66 | 182.46 |
| Transthyretin | P02766 | 0.27 | 13 | 1.27 | 1482.36 |
| Tryptophan--tRNA ligase, cytoplasmic | P23381 | 0.32 | 2 | 27.53 | 77.63 |
| Tubulin beta-1 chain | Q9H4B7 | 0.38 | 2 | 1.12 | 54.29 |
| Tyrosine-protein phosphatase non-receptro type 4 | P29074 | 0.07 | 2 | 1.87 | 13.84 |

| | | | | | |
|---|---|---|---|---|---|
| UTP--glucose 1-phosphate uridylyltransferase | Q16851 | 0.46 | 4 | 1.47 | 61.34 |
| Vacular cell adhesion protein 1 | P19320 | 0.09 | 10 | 3.67 | 329.99 |
| Vacuolar protein sortin-associated protein 11 homolog | Q9H270 | 0.47 | 2 | 1.01 | 13.96 |
| Vasorin | Q6EMK4 | 0.30 | 2 | 1.30 | 60.04 |
| Versican core protein | P13611 | 0.25 | 6 | 1.43 | 114.52 |
| Vinculin | P18206 | 0.02 | 3 | 5.05 | 64.08 |
| Vitamin K-dependent protein C | P04070 | 0.00 | 6 | 3.53 | 163.29 |
| Vitamin K-dependent protein S | P07225 | 0.29 | 28 | 1.14 | 1809.28 |
| Vitamin K-dependent protein z | P22891 | 0.47 | 9 | 1.03 | 403.73 |
| Vitamine D-binding protein | P02774 | 0.00 | 30 | 2.88 | 2213.23 |
| Vitelline mmbrane outer layer protein 1 homolg | Q7Z5L0 | 0.18 | 2 | 62.39 | 201.5 |
| Vitronectin | P04004 | 0.03 | 21 | 1.55 | 1569.07 |
| von Willbrand factor | P04275 | 0.48 | 98 | 1.49 | 6619.24 |
| Xaa-Pro dipeptidase | P12955 | 0.05 | 10 | 2.75 | 384.41 |
| Zinc finger protein 343 | Q6P1L6 | 0.37 | 2 | 1.04 | 24.17 |
| Zinc-alpha-2-glycoprotein | P25311 | 0.23 | 21 | 1.19 | 1341.12 |
| Zymogen granule protein 16 homolog B | Q96DA0 | 0.28 | 6 | 10.29 | 196.18 |

*Appendix B 2. 357 protein identified in all sequential samples from pergnant woman with HFRS*

| Description | Accession | q Value | Unique peptides | Max fold change | Confidence score |
|---|---|---|---|---|---|
| 14-3-3 protein epsilon | P62258 | 0.00 | 2 | Infinity | 172.63 |
| 14-3-3 protein gamma | P61981 | 0.07 | 2 | Infinity | 164.45 |
| 14-3-3 protein zeta/delta | P63104 | 0.02 | 4 | 19.22 | 399.58 |
| 78 kDa glucose-regulated protein | P05534 | 0.01 | 8 | 7.49 | 605.29 |
| Actin, cytoplasmic 1 | P02763 | 0.00 | 10 | 2.87 | 1980.53 |
| Adenylyl cyclase-associated protein 1 | P19652 | 0.02 | 11 | 1.65 | 1936.79 |
| Adiponectin | P01009 | 0.00 | 52 | 1.41 | 5929.02 |
| Afamin | P04217 | 0.06 | 21 | 1.41 | 2860.38 |
| Alpha-1-acid glycoprotein 1 | P08697 | 0.04 | 22 | 1.71 | 3029.33 |
| Alpha-1-acid glycoprotein 2 | P02750 | 0.03 | 16 | 2.16 | 2017.87 |
| Alpha-1-antichymotrypsin | P01023 | 0.00 | 93 | 6.70 | 16163.67 |
| Alpha-1-antitrypsin | P01011 | 0.01 | 53 | 2.33 | 6793.62 |
| Alpha-1B-glycoprotein | P17174 | 0.01 | 5 | 18.83 | 232.07 |
| Alpha-2-antiplasmin | P60709 | 0.00 | 8 | 4.20 | 2226.46 |
| Alpha-2-HS-glycoprotein | O43184 | 0.00 | 10 | 15.43 | 741.12 |
| Alpha-2-macroglobulin | Q15848 | 0.00 | 2 | 10.45 | 276.02 |
| Alpha-enolase | P43652 | 0.00 | 36 | 4.28 | 4785.93 |
| Amiloride-sensitive amine oxidase [copper-containing] | P02768 | 0.00 | 68 | 134.91 | 11509.36 |
| Aminopeptidase N | P04075 | 0.01 | 4 | 7.09 | 244.7 |
| Angiogenin | P05062 | 0.00 | 9 | 193.98 | 655.46 |
| Angiotensinogen | P35858 | 0.02 | 22 | 3.05 | 2787.64 |

| | | | | | |
|---|---|---|---|---|---|
| Annexin A1 | P02760 | 0.00 | 28 | 1.61 | 3444.31 |
| Antithrombin-III (Chain 33-464) | P28838 | 0.05 | 6 | 56687.60 | 318.88 |
| Apolipoprotein A-I | P15144 | 0.08 | 8 | 1.86 | 556.65 |
| Apolipoprotein A-II | P03950 | 0.00 | 3 | 23.51 | 132.83 |
| Apolipoprotein A-IV | P01019 | 0.07 | 27 | 1.73 | 4270.08 |
| Apolipoprotein B-100 | P01008 | 0.04 | 45 | 1.68 | 5637.01 |
| Apolipoprotein C-I | P04083 | 0.19 | 2 | 349.11 | 153.36 |
| Apolipoprotein C-II | P19801 | 0.04 | 3 | 54.61 | 177.43 |
| Apolipoprotein C-III | P08519 | 0.00 | 6 | 3.01 | 599.14 |
| Apolipoprotein C-IV | P02647 | 0.00 | 49 | 3.71 | 5589.85 |
| Apolipoprotein D | P02652 | 0.00 | 8 | 4.13 | 1038.41 |
| Apolipoprotein E | P06727 | 0.00 | 37 | 2.01 | 4037.02 |
| Apolipoprotein F | P04114 | 0.01 | 371 | 2.43 | 48749.19 |
| Apolipoprotein L1 | P02654 | 0.00 | 5 | 4.35 | 402.04 |
| Apolipoprotein M | P02655 | 0.00 | 5 | 3.43 | 750.44 |
| Apolipoprotein(a) | P02656 | 0.00 | 5 | 5.28 | 881.53 |
| Asialoglycoprotein receptor 2 | P55056 | 0.00 | 8 | 4.00 | 737.84 |
| Aspartate aminotransferase, cytoplasmic | P05090 | 0.00 | 11 | 2.20 | 1245.6 |
| Attractin | P02649 | 0.00 | 30 | 2.33 | 3597.58 |
| Azurocidin | Q13790 | 0.01 | 4 | 11.75 | 376.96 |
| Band 3 anion transport protein | P02749 | 0.00 | 25 | 2.92 | 3201.91 |
| Basement membrane-specific heparan sulfate proteoglycan core protein | O14791 | 0.00 | 11 | 2.45 | 1218.99 |
| Beta-1,4-galactosyltransferase 1 | O95445 | 0.00 | 14 | 2.76 | 1123.75 |

| | | | | | |
|---|---|---|---|---|---|
| Beta-2-glycoprotein 1 | P07307 | 0.06 | 2 | 14.90 | 166.55 |
| Beta-2-microglobulin | O75882 | 0.00 | 36 | 2.41 | 3278.48 |
| Beta-Ala-His dipeptidase | P61769 | 0.00 | 4 | 6.10 | 359.38 |
| Biotinidase | P02730 | 0.01 | 12 | 173.57 | 1123.63 |
| Bone marrow proteoglycan | P15291 | 0.09 | 3 | 3.04 | 211.76 |
| C-reactive protein (Chain 19-224) | Q15582 | 0.07 | 15 | 1.91 | 1188.68 |
| C4b-binding protein alpha chain | P30043 | 0.02 | 3 | 10440.34 | 178.88 |
| C4b-binding protein beta chain | P43251 | 0.03 | 11 | 1.65 | 1194.49 |
| Cadherin-1 | Q86VB7 | 0.00 | 12 | 10.59 | 1014.12 |
| Cadherin-5 | P02745 | 0.01 | 4 | 1.70 | 177 |
| Calmodulin | P02746 | 0.01 | 8 | 2.02 | 960.23 |
| Calreticulin | P02747 | 0.00 | 6 | 1.95 | 559.85 |
| Carbonic anhydrase 1 | P00736 | 0.01 | 33 | 1.48 | 3872.99 |
| Carbonic anhydrase 2 | Q9NZP8 | 0.01 | 9 | 1.50 | 1101.6 |
| Carboxypeptidase B2 | P09871 | 0.02 | 30 | 1.46 | 3496.17 |
| Carboxypeptidase N catalytic chain | P20160 | 0.00 | 2 | 9.67 | 69.03 |
| Carboxypeptidase N subunit 2 | P04003 | 0.00 | 36 | 2.01 | 3730.25 |
| Cartilage oligomeric matrix protein | P20851 | 0.00 | 5 | 1.74 | 565.6 |
| Catalase | P12830 | 0.23 | 2 | 30.37 | 146.16 |
| Cathelicidin antimicrobial peptide | P33151 | 0.03 | 7 | 11.35 | 481.48 |
| Cathepsin D | P00915 | 0.00 | 10 | 28.73 | 1185.9 |
| Cathepsin G | P00918 | 0.00 | 4 | 542.52 | 249.16 |
| CD44 antigen | P62158 | 0.04 | 3 | 55.30 | 159.4 |

| | | | | | |
|---|---|---|---|---|---|
| CD5 antigen-like | P27797 | 0.03 | 2 | 12.46 | 76.21 |
| Cell surface glycoprotein MUC18 | P49913 | 0.03 | 4 | 2.73 | 194.82 |
| Ceruloplasmin | Q01518 | 0.10 | 2 | 486.30 | 79.28 |
| Cholesteryl ester transfer protein | P04040 | 0.01 | 9 | 21.58 | 781.07 |
| Cholinesterase | P07339 | 0.02 | 2 | 34.32 | 54.13 |
| Choriogonadotropin subunit beta variant 1 | P08311 | 0.03 | 6 | 9.31 | 364.68 |
| Chorionic somatomammotropin hormone 1 | P08185 | 0.02 | 20 | 2.36 | 2777.98 |
| Clusterin | Q96IY4 | 0.00 | 14 | 2.29 | 1434.74 |
| Coactosin-like protein | P15169 | 0.01 | 18 | 1.94 | 1615.31 |
| Coagulation factor IX | P08571 | 0.01 | 11 | 2.66 | 992.4 |
| Coagulation factor V | P16070 | 0.23 | 2 | 1.41 | 114.19 |
| Coagulation factor VII | O43866 | 0.00 | 14 | 7.52 | 1820.85 |
| Coagulation factor X | P00450 | 0.02 | 87 | 1.34 | 15345.55 |
| Coagulation factor XI | P11597 | 0.01 | 7 | 19.64 | 476.31 |
| Coagulation factor XII | P00751 | 0.00 | 52 | 1.37 | 6071.33 |
| Coagulation factor XIII A chain | P00746 | 0.01 | 11 | 2.85 | 954.68 |
| Coagulation factor XIII B chain | P08603 | 0.00 | 70 | 1.69 | 9924.05 |
| Collagen alpha-1(III) chain | P05156 | 0.00 | 26 | 1.51 | 3048.83 |
| Collagen alpha-1(VI) chain | A6NKQ9 | 0.01 | 2 | 630.76 | 205.94 |
| Collagen alpha-1(XVIII) chain | P06276 | 0.00 | 12 | 3.18 | 953.58 |
| Collagen alpha-3(VI) chain | P10909 | 0.03 | 26 | 1.31 | 3089.26 |
| Collectin-11 | Q96KN2 | 0.01 | 16 | 2.11 | 984.07 |
| Complement C1q subcomponent subunit A | P06681 | 0.00 | 30 | 1.44 | 3390.61 |

| | | | | | |
|---|---|---|---|---|---|
| Complement C1q subcomponent subunit B | P01024 | 0.00 | 194 | 1.74 | 28824.39 |
| Complement C1q subcomponent subunit C | P02461 | 0.00 | 2 | Infinity | 124.91 |
| Complement C1r subcomponent | P0C0L4 | 0.04 | 4 | 1.56 | 14917.33 |
| Complement C1r subcomponent-like protein | P01031 | 0.01 | 104 | 1.60 | 11953.51 |
| Complement C1s subcomponent | P13671 | 0.02 | 44 | 1.98 | 5094.78 |
| Complement C2 | P12109 | 0.01 | 4 | 24.62 | 233.08 |
| Complement C3 | P12111 | 0.21 | 3 | 68.76 | 166.69 |
| Complement C4-A | P10643 | 0.00 | 37 | 1.43 | 3906.11 |
| Complement C5 | P07357 | 0.00 | 20 | 2.26 | 2829.81 |
| Complement component C6 | P07358 | 0.00 | 24 | 2.25 | 2756.11 |
| Complement component C7 | P07360 | 0.00 | 11 | 1.62 | 1626.49 |
| Complement component C8 alpha chain | P02748 | 0.01 | 33 | 1.36 | 4239.14 |
| Complement component C8 beta chain | P39060 | 0.02 | 3 | 4.87 | 224.81 |
| Complement component C8 gamma chain | Q9BWP8 | 0.03 | 3 | 3.77 | 151.67 |
| Complement component C9 | P49747 | 0.01 | 5 | 5.32 | 661.58 |
| Complement factor B | Q14019 | 0.26 | 3 | 75.67 | 124.01 |
| Complement factor D | P22792 | 0.21 | 14 | 1.39 | 1719.03 |
| Complement factor H | P54108 | 0.03 | 2 | 1.94 | 112.07 |
| Complement factor H-related protein 1 | P02741 | 0.00 | 9 | 52.19 | 685.54 |
| Complement factor H-related protein 2 | P07333 | 0.01 | 7 | 6.62 | 504.69 |
| Complement factor H-related protein 3 | P0DML2 | 0.00 | 6 | 4.97 | 829.34 |
| Complement factor H-related protein 5 | P13611 | 0.02 | 12 | 50.63 | 726.98 |
| Complement factor I | P02775 | 0.00 | 6 | 6.13 | 904.79 |

| | | | | | |
|---|---|---|---|---|---|
| Corticosteroid-binding globulin | P01034 | 0.01 | 7 | 8.15 | 667.03 |
| Cystatin-C | Q14118 | 0.03 | 3 | 20.03 | 80.58 |
| Cysteine-rich secretory protein 3 | P81605 | 0.00 | 3 | 3.96 | 200.83 |
| Cytosol aminopeptidase | P59665 | 0.00 | 3 | 2.86 | 209.89 |
| Dermcidin | Q01459 | 0.02 | 3 | 2.13 | 163.88 |
| Di-N-acetylchitobiase | P09172 | 0.00 | 8 | 3.97 | 711.48 |
| Disintegrin and metalloproteinase domain-containing protein 12 | Q16610 | 0.00 | 12 | 3.91 | 940.23 |
| Dopamine beta-hydroxylase | P08246 | 0.11 | 3 | 4.79 | 113.75 |
| Dystroglycan | P06733 | 0.08 | 3 | 32.28 | 140.1 |
| Ectonucleotide pyrophosphatase/phosphodiesterase family member 2 | P14625 | 0.14 | 3 | 81.60 | 205.94 |
| EGF-containing fibulin-like extracellular matrix protein 1 | Q13822 | 0.00 | 14 | 4.36 | 1066.78 |
| Endoplasmin | Q9UNN8 | 0.00 | 2 | 13.21 | 148.39 |
| Endothelial protein C receptor | P00488 | 0.16 | 2 | 219.88 | 94.77 |
| Extracellular matrix protein 1 | P05160 | 0.01 | 8 | 3.28 | 442.63 |
| Ferritin light chain | P00742 | 0.00 | 18 | 1.47 | 1453.77 |
| Fetuin-B | P03951 | 0.01 | 14 | 4.38 | 883.5 |
| Fibrinogen alpha chain | P00748 | 0.00 | 21 | 1.77 | 2062.41 |
| Fibrinogen beta chain | P12259 | 0.00 | 37 | 2.18 | 2391.36 |
| Fibrinogen gamma chain | P08709 | 0.01 | 3 | 5.55 | 288.08 |
| Fibrinogen-like protein 1 | P00740 | 0.00 | 16 | 3.53 | 1280.12 |
| Fibronectin | P23142 | 0.00 | 19 | 11.17 | 2140.42 |
| Fibulin-1 | Q12805 | 0.00 | 12 | 5.93 | 941.16 |
| Ficolin-2 | Q9Y6R7 | 0.01 | 10 | 10.25 | 462.8 |

| | | | | | |
|---|---|---|---|---|---|
| Ficolin-3 | Q15485 | 0.00 | 5 | 6.69 | 432.59 |
| Filamin-A | O75636 | 0.01 | 12 | 1.51 | 1517.03 |
| Flavin reductase (NADPH) | P02765 | 0.00 | 14 | 2.70 | 3262.98 |
| Follistatin-related protein 1 | Q9UGM5 | 0.01 | 9 | 1.47 | 979.26 |
| Fructose-bisphosphate aldolase A | Q08830 | 0.17 | 2 | 49.14 | 62.98 |
| Fructose-bisphosphate aldolase B | Q03591 | 0.00 | 2 | 2.84 | 1679.54 |
| G-protein coupled receptor 126 | P36980 | 0.03 | 2 | 1.57 | 585.29 |
| Galectin-3-binding protein | Q02985 | 0.08 | 4 | 1.80 | 525.25 |
| Gamma-glutamyl hydrolase | Q9BXR6 | 0.01 | 6 | 6.87 | 510.09 |
| Gelsolin | P02671 | 0.00 | 11 | 6.11 | 716.56 |
| Glucose-6-phosphate isomerase | P02675 | 0.00 | 12 | 23.19 | 994.83 |
| Glutathione peroxidase 3 | P02679 | 0.00 | 7 | 17.43 | 648.86 |
| Glutathione S-tanferase P | P02751 | 0.00 | 73 | 24.63 | 7767.52 |
| Glutathione S-transferase omega-1 | P21333 | 0.11 | 4 | 780.77 | 208.12 |
| Glyceraldehyde-3-phosphate dehydrogenase | P02792 | 0.00 | 7 | 38.65 | 566.93 |
| Glycoprotein hormones alpha chain | Q12841 | 0.15 | 2 | 41.20 | 55.77 |
| Haptoglobin | P04406 | 0.03 | 5 | 4.50 | 630.75 |
| Haptoglobin-related protein | P06744 | 0.17 | 2 | 105.39 | 118.92 |
| Heat shock protein HSP 90-alpha | P52566 | 0.04 | 2 | 64.19 | 103.44 |
| Hemoglobin subunit alpha | P06396 | 0.00 | 42 | 2.97 | 4407.8 |
| Hemoglobin subunit beta | Q92820 | 0.04 | 4 | 2.12 | 218.79 |
| Hemoglobin subunit delta | P01215 | 0.00 | 3 | 6.35 | 113.87 |
| Hemopexin | Q86SQ4 | 0.01 | 5 | 16.77 | 312.58 |

| | | | | | |
|---|---|---|---|---|---|
| Heparin cofactor 2 | P07359 | 0.02 | 6 | 2.58 | 631.66 |
| Hepatocyte growth factor activator | P40197 | 0.01 | 6 | 39.17 | 640.62 |
| Hepatocyte growth factor-like protein | P22352 | 0.00 | 7 | 2.19 | 423.63 |
| Histidine-rich glycoprotein | P11021 | 0.02 | 4 | 3.69 | 319.12 |
| Histone H2A type 2-C | P78417 | 0.02 | 2 | 9802.37 | 108.37 |
| Histone H3.2 | P09211 | 0.02 | 2 | 28.77 | 126.87 |
| Histone H4 | Q16777 | 0.00 | 3 | 23.94 | 121.4 |
| HLA class I histocompatibility antigen, A-24 alpha chain | Q71DI3 | 0.01 | 2 | 7.21 | 58.01 |
| Hornerin | P62805 | 0.00 | 6 | 11.35 | 468.23 |
| Hyaluronan-binding protein 2 | Q14520 | 0.01 | 19 | 1.82 | 1632.26 |
| Ig alpha-1 chain C region | P69905 | 0.01 | 11 | 13.90 | 1331.68 |
| Ig alpha-2 chain C region | P68871 | 0.00 | 9 | 16.91 | 1929.11 |
| Ig delta chain C region | P02042 | 0.00 | 2 | 31.58 | 1404.05 |
| Ig gamma-1 chain C region | P02790 | 0.00 | 35 | 1.91 | 4488.09 |
| Ig gamma-2 chain C region | P05546 | 0.00 | 29 | 2.23 | 2455.42 |
| Ig gamma-3 chain C region | Q04756 | 0.00 | 8 | 23.27 | 461.44 |
| Ig gamma-4 chain C region | P26927 | 0.00 | 14 | 2.52 | 1386.49 |
| Ig heavy chain V-I region HG3 | Q86YZ3 | 0.23 | 2 | 50.26 | 206.68 |
| Ig heavy chain V-I region V35 | P00738 | 0.00 | 20 | 4.31 | 5369.83 |
| Ig heavy chain V-II region ARH-77 | P00739 | 0.00 | 7 | 4.13 | 2920.48 |
| Ig heavy chain V-III region BUT | P04196 | 0.00 | 24 | 5.51 | 3217.09 |
| Ig heavy chain V-III region GA | P07900 | 0.08 | 2 | 26.46 | 178.33 |
| Ig heavy chain V-III region GAL | P01743 | 0.00 | 2 | 7.34 | 201.11 |

| | | | | | |
|---|---|---|---|---|---|
| Ig heavy chain V-III region WEA | P23083 | 0.00 | 3 | 5.61 | 445.61 |
| Ig kappa chain C region | P06331 | 0.00 | 2 | 3.34 | 330.64 |
| Ig kappa chain V-I region CAR | P01763 | 0.05 | 2 | 15.35 | 262.83 |
| Ig kappa chain V-I region HK102 (Fragment) | P01767 | 0.00 | 3 | 6.69 | 398.8 |
| Ig kappa chain V-I region WEA | P01769 | 0.01 | 2 | 35.53 | 61.12 |
| Ig kappa chain V-III region VG (Fragment) | P01781 | 0.00 | 4 | 4.80 | 257.93 |
| Ig kappa chain V-IV region Len | P18065 | 0.19 | 3 | 104.41 | 242.51 |
| Ig lambda chain V region 4A | P17936 | 0.01 | 7 | 2.58 | 571.67 |
| Ig lambda chain V-I region NIG-64 | P22692 | 0.01 | 3 | 10.69 | 174.78 |
| Ig lambda chain V-III region LOI | P24592 | 0.16 | 2 | 6.23 | 111 |
| Ig lambda chain V-III region SH | P05155 | 0.05 | 37 | 1.65 | 4646.01 |
| Ig lambda chain V-IV region MOL | P05362 | 0.01 | 7 | 21.27 | 622.81 |
| Ig lambda-7 chain C region | P01344 | 0.00 | 4 | 2.67 | 422.25 |
| Ig mu chain C region | P01876 | 0.00 | 6 | 9.70 | 2229.61 |
| IgGFc-binding protein | P01877 | 0.00 | 3 | 14.44 | 1573 |
| Immunoglobulin J chain | P01880 | 0.03 | 7 | 19.18 | 605.2 |
| Immunoglobulin lambda-like polypeptide 5 | P01857 | 0.00 | 6 | 13.08 | 2048.44 |
| Insulin-like growth factor II (Chain 25-91) | P01859 | 0.00 | 5 | 31.53 | 1491.8 |
| Insulin-like growth factor-binding protein 2 | P01860 | 0.00 | 6 | 18.62 | 1758.66 |
| Insulin-like growth factor-binding protein 3 | P01861 | 0.00 | 3 | 47.85 | 1042.33 |
| Insulin-like growth factor-binding protein 4 | P01871 | 0.00 | 9 | 2.85 | 3984.06 |
| Insulin-like growth factor-binding protein 6 | P01591 | 0.00 | 7 | 3.07 | 722.78 |
| Insulin-like growth factor-binding protein complex acid labile subunit | P01834 | 0.00 | 8 | 8.27 | 1914.79 |

| | | | | | |
|---|---|---|---|---|---|
| Inter-alpha-trypsin inhibitor heavy chain H1 | B9A064 | 0.00 | 3 | 9.40 | 1210.73 |
| Inter-alpha-trypsin inhibitor heavy chain H2 | P05154 | 0.00 | 15 | 4.77 | 1042.4 |
| Inter-alpha-trypsin inhibitor heavy chain H3 | Q6H9L7 | 0.02 | 5 | 20.76 | 232.44 |
| Inter-alpha-trypsin inhibitor heavy chain H4 | P19827 | 0.01 | 51 | 2.30 | 7548.04 |
| Intercellular adhesion molecule 1 | P19823 | 0.00 | 55 | 2.52 | 7261.15 |
| Isthmin-2 | Q06033 | 0.00 | 45 | 3.04 | 4989.64 |
| Kallistatin | Q14624 | 0.01 | 63 | 1.71 | 8607.9 |
| Keratin-associated protein 11-1 | P13645 | 0.04 | 27 | 2.02 | 4556 |
| Keratin, type I cytoskeletal 10 | P02533 | 0.02 | 5 | 5.00 | 1256.91 |
| Keratin, type I cytoskeletal 14 | P04264 | 0.00 | 30 | 1.79 | 3760.58 |
| Keratin, type II cytoskeletal 1 | P13647 | 0.00 | 7 | 2.54 | 973.54 |
| Keratin, type II cytoskeletal 5 | P48668 | 0.11 | 2 | 17.57 | 851.76 |
| Keratin, type II cytoskeletal 6C | P29622 | 0.00 | 16 | 5.21 | 1672.78 |
| Kininogen-1 | P03952 | 0.00 | 37 | 2.10 | 3772.72 |
| L-lactate dehydrogenase A chain | P01042 | 0.00 | 39 | 1.76 | 4221.49 |
| L-lactate dehydrogenase B chain | P14618 | 0.25 | 2 | 98.90 | 122.29 |
| L-selectin | Q8IUC1 | 0.03 | 2 | Infinity | 129.85 |
| Lactotransferrin | P01596 | 0.07 | 2 | 56.91 | 91.87 |
| Leucine-rich alpha-2-glycoprotein | P01602 | 0.00 | 2 | 3.66 | 284.72 |
| Leucyl-cystinyl aminopeptidase | P01610 | 0.23 | 2 | 39.19 | 213.65 |
| Leukocyte immunoglobulin-like receptor subfamily A member 3 | P04433 | 0.00 | 3 | 6.48 | 244.19 |
| Lipopolysaccharide-binding protein | P01625 | 0.00 | 3 | 8.81 | 621.68 |
| Lumican | A0M8Q6 | 0.00 | 2 | 9.43 | 650.93 |

| | | | | | |
|---|---|---|---|---|---|
| Lymphatic vessel endothelial hyaluronic acid receptor 1 | P18428 | 0.01 | 17 | 5.43 | 1769.49 |
| Lysozyme C | Q9UIQ6 | 0.00 | 5 | 48.52 | 344.07 |
| Macrophage colony-stimulating factor 1 receptor | P04180 | 0.01 | 7 | 1.89 | 874.1 |
| Macrophage mannose receptor 1 | P00338 | 0.10 | 2 | Infinity | 193.12 |
| Mannan-binding lectin serine protease 1 | P07195 | 0.01 | 4 | 7.64 | 344.29 |
| Mannan-binding lectin serine protease 2 | Q08380 | 0.00 | 24 | 3.64 | 3292.45 |
| Mannose-binding protein C | Q8N6C8 | 0.03 | 3 | 6.96 | 213.11 |
| Mannosyl-oligosaccharide 1,2-alpha-mannosidase IA | Q07954 | 0.01 | 4 | 38.96 | 265.37 |
| Matrix metalloproteinase-9 | P51884 | 0.01 | 13 | 1.81 | 1502.96 |
| Metalloproteinase inhibitor 1 | P04211 | 0.04 | 2 | 4.16 | 91.49 |
| Moesin | P01702 | 0.01 | 2 | 2.24 | 63.55 |
| Monocyte differentiation antigen CD14 | P01714 | 0.01 | 3 | 3.64 | 409.8 |
| Myeloperoxidase | P80748 | 0.00 | 2 | 7.46 | 265.87 |
| N-acetylmuramoyl-L-alanine amidase | P06889 | 0.01 | 2 | 3.21 | 172.43 |
| Neuropilin-1 | P14151 | 0.06 | 4 | 1.73 | 153.4 |
| Neutrophil collagenase | P61626 | 0.00 | 6 | 1.87 | 279.78 |
| Neutrophil defensin 1 | Q9Y5Y7 | 0.04 | 4 | 2.68 | 173.45 |
| Neutrophil elastase | P33908 | 0.08 | 4 | 2.62 | 282.52 |
| Neutrophil gelatinase-associated lipocalin | P48740 | 0.01 | 13 | 1.47 | 1433.51 |
| Nidogen-1 | O00187 | 0.00 | 10 | 2.00 | 696.32 |
| Nucleobindin-1 | P11226 | 0.01 | 7 | 1.84 | 1023.75 |
| Olfactomedin-4 | P22894 | 0.01 | 2 | 11.75 | 161.6 |
| Out at first protein homolog | P14780 | 0.01 | 14 | 1.86 | 990.76 |

| | | | | | |
|---|---|---|---|---|---|
| Pantetheinase | P26038 | 0.21 | 3 | 7.31 | 131.46 |
| Pappalysin-1 | P22897 | 0.01 | 5 | 15.62 | 200.83 |
| Pentraxin-related protein PTX3 | P43121 | 0.07 | 2 | 3.33 | 124.72 |
| Peptidase inhibitor 16 | P80188 | 0.00 | 3 | 3.18 | 228.36 |
| Peptidyl-prolyl cis-trans isomerase A | P14543 | 0.00 | 15 | 2.93 | 867.79 |
| Periostin | Q6P988 | 0.01 | 4 | 10.90 | 302.7 |
| Peroxiredoxin-2 | O14786 | 0.28 | 2 | 15.90 | 136.12 |
| Peroxiredoxin-6 | Q02818 | 0.02 | 5 | 32.72 | 330.22 |
| Phosphatidylcholine-sterol acyltransferase | Q86UD1 | 0.03 | 3 | 5.94 | 149.78 |
| Phosphatidylinositol-glycan-specific phospholipase D | Q6UX06 | 0.05 | 3 | 13.02 | 225.86 |
| Phospholipid transfer protein | Q13219 | 0.00 | 37 | 38.02 | 3617.2 |
| Pigment epithelium-derived factor | Q9UHG3 | 0.01 | 13 | 4.32 | 908.17 |
| Plasma kallikrein | P36955 | 0.03 | 20 | 1.51 | 2063.15 |
| Plasma protease C1 inhibitor | P12955 | 0.15 | 4 | 1.49 | 263.08 |
| Plasma serine protease inhibitor | P05164 | 0.00 | 14 | 4.45 | 1044.77 |
| Plasminogen | P98160 | 0.09 | 5 | 11.67 | 194.38 |
| Plastin-2 | Q96PD5 | 0.00 | 21 | 3.74 | 3611.86 |
| Platelet basic protein | P80108 | 0.03 | 19 | 2.33 | 1911.43 |
| Platelet factor 4 | Q6UXB8 | 0.05 | 2 | 1.73 | 180.36 |
| Platelet glycoprotein Ib alpha chain | P01833 | 0.00 | 17 | 6.21 | 1496.35 |
| Platelet glycoprotein V | P02776 | 0.00 | 3 | 5.39 | 306.07 |
| Poliovirus receptor | P00747 | 0.00 | 68 | 2.29 | 9045.17 |
| Polymeric immunoglobulin receptor | P13796 | 0.00 | 18 | 5.00 | 1542.8 |

| | | | | | |
|---|---|---|---|---|---|
| Polyubiquitin-C | P55058 | 0.04 | 13 | 2.46 | 1290.42 |
| Pregnancy zone protein | P27169 | 0.00 | 22 | 5.56 | 2816.57 |
| Pregnancy-specific beta-1-glycoprotein 1 | Q15063 | 0.03 | 4 | 10.18 | 263.47 |
| Pregnancy-specific beta-1-glycoprotein 11 | P62937 | 0.00 | 6 | 15.05 | 443.38 |
| Pregnancy-specific beta-1-glycoprotein 2 | P32119 | 0.01 | 8 | 47.58 | 425 |
| Pregnancy-specific beta-1-glycoprotein 4 | P30041 | 0.01 | 3 | 7.20 | 229.56 |
| Pregnancy-specific beta-1-glycoprotein 6 | P13727 | 0.00 | 11 | 12.49 | 1118.35 |
| Pregnancy-specific beta-1-glycoprotein 9 | Q92954 | 0.03 | 8 | 2.11 | 654.72 |
| Prenylcysteine oxidase 1 | P04070 | 0.00 | 7 | 2.99 | 561.74 |
| Profilin-1 | P07737 | 0.00 | 3 | 17.00 | 223.51 |
| Prolow-density lipoprotein receptor-related protein 1 | P27918 | 0.00 | 7 | 4.87 | 523.11 |
| Properdin | P07225 | 0.01 | 24 | 2.09 | 3261.23 |
| Prostaglandin-H2 D-isomerase | P22891 | 0.00 | 12 | 2.20 | 982.69 |
| Proteasome subunit alpha type-2 | P25787 | 0.01 | 2 | 94.80 | 149.41 |
| Proteasome subunit alpha type-3 | P25788 | 0.11 | 2 | 303.43 | 149.18 |
| Proteasome subunit alpha type-5 | P28066 | 0.13 | 4 | 363.02 | 301.64 |
| Proteasome subunit alpha type-6 | P60900 | 0.04 | 3 | 716.32 | 261.71 |
| Proteasome subunit alpha type-7 | O14818 | 0.00 | 5 | 27.68 | 336.78 |
| Proteasome subunit beta type-1 | P20618 | 0.00 | 2 | 17.13 | 251.37 |
| Proteasome subunit beta type-3 | P49720 | 0.19 | 2 | 149.38 | 61.91 |
| Proteasome subunit beta type-4 | P28070 | 0.00 | 2 | Infinity | 134.23 |
| Proteasome subunit beta type-9 | P28065 | 0.06 | 2 | 1844.03 | 182.97 |
| Protein AMBP | P11464 | 0.00 | 3 | 9.30 | 1249.66 |

| | | | | | |
|---|---|---|---|---|---|
| Protein notum homolog | Q9UQ72 | 0.01 | 3 | 42.75 | 755.62 |
| Protein S100-A7 | P11465 | 0.01 | 2 | 107.36 | 859.05 |
| Protein S100-A8 | Q00888 | 0.00 | 4 | 15.45 | 853.98 |
| Protein S100-A9 | Q00889 | 0.01 | 2 | 13.81 | 635.33 |
| Protein Z-dependent protease inhibitor | Q13046 | 0.02 | 4 | 5.11 | 978.28 |
| Proteoglycan 4 | Q00887 | 0.01 | 8 | 6.89 | 1105.15 |
| Prothrombin | P41222 | 0.10 | 2 | 3.69 | 215.91 |
| Putative pregnancy-specific beta-1-glycoprotein 7 | P26022 | 0.00 | 7 | 79.12 | 521.78 |
| Pyruvate kinase PKM | P15151 | 0.00 | 3 | 6.02 | 165.54 |
| Retinoic acid receptor responder protein 2 | P20742 | 0.01 | 51 | 2.78 | 8179.84 |
| Retinol-binding protein 4 | O00391 | 0.01 | 12 | 1.91 | 1100.1 |
| Rho GDP-dissociation inhibitor 2 | Q99969 | 0.02 | 2 | 3.94 | 80.73 |
| Ribonuclease 4 | P02753 | 0.00 | 15 | 5.00 | 2008.66 |
| Ribonuclease pancreatic | P07998 | 0.00 | 2 | 64.15 | 164.79 |
| Scavenger receptor cysteine-rich type 1 protein M130 | P34096 | 0.02 | 5 | 14.15 | 245.52 |
| Secreted phosphoprotein 24 | P31151 | 0.21 | 2 | 5.58 | 135.65 |
| Selenoprotein P | P05109 | 0.00 | 4 | 4.48 | 281.82 |
| Serotransferrin | P06702 | 0.00 | 8 | 6.00 | 860.88 |
| Serpin A11 | P0DJI8 | 0.00 | 3 | 226.16 | 1293.71 |
| Serum albumin | P0DJI9 | 0.00 | 2 | 18.76 | 894.78 |
| Serum amyloid A-1 protein | P35542 | 0.00 | 5 | 2.23 | 691.5 |
| Serum amyloid A-2 protein | P02743 | 0.04 | 6 | 1.35 | 827.48 |
| Serum amyloid A-4 protein | P49908 | 0.00 | 5 | 4.22 | 455.32 |

| | | | | | |
|---|---|---|---|---|---|
| Serum amyloid P-component | Q9H299 | 0.02 | 2 | 23.50 | 66.11 |
| Serum paraoxonase/arylesterase 1 | P04278 | 0.03 | 22 | 2.83 | 3159.95 |
| Sex hormone-binding globulin | Q86U17 | 0.04 | 2 | 2.61 | 74.07 |
| SH3 domain-binding glutamic acid-rich-like protein 3 | Q13103 | 0.02 | 4 | 1.86 | 618.89 |
| SPARC | P09486 | 0.10 | 2 | 6.42 | 104.4 |
| SPARC-like protein 1 | Q14515 | 0.33 | 2 | 7.39 | 42.75 |
| Spectrin alpha chain, erythrocytic 1 | P02549 | 0.15 | 3 | 622.34 | 108.18 |
| Spectrin beta chain, erythrocytic | P11277 | 0.16 | 2 | Infinity | 154.55 |
| Sulfhydryl oxidase 1 | P23381 | 0.02 | 5 | 59.40 | 297.25 |
| Talin-1 | P37802 | 0.00 | 5 | 39.33 | 376.11 |
| Tenascin | P24821 | 0.06 | 6 | 7.65 | 318.9 |
| Tenascin-X | P22105 | 0.09 | 5 | 4.22 | 244.47 |
| Tetranectin | P05452 | 0.00 | 8 | 3.29 | 945.88 |
| Thrombospondin-1 | P05543 | 0.05 | 22 | 1.55 | 2729.16 |
| Thrombospondin-4 | P00734 | 0.00 | 42 | 2.32 | 7064.65 |
| Thyroxine-binding globulin | P01033 | 0.01 | 4 | 6.84 | 338.89 |
| Transforming growth factor-beta-induced protein ig-h3 | P29401 | 0.02 | 5 | 13.51 | 258.23 |
| Transgelin-2 | Q9Y490 | 0.03 | 6 | 261.89 | 441.48 |
| Transketolase | P60174 | 0.17 | 2 | 340.98 | 182 |
| Transthyretin | P67936 | 0.21 | 2 | 116.57 | 200.27 |
| Triosephosphate isomerase | P02787 | 0.00 | 80 | 4.39 | 12211.26 |
| Tropomyosin alpha-4 chain | P02788 | 0.00 | 27 | 4.76 | 2256.95 |
| Tryptophan--tRNA ligase, cytoplasmic | P07996 | 0.00 | 30 | 6.33 | 3132.49 |

| | | | | | |
|---|---|---|---|---|---|
| U5 small nuclear ribonucleoprotein 200 kDa helicase | P35443 | 0.02 | 7 | 33.20 | 847.99 |
| UTP--glucose-1-phosphate uridylyltransferase | P02766 | 0.00 | 13 | 5.21 | 3142.71 |
| Vascular cell adhesion protein 1 | O75643 | 0.32 | 2 | 2.15 | 30.81 |
| Vasorin | P0CG48 | 0.00 | 4 | 5.96 | 235.84 |
| Versican core protein | Q16851 | 0.00 | 7 | 46.28 | 362.77 |
| Vinculin | Q6EMK4 | 0.06 | 3 | 3.30 | 253.74 |
| Vitamin D-binding protein | P19320 | 0.01 | 15 | 3.62 | 865.28 |
| Vitamin K-dependent protein C | P18206 | 0.02 | 6 | 12.57 | 347.65 |
| Vitamin K-dependent protein S | O95497 | 0.03 | 5 | 2.08 | 363.57 |
| Vitamin K-dependent protein Z | P02774 | 0.03 | 48 | 1.50 | 7746.83 |
| Vitronectin | P04004 | 0.00 | 26 | 1.86 | 3054.04 |
| von Willebrand factor | P04275 | 0.00 | 107 | 8.58 | 11433.97 |
| Xaa-Pro dipeptidase | P25311 | 0.01 | 23 | 2.47 | 2582.1 |
| Zinc-alpha-2-glycoprotein | Q9UK55 | 0.01 | 11 | 1.65 | 1188.48 |

*Appendix B 3. Proteins clustered by GProX*

| Biological function (GO annotation) | Description | Accession | Cluster membership |
|---|---|---|---|
| **Cluster 1** | | | |
| Cell adhesion | Disintegrin and metalloproteinase domain-containing protein 12 | O43184 | 0.7 |
| Pregnancy | Pregnancy-specific beta-1-glycoprotein 1 | P11464 | 0.7 |
| Oxidoreductase | Flavin reductase (NADPH) | P30043 | 0.6 |
| Pregnancy | Fibrinogen alpha chain | P02671 | 0.6 |
| Protease | Mannan-binding lectin serine protease 2 | O00187 | 0.8 |
| Pregnancy | Adiponectin | Q15848 | 0.7 |
| Pregnancy/ Coagulation | Coagulation factor VII | P08709 | 0.7 |
| Immunity/ Inflammation | Macrophage colony-stimulating factor 1 receptor | P07333 | 0.8 |
| Receptor | G-protein coupled receptor 126 | Q86SQ4 | 0.8 |
| Pregnancy | Pregnancy-specific beta-1-glycoprotein 4 | Q00888 | 0.9 |
| Pregnancy | Pregnancy-specific beta-1-glycoprotein 9 | Q00887 | 0.9 |
| Vitamin B5 metabolism | Pantetheinase | O95497 | 0.9 |
| Pregnancy | Leucyl-cystinyl aminopeptidase | Q9UIQ6 | 0.9 |
| Pregnancy | Chorionic somatomammotropin hormone 1 | P0DML2 | 0.9 |
| Pregnancy | Pappalysin-1 | Q13219 | 0.9 |
| Pregnancy | Pregnancy-specific beta-1-glycoprotein 2 | P11465 | 0.9 |
| Pregnancy | Bone marrow proteoglycan | P13727 | 0.9 |
| Pregnancy | Pregnancy-specific beta-1-glycoprotein 11 | Q9UQ72 | 0.9 |
| Pregnancy | Pregnancy-specific beta-1-glycoprotein 6 | Q00889 | 0.9 |
| Lipid metabolism | Apolipoprotein C-IV | P55056 | 0.6 |

| | | | |
|---|---|---|---|
| Structural protein | Collagen alpha -1(VI) chain | P12109 | 0.6 |
| Oxidoreductase | Amiloride-sensitive amine oxidase (copper-containing) | P19801 | 0.6 |
| **Cluster 2** | | | |
| Acute phase response | Fibrinogen gamma chain | P02679 | 0.6 |
| Cell adhesion | Galectin-3-binding protein | Q08380 | 0.9 |
| Acute phase response | C-reactive protein (Chain 19-224) | P02741 | 0.9 |
| Cell movement | EGF-containing fibulin-like extracellular matrix protein 1 | Q12805 | 0.6 |
| Proteolysis | Proteasome subunit beta type-4 | P28070 | 0.6 |
| Proteolysis | Proteasome subunit beta type-1 | P20618 | 0.7 |
| Coagulation | Endothelial protein C receptor | Q9UNN8 | 0.6 |
| Angiogenesis | Angiogenin | P03950 | 0.7 |
| Acute phase response | Alpha-1-acid glycoprotein 1 | P02763 | 0.8 |
| Growth factor binding | Insulin-like growth factor-binding protein 4 | P22692 | 0.6 |
| Acute phase response | Lipopolysaccharide-binding protein | P18428 | 0.6 |
| Innate immunity | Macrophage mannose receptor 1 | P22897 | 0.6 |
| Protease inhibitor | Cystatin-C | P01034 | 0.6 |
| Acid protease | Cathepsin D | P07339 | 0.6 |
| Cell adhesion/ angiogenesis | Thrombospondin-4 | P35443 | 0.6 |
| Innate immunity | Scavenger receptor cysteine-rich type 1 protein M130 | Q86VB7 | 0.6 |
| Actin-binding | Plastin-2 | P13796 | 0.6 |
| Cell adhesion | Olfactomedin-4 | Q6UX06 | 0.6 |
| Platelet activation | Inter-alpha-trypsin inhibitor heavy chain H3 | Q06033 | 0.6 |
| Endonuclease | Ribonuclease pancreatic | P07998 | 0.9 |

| | | | |
|---|---|---|---|
| Angiogenesis | Leucine-rich alpha-2-glycoprotein | P02750 | 0.6 |
| Cell adhesion | Collagen alpha-1(XVIII) chain | P39060 | 0.6 |
| Oxidoreductase/ transferase | Glutathione S-transferase omega-1 | P78417 | 0.7 |
| Wnt signalling pathway | Protein notum homolog | Q6P988 | 0.8 |
| Lactate metabolism | L-lactate dehydrogenase B chain | P07195 | 0.8 |
| Acute phase response | Ferritin light chain | P02792 | 0.7 |
| Acute phase response | Pentraxin-related protein PTX3 | P26022 | 0.8 |
| Acute phase response | Serum amyloid A-1 protein | P0DJI8 | 0.7 |
| Structural | Collagen alpha-1(III) chain | P02461 | 0.8 |
| Humoral immunity | HLA class I histocompatibility antigen, A-24 alpha chain | P05534 | 0.7 |
| Proteolysis | Proteasome subunit alpha type-2 | P25787 | 0.8 |
| Acute phase response / platelet activation | Alpha-1-antichymotrypsin | P01011 | 0.8 |
| Platelet activation | Metalloproteinase inhibitor 1 | P01033 | 0.8 |
| Endocytic receptor | Prolow-density lipoprotein receptor-related protein 1 | Q07954 | 0.9 |
| Cell adhesion | Vascular cell adhesion protein 1 | P19320 | 0.9 |
| Secreted glycoprotein | Isthmin-2 | Q6H9L7 | 0.8 |
| - | Out at first protein homolog | Q86UD1 | 0.9 |
| Proteolysis | Proteasome subunit alpha type-6 | P60900 | 0.8 |
| Proteolysis | Proteasome subunit alpha type-7 | O14818 | 0.6 |
| Humoral immunity | Beta-2-microglobulin | P61769 | 0.7 |
| Endonuclease | Ribonuclease 4 | P34096 | 0.6 |
| **Cluster 3** | | | |
| Oxidative stress | Carbonic anhydrase 2 | P00918 | 0.7 |

| | | | |
|---|---|---|---|
| Oxidative stress | Haemoglobin subunit beta | P68871 | 0.8 |
| Ubiquitin | Polyubiquitin-C | P0CG48 | 0.8 |
| Oxidative stress | Protein S100-A9 | P06702 | 0.6 |
| Oxidative stress | Protein S100-A8 | P05109 | 0.8 |
| Oxidative stress | Peptidyl-prolyl cis-trans isomerase A | P62937 | 0.8 |
| Oxidative stress | Haemoglobin subunit delta | P02042 | 0.8 |
| Oxidative stress / neutrophil activity | Myeloperoxidase | P05164 | 0.8 |
| Cell motility | Actin, cytoplasmic 1 | P60709 | 0.7 |
| Neutrophil activity | Neutrophil defensin 1 | P59665 | 0.7 |
| Neutrophil activity | Neutrophil collagenase | P22894 | 0.6 |
| Oxidative stress | Haemoglobin subunit alpha | P69905 | 0.6 |
| Oxidative stress | Glutathione S-transferase P | P09211 | 0.7 |
| Cellular $Ca^{2+}$-response | Calmodulin | P62158 | 0.9 |
| Oxidative stress | Haemoglobin subunit alpha | P69905 | 0.7 |
| Nucleasome component | Histone H4 | P62805 | 0.6 |
| Cell motility | Profilin-1 | P07737 | 0.6 |
| Oxidative stress | Band 3 anion transport protein | P02730 | 0.6 |
| Oxidative stress | Peroxiredoxin-2 | P32119 | 0.6 |
| **Cluster 4** | | | |
| Humoral immunity | Ig heavy chain V-II region ARH-77 | P06331 | 0.7 |
| Humoral immunity | Immunoglobulin J chain | P01591 | 0.7 |
| Humoral immunity | Ig mu chain C region | P01871 | 0.7 |
| Humoral immunity | Ig kappa chain V-I region HK102 (Fragment) | P01602 | 0.6 |

| | | | |
|---|---|---|---|
| Acute phase response | Albumin | P02768 | 0.8 |
| Humoral immunity | Ig alpha-1 chain C region | P01876 | 0.9 |
| Humoral immunity | Ig gamma-4 chain C region | P01861 | 0.9 |
| Humoral immunity | Ig alpha-2 chain C region | P01877 | 0.9 |
| Humoral immunity | Immunoglobulin lambda-like polypeptide 5 | B9A064 | 0.9 |
| Humoral immunity | Ig kappa chain C region | P01834 | 1 |
| Humoral immunity | Ig gamma-1 chain C region | P01857 | 0.9 |
| Humoral immunity | Ig lambda-7 chain C region | A0M8Q6 | 0.9 |
| Haemoglobin binding | Haptoglobin-related protein | P00739 | 0.9 |
| Humoral immunity | Ig gamma-2 chain C region | P01859 | 0.8 |
| Immunity/Inflammation | CD5 antigen-like | O43866 | 0.8 |
| Acute phase response | Serotransferrin | P02787 | 0.8 |
| Humoral immunity | Ig lambda chain V-III region LOI | P80748 | 0.9 |
| Humoral immunity | Ig gamma-3 chain C region | P01860 | 0.9 |
| Protease inhibitor | Alpha-2-macroglobulin | P01023 | 0.8 |
| Acute phase response | Apolipoprotein A-II | P02652 | 0.9 |
| Acute phase response | Apolipoprotein A-I | P02647 | 0.6 |
| Humoral immunity | Ig heavy chain V-I region HG3 | P01743 | 0.7 |
| Humoral immunity | Ig heavy chain V-III region GA | P01769 | 0.9 |
| Humoral immunity | Ig delta chain C region | P01880 | 0.9 |
| Humoral immunity | Ig heavy chain V-I region V35 | P23083 | 0.9 |
| Humoral immunity | Ig kappa chain V-III region VG (Fragment) | P04433 | 0.9 |
| Humoral immunity | Ig kappa chain V-I region HK102 (Fragment) | U6CXY5 | 0.7 |

| | | | |
|---|---|---|---|
| Humoral immunity | Ig heavy chain V-III region GAL | P01781 | 0.9 |
| Humoral immunity | Ig lambda chain V-III region SH | P01714 | 0.9 |
| Humoral immunity | Ig lambda chain V region 4A | P04211 | 0.9 |
| Humoral immunity | Ig heavy chain V-III region BUT | P01767 | 0.9 |
| Complement | C4b-binding protein alpha chain | P04003 | 0.7 |
| Hydrolase | Serum paraoxonase/arylesterase 1 | P27169 | 0.7 |
| Humoral immunity | Ig kappa chain V-IV region LEN | P01625 | 1 |
| Pregnancy | Choriogonadotropin subunit beta variant 1 | A6NKQ9 | 0.6 |
| Oxidative stress | Peroxiredoxin 6 | P30041 | 0.6 |
| Complement | Complement C1q subcomponent subunit B | P02746 | 0.6 |
| **Cluster 5** | | | |
| Coagulation | Platelet glycoprotein V | P40197 | 0.8 |
| Vitamin-E-binding protein / Acute phase response | Afamin | P43652 | 0.7 |
| Acute phase response | Inter-alpha-trypsin inhibitor heavy chain H2 | P19823 | 0.8 |
| Acute phase response | Inter-alpha-trypsin inhibitor heavy chain H1 | | 0.8 |
| Complement | Properdin | P27918 | 0.8 |
| Coagulation | Heparin cofactor 2 | P05546 | 0.8 |
| Platelet activation | Selenoprotein P | P49908 | 0.9 |
| Innate immunity | N-acetylmuramoyl-L-alanine amidase | Q96PD5 | 0.9 |
| Platelet activation | Beta-2-glycoprotein 1 | P02749 | 0.9 |
| Coagulation | Plasminogen | P00747 | 0.9 |
| Coagulation | Prothrombin | P00734 | 0.9 |
| Coagulation / Acute phase response | Transthyretin | P02766 | 0.9 |

| | | | |
|---|---|---|---|
| Acute phase response | Retinol-binding protein 4 | P02753 | 0.6 |
| Complement/ Innate immunity | Ficolin-2 | Q15485 | 0.9 |
| Coagulation | Kallistatin | P29622 | 0.9 |
| Coagulation | Plasma serine protease inhibitor | P05154 | 0.9 |
| Coagulation | Plasma kallikrein | P03952 | 1 |
| Coagulation | Histidine-rich glycoprotein | P04196 | 1 |
| Coagulation | Vitamin K-dependent protein S | P07225 | 0.9 |
| Coagulation | Vitamin K-dependent protein C | P04070 | 0.6 |
| Platelet activation | Thrombospondin-1 | P07996 | 0.7 |
| Platelet activation | Platelet basic protein | P02775 | 0.7 |
| Platelet activation | Tetranectin | P05452 | 0.6 |
| Lipid metabolism | Apolipoprotein C-I | P02654 | 0.6 |
| Coagulation | Coagulation factor XI | P03951 | 0.7 |
| Protein binding and transport | Zinc--alpha-2-glycoprotein | P25311 | 0.9 |
| Inflammatory response | Attractin | O75882 | 0.6 |
| Coagulation | Carboxypeptidase B2 | Q96IY4 | 0.6 |

*Appendix B 4. 211 proteins identified in HEK213T cells by MS*

| Description | Accession | -LOG P-value | Unique peptides | Max fold change | Confidence score |
|---|---|---|---|---|---|
| 10 kDa heat shock protein, mitochondrial | P61604 | 1.073 | 3 | 1.56 | 12.74 |
| 3-hydroxyacyl-CoA dehydrogenase type-2 | Q99714 | 0.617 | 2 | -1.09 | 9.47 |
| 39S ribosomal protein L39, mitochondrial | Q9NYK5 | 0.433 | 3 | -0.23 | 19.26 |
| 40S ribosomal protein S11 | P62280 | 0.724 | 4 | 1.42 | 21.04 |
| 40S ribosomal protein S12 | P25398 | 0.308 | 3 | 0.47 | 25.94 |
| 40S ribosomal protein S14 | P62263 | 0.49 | 5 | 1.44 | 47.41 |
| 40S ribosomal protein S19 | P39019 | 0.291 | 7 | -0.55 | 62.08 |
| 40S ribosomal protein S2 | P15880 | 0.347 | 3 | -0.24 | 8.22 |
| 40S ribosomal protein S20 | P60866 | 1.049 | 5 | -0.98 | 12.03 |
| 40S ribosomal protein S21 | P63220 | 0.101 | 6 | 0.12 | 62.96 |
| 40S ribosomal protein S28 | P62857 | 0.668 | 5 | 1.79 | 37.13 |
| 40S ribosomal protein S29 | P62273 | 0.238 | 4 | 0.69 | 7.62 |
| 40S ribosomal protein S30 | P62861 | 0.14 | 2 | 0.32 | 7.26 |
| 40S ribosomal protein S3a | P61247 | 0.814 | 6 | 1.07 | 21.05 |
| 40S ribosomal protein S4, X isoform | P62701 | 0.853 | 2 | 0.52 | 7.35 |
| 40S ribosomal protein S6 | P62753 | 0.795 | 2 | -2.23 | 14.81 |
| 40S ribosomal protein S7 | P62081 | 0.003 | 2 | 0.02 | 21.47 |
| 40S ribosomal protein S8 | P62241 | 0.248 | 2 | 0.24 | 36.96 |
| 40S ribosomal protein SA | P08865 | 2.04 | 2 | -1.25 | 5.68 |
| 4F2 cell-surface antigen heavy chain | P08195 | 0.45 | 2 | 0.91 | 11.69 |
| 60 kDa heat shock protein, mitochondrial | P10809 | 0.16 | 28 | 0.21 | 323.31 |

| | | | | | |
|---|---|---|---|---|---|
| 60S ribosomal protein L12 | P30050 | 0.787 | 2 | 0.63 | 11.22 |
| 60S ribosomal protein L13 | P26373 | 0.772 | 6 | 0.91 | 90.37 |
| 60S ribosomal protein L14 | P50914 | 0.335 | 2 | 0.32 | 5.98 |
| 60S ribosomal protein L15 | P61313 | 2.83 | 2 | -3.11 | 5.40 |
| 60S ribosomal protein L19 | P84098 | 0.359 | 3 | 0.29 | 9.16 |
| 60S ribosomal protein L21 | P46778 | 0.012 | 2 | -0.08 | 8.06 |
| 60S ribosomal protein L23a | P62750 | 2.307 | 3 | 1.83 | 5.93 |
| 60S ribosomal protein L24 | P83731 | 0.543 | 3 | 2.13 | 9.68 |
| 60S ribosomal protein L26 | P61254 | 0.024 | 8 | -0.06 | 39.07 |
| 60S ribosomal protein L28 | P46779 | 0.104 | 7 | 0.15 | 40.85 |
| 60S ribosomal protein L29 | P47914 | 0.457 | 5 | 1.45 | 25.56 |
| 60S ribosomal protein L31 | P62899 | 1.194 | 3 | 2.78 | 5.13 |
| 60S ribosomal protein L34 | P49207 | 0.022 | 2 | -0.08 | 8.81 |
| 60S ribosomal protein L4 | P36578 | 0.024 | 2 | 0.13 | 12.23 |
| 60S ribosomal protein L6 | Q02878 | 0.024 | 4 | 0.02 | 10.93 |
| 60S ribosomal protein L7a | P62424 | 0.165 | 4 | 0.38 | 11.69 |
| 60S ribosomal protein L8 | P62917 | 0.294 | 6 | 0.76 | 17.78 |
| 7-dehydrocholesterol reductase | Q9UBM7 | 0.363 | 3 | 1.39 | 11.93 |
| 78 kDa glucose-regulated protein | P11021 | 0.088 | 5 | 0.58 | 39.31 |
| Actin, cytoplasmic 1 | P60709 | 2.237 | 2 | -1.47 | 323.31 |
| Actin, cytoplasmic 2 | P63261 | 0.055 | 2 | -0.56 | 87.37 |
| Alanine aminotransferase 2 | Q8TD30 | 0.586 | 2 | -0.74 | 6.19 |
| Alpha-enolase | P06733 | 1.229 | 7 | -1.18 | 19.02 |

| | | | | | |
|---|---|---|---|---|---|
| Annexin A2 | P07355 | 0.486 | 2 | -0.46 | 9.04 |
| ATP synthase subunit alpha, mitochondrial | P25705 | 1.177 | 10 | 1.72 | 86.47 |
| ATP synthase subunit beta, mitochondrial | P06576 | 0.62 | 10 | 1.55 | 108.66 |
| ATP synthase subunit d, mitochondrial | O75947 | 1.156 | 2 | 1.92 | 3.71 |
| ATP synthase subunit e, mitochondrial | P56385 | 1.275 | 2 | 2.59 | 15.42 |
| ATP synthase subunit O, mitochondrial | P48047 | 0.683 | 4 | 1.36 | 11.42 |
| B-cell receptor-associated protein 31 | P51572 | 0.277 | 2 | 0.38 | 5.21 |
| Basigin | P35613 | 1.2 | 3 | 2.19 | 32.82 |
| Beta-2-microglobulin | P61769 | 0.331 | 2 | 0.88 | 2.91 |
| BolA-like protein 2 | Q9H3K6 | 0.448 | 4 | -0.73 | 39.42 |
| CAAX prenyl protease 1 homolog | O75844 | 0.79 | 2 | 2.76 | 2.92 |
| Calmodulin-like protein 5 | Q9NZT1 | 1.018 | 2 | 2.27 | 12.38 |
| Calnexin | P27824 | 0.041 | 6 | 0.22 | 25.48 |
| CD151 antigen | P48509 | 0.318 | 2 | 1.15 | 5.95 |
| Cellular nucleic acid-binding protein | P62633 | 0.387 | 5 | -0.71 | 59.47 |
| Cofilin-1 | P23528 | 0.204 | 5 | 0.29 | 69.41 |
| Coiled-coil domain-containing protein 47 | Q96A33 | 0.4 | 2 | 0.77 | 5.08 |
| Cold-inducible RNA-binding protein | Q14011 | 0.612 | 2 | 1.01 | 7.21 |
| Complement component 1 Q subcomponent-binding protein, mitochondrial | Q07021 | 0.792 | 2 | -2.94 | 47.81 |
| Crk-like protein | P46109 | 0.471 | 3 | -1.64 | 32.34 |
| CTP synthase 1 | P17812 | 1.541 | 5 | -1.63 | 51.29 |
| Cystathionine beta-synthase | P0DN79 | 1.63 | 4 | -1.86 | 29.23 |
| Cysteine and glycine-rich protein 2 | Q16527 | 1.353 | 4 | -1.60 | 34.62 |

| | | | | | |
|---|---|---|---|---|---|
| Cytochrome b-c1 complex subunit 1, mitochondrial | P31930 | 0.38 | 4 | -1.15 | 16.82 |
| Cytochrome b-c1 complex subunit 2, mitochondrial | P22695 | 0.909 | 2 | 1.67 | 41.98 |
| Cytochrome b-c1 complex subunit 6, mitochondrial | P07919 | 1.66 | 4 | 1.68 | 62.00 |
| Cytochrome c oxidase subunit 5A, mitochondrial | P20674 | 0.724 | 4 | 2.43 | 27.46 |
| Cytochrome c oxidase subunit 5B, mitochondrial | P10606 | 2.046 | 5 | 3.86 | 15.56 |
| Cytochrome c oxidase subunit 6B1 | P14854 | 1.136 | 4 | 3.29 | 25.94 |
| Cytochrome c oxidase subunit 6C | P09669 | 0.645 | 3 | 2.73 | 7.09 |
| Cytoplasmic dynein 1 intermediate chain 2 | Q13409 | 0.797 | 2 | 1.25 | 42.34 |
| D-3-phosphoglycerate dehydrogenase | O43175 | 1.645 | 6 | 0.24 | 60.06 |
| Deoxyuridine 5-triphosphate nucleotidohydrolase, mitochondrial | P33316 | 1.545 | 6 | -2.19 | 77.66 |
| DnaJ homolog subfamily A member 1 | P31689 | 0.17 | 2 | 0.57 | 15.70 |
| DnaJ homolog subfamily A member 2 | O60884 | 0.976 | 2 | 1.28 | 19.90 |
| Dolichol-phosphate mannosyltransferase subunit 1 | O60762 | 1.368 | 2 | 1.92 | 6.19 |
| Dolichyl-diphosphooligosaccharide--protein glycosyltransferase 48 kDa subunit | P39656 | 2.775 | 2 | 4.03 | 10.48 |
| Dolichyl-diphosphooligosaccharide--protein glycosyltransferase subunit 1 | P04843 | 1.203 | 10 | 2.06 | 78.34 |
| Dynamin-like 120 kDa protein, mitochondrial | O60313 | 1.02 | 6 | -1.11 | 47.85 |
| Elongation factor 1-alpha 1 | P68104 | 0.806 | 11 | -0.92 | 51.78 |
| Elongation factor 1-gamma | P26641 | 0.041 | 5 | -0.05 | 40.30 |
| Elongation factor 2 | P13639 | 0.361 | 9 | -0.24 | 45.89 |
| Elongation factor Tu, mitochondrial | P49411 | 0.342 | 11 | -0.64 | 64.84 |
| Emerin | P50402 | 1.47 | 3 | 1.93 | 35.01 |
| Endoplasmin | P14625 | 1.221 | 2 | 1.76 | 6.72 |

| | | | | | |
|---|---|---|---|---|---|
| ES1 protein homolog, mitochondrial | P30042 | 2.293 | 4 | -0.93 | 11.16 |
| Eukaryotic translation initiation factor 3 subunit I | Q13347 | 1.89 | 3 | 2.07 | 10.27 |
| F-actin-capping protein subunit alpha-1 | P52907 | 0.094 | 3 | -0.46 | 37.60 |
| F-actin-capping protein subunit beta | P47756 | 0.738 | 3 | -2.09 | 32.66 |
| Far upstream element-binding protein 2 | Q92945 | 0.552 | 6 | 1.61 | 25.63 |
| Fatty acid synthase | P49327 | 0.516 | 3 | -1.51 | 10.65 |
| Fructose-bisphosphate aldolase A | P04075 | 0.002 | 4 | 0.01 | 43.68 |
| Glucosidase 2 subunit beta | P14314 | 0.444 | 4 | 1.07 | 21.73 |
| Glutamine synthetase | P15104 | 0.314 | 3 | -0.81 | 35.70 |
| GTP-binding nuclear protein Ran | P62826 | 0.213 | 3 | 0.28 | 8.46 |
| Guanine nucleotide-binding protein subunit beta-2-like 1 | P63244 | 0.201 | 2 | -0.51 | 7.74 |
| Guanine nucleotide-binding protein subunit beta-like protein 1 | Q9BYB4 | 0.951 | 3 | -1.92 | 14.94 |
| Heat shock 70 kDa protein 1B;Heat shock 70 kDa protein 1A | P0DMV9 | 0.357 | 6 | 0.37 | 113.74 |
| Heat shock cognate 71 kDa protein | P11142 | 0.139 | 10 | 0.20 | 105.76 |
| Heat shock protein HSP 90-beta | P08238 | 1.141 | 3 | 1.36 | 58.95 |
| Heme oxygenase 1 | P09601 | 1.178 | 2 | 2.00 | 11.10 |
| Heme oxygenase 2 | P30519 | 0.691 | 3 | 1.81 | 25.80 |
| Heterogeneous nuclear ribonucleoprotein A1 | P09651 | 0.118 | 4 | 0.49 | 50.41 |
| Heterogeneous nuclear ribonucleoprotein K | P61978 | 1.188 | 3 | -1.89 | 11.31 |
| Heterogeneous nuclear ribonucleoprotein M | P52272 | 0.353 | 7 | -0.86 | 11.65 |
| Heterogeneous nuclear ribonucleoproteins A2/B1 | P22626 | 0.01 | 4 | 0.05 | 16.79 |
| Heterogeneous nuclear ribonucleoproteins C1/C2 | P07910 | 0.122 | 2 | -0.56 | 14.12 |
| Histone H1.4 | P10412 | 0.275 | 2 | 0.64 | 7.35 |

| | | | | | |
|---|---|---|---|---|---|
| Histone H2A.V | Q71UI9 | 0.931 | 2 | -2.60 | 3.98 |
| Hydroxysteroid dehydrogenase-like protein 2 | Q6YN16 | 0.409 | 3 | -0.86 | 23.64 |
| Importin subunit beta-1 | Q14974 | 0.744 | 2 | 1.37 | 12.50 |
| Inosine-5-monophosphate dehydrogenase 2 | P12268 | 0.319 | 3 | -0.56 | 4.84 |
| Ketosamine-3-kinase | Q9HA64 | 0.769 | 4 | -2.15 | 31.41 |
| L-lactate dehydrogenase A chain | P00338 | 0.502 | 4 | 1.41 | 29.22 |
| Lamina-associated polypeptide 2, isoforms beta/gamma | P42167 | 0.396 | 2 | 0.73 | 0.88 |
| Large neutral amino acids transporter small subunit 1 | Q01650 | 0.192 | 3 | 0.44 | 30.16 |
| LIM domain and actin-binding protein 1 | Q9UHB6 | 0.743 | 3 | 0.81 | 13.16 |
| Macrophage migration inhibitory factor | P14174 | 0.186 | 8 | -0.46 | 89.56 |
| Malate dehydrogenase, mitochondrial | P40926 | 0.054 | 2 | 0.08 | 7.98 |
| MARCKS-related protein | P49006 | 2.388 | 6 | 5.09 | 62.64 |
| Membrane-associated progesterone receptor component 1 | O00264 | 1.022 | 6 | 1.69 | 16.09 |
| Methionine-R-sulfoxide reductase B2, mitochondrial | Q9Y3D2 | 0.321 | 2 | 0.55 | 2.52 |
| MICOS complex subunit MIC19 | Q9NX63 | 0.523 | 7 | 2.11 | 35.26 |
| MICOS complex subunit MIC25 | Q9BRQ6 | 0.451 | 2 | 1.45 | 11.06 |
| MICOS complex subunit MIC60 | Q16891 | 0.051 | 4 | -0.17 | 10.32 |
| Myosin light polypeptide 6 | P60660 | 0.672 | 7 | -2.65 | 72.27 |
| Myosin-10 | P35580 | 0.524 | 2 | -0.40 | 10.13 |
| NAD(P) transhydrogenase, mitochondrial | Q13423 | 0.803 | 2 | 1.72 | 4.57 |
| NADH dehydrogenase [ubiquinone] 1 alpha subcomplex subunit 7 | O95182 | 1.663 | 3 | 2.69 | 19.25 |
| NADH dehydrogenase [ubiquinone] 1 beta subcomplex subunit 10 | O96000 | 0.524 | 3 | 1.51 | 17.83 |

| | | | | | |
|---|---|---|---|---|---|
| NADH dehydrogenase [ubiquinone] iron-sulfur protein 6, mitochondrial | O75380 | 1.393 | 3 | 2.91 | 25.68 |
| NADPH--cytochrome P450 reductase | P16435 | 0.315 | 2 | 0.69 | 2.33 |
| Neutral amino acid transporter B(0) | Q15758 | 1.178 | 4 | 2.63 | 30.28 |
| Non-POU domain-containing octamer-binding protein | Q15233 | 1.523 | 3 | -2.19 | 15.87 |
| Nuclease-sensitive element-binding protein 1 | P67809 | 0.559 | 6 | 0.53 | 88.87 |
| Nucleolin | P19338 | 0.905 | 5 | 2.22 | 55.45 |
| Nucleophosmin | P06748 | 0.045 | 3 | -0.18 | 13.77 |
| OCIA domain-containing protein 1 | Q9NX40 | 0.439 | 2 | 1.54 | 4.35 |
| Peptidyl-prolyl cis-trans isomerase A | P62937 | 0.411 | 9 | -0.83 | 37.77 |
| Peroxiredoxin-1 | Q06830 | 1.889 | 7 | -2.73 | 62.15 |
| Phenylalanine--tRNA ligase alpha subunit | Q9Y285 | 0.128 | 2 | -0.22 | 15.53 |
| Phenylalanine--tRNA ligase beta subunit | Q9NSD9 | 1.352 | 4 | -1.38 | 7.89 |
| Plasma membrane calcium-transporting ATPase 4 | P23634 | 0.423 | 2 | 1.48 | 12.42 |
| Plasminogen activator inhibitor 1 RNA-binding protein | Q8NC51 | 0.647 | 6 | 1.56 | 51.47 |
| Plastin-3 | P13797 | 0.566 | 3 | -1.54 | 13.54 |
| Poly [ADP-ribose] polymerase 1 | P09874 | 0.421 | 2 | 1.22 | 6.72 |
| Poly(rC)-binding protein 1 | Q15365 | 0.681 | 2 | -1.39 | 56.41 |
| Polypeptide N-acetylgalactosaminyltransferase 2 | Q10471 | 0.75 | 5 | 1.56 | 36.11 |
| PRA1 family protein 2 | O60831 | 1.029 | 2 | 2.39 | 15.88 |
| Prohibitin | P35232 | 0.402 | 7 | 1.15 | 45.32 |
| Prohibitin-2 | Q99623 | 0.743 | 7 | 2.91 | 27.28 |
| Proteasomal ubiquitin receptor ADRM1 | Q16186 | 1.682 | 2 | 1.62 | 26.27 |
| Protein deglycase DJ-1 | Q99497 | 0.445 | 4 | 0.45 | 19.73 |

| | | | | | |
|---|---|---|---|---|---|
| Protein disulfide-isomerase | P07237 | 0.558 | 4 | 0.87 | 7.63 |
| Protein disulfide-isomerase A3 | P30101 | 1.021 | 3 | 0.79 | 35.62 |
| Protein disulfide-isomerase A6 | Q15084 | 0.068 | 5 | 0.22 | 41.32 |
| Protein FAM3C | Q92520 | 0.256 | 4 | 1.15 | 14.81 |
| Protein S100-A8 | P05109 | 0.574 | 3 | -1.47 | 9.82 |
| Protein S100-A9 | P06702 | 0.536 | 2 | -1.33 | 11.00 |
| Protein transport protein Sec61 subunit beta | P60468 | 0.23 | 3 | -0.78 | 37.67 |
| Prothymosin alpha | P06454 | 0.551 | 3 | 2.49 | 62.35 |
| Putative transferase CAF17, mitochondrial | Q5T440 | 2.379 | 2 | -1.82 | 16.34 |
| Pyruvate dehydrogenase E1 component subunit alpha, somatic form, mitochondrial | P08559 | 2.162 | 3 | 1.87 | 17.03 |
| Ras-related protein Rab-1A | P62820 | 0.037 | 2 | -0.12 | 8.11 |
| Ras-related protein Rab-21 | Q9UL25 | 0.246 | 2 | 0.59 | 12.15 |
| Ras-related protein Rab-6A | P20340 | 0.439 | 3 | 1.18 | 6.12 |
| Ras-related protein Rab-7a | P51149 | 0.051 | 4 | 0.18 | 48.91 |
| Retinol dehydrogenase 14 | Q9HBH5 | 0.36 | 2 | 1.01 | 6.01 |
| RuvB-like 1 | Q9Y265 | 0.433 | 2 | 0.42 | 6.47 |
| RuvB-like 2 | Q9Y230 | 0.544 | 2 | 1.30 | 3.93 |
| Secretory carrier-associated membrane protein 1 | O15126 | 0.073 | 2 | 0.47 | 42.01 |
| SEOV glycoprotein | NP_942557.1 | 1.788 | 17 | 6.28 | 106.14 |
| Sideroflexin-1 | Q9H9B4 | 2.382 | 2 | 3.71 | 28.26 |
| Single-stranded DNA-binding protein, mitochondrial | Q04837 | 2.478 | 3 | 3.13 | 20.38 |
| Small nuclear ribonucleoprotein Sm D2 | P62316 | 2.927 | 2 | 4.49 | 13.50 |
| Sodium/potassium-transporting ATPase subunit alpha-1 | P05023 | 0.821 | 12 | 1.41 | 238.29 |

| | | | | | |
|---|---|---|---|---|---|
| Solute carrier family 35 member F6 | Q8N357 | 0.242 | 2 | 0.57 | 5.36 |
| Stress-70 protein, mitochondrial | P38646 | 0.055 | 12 | -0.10 | 128.45 |
| Stress-induced-phosphoprotein 1 | P31948 | 1.482 | 4 | 3.68 | 70.66 |
| Stromal cell-derived factor 2-like protein 1 | Q9HCN8 | 2.74 | 4 | 4.54 | 53.78 |
| Succinate dehydrogenase [ubiquinone] flavoprotein subunit, mitochondrial | P31040 | 1.317 | 7 | 1.69 | 22.20 |
| Succinate dehydrogenase [ubiquinone] iron-sulfur subunit, mitochondrial | P21912 | 0.685 | 2 | 1.23 | 4.06 |
| Superoxide dismutase [Cu-Zn] | P00441 | 2.365 | 2 | 3.93 | 1.77 |
| Thioredoxin domain-containing protein 5 | Q8NBS9 | 0.162 | 5 | 0.61 | 62.89 |
| Thioredoxin-related transmembrane protein 2 | Q9Y320 | 0.26 | 2 | 0.54 | 10.15 |
| THO complex subunit 4 | Q86V81 | 0.83 | 4 | 2.17 | 25.09 |
| Threonine--tRNA ligase, mitochondrial | Q9BW92 | 0.509 | 3 | -0.27 | 7.79 |
| Transferrin receptor protein 1 | P02786 | 0.12 | 4 | -0.72 | 25.66 |
| Transgelin-2 | P37802 | 0.031 | 2 | -0.09 | 21.71 |
| Transitional endoplasmic reticulum ATPase | P55072 | 1.55 | 4 | 1.42 | 22.36 |
| Transmembrane emp24 domain-containing protein 10 | P49755 | 2.268 | 2 | 2.55 | 9.01 |
| Transmembrane protein 109 | Q9BVC6 | 1.307 | 2 | -1.03 | 8.53 |
| Trifunctional purine biosynthetic protein adenosine-3 | P22102 | 1.231 | 5 | -1.86 | 21.38 |
| Tropomyosin alpha-3 chain | P06753 | 0.505 | 7 | -0.73 | 46.05 |
| Tubulin alpha-1A chain | Q71U36 | 1.833 | 8 | -0.74 | 185.92 |
| Tubulin beta chain;Tubulin beta-2A chain | P07437 | 0.019 | 3 | 0.02 | 36.52 |
| Tubulin beta-4B chain | P68371 | 0.362 | 4 | -0.23 | 108.30 |
| Ubiquitin-60S ribosomal protein L40 | P62987 | 1.355 | 3 | 2.51 | 23.99 |

| | | | | | |
|---|---|---|---|---|---|
| UDP-glucose:glycoprotein glucosyltransferase 1 | Q9NYU2 | 0.821 | 5 | 2.07 | 14.67 |
| Uncharacterized protein C4orf3 | Q8WVX3 | 0.844 | 2 | 2.51 | 11.20 |
| UPF0449 protein C19orf25 | Q9UFG5 | 0.597 | 3 | 1.84 | 40.50 |
| Vesicle-associated membrane protein-associated protein B/C | O95292 | 1.363 | 3 | 2.66 | 9.15 |
| Vesicle-fusing ATPase | P46459 | 0.947 | 2 | 1.59 | 18.47 |
| Vesicle-trafficking protein SEC22b | O75396 | 0.901 | 4 | 1.73 | 80.33 |
| Vimentin | P08670 | 0.657 | 25 | -0.63 | 323.31 |
| Voltage-dependent anion-selective channel protein 2 | P45880 | 0.5 | 2 | 1.22 | 4.10 |
| Y-box-binding protein 3 | P16989 | 0.649 | 2 | 1.80 | 13.63 |
| Zinc finger CCCH-type antiviral protein 1-like | Q96H79 | 0.584 | 4 | -2.45 | 10.39 |

# *Appendix C. Published data*

## *Oral presentations*

- April 2017: **Microbiology Society Annual Conference 2017, Edinburgh**; *Serum proteins associated with acute hantavirus infection in a pregnant woman*
- January 2017: **HPRU Phd Meeting, London**; *Using label free proteomics for discovery of host biomarkers of hantavirus infection*
- December 2016: **HPRU EZI 3rd Annual Conference, Liverpool;** *Serum proteins associated with acute hantavirus infection in a pregnant woman*
- February 2016: **Hantavirus Workshop, Liverpool**; *Proteomic analysis of hantavirus-infected human serum*
- January 2016: **HPRU EZI 2nd Annual Conference, London**; *Proteomic analysis of hantavirus-infected human serum*
- March 2015: **HPRU EZI Meeting, Porton Down;** *Diagnostic and immune predictors of acute kidney injury in patients infected with hantaviruses in the UK*

## *Poster presentations*

- April 2017: **27th ECCMID, Vienna**; *Serum proteins associated with acute hantavirus infection in a pregnant woman*
- November 2016: **Infection and Global Health Day, University of Liverpool**: *Serum proteins associated with acute hantavirus infection in a pregnant woman*
- November 2015: **Infection and Global Health Day, University of Liverpool;** *Proteomic analysis of hantavirus-infected human serum*
- September 2015: **Public Health England Annual Conference, Coventry**; *Proteomic analysis of hantavirus-infected human serum*

*Publications*

- **Longitudinal characterisation of the serum plasma proteome in a pregnant woman during acute orthohantavirus infection**. Sarah B. Bar-Yaacov, Stuart D. Armstrong, Ollie Wildman, Ewa Zatyka, Jackie M. Duggan, Tim J.G. Brooks, Nicholas J. Beeching, Julian A. Hiscox – *in submission.*